INVESTIGATING THE ROLE OF VESICLE TRAFFICKING IN EPITHELIAL CELL MIGRATION

by

SARAH JANE FLETCHER

A thesis submitted to
The University of Birmingham
for the degree of
DOCTOR OF PHILOSOPHY

School of Biosciences
The University of Birmingham
September 2012

ABSTRACT

Cell migration is required for re-epithelisation following wounding. Vesicle trafficking is widely implicated in regulation of cell migration. The scratch wound healing assay was utilised throughout this study to determine mechanistic linkages between endocytosis and migration in the Madin-Darby Canine Kidney (MDCK) epithelial cell line.

Time-lapse epifluorescence imaging studies demonstrated specific inhibition of clathrin-mediated, dynamin-dependent and caveolar endocytosis, Rab4- and Rab11-mediated trafficking significantly reduced the rate of epithelial cell migration. Further wound healing studies combined with total-internal reflection fluorescence (TIRF) microscopy of cells expressing GFP-labelled trafficking markers identified polarised caveolar endocytosis to the cell rear, whilst exocytosis of vesicles derived from the Rab11 and Rab25 trafficking pathways were not polarised during epithelial wound healing.

Additionally, although the dynamin-dependent endocytosis pathways do have a function in MDCK cell migration, TIRF imaging combined with co-localisation analysis of migrating cells expressing fluorescently labelled focal adhesion (FA) and endocytosis pathway markers suggest endocytosis does not regulate FA turnover. Alternatively, immunocytochemistry, confocal imaging and co-localisation analysis demonstrated clathrin-mediated endocytosis of the tight junction (TJ) protein occludin from the wound edge to Rab5 positive early endosomal compartments occurs shortly after wound healing. Wound healing analysis also suggested internalisation of occludin from the leading edge as a novel mechanism for regulating epithelial cell motility.

However, little is known about occludin trafficking under non-stimulated conditions. This study utilised stable-isotope labelling by amino acids in cell culture (SILAC) combined with immunoprecipitation (IP) and mass spectrometry to identify proteins/protein complexes which may regulate occludin trafficking. Although no such proteins were identified, the data did indicate a high level of occludin synthesis. Sulfo-NHS-SS-Biotin based trafficking assays were combined with confocal imaging, immunocytochemistry of endogenous occludin and co-localisation analysis between occludin and fluorescent endosomal markers to examine steady-state occludin trafficking. These studies suggest that under non-stimulated conditions occludin is continuously internalised, with a large proportion of endocytosed occludin undergoing lysosomal degradation. Occludin degradation is coupled to a high level of biosynthesis and trafficking to the plasma membrane. These findings are important as regulation of TJ structure is integral in maintenance of epithelial membranes whilst loss of cell-cell junctions is a hallmark of epithelial mesenchymal transition during cancer metastasis. Therefore this work demonstrates a clear link between regulation of TJ proteins and directed epithelial cell migration.

I dedicate this thesis to my mother, Anita. Thank you for everything.

ACKNOWLEDGEMENTS

Firstly, I would like to express my gratitude to my supervisor Dr Joshua Rappoport, who throughout my PhD has supported me continuously. His endless patience, motivation, knowledge and enthusiasm has guided me through my research and thesis writing. I could not have wished for a better mentor and advisor during my PhD study. I would also like to thank my internal assessor Professor John Heath for his continual guidance, advice and discussion and the members of the Friday lunchtime lab meeting group for their invaluable advice and tips. My gratitude is also expressed to Professor Jane McKeating and members of her lab (especially Michelle Farquhar) for sharing both knowledge and reagents during my research. I am also thankful to Dr Michael Tomlinson (the King of Westerns) for all of his advice, sharing of reagents, knowledge and hilarious stories. My thanks also goes out to current and previous members of the Rappoport Lab: Giulio Auciello, Dr Natalie Poulter, Jennifer Thorley, Dr Julie Mazzolini, Sylwia Krawczyk, Phil Smith, Laura Mutch and Eric Pitkeathly for making the lab such a wonderful working environment and helping me throughout my research. I also thank members of the Tomlinson Lab: Dr Jing Yang, Elizabeth Haining and Rebecca Bailey for their help and advice. I would also like to thank Debbie Cunningham and Andrew Creese for their help with SILAC and mass spectrometry analysis. I particularly want to thank Elizabeth Haining and Dr Natalie Poulter for their direct contributions to my research.

I also thank all of the lunch time crew for keeping me sane during my PhD study, for some excellent scientific advice and truly amazing times (and cakes): In particular I would like to thank Rachel Gurney, Richard Logan and Jennifer Morris.

I want to thank my family, especially my Mum who has always been there and encouraged me. Thank you for your continued support and love. I also want to thank my Dad, Phil and Val, Alan and Lisa, Keith and Carol, Nicole and Marie for their help and support over the years. Thank you to my great friends Jodie, Leigh and Kat you guys are the best. Finally, I would like to thank Matthew for all of his support, coming into the lab with me on weekends and putting up with me during the write up stage (and not complaining).

TABLE OF CONTENTS

LIST OF FIGURES AND TABLES

CHAPTER 1- INTRODUCTION

CHAPTER 2 – METHODS

CHAPTER 3 - THE ROLE OF VESICLE TRAFFICKING IN EPITHELIAL CELL MIGRATION

CHAPTER 4 - POLARISED TRAFFICKING IN MIGRATING EPITHELIAL CELLS

CHAPTER 5 - TRAFFICKING OF ADHESION COMPLEXES DURING EPITHELIAL CELL MIGRATION

CHAPTER 6 - STEADY-STATE OCCLUDIN TRAFFICKING

LIST OF DEFINITIONS

Adherens junction	**AJ**
Ammonium Persulphate	**APS**
Bafilomycin A	**BafA**
Bovine serum albumin	**BSA**
Brain-derived neurotrophic factor	**BDNF**
Cell imaging media	**CIM**
Cholera Toxin B subunit	**CTxB**
Cholera Toxin Subunit B conjugated to Alexa Fluor 555	**CTxB-AF555**
Clathrin-mediated endocytosis	**CME**
Collision-induced dissociation	**CID**
Cycloheximide	**CHX**
Dimethylpimelimidate	**DMP**
Dithiothreitol	**DTT**
Dorsal root ganglion cell	**DRG**
Dulbecco's Modified Eagle Medium	**DMEM**
Early Endosome	**EE**
Endothelial cells	**EC**
Endothelial Growth Factor Receptor	**EGFR**
Epidermal growth factor receptor substrate 15	**Eps15**
Epithelial Mesenchymal Transition	**EMT**
Electron Microscopy	**EM**
Extracellular matrix	**ECM**
Fibroblast growth factor	**FGF**
Focal Adhesion	**FA**
Foetal bovine serum	**FBS**
Formyl-Methionyl-Leucyl-Phenylalanine	**fMLP**
Focal adhesion kinase	**FAK**
Goat serum	**GS**
Hepatitis C Virus	**HCV**
Human basement membrane heparin sulfate proteoglycan core protein	**HSPG**
Immunocytochemistry	**IC**
Immunoprecipitation	**IP**
Junctional adhesion molecule	**JAM**
Low density lipoprotein	**LDL**
Luria Broth	**LB**
Madin-Darby canine kidney cell	**MDCK**
Microtubule Organising Centre	**MTOC**
Mouse embryonic fibroblast	**MEF**
Myxovirus hemagglutinin	**HA**
Neuropeptide Y	**NPY**
Normal rat kidney fibroblast cell	**NRK**
Paraformaldehyde	**PFA**
Perinuclear Recycling Compartment	**PNRC**
Phosphorylated focal adhesion kinase	**pFAK**

Platelet derived growth factor	**PDGF**
Protein kinase C	**PKC**
Protein kinase D	**PKD**
Room temperature	**RTP**
Serum free DMEM	**SFM**
Sodium Dodecyl Sulphate	**SDS**
Src family kinase	**SFK**
Stable-isotope labelling by amino acids in cell culture	**SILAC**
Sulfosuccinimidyl-2-(biotinamido)-ethyl-1,3'-dithiopropionate	**Sulfo-NHS-SS-Biotin**
Region of interest	**ROI**
Total-internal reflection fluorescence	**TIRF**
Tight Junction	**TJ**
Tumour necrosis factor	**TNF**
Vascular Endothelial Growth Factor Receptor-2	**VEGFR-2**
Vesicular stomatitis virus G-protein	**VSVG**
Zonula occludens	**ZO**

CHAPTER 1

INTRODUCTION

Cell migration is a requirement for many physiological processes, from the flagella-based swimming of sperm to the amoeboid crawling of *Dictyostelium* and the collective healing of an epithelial wound. In particular epithelial wound healing is a critical physiological process. Failure of wounds to heal to completion can lead to fibrosis of surrounding tissue, impairing solute and gas exchange when the kidneys and lungs are affected. Furthermore, inability to repair wounds correctly leads to increased likelihood of wound infection. This is particularly a problem in patients suffering diabetes. A significant side effect of diabetes is the formation of non-healing dermal ulcers which occur in 15% of patients (Reiber et al., 1999) as a result of localised tissue ischemia (Kolluru, Bir, & Kevil, 2012). 87% of ulcers lead to lower foot amputations (McNeely et al., 1995) and 70% of patients who have undergone amputation die within the first five years (Stratton et al., 2000). Moreover, this is a problem which is on the rise as a significant increase in type 2 diabetes has been observed in recent years (Diabetes in the U.K., 2012). Thus, the increased prevalence of disorders such as diabetes emphasises the importance of research investigating the mechanisms through which epithelial wound healing is regulated. This research

may aid in identification of therapeutic targets and pharmacological tools to aid wound healing.

1.1 Cell migration

Cell migration is a key requirement during embryonic development and in maintenance of multicellular organisms. It describes the process of translocation of cells from one region to another. Cell motility can be directed or random, and can occur through a variety of stimuli. There are several types of directed cell migration, yet the two most widely studied *in vitro* models of directed cell migration are chemotaxis and wound healing. Chemotaxis is a process where directed migration occurs as a response to external cues in the form of soluble ligands (growth factors and cytokines) which when released into the local environment bind their cognate receptor at the plasma membrane. Ligand-receptor binding mediates activation of downstream signalling cascades leading to generation and maintenance of a migratory phenotype in the direction of the ligand source (reviewed fully in Iglesias & Devreotes, 2008). During chemotaxis, directed cell migration is reliant upon a chemical gradient, however during wound healing the external stimuli is a release of contact inhibition from neighbouring cells (Huttenlocher et al., 2012). Examples of these processes *in-vivo* include chemotactic motility of neutrophils seeking out pathogens (Nuzzi, Senetar, & Huttenlocher, 2007), and the sheet-like motion of epithelial monolayers into a denuded region such as in conjunctival scratches (Geggel, Friend, & Thoft, 1984). The mechanisms through which chemotaxis and wound

healing are regulated are likely to be very different; however, a cohesive model of the processes which regulate motility is yet to be made.

Multiple cellular processes have been demonstrated to play an important function in cell migration. When a migratory stimulus is received by the cell, several morphological changes occur leading to development of a polarised phenotype (Lauffenburger & Horwitz, 1996). This phenotype is identified by extension of dynamic membrane protrusions in the direction of migration, formation and disassembly of FAs, extensive reorganisation of the actin cytoskeleton, and re-orientation of the Golgi and microtubule organising centre (MTOC) (Casanova, 2002; Grande-Garcia et al., 2007; Lauffenburger & Horwitz, 1996).

One of the initial stages of polarisation is generation of a dynamic lamellipodia/filopodia at the leading edge (Chou et al., 2003) (Figure 1.1). These protrusions are formed by extensive actin polymerisation and function in generation of a protrusive force (Lauffenburger & Horwitz, 1996). This process is regulated by several members of the Rho-GTPase family (Cdc42 and Rac), the Arp2/3 complex activated by N-Wasp, and Ena/VASP proteins localised to the leading edge (Grande-Garcia et al., 2007; Ridley et al., 2003; Krause et al., 2003). However, development of membrane protrusions alone are unable to generate motile force, thus new membrane extensions develop attachments between the extracellular matrix (ECM) and the cell, utilising traction forces to drive cell migration (Figure 1.1). These attachments with the substratum are known as focal complexes (Izzard & Lochner, 1976), which mature into FAs

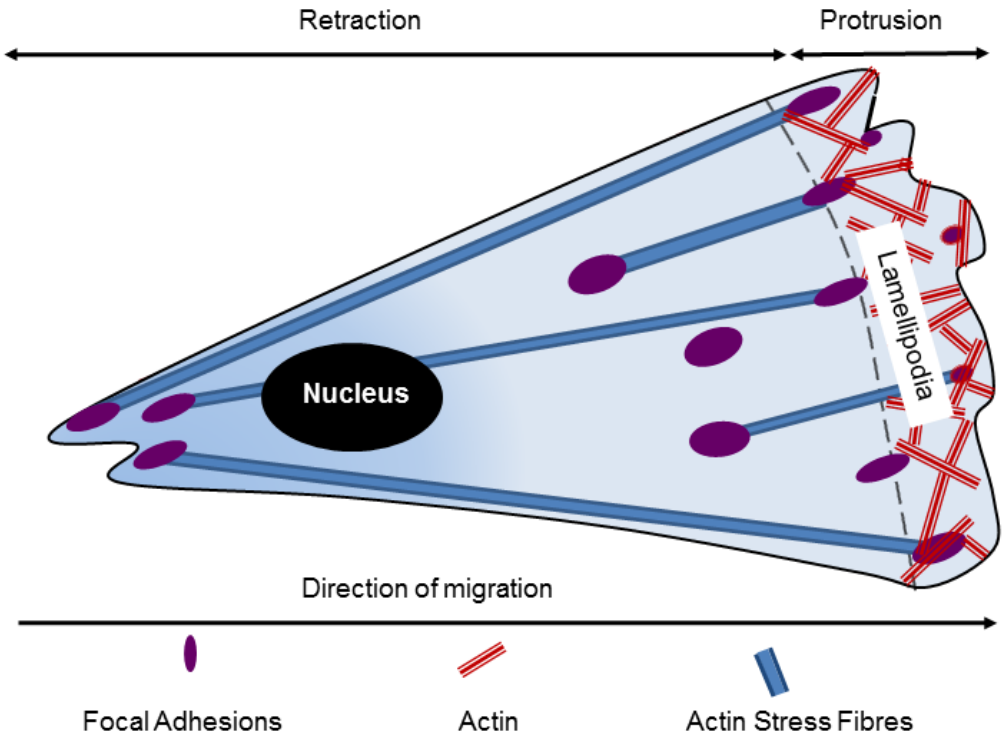

Figure 1.1. The polarised migratory phenotype. Depiction of a polarised migrating cell. Figure shows extensive actin polymerisation in the lamellipodial region mediating membrane protrusion. Focal adhesions form in the adherent surface of regions of membrane protrusion, coupling the actin cytoskeleton to the extracellular matrix. Thick actin stress fibres aid in regulation of tension, whilst actomyosin contraction of these fibres facilitate retraction of the cell rear.

(Burridge & Chrzanowska-Wodnicka, 1996). FAs are linked to the actin cytoskeleton via actin stress fibres which regulate and maintain tension on the axis of the cell (Ridley et al., 1992) (Figure 1.1). However, for directed cell migration to be successful, protrusion and generation of motile force must be coupled to retraction of the cell rear and disassembly of adhesive complexes. This process is mediated by retraction of the trailing edge and is regulated by Rho-GTPase, Rho kinase, myosin light chain phosphorylation, and interactions with myosin II (Katoh et al., 2001). Moreover, cell-substrate adhesion and disassembly have been hypothesised to be regulated by several mechanisms including: mechanical disruption driven by actomyosin contraction, extracellular disruption by proteases and sheddases and post-translational modification of scaffolding proteins (reviewed fully in Kirfel et al., 2004). These processes require a high level of regulation to enable successful directed migration (Friedl & Wolf, 2003).

1.2 Epithelial wound healing

Epithelial cell layers are required for regulation of gas and solute exchange and also aid in protection of underlying tissue from injury and infection. When injury occurs repair must take place. Two mechanisms of wound healing have been identified: the “purse-string” model (identified predominantly in smaller wounds) which is regulated by actomyosin based contraction (Kiehart, 1999); and re-epithelialisation occurring via collective migration of epithelial monolayers (Figure 1.2) (Fenteany, Janmey, & Stossel, 2000). Re-epithelialisation is the final phase of tissue repair (Castor, 1968; Falanga, 2005; Lampugnani, 1999;

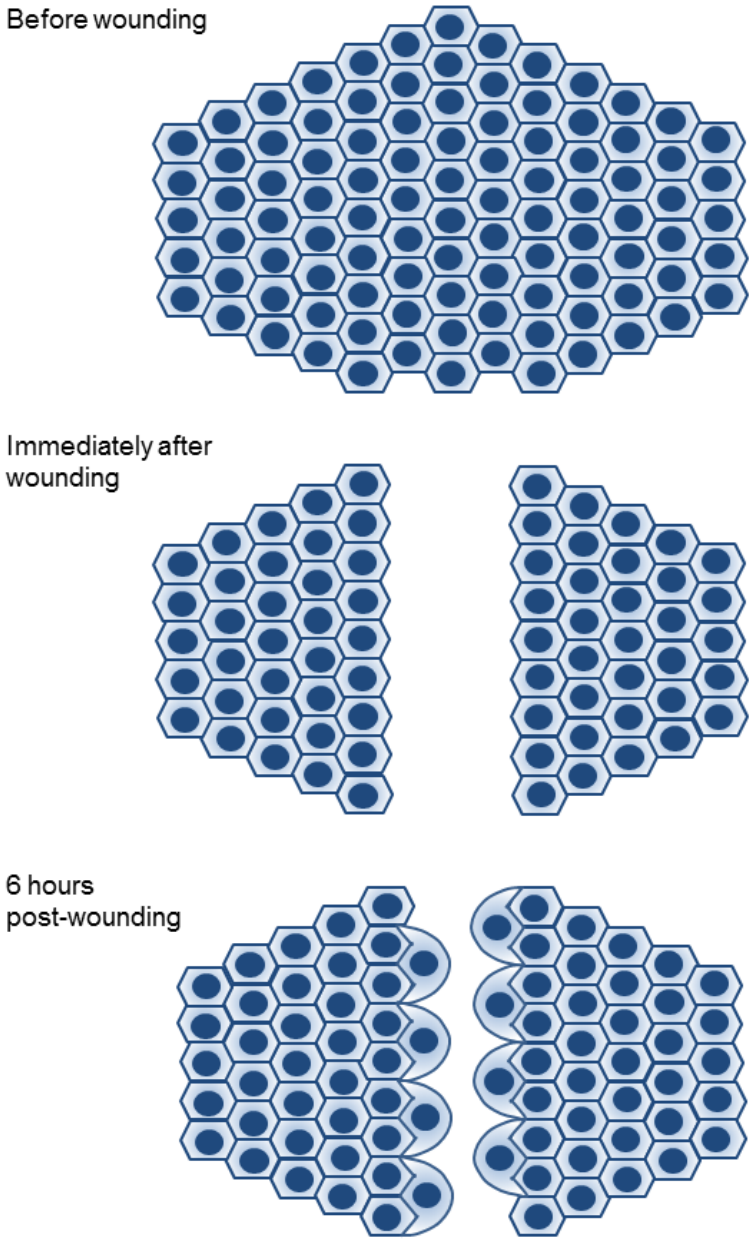

Figure 1.2. Collective epithelial migration. Diagram depicting epithelial wound healing. Before wounding, epithelial cells have tight cell-cell junctions to maintain the integrity of the epithelial monolayer. Immediately after wounding epithelial cells maintain cell-cell interactions and cells on the wound edge begin to develop a polarised phenotype with a broad lamellipodia. Once development of the motile morphology has occurred cells undergo collective directed migration to close the wound.

Marti et al., 2004) and is important for healing dermal wounds and injuries to internal organs. Collective epithelial motility differs significantly from the migratory strategy employed by non-epithelial derived cell lines such as fibroblasts and endothelial cells (ECs). This is due to the presence of significant cell-cell junctions which are maintained during epithelial cell migration.

Intercellular adhesion structures are highly important for maintaining the structural integrity and function of epithelial monolayers. There are four types of cell-cell adhesion structure; Adherens Junctions (AJ), TJs, GAP Junctions and Desmosomes (Figure 1.3). AJs function predominantly in intercellular adhesion (Yonemura et al., 1995) whilst TJs aid in regulation of paracellular permeability and apical-basolateral polarity (van Meer & Simons, 1986). GAP junctions allow flux of solute and ions from one cell to its neighbour (Lampe & Lau, 2004) while desmosomes aid in cell-cell adhesion and also in resistance to sheering forces (Green & Jones, 1996). Several studies have been performed linking regulation of cell-cell junctions with cell migration, particularly during epithelial-mesenchymal transition (EMT) (Du et al., 2010; Sander et al., 1998; Brennan et al., 2010). EMT is a process characterised by loss of cell-cell junctions where epithelial cells lose their epithelial morphology, become more fibroblastic and develop a more migratory and invasive phenotype. EMT is observed in some epithelial derived carcinoma (Brennan et al., 2010), identifying a role for cell-cell junction disassembly in epithelial cell migration (Brennan et al., 2010; Niessen, 2007). Cell-cell adhesion may have an important function in regulation of cell migration, combined with the physiological importance of epithelial wound

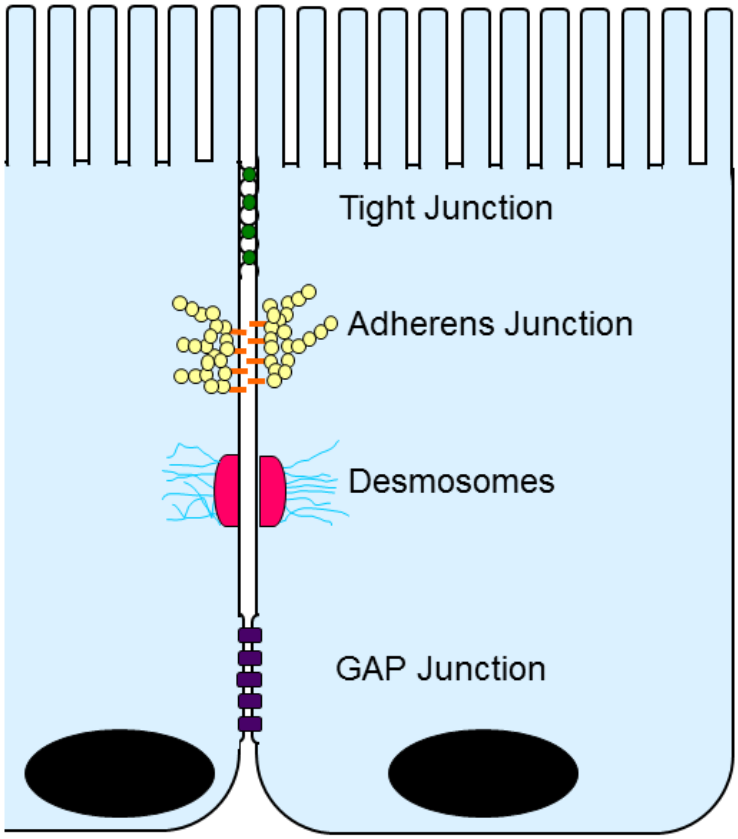

Figure 1.3. Cell-cell adhesive structures in polarised epithelial cells. There are four types of adhesive structure in polarised epithelial cells, the most apical structures are tight junctions, below them the adherens junctions and desmosomes. The most basolateral adhesive structures are GAP junctions.

healing, collective migration of epithelial cells is a system requiring further investigation.

1.3 MDCK cells

One of the most widely used epithelial models is the MDCK epithelial cell model. MDCK cells were isolated from the apparently normal kidney distal tubule of a female cocker spaniel in 1958 by S.H. Madin and N.B. Darby (Madin & Darby, 1958). MDCK cells are an excellent epithelial model as their trafficking pathways are well established (Weisz & Rodriguez-Boulan, 2009), they are capable of forming fully polarised monolayers and form well defined cell-cell junctions (AJ, TJ, Gap junctions, Desmosomes) (Dukes, Whitley, & Chalmers, 2011). They have been widely utilised to examine mechanisms of wound healing (Fenteany, Janmey, & Stossel, 2000). Moreover, MDCK cells are an excellent tool for examining wound healing as their mechanism of wound closure utilises collective cell migration rather than cell division to fill in the denuded region (Fenteany, Janmey, & Stossel, 2000). However MDCK cells do have several draw-backs, mostly due to the fact they are a canine derived cell line. For example most antibodies are raised against human or mouse sequences and may not be able to recognise the canine protein target. Furthermore, gene silencing techniques such as RNAi and siRNA are difficult in MDCK cells, as the canine genome although fully sequenced is not fully annotated making target sequence identification difficult. Moreover, the canine sequence database is limited, hindering mass spectrometry based proteomic studies of MDCK cells. Although there are negative aspects of using MDCK

cells as an epithelial model, the benefits far outweigh the negative features of this cell line. Their ease of culturing, known trafficking pathways, and ability to polarise and form excellent cell-cell adhesions makes this an invaluable model to study trafficking of adhesion complexes during epithelial wound healing.

1.4 Vesicle trafficking

Vesicles are intracellular structures, enclosed by a lipid bilayer and required for transport of cargo between cellular compartments. Endosomal recycling is initiated when lipids, membrane proteins and soluble ligands are internalised from the cell-surface. Once inside the cell body, endosomal cargo is either recycled via intracellular organelles and returned to the plasma membrane or targeted for degradation (Maxfield & McGraw, 2004).

One of the most widely studied internalisation pathways is clathrin-mediated endocytosis (CME) (Figure 1.4). CME is initiated by formation of clathrin coated pits. Adaptor proteins such as AP2 facilitate recruitment of clathrin triskelia to the plasma membrane (Pearse, Smith, & Owen, 2000). Clathrin triskelia are three-legged pinwheel shaped heteropolymers, each “leg” is composed of a heavy and light clathrin chain, the C terminus ending in a common hub (Ferguson et al., 2008). Upon recruitment to the plasma membrane the triskelia polymerise into a clathrin lattice, mediating plasma membrane curvature (Boucrot & McMahon, 2011). Accessory proteins such as AP180 and epsin are recruited to the plasma, which function both directly in membrane curvature and recruit molecules with similar function (Ford et al., 2002; Ford et al., 2001). Once the pit has formed, dynamin polymerises in a spiral formation at the neck

of the vesicle. This molecule utilises GTP hydrolysis to induce a conformational change leading to vesicle fission (Sweitzer & Hinshaw, 1998). Once the clathrin coated vesicle has been formed and is disconnected from the plasma membrane, it undergoes an uncoating process mediated by auxillin and Hsc70 where clathrin is removed from the vesicle (Rapoport et al., 2008). When vesicles have been uncoated they are capable of fusion with endosomal organelles delivering cargo for recycling or degradation.

Another dynamin-dependent internalisation pathway is caveolar endocytosis (Figure 1.4). Caveolar endocytosis takes place through structures known as caveolae, which are flask-shaped invaginations rich in cholesterol and sphingolipids. The most important structural component of caveolae are the caveolin coat proteins. There are 3 members of the caveolin family, caveolin1 (required for caveolae biogenesis), caveolin2 and caveolin3 (muscle specific) (Fra et al., 1995). Caveolins are hairpin transmembrane proteins which bind cholesterol, both the N and C terminus are cytoplasmic (Murata et al., 1995). The first stage of caveolar biogenesis involves trafficking of newly synthesised caveolin1 to the endoplasmic reticulum where it is oligomerised into homo oligomers of 7-14 caveolin1 molecules, which are transported to the plasma membrane as a stationary unit (Monier et al., 1995; Scheiffele et al., 1998; Tagawa et al., 2005). Recent studies have identified members of the cavin family of proteins associated with the plasma membrane of mature caveolae, where its appears to function in sequestration of mobile caveolin1 into caveolae, aiding biogenesis and regulation of membrane curvature (Hansen et al., 2009; Hill et al., 2008). The exact mechanism through which cargo is recruited

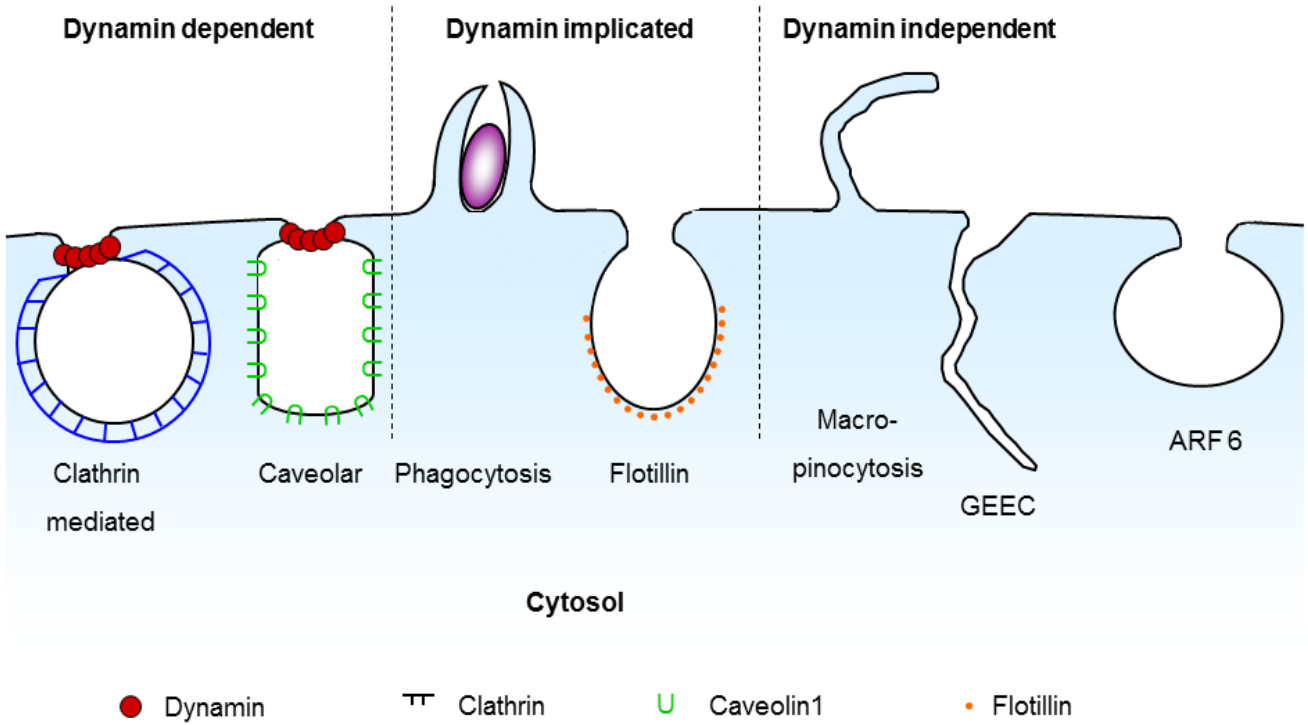

Figure 1.4. Endocytosis pathways. There are several internalisation pathways, the most widely studied are the dynamin-dependent pathways particularly clathrin-mediated and caveolar endocytosis. Moreover, dynamin has been implicated in other internalisation pathways such as phagocytosis and flotillin endocytosis. However, there are dynamin-independent internalisation pathways including macropinocytosis, GEEC and ARF 6-mediated pathways.

to caveolae and internalised is unknown, however the large GTPase dynamin appears to play a role in vesicle fission (Oh, McIntosh, & Schnitzer, 1998). Like CCVs, caveolar derived vesicles undergo subsequent trafficking to endosomal organelles (Zhang et al., 2000) and are capable of plasma membrane fusion (Salanueva et al., 2007).

Upon internalisation of cargo by endocytosis, the cargo can be recycled through several organelles back to the cell-surface or be targeted for degradation (Maxfield & McGraw, 2004). Recycling can occur via many endosomal organelles (reviewed extensively in Maxfield & McGraw 2004). However, this study is particularly interested in the trafficking pathways mediated by the GTP ases Rab4 and Rab11 (Figure 1.5). In many cells undergoing single cell migration, Rab4-mediated recycling describes rapid transport of cargo to peripheral early endosomes (EE) and recycling directly back to the plasma membrane (Figure 1.5) (van der Sluijs et al., 1992a; van der Sluijs et al., 1992b). An alternative route for cargo from the EE is to the perinuclear recycling compartment (PNRC) then to the plasma membrane (Figure 1.5) (Ullrich et al., 1996). This route is slower and is known as the Rab11-dependent pathway (Maxfield & McGraw, 2004). This model describes the classical pathway of endosomal sorting and targeting of proteins, however there is a significant difference in these pathways between cell lines. For example, in polarised MDCK cells the endosomal recycling pathway utilised by these cells to recycle cargo is complex, complicated by the presence of apical and basolateral domains (Figure 1.6). Each domain has its own set of recycling

Figure 1.5. Classical vesicle trafficking pathways. Figure demonstrating several vesicle trafficking pathways. The Rab4 pathway shows internalisation from the plasma membrane to early endosomal (EE) compartments followed by rapid recycling back to the plasma membrane. An alternative recycling pathway is the slower Rab11 trafficking pathway. Cargo destined for this pathway, still traverses the EE but is transported from the EE to the perinuclear recycling compartment (PNRC). From the PNRC cargo is transported to the plasma membrane. This diagram also shows how some internalised cargo is targeted for lysosomal degradation via the late endosome (LE). The final trafficking pathway demonstrated shows trafficking of newly synthesised cargo via the biosynthetic secretory pathway and transported to the plasma membrane.

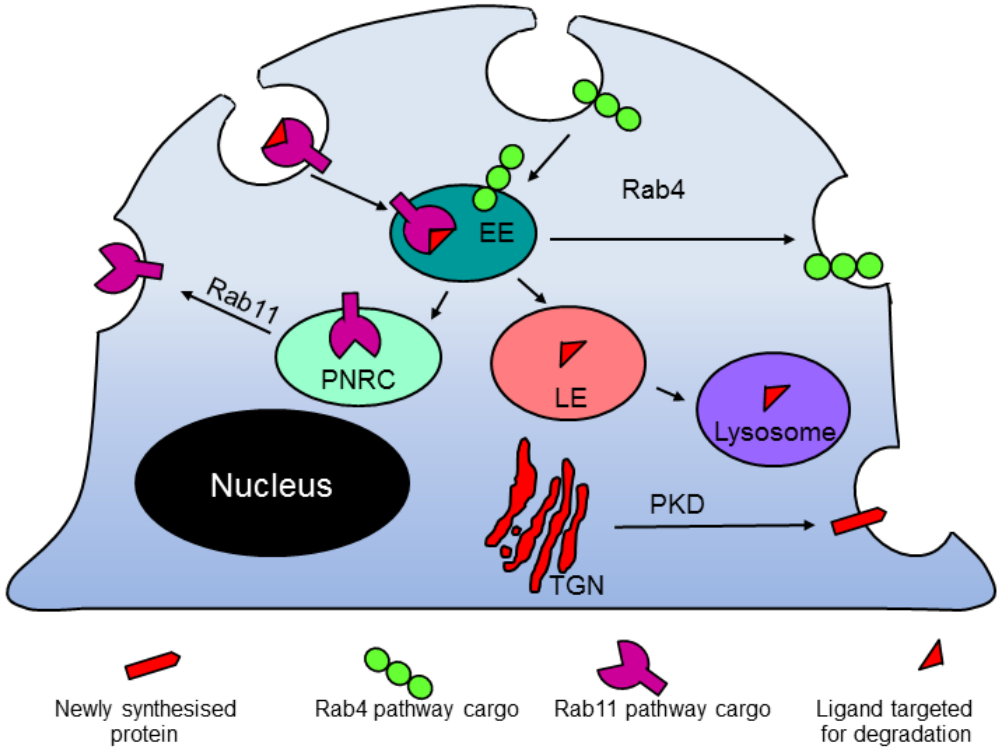

endosomes, through which cargo can be transported for targeting to apical/basolateral membranes (Figure 1.6). As shown in Figure 1.6, Rab4 still has an important role in regulating trafficking of cargo through the apical and basolateral EEs (Weisz & Rodriguez-Boulan, 2009), however the function for Rab11 in regulation of vesicle trafficking is significantly different to that observed in migrating CHO and BHK cells (Ullrich et al., 1996). Instead of modulating transport of cargo through the PNRC compartment, Rab11 appears to function by regulating trafficking through the apical recycling endosome regulating apical recycling and transcytosis (trafficking from apical to basolateral membranes) (Figure 1.6) (Casanova et al., 1999; Casanova, 2002; Wang et al., 2000). However, during cell migration apical and basolateral polarity is lost, instead cells develop a front-rear axis of polarity. This phenotype change may alter both function and organelle localisation of Rab11 during MDCK cell migration, but the extent to which it is altered is unknown. Yet it has been demonstrated in non-polarised MDCK cells grown on glass, Rab11 localises to an organelle similar to the apical recycling endosome adjacent to the nucleus, however it is not involved in transferrin recycling so is unlikely to be comparable to the PNRC (Brown et al., 2000). Thus, the trafficking pathways involved in regulation of directed epithelial cell migration differ from that of cells migrating singularly, further emphasising the need to examine vesicle trafficking during collective epithelial cell migration.

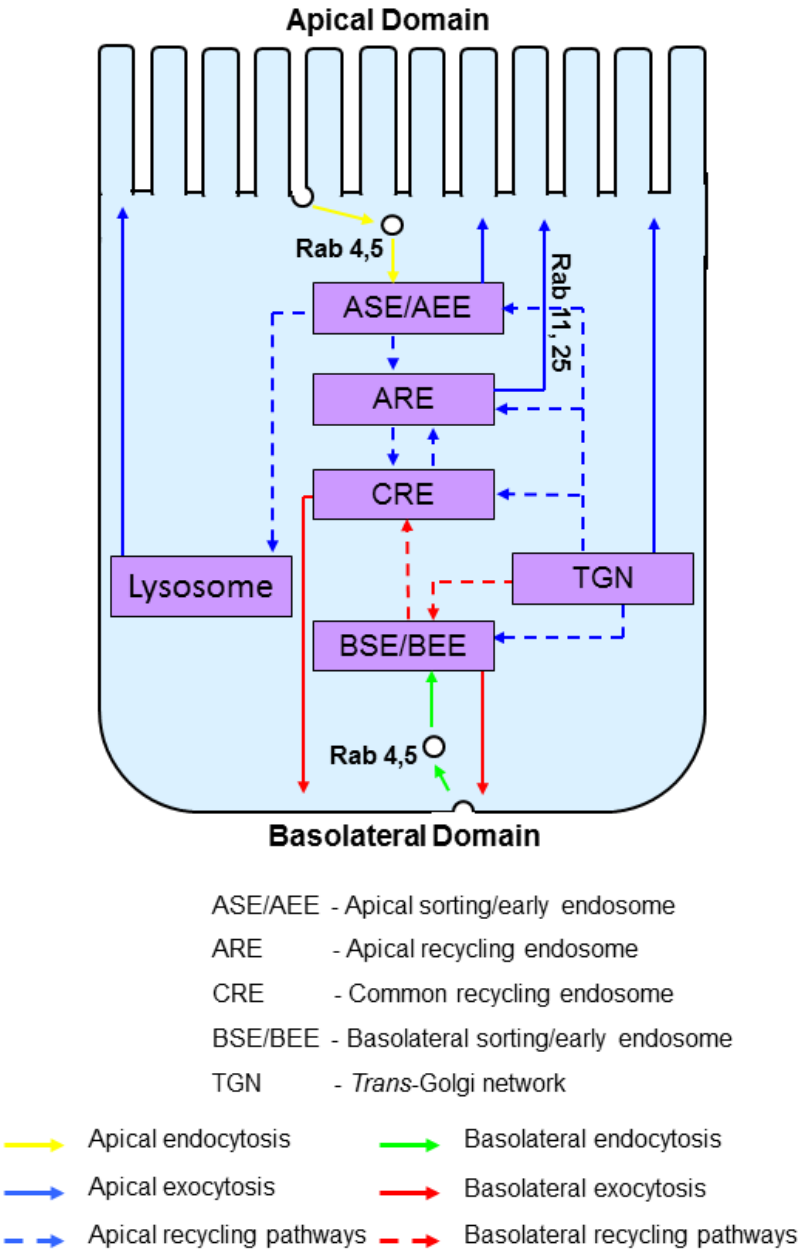

Figure 1.6. Vesicle trafficking pathways in polarised MDCK cells. Diagram demonstrating vesicle trafficking pathways in polarised MDCK cells.

1.5 A role for vesicle trafficking in cell migration

Vesicle trafficking has been shown to be critical in regulation of cell migration, which could be orchestrated by regulation of several processes including regulation of signalling and correct protein targeting (Mukherjee, Tessema, & Wandinger-Ness, 2006). Recently, vesicle trafficking has been suggested to aid regulation of cell migration via several mechanisms.

One such mechanism is through regulation of FAs. As described previously, FA assembly and disassembly is vital for efficient cell migration. An important component of FAs are integrins. Integrins are hetero-dimeric complexes, which in their active state bind to immobilised ligands in the ECM and are mechanically coupled to the actin cytoskeleton (Zamir & Geiger, 2001). Integrins play a pivotal role in adhesion and have emerged as an important mechanism for controlling cell motility in several models (Caswell & Norman, 2006). Vesicle trafficking has the potential to modulate cell migration through trafficking of integrins (Caswell et al., 2007; Roberts et al., 2001). Other ways in which vesicle trafficking may regulate cell migration is through transport of lipids to facilitate membrane extension (Bretscher, 1996), trafficking of receptors for soluble ligands (e.g. chemoattractants) (Zieske et al., 2001) and v-SNAREs (proteins which are incorporated into vesicles which enable vesicle fusion at target membranes) introduced into the plasma membrane following vesicle fusion (Gerst, 1999). Vesicle trafficking may play a role in cell motility by regulation of a range of mechanisms. However, the exact trafficking pathways involved in regulation of cell migration are unclear and are further complicated by conflicting opinions on the function of each pathway during polarisation and

steady-state migration. This inconsistency may be due to cell specific variances, altering migratory stimuli (chemotaxis versus loss of contact inhibition) and differing assay systems, highlighting the requirement for analysis of several trafficking pathways within a single migratory model.

1.6 Polarised trafficking in cell migration

Although several roles for vesicle trafficking in cell migration have been hypothesised, the precise mechanistic linkages between the two processes are not clear. The longstanding “back to front” hypothesis proposes transport of cell adhesion molecules from the rear of a motile cell to the front (Sheetz et al., 1999) (Figure 1.7A), whilst it has also been suggested that internalisation of lipid occurs throughout the cell body but exocytosis is polarised to the leading edge (Figure 1.7B) (Bretscher, 1984). Additionally, polarised trafficking of receptors to soluble ligands has been connected with cell migration and recycling during chemotaxis (Figure 1.7C) (Bailly et al., 2000; Hopkins et al., 1994).

Several receptors for soluble ligands have been demonstrated to cycle between the cell-surface and endosomal compartments, including the epidermal growth factor receptor (EGFR) (extensively reviewed by Husnjak & Dikic, 2006) and the insulin receptor (Kublaoui, Lee, & Pilch, 1995). Bailly et al., (2000), examined polarised trafficking of EGFR during chemotaxis in an EGF gradient. Live cell imaging of EGFR-GFP in MTLn3 adenocarcinoma cells demonstrated increased EGFR-containing vesicles towards an EGF source, potentially due to polarised internalisation at the leading edge. Later work by

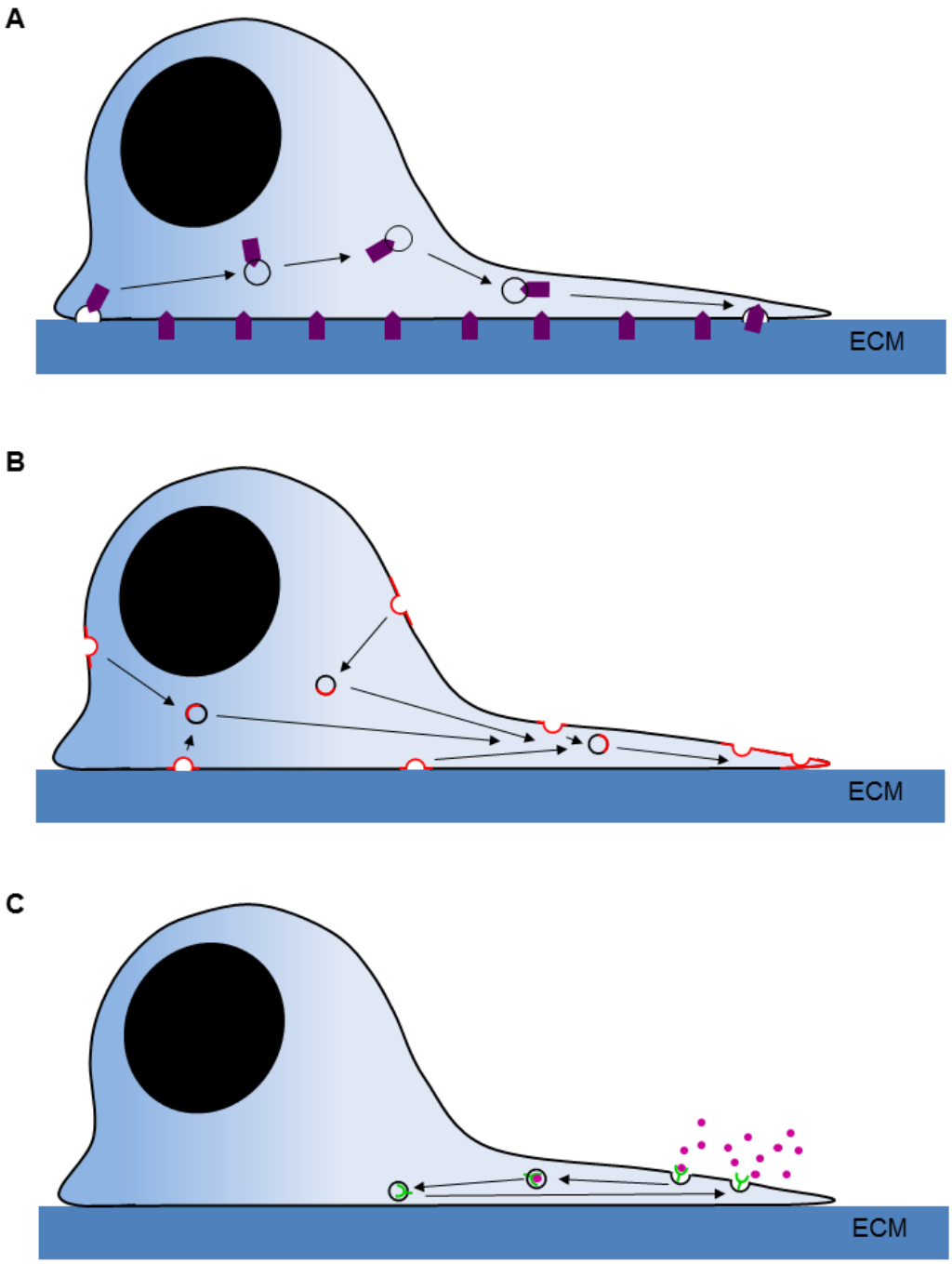

Figure 1.7. Three proposed mechanisms for polarised vesicle trafficking. (A) Internalisation and transport of cell-adhesion molecules from the rear of a motile cell to the front. (B) Internalisation of bulk membrane during plasma-membrane lipid trafficking to the leading edge. (C) Receptor recycling during chemotaxis.

Zhou et al., (2007), utilised cerebellar granule precursor cells undergoing migration in a chemotactic gradient of brain-derived neurotrophic factor (BDNF), to identify polarised trafficking of the BDNF receptor TrkB. They identified asymmetrical distribution of TrkB containing endosomes to areas where BDNF concentration was highest (Zhou et al., 2007). Thus, evidence does suggest that some receptors do undergo polarised trafficking during chemotaxis, however not all receptors show the same behaviour. For example in the leukaemia cell line PLB-985, undergoing chemotaxis towards formyl-methionyl-leucyl-phenylalanine (fMLP), no alteration in distribution of the complement component C5a receptor was observed during either generation of a motile phenotype or migration (Servant et al., 1999). Evidently, receptors to soluble ligands represent one cargo which may be subject to polarised trafficking during cell migration, another are the FA components integrins.

Work from the laboratory of Jim Norman suggests specific integrin heterodimers undergo endocytosis in the middle to front regions of the migrating cell. Potentially these internalised integrins may be transported to the leading edge in a polarised manner, where they can form new FA complexes (Caswell & Norman, 2006). This hypothesis is further supported by the increased localisation of CME to middle to front regions of migrating MDCK cells (Rappoport & Simon, 2003) and observations of β_1 integrin undergoing CME during FA disassembly (Ezratty et al., 2009). However it must be noted, work in the MDCK cell line has identified a minimal role for dynamin-dependent, CME or caveolar endocytosis in regulation of FAs during cell migration (Fletcher et al.,

2012). This suggests integrin endocytosis and trafficking may be cell line specific, dependent on the heterodimer studied or subject to alteration dependent on migratory stimulus.

Additionally, work from the Bretscher lab has suggested the importance of polarised delivery of lipids to the leading edge as a means of facilitating membrane extension (Bretscher, 1984; Bretscher, 1996). Several other groups have tested this hypothesis by examining rearward membrane flow. Rearward flow is a process where extensive addition of membrane to the leading edge should displace adjacent membranes leading to rearward flow of membrane from the lamellipodial region. This process has been observed in migrating chick dorsal root ganglion cells (DRGs) where the trajectories of beads anchored to the plasma membrane were measured as a means of quantifying membrane extension (Dai & Sheetz,1995). However, similar experiments in randomly migrating Leukocytes did not find evidence of rearward flow (Lee et al. 1990).

1.7 Vesicle trafficking in differing cell lines

Variations between different cellular models is an important factor when examining cell migration, as there are a several types of cell motility as well as a wide variety of migratory stimuli. There are two main types of cell motility; single cell and collective migration. These categories can then be further divided into two types of single cell migration (amoeboid or mesenchymal), or in collective migration can be divided into cell sheets, strands, tubes or clusters (Friedl, 2004). Different cell types exhibit different migratory strategies; for

example MDCK cells migrate collectively, leukocytes undergo amoeboid motility (Friedl, Borgmann, & Brocker, 2001), whilst fibroblast cells migrate in a mesenchymal manner (Grinnell, 1994). Moreover, cells can alter migratory strategy such as during EMT when epithelial collective migration is lost and the cells develop a more mesenchymal migratory phenotype (Thiery, 2002). Migratory behaviour will also vary dependent upon the type of motility being studied i.e. planar migration vs. invasion through matrix. These migratory mechanisms are likely to require different regulation, therefore, the role of vesicle trafficking in regulation of cell migration may vary depending upon cell type, preventing extrapolation of findings onto other cell lines. For example, cells such as the rapidly migrating fish keratocytes have a differing migratory morphology and mechanism in comparison to cells such as the MDCK cell line. Fish keratocytes migrate individually at 30μm/minute (Schwab, 2001), whilst MDCK cells migrate collectively at approximately ~20μm/hr (Fletcher et al., 2012). The fish cells exhibit a crescent shaped morphology due to lamellipodia extending halfway around the cell body (Kucik, Elson, & Sheetz, 1990), whist MDCK cells maintain cell-cell contacts and form a triangular polarised morphology with a broad leading lamella (Rappoport & Simon, 2003). These cell specific variances are likely to require highly different regulatory mechanisms e.g. in keratocytes FA turnover is likely to be more rapid than in motile MDCK cells, therefore integrin recycling may occur via a faster pathway than in MDCK cells, or trafficking may be more localised. Evidently, the function for vesicle trafficking in regulation of cell migration in these cell lines will vary. However, factors such as cell adhesion molecule expression level, differing

requirements for actin polymerisation and actomyosin contraction are also likely to be responsible for differences in migratory phenotype between cell lines.

1.8 Clathrin-mediated endocytosis

CME is an internalisation pathway which has been widely implicated in functioning in regulation of epithelial cell migration via endocytosis of numerous receptors to chemoattractants and cell adhesion molecules (Chao & Kunz, 2009; Ezratty et al., 2009; Rappoport & Simon, 2009; Sturge, Hamelin, & Jones, 2002). Thus, this pathway may be integral in regulation of cell motility (Sheetz et al., 1999). Yet, experiments to determine the function of CME and the extent to which it is polarised during cell migration have been difficult to integrate into a cohesive understanding.

One of the first investigations into the potential for polarised CME was performed in 1983 by Mark Bretscher (Bretscher, 1983). Distribution of coated pits on the dorsal surface of so-called “giant” HeLa cells was measured by electron microscopy and a non-polarised distribution was observed as cells underwent random spreading. Conversely, several studies have been performed which demonstrated polarisation of CME during cell migration (Damer & O'Halloran, 2000; Davis et al., 1982; Kamiguchi et al., 1998; Nishimura & Kaibuchi, 2007; Rappoport & Simon 2003; Samaniego et al., 2007). However, the domain to which it is polarised has not always been consistent from study to study.

Investigations in the early 1980s identified polarised distribution of CCPs in chemotactic neutrophils. CCPs were excluded from the lamellipodium and instead localised towards the uropod (a trailing non-adherent projection) (Davis et al., 1982). Similar observations were reported in T-lymphocytes undergoing random migration (Samaniego et al., 2007). Confocal microscopy demonstrated co-localisation of clathrin light chain with AP2 and transferrin at the uropod and away from the leading edge (Samaniego et al., 2007). This rearwards polarisation was also observed in *Dictyostelium* cells, where transient recruitment of GFP-tagged clathrin heavy chain was observed at the trailing edge (Damer & O'Halloran, 2000). Similarly CME of the adhesion molecule L1 was shown to occur preferentially at the cell rear and centre of chick DRG growth cones (Kamiguchi et al., 1998).

However, this rearwards CME localisation has not been observed in other cell lines. Two recent studies utilising epithelial-derived cells have challenged the view that endocytosis is polarised to the rear of motile cells. Total-internal reflection fluorescence (TIRF) microscopy enables selective excitation of fluorophores 100nm above the glass coverslip allowing imaging of the adherent plasma membrane. Using the TIRF imaging platform Rappoport and Simon (2003), identified clathrin light chain, dynamin2aa, and the transferrin receptor excluded from the cell rear and localised towards the front of MDCK cells during wound healing (Rappoport & Simon, 2003). Moreover, the clathrin adaptor AP2 was found to be polarised towards the leading edge of HeLa cells during wound healing assays (Nishimura & Kaibuchi, 2007).

Evidently, there does appear to be a high degree of variability to the domain to which CME is polarised. This is potentially due to differing cell lines, migratory stimuli as well as experimental differences. For example in research by Bretscher et al., (1983), analysis was performed on the non-adherent plasma membrane of non-motile cells. This is important as regions where polarised endocytosis of cell adhesion molecules might be expected to arise, i.e. the adherent plasma membrane, were not measured. This was also the case in studies where rearwards polarisation of CME was demonstrated to occur (Davis et al., 1982; Samaniego et al., (2007); Damer & O'Halloran, 2000). In observations in neutrophils undergoing chemotaxis, analysis was performed on horizontal EM sections (the non-adherent plasma membrane) (Davis et al., 1982). Whilst the uropod and "neck region" of T-lymphocytes studied by Samaniego et al., (2007) is a trailing projection which is non-adherent. Conversely, in studies where TIRF microscopy was employed to observe CME at the adherent plasma membrane (Rappoport & Simon, 2003; Nishimura & Kaibuchi, 2007), CME localisation was not observed in the non-adherent plasma membrane, potentially missing polarised CME in dorsal membranes. Therefore, to build a more cohesive model of polarised CME during cell migration the localisation of CME in the entire plasma membrane should be measured.

1.9 Caveolar endocytosis

The exact role for caveolar endocytosis during directed migration has been widely debated, and is disputed by several groups. Initial studies which utilised

overexpression of caveolin1 demonstrated inhibition of lamellipodial extension and migration in the MTLn3 carcinoma cell line (Zhang et al., 2000), thus the authors concluded caveolin1 functioned as a negative regulator of cell migration. Yet later studies examining invasion of human ECs into collagen I gel, found inhibition of caveolar internalisation by the cholesterol sequestering agent filipin, decreased migration and invasion (Galvez et al., 2004). However, these results may be non-specific as filipin induced cholesterol depletion may effect plasma membrane architecture and function as well as caveolar endocytosis (Kwik et al., 2003). Importantly, these findings were replicated in caveolin1 deficient mouse embryonic fibroblasts during wound healing (Grande-Garcia et al., 2007). The fibroblasts displayed increased migration speed, poor directionality, a non-polarised morphology and an irregular cytoskeleton. These migrational and cytoskeletal defects were suggested to be due to caveolin1 regulation of Src kinase and effectors Rho, Rac and CDC42 GTPases. However, recent research may explain the contradictory results observed when examining the role of caveolar endocytosis and cell migration (Zhang et al., 2000; Galvez et al., 2004; Grande-Garcia et al., 2007), with work by Vassilieva et al., (2008) suggesting caveolin1 overexpression exerts a dominant negative effect.

Evidently caveolar endocytosis does have an important function in regulation of cell migration, the exact role for caveolar endocytosis has not been identified. Although caveolin1 may regulate cell migration through interactions with the Rho family of GTPases (Grande-Garcia et al., 2007), an alternative way in which caveolar endocytosis may regulate cell migration is via endocytosis of

specific integrin heterodimers and receptors for soluble ligands as demonstrated in table 1.1 (Caswell & Norman, 2006; Samaniego et al., 2007; Zhu et al., 2005).

Interestingly, like CME, caveolar endocytosis has been shown to be polarised during cell motility, again with conflicting observations recorded. The majority of studies examining caveolar endocytosis in cell migration have been performed in ECs. ECs have a high abundance of caveolae making them an ideal model in which to examine caveolar endocytosis (Frank et al., 2003). Moreover, motility of ECs is integral during angiogenesis, making identification of the role of caveolar endocytosis during EC migration particularly important (Isshiki et al., 2002; Severs, 1988). Therefore, several studies have been performed examining polarised caveolar endocytosis during EC migration. One of the first demonstrations of polarised caveolin1 distribution during cell migration was observed in ECs undergoing directed migration during wound healing. In cells migrating on a 2D surface, immunofluorescence showed endogenous caveolin1 was localised to the cell rear (Isshiki et al., 2002). Moreover, further analysis of polarised caveolar endocytosis during EC migration was performed in studies by Parat, Anand-Apte, & Fox (2003). This group utilised confocal and electron microscopy to verify the increased presence of caveolae polarised to the rear of ECs during two-dimensional wound healing. They also described non-membrane localised polarisation of caveolin1 to anterior protrusions during EC invasion through pores in a Boyden chamber in cells undergoing chemotaxis towards a fibroblast growth factor (FGF) source. This study elegantly demonstrated how alteration of migratory mechanisms can affect the function

Table 1.1 Integrin internalisation and recycling pathways. (Table adapted from Fletcher and Rappoport, 2010).

Integrin	Internalisation	Recycling Pathway
$\alpha?\beta_1$	Dynamin-dependent (Ng et. al., 1999)	Rab11 (Powelka et. al., 2004)
$\alpha_5\beta_1$	Clathrin-independent (Altankov & Grinnell 1995) Caveolin1-dependent (Shi & Sottile 2008)	Rab11 (Roberts et. al., 2001;Roberts et. al., 2004;Skalski & Coppolino 2005;Tayeb et. al., 2005)
$\alpha_2\beta_1$	Caveolae (Upla, et al., 2004) Pak1 dependent (Karjalainen et. al., 2008)	-
$\alpha_6\beta_1$	-	Rab11 (Roberts et. al., 2004)
$\alpha_6\beta_4$	-	Rab11 (Yoon, Shin, & Mercurio, 2005)
$\alpha_L\beta_2$	Filipin sensitive (Caswell & Norman 2006)	Rab11 (Caswell & Norman 2006)
$\alpha_v\beta_3$- unstimulated	NXXY motif not req (Woods et. al., 2004) Clathrin coated pits (Sancey et. al., 2009)	Rab11 (Roberts et. al., 2001;Roberts et. al., 2004)
$\alpha_v\beta?$	Clathrin coated pits (Upla et al, 2004)	-
$\alpha_v\beta_6$	Clathrin coated pits (Ramsay et. al., 2007)	-
$\alpha_v\beta_3$- PDGF stimulated	-	Rab4 (Roberts et. al., 2001;Woods et. al., 2004)
$\alpha_v\beta_5$	Clathrin coated pits (De Deyne et. al., 1998)	-
β_1	Dynamin-dependent, clathrin dependent (Chao and Kunz 2009; Ezratty et al., 2009)	-
β_3 – PDGF stimulated	Macropinocytosis (Gu et al., 2011)	-

and localisation of a specific endocytic pathway. Furthermore, the group also performed important control experiments observing effects on caveolae distribution when factors such as cell culture technique, chemotactic stimulus, gravitational forces and substrate were altered. On the contrary, work by Galvez et al., 2005 again employing ECs observed co-localisation of caveolin1 with the matrix metalloproteinase MT1-MMP and $\alpha_v\beta_3$ integrin within dynamic membrane protrusions, therefore polarisation away from the cell rear may exist (Galvez et al., 2004).

Clearly, evidence from the aforementioned studies implicates an important function for the role of caveolar endocytosis during EC migration as well as the potential for caveolar endocytosis to be polarised to a specific domain within the plasma membrane. However it must be noted, that these studies observed caveolae localisation rather than actual caveolar endocytosis events. Caveolae may have functions other than to internalise cargo, such as in regulation of membrane tension (Sinha et al., 2011). Thus the polarised localisation of caveolae observed within the previous studies may not represent polarised caveolar endocytosis, instead it might indicate a requirement for a polarised caveolae localisation to regions of increased plasma membrane tension.

Caveolae have an important function during cell migration yet the extent to which caveolar endocytosis is polarised during migration is not fully understood in non-EC derived cell lines. The function of caveolar endocytosis is of particular importance during epithelial cell migration as intercellular and cell-ECM adhesion molecules undergo extensive reorganisation during collective migration. One way in which caveolae may function in regulation of epithelial

cell migration is through modulation of adhesion complexes; caveolar endocytosis has been demonstrated to regulate internalisation of integrins and TJ components (Upla et al., 2004; Marchiando et al., 2010). Therefore, both the role of caveolar endocytosis and its potential polarisation during epithelial wound healing requires further investigation.

1.10 Endosomal recycling

Within the last two decades, many studies have focussed on the role of vesicle trafficking in regulation of cell migration; however the extent to which vesicle trafficking pathways are polarised during cell migration has not been as widely examined. Internalisation and recycling of cargo important for cell migration may be a way through which vesicle trafficking may regulate cell migration. For example polarised recycling of chemoattractant receptors during processes such as detection and response to chemotactic signals may function to maintain cell migration (Zhou et al., 2007), whilst motile force could be regulated by recycling of cell adhesion molecules (Roberts et al., 2001).

One of the key regulators of vesicle trafficking and recycling are members of the Rab-GTPase family. They function to regulate several aspects of cargo trafficking acting via recruitment of effector proteins, they ensure correct vesicle targeting, cargo selection, vesicle budding, motility of vesicles, uncoating, docking and fusion (reviewed extensively in Subramani & Alahari, 2010). Of the 51 known Rab family members, the ones of particular interest to this study are Rab4 and Rab11, both are associated with vesicle trafficking events which

intersect with the plasma membrane. Rab4 is localised to the EE compartments and is required for cargo sorting and rapid recycling from EEs to the plasma membrane (Daro et al., 1996; McCaffrey et al., 2001). Expression of dominant negative Rab4(S22N) is a tool which can be utilised to inhibit Rab4-mediated recycling and has been used widely. This mutant has been demonstrated to decrease recycling of the transferrin receptor and affect degradation of EGF receptors in HeLa cells (McCaffrey et al., 2001). Moreover increased localisation of transferrin receptor to perinuclear compartments was observed, potentially due to diversion of cargo to the Rab11-mediated pathway (Figure 1.5). However, this hypothesis was not proven as the perinuclear compartment identified was not confirmed to be that which is regulated by Rab11 (Figure 1.5).

The exact function of Rab4-mediated recycling in cell migration is unknown, yet its significance is becoming clear. In migrating NIH3T3 fibroblasts, inhibition of Rab4 by expression of Rab4(121I) increased migratory tortuosity in wound healing studies, decreased $\alpha_v\beta_3$ integrin trafficking but did not affect migration speed (White, Caswell, & Norman, 2007). These findings suggest Rab4-mediated trafficking may be required for cell spreading and polarised trafficking of $\alpha_v\beta_3$ to the leading edge (Roberts et al., 2001; Woods et al., 2004). Due to the importance of correct integrin function during cell migration, regulation of adhesion and signalling; the directional effects observed upon inhibition of Rab4 may be due to alterations in $\alpha_v\beta_3$ trafficking (White, Caswell, & Norman, 2007). The authors suggested a model where Rab4-mediated recycling could regulate directionality by re-sensitising $\alpha_v\beta_3$ to ligand (Danen et al., 2005; White,

Caswell, & Norman, 2007). Yet there are numerous other mechanisms through which Rab4 recycling may regulate cell migration either directly or by affecting downstream effectors.

An alternative cargo recycling pathway of interest to this study is the Rab11-mediated trafficking pathway (Figure 1.5). Rab11-dependent recycling has been demonstrated to play an important role in regulation of cell migration. Initial findings by Mammoto et al., 1999, found expression of a dominant negative mutant of Rab11, Rab11(S25N) decreased MDCK epithelial cell migration (Mammoto et al., 1999). In later studies, expression of this mutant in the PtK1 epithelial cell line also led to an alteration in migratory phenotype (Prigozhina & Waterman-Storer, 2006). PtK1 cells expressing Rab11b(S25N) displayed an increased frequency of directional changes when cells underwent random migration in comparison to control cells (Prigozhina & Waterman-Storer, 2006). Furthermore, an augmented number of membrane protrusions were observed, as well as difficulty in retraction of the cell rear (Prigozhina & Waterman-Storer, 2006). These observations were replicated during directed migration in a wound healing assay, and suggest an important role for Rab11 in regulation of both random and directed cell motility (Prigozhina & Waterman-Storer, 2006).

As demonstrated in the aforementioned studies, Rab11-mediated recycling plays an important role in cell migration. One way in which trafficking via the Rab11-dependent pathway may regulate cell migration is through trafficking of specific integrin heterodimers (Roberts et al., 2001; Yoon, Shin, & Mercurio, 2005). Work from the laboratory of Jim Norman demonstrated in NIH3T3

fibroblasts that expression of Rab11(N124I) significantly reduced recycling of both $\alpha_v\beta_3$ and $\alpha_5\beta_1$ under basal conditions, and demonstrated co-localisation between PNRC localised Rab11 and $\alpha_v\beta_3$ integrin (Roberts et al., 2001). Further evidence supporting a function for Rab11 in regulation of integrin trafficking was performed in CHO cells treated with fMLF (to induce membrane ruffling), where a decreased localisation of α_L/β_2 integrin to lamellipodia was observed upon expression of Rab11(S25N) (Fabbri et al., 2005). This group also identified a high level of co-localisation between Rab11 and α_L/β_2 in polymorphonuclear cells and found expression of Rab11(S25N) led to accumulation of α_L/β_2 in the PNRC (Fabbri et al., 2005). Therefore, one hypothesis which can be formed from the work of Fabbri et al., 2005 suggests that α_L/β_2 is transported via the Rab11-dependent recycling pathway under both non-motile and motile conditions and that during cell migration Rab11-mediated trafficking is required for polarised delivery of α_L/β_2 to the leading edge via a Rab11-mediated recycling pathway (Fabbri et al., 2005).

Additionally, another epithelial specific member of the Rab11 GTPase family, Rab25 exists (Goldenring et al., 1993). Rab25 has not been widely studied, however several findings have linked Rab25 to regulation of cell migration, correlating augmentation of Rab25 expression with increased invasiveness *in vivo* and *in vitro* (Caswell et al., 2007; Cheng et al., 2004). Yet, in other cell types (A2780 ovarian carcinoma cells) overexpression of Rab25 had no effect on migration speed or directionality (White, Caswell, & Norman, 2007). Although little is known of the function for Rab25 in cell migration it has been demonstrated to be important for trafficking of cargo via the apical EE,

regulating apical to basolateral transcytosis (Figure 1.6) in polarised MDCK cells (Casanova et al., 1999; Tzaban et al., 2009). Evidently Rab25 has a function in regulating vesicle trafficking in epithelial cells yet whether this trafficking pathway is required during collective epithelial cell migration is not known, however it is a question which requires further study.

Undoubtedly vesicle trafficking plays a significant role in regulation of cell migration. However the extent to which polarised endocytosis and recycling is required during cell migration is less well understood. Most of our current understanding of the function for polarised vesicle trafficking during cell motility is based upon data obtained from randomly migrating fibroblast-derived cell lines, with less evidence available for the function of polarised trafficking in other cell types and cells undergoing directed migration. One of the most widely utilised tools in the study of trafficking is the iron-binding protein transferrin which binds to the transferrin receptor and is recycled via several endosomal compartments including the EE and the PNRC. Transferrin is easily labelled with fluorescent probes and the ^{125}I isotope making it ideal for use in both imaging and biochemical based trafficking assays. In studies by Hopkins et al., 1994, randomly migrating chick embryonic fibroblasts were used along with pulse-chase transferrin recycling, live cell time-lapse microscopy and EM imaging of immuno-gold-labelled transferrin receptors, to identify polarised trafficking of both transferrin and its receptor via a juxtanuclear compartment to the leading lamella (Hopkins et al., 1994).

There is clearly evidence suggesting some proteins do undergo polarised recycling during cell motility. However the majority of research has been performed examining polarised trafficking of cell adhesion molecules as means through which cell migration and adhesion can be regulated. Work by Laukaitis et al., 2001 demonstrated polarised recycling of α_5-GFP integrin containing vesicles from a perinuclear region to the base of the lamellipodia in randomly migrating WI38 fibroblast cells (Laukaitis et al., 2001). Although a polarised vesicular localisation of α_5-GFP was observed, the authors never performed fusion analysis to identify whether these α_5-GFP containing vesicles ever fuse with the leading edge to confirm true polarised trafficking of α_5 integrin. Also expression of exogenous α_5-GFP makes it is impossible to determine the proportion of α_5-GFP- containing vesicles undergoing recycling or secretion via the biosynthetic secretory pathway. Further evidence of polarised integrin trafficking was also observed in randomly migrating skeletal muscle fibroblasts where trafficking of β_1 integrin from the lagging edge into the cell body was seen (Palecek et al., 1996).

Although much work of the work examining polarised trafficking has been performed in migrating fibroblasts, studies in randomly migrating neutrophils have also provided evidence for polarised trafficking of cell adhesion molecules. Work from the laboratory of Frederick Maxfield in neutrophils undergoing chemotaxis towards fMLP demonstrated polarised recycling of the $\alpha_v\beta_3$ integrin heterodimer and α_5-integrin subunit (Lawson & Maxfield, 1995; Pierini et al., 2000). In both of these studies, calcium buffering was utilised to prevent integrin disassembly at FAs. During cell migration transient intracellular calcium

spikes can lead to FA disassembly (Giannone et al., 2002). Inhibition of these calcium spikes using the calcium chelating agent Quin 2 prevents detachment of integrins from their immobilised ligand (Lawson and Maxfield, 1995). In cells where intracellular calcium levels had been buffered a redistribution of $\alpha_v\beta_3$ integrin (Lawson & Maxfield, 1995) and α_5-integrin (Pierini et al., 2000) from the lamellipodia region to the cell rear was observed. Additionally in the latter study by Pierini et al., an endosomal recycling compartment localised behind the leading lamella was identified which was responsible for polarised α_5 recycling during polymorphonuclear neutrophil migration (Pierini et al., 2000). Although the accumulation of integrins at the cell rear and loss from the cell front may be indicative of back to front integrin trafficking, the techniques employed (although highly innovative) did not quantitatively measure polarised recycling (Lawson & Maxfield, 1995; Pierini et al., 2000).

Clearly, studies in both fibroblast- and neutrophil-derived cell lines propose a role for polarised recycling of cell adhesion molecules during cell migration. One hypothesis which can be formed from the aforementioned observations is that polarised trafficking of cell adhesion molecules regulates cell migration through polarised endocytosis of integrins (and potentially other FA components) at the cell rear as FAs undergo disassembly. This endocytosis is then coupled to a polarised endosomal recycling pathway leading to delivery of recycled integrins to the leading edge where they can be incorporated into newly formed FAs. This hypothesis would support a role for polarised trafficking in cell migration as it would facilitate detachment of the cell rear from the substrate but also aid in anchoring newly formed membrane protrusions at the

leading edge, aiding in cell motility. However, an important observation was made in the study by Palecek et al., (1996) which questions the relevance of cell adhesion molecule recycling in cell motility (Palecek et al., 1996). This study used an anti-β_1 antibody (validated to not affect adhesions) conjugated to photo-activateable caged carboxy-fluorescine to observe integrin dynamics in randomly migrating chick skeletal muscle cells. Fluorophores were selectively activated at the rear of migrating cells by UV light passing through a pin-hole to activate fluorophores within a 10µm circle at the adherent plasma membrane. They determined that approximately 80% of the total amount of photo-activated anti-β_1 bound integrin remained attached to the ECM in a trail behind the cells (Palecek et al., 1996). This would suggest that β_1-integrin undergoes a high level of biosynthesis during cell migration to replace β_1-integrin left attached to the substrate. This may indicate that a large proportion of intracellular β_1 integrin containing vesicles are actually derived from the biosynthetic trafficking pathway rather than recycling. This hypothesis may be supported by data from other laboratories where inhibition of protein biosynthesis has been shown to severely alter the migratory phenotype of motile fibroblasts (Bershadsky & Futerman, 1994; Prigozhina & Waterman-Storer, 2004).

As described in section 1.7 differences in migratory stimulus and cell line are factors which can affect polarised trafficking. Another factor which has been shown to influence polarised trafficking within a single model is the substrate upon which the cells migrate/are plated. Kamiguchi et al., (2000), demonstrated in chick DRG cells, that post-endocytosis the cell adhesion molecule L1 underwent polarised endosomal recycling in a manner dependent on substrate

(Kamiguchi et al., 2000). In cells plated on laminin, L1 was recycled locally to the distal axonal shaft and central domain of the growth cone. However L1 can function as both a ligand and a receptor, and homotypic L1-L1 interactions promote axonal growth *in vivo*. When DRG cells were plated on a chimeric protein made from the Fc region of human IgG and the extracellular domain of human L1, L1 trafficking was polarised to the peripheral zone (an actin rich lamellipodial and filopodial region). Therefore, this study demonstrates both polarised recycling of adhesion receptors during growth cone remodelling and the importance of cell substrate on polarisation of vesicle trafficking pathways.

Evidently, vesicle trafficking has an important function during epithelial cell migration (Mammoto et al., 1999, Prigozhina and Waterman-Storer, 2006), the extent to which vesicle trafficking is polarised during epithelial cell migration has not been well researched. As epithelial wound healing is such a physiologically important process, further research into the role of vesicle trafficking and the extent to which it is polarised during collectively motility is a question requiring further investigation.

1.11 Biosynthetic secretory pathway

The biosynthetic secretory pathway is a mechanism through which newly synthesised molecules are transported to the plasma membrane. Newly synthesised proteins are transported to the endoplasmic reticulum where they are correctly folded and undergo post-translational modification. They are then transported to the Golgi where they pass through the various cisternae and are

packaged into vesicles for secretion at the *trans*-most cisternae (Figure 1.5). Several hypotheses have been made that suggest a function for exocytosis of newly synthesised biosynthetic cargo in cell migration, such as supplying membrane to the leading edge for pseudopod formation and in regulation of membrane tension and surface area (Traynor & Kay, 2007).

Interest in polarised post-Golgi trafficking arose in 1962, when studies performed in giant HeLa cells not undergoing directed motility, demonstrated exocytosis polarised to the cell circumference (Marcus, 1962). This report followed the expression and localisation of the Myxovirus Hemagglutinin (HA) protein over time through microscopy, analysing binding of red blood cells to Myxovirus infected giant HeLa cells. Although RBC binding to HA was eventually observed across the entire surface of infected cells, at early time points it selectively occurred at the cell periphery. This was followed subsequently in 1981, when re-orientation of the Golgi between the nucleus and leading edge was observed in migrating ECs (Gotlieb et al., 1981). In later studies, polarised secretion of labelled marker proteins was directly observed in migrating cells. A temperature sensitive mutant of the vesicular stomatitis virus G-protein (VSVG) was employed in a study performed in normal rat kidney (NRK) fibroblast cells (Bergmann, Kupfer, & Singer, 1983). In these experiments, VSVG was found towards the leading edge of fixed NRK cells in a wound healing assay. Importantly, by performing immunocytochemistry on cells without permeabilisation, cell-surface VSVG was selectively labelled, unequivocally demonstrating plasma membrane association of proteins post-exocytosis (Bergmann, Kupfer, & Singer, 1983). Recent work has supported

these findings in live cells using TIRF microscopy (Schmoranzer, Kreitzer, & Simon, 2003).

Further, evidence highlighting the importance of Golgi localisation and secretion in both generation of a polarised phenotype and steady-state migration has recently been identified (Yadav, Puri, & Linstedt, 2009). This study examined the function of golgins (proteins localised to the cytoplasmic surface of Golgi membranes and implicated in Golgi positioning) during wound healing in HeLa cells. The group found siRNA targeting golgin prevented polarised secretion to the wound edge and an inability of the cells to polarise and effectively heal the scratch wound. This evidence certainly implies synthesis of protein and its polarised post-Golgi secretion as an important factor in cell migration. Work by Bershadsky and Futerman, 1994 examining the role of post-Golgi secretion in cell migration used Brefeldin A to disrupt the Golgi apparatus (Bershadsky & Futerman, 1994). Brefeldin A treatment of Swiss 3T3 fibroblasts inhibited polarisation, cell migration, affected membrane protrusion and disrupted the actin cytoskeleton (Bershadsky & Futerman, 1994). However, Brefeldin A causes non-specific effects, such as tubulation of peripheral organelles such as the EE (Klausner, Donaldson, & Lippincott-Schwartz, 1992), indicating changes in migratory phenotype may not solely be due to biosynthetic pathway inhibition. New insights into post-Golgi trafficking found post-Golgi secretion is dependent upon protein kinase D (PKD) for vesicle fission from the Golgi (Liljedahl et al., 2001; White, Caswell, & Norman, 2007). Blocking this biosynthetic secretory pathway by expression of a dominant negative mutant (PKD(K618N)) inhibited lamellipodial activity at the leading edge, retrograde flow, and decreased motility

in Swiss 3T3 fibroblasts (Prigozhina & Waterman-Storer, 2004). However it must be noted that PKD has also been implicated in regulation of endosomal recycling via the Rab4-dependent trafficking pathway (Woods et al., 2004). Therefore studies where perturbations on PKD activity have been made may also be affecting Rab4-dependent trafficking. None the less, there are clear indications of a function for the biosynthetic pathway in generation of a polarised phenotype and persistent migration. Obviously, identifying a specific role for the biosynthetic secretory pathway is complex, as inhibition of this pathway affects trafficking of numerous newly synthesised proteins. However the biosynthetic secretory pathway is likely to play an important role in cell migration, conversion of proto-oncogenes to oncogenes by genetic mutations can lead to up-regulation of proteins such as matrix metalloproteinases and growth factor receptors in some tumour cells, facilitating increased dissemination and metastasis *in vivo* (Friedl and Wolf, 2003).

1.12 Focal adhesions and cell migration

Adhesion of cells to an ECM is fundamental for many physiological processes, but is particularly relevant for effective cell migration. Adhesion of the adherent plasma membrane of cells to the ECM occurs via FAs. FAs are multi-protein complexes, their composition varying dependent upon external cues, however only a few proteins will be discussed here (Petit & Thiery, 2000). A key component of FAs are integrins. Integrins are dimers of α and β – transmembrane protein subunits (Figure 1.8). Both α and β subunits have large extracellular domains that participate in binding to immobilised ligands in protein

substrates (e.g. fibronectin, laminin, collagens, vitronectin) in the ECM, and a small cytoplasmic domain that anchors the protein to the cytoskeleton through various scaffolding proteins.

Once the cytoskeleton is mechanically coupled to the ECM, integrins are capable of bi-directional signalling (known as inside-out and outside-in) allowing transmission of biochemical and mechanical signalling at the plasma membrane facilitating cell functions such as adhesion, division, growth and differentiation (Calderwood, 2004). Inside-out signalling is stimulated by many agents including protein kinase C (PKC), phosphoinositide-3-kinase, chemoattractants and calcium ionophores (reviewed in Kolanus & Seed, 1997). Once activation signals are received, talin (an actin binding protein that links integrins to the cytoskeleton (Gingras et al., 2010; Goult et al., 2009) binds to the cytoplasmic tail of the β-subunit, mediating a conformational change that increases the affinity of the integrin to its ECM ligand, facilitating increased adhesion (Calderwood, 2004).

Additionally, integrins are capable of outside-in signalling. This occurs when an integrin binds to its ligand in the ECM and initiates clustering (Ingber, 2003). At this point, the inside-out and outside-in signalling pathways converge, and formation of large multi-protein FAs is initiated. Initially, talin is recruited to individual integrins and small integrin clusters to form nascent FAs. As a link between the ECM and cytoskeleton has been made, these nascent FAs aid in mechanosensation of the external environment, and depending upon tension, can begin to mature into larger FAs by recruitment of signalling molecules and scaffolding proteins (Ingber, 2003). Further recruitment of scaffolding proteins

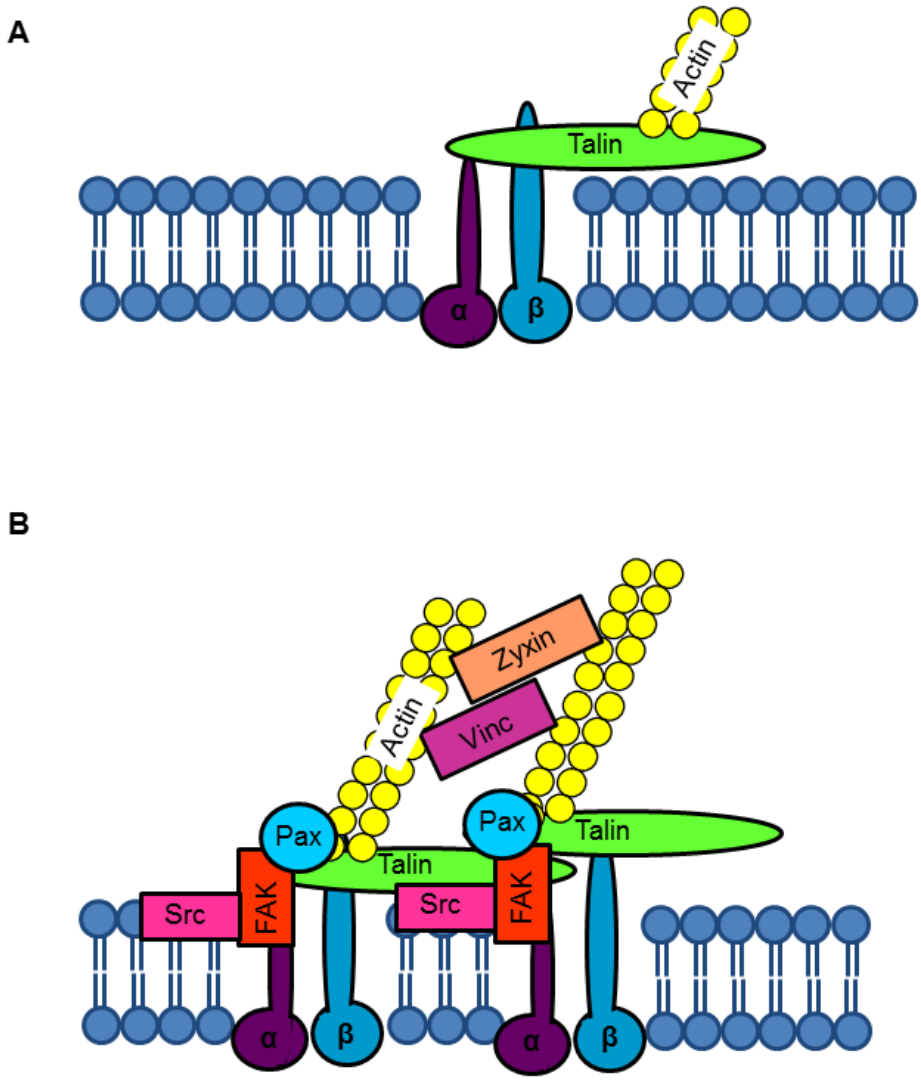

Figure 1.8. Focal adhesion structure. (A) Diagram showing formation of a nascent focal adhesion. (B) Shows the structure of a mature focal adhesion. FAK = focal adhesion kinase, Pax = paxillin and Vinc = vinculin.

such as paxillin forms additional links between integrins and the cytoskeleton (Mitra, Hanson, & Schlaepfer, 2005). This in turn leads to recruitment and phosphorylation of focal adhesion kinase (FAK) (Calalb, Polte, & Hanks, 1995). Phosphorylated FAK binds to another cytoplasmic scaffolding protein called vinculin that cross links actomyosin stress fibres, binding them to focal contacts (Pasapera et al., 2010). As contacts mature into FAs, further recruitment of actomyosin binding scaffolding proteins α-actinin and zyxin occurs (Figure 1.8) (Mitra, Hanson, & Schlaepfer, 2005). Members of the Src family kinases (SFKs) are also localised to FAs and are implicated in migration (Figure 1.8) (Li, Okura, & Imamoto, 2002). SFKs are known to be involved in regulating FA dynamics during cell migration and have been suggested to exert effects via phosphorylation of Src by FAK, which in turn mediates further phosphorylation of FAK (Calalb, Polte, & Hanks, 1995). This then leads to phosphorylation and recruitment of other scaffolding proteins (Huveneers & Danen, 2009).

During cell migration, focal complexes have been shown to assemble at the migrating front, and disassemble at the trailing edge, as the cell migrates. (Caswell, Vadrevu, & Norman, 2009; Lauffenburger & Horwitz, 1996; Valdembri et al., 2009). FAs are likely to function as traction points for the propulsive forces which move the cell body in the direction of migration (Webb, Parsons, & Horwitz, 2002). Nascent FAs are believed to function during rapid movement, whilst mature FAs are thought to aid in generation of contractile force by actomyosin based contractions (Webb, Parsons, & Horwitz, 2002).

Several mechanisms have been suggested for regulation of FA dynamics with particular focus on regulation of FA disassembly during cell migration. Three main mechanisms of FA disassembly have been suggested, as seen in Figure 1.9. Firstly, disassembly of FAs occurring at the cell rear and subsequent internalisation of FA components (Fig. 1.9a) (Chao & Kunz, 2009; Ezratty et al., 2009). Secondly FAs remaining tightly bound to the ECM are "ripped" out of the trailing edge of migrating cells (Fig.1.9b) (Palecek et al., 1996). Finally, a mechanism suggested by Ballestrem et al., 2001 where FAs undergo disassembly and passively diffuse away from the FA site (Fig 1.9c) (Ballestrem et al., 2001).

Reports from many groups have suggested a role for endocytosis as an integral factor in FA disassembly. The most widely studied FA protein used to observe FA dynamics are integrins. However, as can be seen in table 1.1, both internalisation and subsequent recycling pathways vary dependent upon the integrin α and β subunit composition. However, there is little research examining internalisation as a potential regulator of FA disassembly in migrating epithelial cells, with the majority of studies being performed in fibroblast derived cell lines. Recent studies from the laboratory of Gregg Gundersen suggest that clathrin is required for microtubule induced disassembly of FAs (Ezratty et al., 2009). Using siRNA techniques to knock-down clathrin, they found a significantly increased number of FAs when using vinculin as a marker for FAs (Ezratty et al., 2009). This group also found CME was responsible for internalisation of $\alpha_5\beta_1$ integrin. Using TIRF microscopy they identified recruitment of clathrin to sites of FAs during FA disassembly (phosphorylated

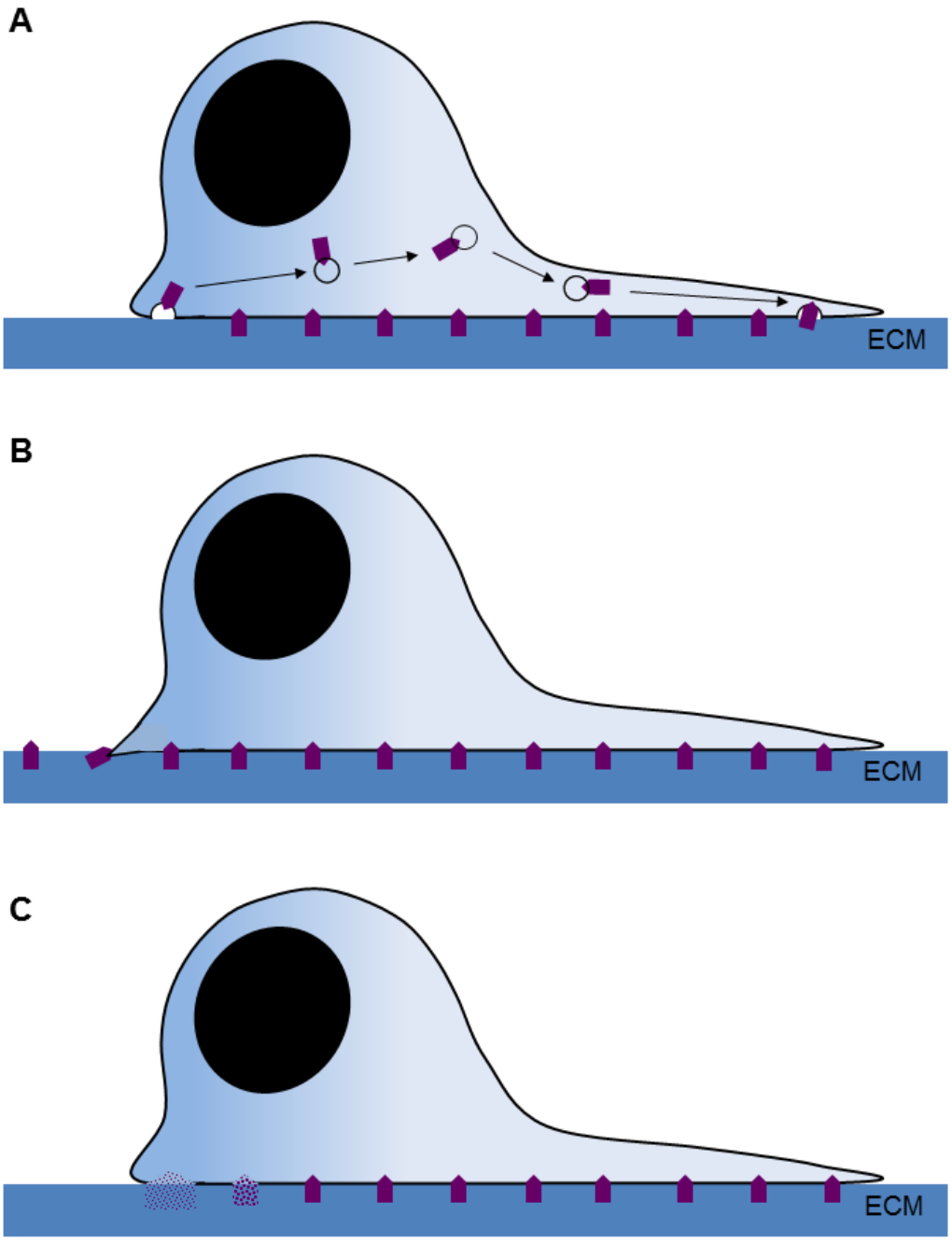

Figure 1.9. Mechanisms of focal adhesion disassembly. (A) Disassembly and internalisation of FAs at the cell rear and recycling to the cell front. (B) FAs remain bound tightly to the extracellular matrix and are pulled out of plasma membrane. (C) FAs undergo disassembly then passive diffusion through the plasma membrane.

FAK (pFAK) and GFP- β_1 were used as FA markers). These results could suggest FA disassembly occurs by internalisation of integrins via CME.

However it should be noted, in some of the studies the fibroblasts were not motile and in others migration was stimulated by wounding a confluent fibroblast monolayer. This is important as during migration you would expect to see increased co-localisation between CME and FAs due to increased FA turnover. Additionally, *in vivo* fibroblasts do not grow in monolayers therefore wounding a fibroblast monolayer is not representative of physiological fibroblast migration. Also the cells were serum-starved and treated with the microtubule depolymerising agent nocodazole, (to increase FA number and enable identification of potential co-localisation) which may affect FA dynamics even after nocodazole wash out. Yet, this study has been corroborated by Chao and Kunz, 2009 who also found internalisation of β_1 integrin and FA disassembly dependent upon CME in the human fibrosarcoma HT180 cell line undergoing chemotaxis towards foetal bovine serum (FBS) (Chao & Kunz, 2009). They also identified the GTPase dynamin2 as functioning in FA disassembly, suggesting a possible role for either dynamin-dependent internalisation in mechanical disassembly of FA complexes (Chao & Kunz, 2009). Moreover a function for CME in integrin endocytosis is supported by findings from Le Roy and Wrana et al., (2005), who identified the cytoplasmic domains of β-integrins contain two conserved NXXY motifs, a known sequence required for CME (Le & Wrana, 2005). This motif has been demonstrated to be important for internalisation of β_1-integrin (Pellinen et al., 2008).

Other internalisation pathways have been implicated in FA disassembly. Recent work by Gu et al., suggests that in NIH3T3 fibroblasts and MDA-MD-231 breast carcinoma cell lines stimulated with platelet derived growth factor (PDGF), β_3-integrin undergoes internalisation at the ventral cell surface via a circular dorsal ruffle. This indicates macropinocytosis may act as a possible FA internalisation mechanism (Gu et al., 2011).

Together these data show that internalisation of FA components such as integrins does occur in migrating cells and evidence described in section 1.10 confirms that both polarised and non-polarised endosomal recycling of integrins has an important function during cell migration. However none of these studies were performed in epithelial cells, thus the role of integrin trafficking as a mechanism through which collective epithelial migration is regulated needs further study.

1.13 Tight junctions, a role in cell migration

Cell-cell adhesion is important for many physiological processes, particularly in maintenance of epithelial linings, such as the epidermis and during tissue remodelling. Cell-cell adhesion is necessary for the assembly of coherent sheets of barrier forming-epithelial cells. Intercellular junctions undergo constant remodelling to regulate paracellular permeability, allow extrusion of apoptotic cells and incorporation of newly formed epithelial cells, whilst still maintaining barrier function.

Cell-cell junction remodelling is a key factor in wound repair. Upon formation of a wound, cellular junctions are severed at the site of injury. A transient increase in proliferation and migration occurs as cells undergo migration to repair the injury. As cell density increases, intercellular junctions are re-assembled (Perez-Moreno & Fuchs, 2006). This study is particularly focused on regulation of TJs (cell-cell junctions described in section 1.2). TJs aid in maintaining apical-basolateral polarity, further stabilise cell-cell adhesions and but also regulate paracellular permeability and aid in regulation of membrane integrity. This study is interested in remodelling of TJs during epithelial wound healing, as well as the potential role for endocytosis and vesicle trafficking as a regulator of this remodelling process.

1.14 Tight junction structure

Similar to FAs, TJs are protein complexes, composed of scaffolding, signalling and transmembrane proteins (Figure 1.10). In transmission electron microscopy, TJs appear as a fusion of plasma membranes of neighbouring cells. Freeze-fracture electron microscopy demonstrates intramembranous networks of strands (Staehelin, 1974). The strands consist of integral transmembrane proteins such as occludin, claudin and tricellulin (Furuse et al., 1993; Ikenouchi et al., 2005; Morita et al., 1999). Occludin, claudin and tricellulin all contain four transmembrane domains, two extracellular loops and cytoplasmic N and C termini (Ikenouchi et al., 2005; Krause, 2008; Li et al., 2005). The extracellular loops of these proteins undergo polymerisation with the extracellular loops of homologous proteins from adjacent cells, forming the

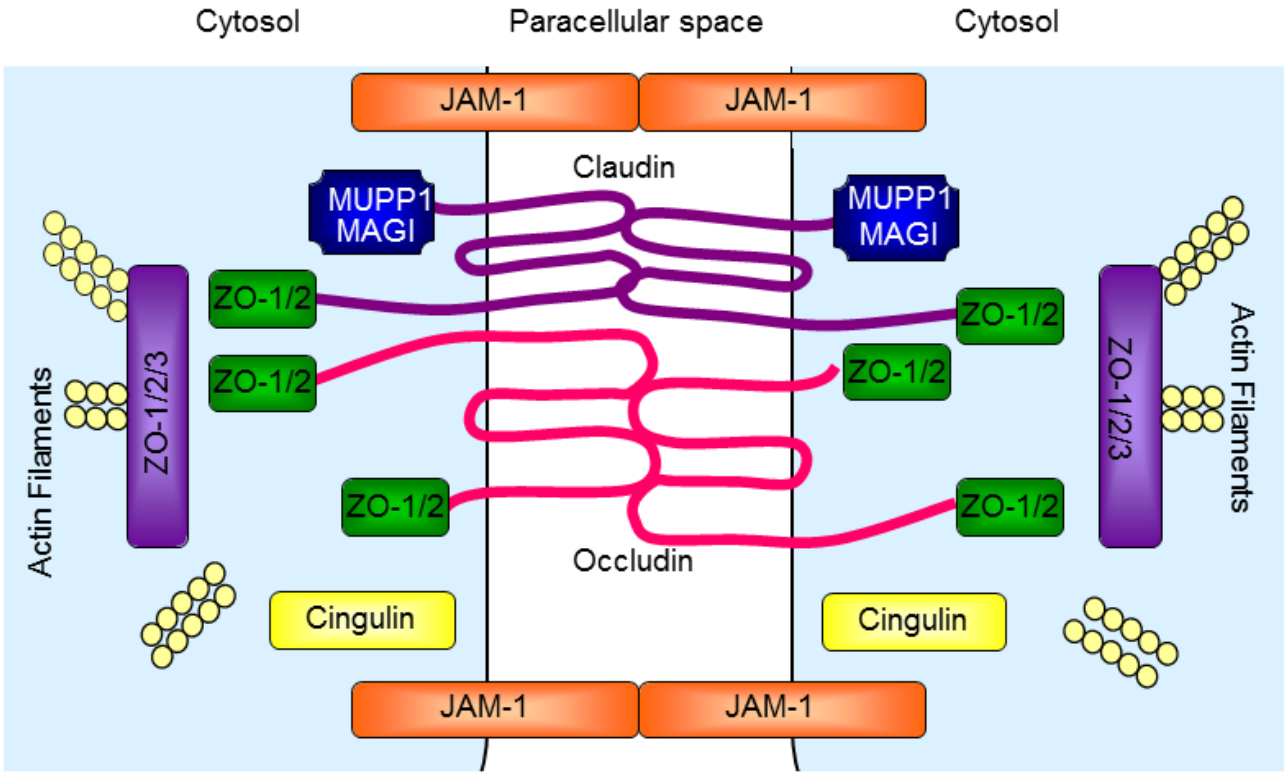

Figure 1.10. Tight junction structure. Diagram showing TJ structure in lateral cell membranes. JAM- junctional adhesion molecule, ZO1=zonula occludens 1.

characteristic TJ strand (Krause, 2008) (Figure 1.10). Junctional adhesion molecules (JAMs), are single TM proteins which contain an extracellular region with two Ig-like domains and an intracellular tail (Liu et al., 2000) also found in TJ strands (Niessen, 2007). These transmembrane domain TJ proteins are then linked directly to the actin cytoskeleton via several scaffolding proteins (Figure 1.10). Zonula occludens (ZO), is one such protein which is thought to bind to and regulate clustering of occludin and claudin, but also has an F-Actin binding domain, stabilising TJ strands by linking them to the actin cytoskeleton (Figure 1.10) (Brennan et al., 2010; Niessen, 2007). Cingulin, MUPP1 and MAGI are other TJ scaffolding proteins, their exact function is yet to be fully elucidated, but cingulin has been shown to interact with JAMs, ZO, myosin and F-actin suggesting a role for cingulin as a linker between TJ membrane and cytoskeleton (Figure 1.10) (reviewed further in Brennan et al., 2010).

1.14 Tight junctions and cell migration

Disassembly of TJs has been widely implicated as having an important function in cell migration. Cells undergoing EMT significantly alter phenotype, from polarised epithelial cells embedded in organized, stratified or single cell layers, the cells convert into single fibroblastoid cells capable of locomotion. A hallmark of EMT is disintegration and disassembly of TJs (Zavadil & Bottinger, 2005). In fully polarised cells polarity complexes are localised to TJs (Martin-Belmonte & Mostov, 2008) and are required to maintain apical basolateral polarity. However, loss of these complexes from TJs during EMT has been widely implicated in cancer (reviewed fully in Ellenbroek, Iden, & Collard, 2012).

Direct links have been made suggesting the TJ protein occludin plays a central role in regulation of directional migration in migrating epithelial cells via interactions with polarity complexes. Initial work by Osanai, et al., (2007) identified over-expression of occludin in AC2M2 mouse breast carcinoma cells mediated increased cell spreading indicating a role for occludin in regulation of cell migration (Osanai et al., 2007). Later work by Du et al., (2010) found localisation of occludin to the leading edge of migrating MDCK cells 6 hours post-wounding. They showed that this localisation is required for recruitment of aPKC, Par 3 and PATJ to the leading edge mediating lamellipodial formation, re-orientation of the MTOC and effective wound closure (Du et al., 2010). Evidently, TJs and occludin have an important function in the regulation of cell migration, potentially through modulation of polarity complexes which mediate effects on the actin cytoskeleton.

1.15 Regulation of occludin distribution by endocytosis and trafficking

Disruption of TJs may play an integral role in regulation of cell motility. In particular, redistribution of the TJ protein occludin, seems to play a key function in modulation of cell migration. Internalisation of occludin has been suggested to occur via several pathways, however these mechanisms seem to vary depending upon both cell type and occludin internalisation stimulus. Depletion of Ca^{2+} has been shown to promote disassembly of both AJs and TJs (Ivanov, Nusrat & Parkos, 2004). In T84 epithelial cells undergoing Ca^{2+} mediated TJ disassembly, occludin was shown by immunocytochemistry to co-localise with markers of CME whilst inhibition of CME blocked occludin internalisation (CME

inhibited by incubation in hypertonic media, a pH drop to pH 5.5 or phenylarsine oxide treatment) (Ivanov, Nusrat & Parkos, 2004). Furthermore, co-localisation of occludin with markers of other endocytosis pathways; macropinocytosis and caveolar endocytosis was not observed. Inhibition of these pathways also had no effect on Ca^{2+} mediated occludin internalisation (Ivanov, Nusrat & Parkos, 2004). Occludin was found to internalise into Rab5 positive EEs, but also into an unidentified intracellular compartment (Ivanov, Nusrat & Parkos, 2004). Further studies were performed in rat Sertoli cells, where TGF-β_3-stimulated internalisation of occludin was mediated by dynamin-dependent pathways (Marchiando et al., 2010; Xia et al., 2009).

Occludin has also been shown to undergo internalisation via caveolar endocytosis. Inhibition of caveolar endocytosis by siRNA and the cholesterol sequestering agent filipin, significantly inhibited internalisation of GFP-occludin in bEnd.3 endothelial cells stimulated with the cytokine CCL2 (shown to promote TJ disassembly) (Stamatovic et al., 2009). GFP-occludin was shown to rapidly cycle back to the plasma membrane, and co-localisation was observed with EEA1 positive EEs and Rab4 positive endosomes (Stamatovic et al., 2009). Internalisation of occludin via caveolar endocytosis was further corroborated in *in vivo* studies performed by Marchiando, et al., (2010) in isolated mouse jejunum. Pharmacological inhibition of caveolar endocytosis was shown to block tumour necrosis factor (TNF)-induced occludin internalisation. Furthermore, TNF was shown to induce co-localisation of occludin with caveolin1 but not clathrin heavy chain or EEA1 (an early endosomal marker) (Marchiando et al., 2010).

Caveolar and CME are both dependent upon the GTPase dynamin for fission of vesicles from the plasma membrane (Doherty & McMahon, 2009). Marchiando, et al., (2010) identified a potential role for dynamin in basal occludin internalisation from the plasma membrane, but not in its internalisation during TNF stimulation (Marchiando et al., 2010). Recently occludin has been shown to co-immunoprecipitate with dynamin (Liu et al., 2010), and this binding was dependent upon the presence of the second extracellular loop of occludin. There are discrepancies between the internalisation pathways of occludin, yet the extent to which this is due to variances in cell line or internalisation stimulus is unclear.

Little is known about how occludin is trafficked, and through which organelles it is recycled both under stimulated and non-stimulated conditions. Occludin is a molecule which undergoes post-translational modification that has been demonstrated to regulate its trafficking. Work by Murakami, Felinski and Antonetti (2009), identified a phosphorylation site, *ser*-490 in the C terminus of occludin, which regulates ubiquitination of occludin (Murakami, Felinski, & Antonetti, 2009).

Ubiquitination is a process which regulates transport of protein both from the plasma membrane and between membrane compartments (Hicke and Dunn, 2003). Proteins can either be mono-ubiquitinated (have one ubiquitin molecule attached) or polyubiquitinated (have ubiquitin chains attached) by ubiquitin ligase proteins (reviewed in Hershko & Ciechanover, 1998). This post-translational modification enables specific trafficking machinery to recognise ubiquitinated cargo proteins and regulate their sorting and trafficking (Hicke &

Dunn, 2003). After VEGF treatment, Murakami, Felinski and Antonetti (2009), identified increased interactions between occludin with the E3 ligase Itch, explaining increased occludin ubiquitination. Furthermore, ubiquitinated occludin was demonstrated to undergo internalisation mediated by epsin and epidermal growth factor receptor substrate 15 (Eps15) (Murakami, Felinski, & Antonetti, 2009; Polo et al., 2002). Epsin and Eps15 are proteins which function in internalisation of ubiquitinated proteins from the plasma membrane (Polo et al., 2002; Shih et al., 2002). These data suggest that occludin internalisation may be regulated by ubiquitination and interactions with epsin and Eps15. However, ubiquitinated occludin was also shown to bind to Hrs (Murakami, Felinski, & Antonetti, 2009). Hrs is a protein that functions at endosomes and functions to sort ubiquitinated proteins into multivesicular bodies prior to lysosomal degradation (Raiborg & Stenmark, 2002). Therefore work from this group suggests VEGF mediated TJ disruption may be mediated by ubiquitination of occludin, leading to its subsequent internalisation and degradation; however, these data go no further in elucidation of the specific trafficking pathways involved in internalisation of occludin.

1.16 Aims

There were four main aims for this PhD examining how vesicle trafficking functions in regulation of epithelial wound healing:

- To perform a systematic analysis of the trafficking pathways required during directed MDCK migration.

- To observe whether trafficking is polarised during epithelial wound healing.
- To identify the role of vesicle trafficking in the regulation of cell adhesion structures during epithelial motility, focussing on trafficking of integrins and the TJ protein occludin.
- To examine how occludin is trafficked under baseline conditions to maintain occludin plasma membrane homeostasis.

CHAPTER 2

METHODS

2.1 Plasmid constructs

All constructs were kindly donated or purchased from:

Table 2.1 Plasmid constructs

Plasmid	Source
β_3-GFP	Prof. Jonathan Jones - Department of Cell and Molecular Biology, Northwestern University Medical School, Chicago. USA.
caveolin1-mCherry	Prof. Ari Helenius - Swiss Federal Institute of Technology Zurich, Zurich, Switzerland.
caveolin1(Y14F)-GFP	Prof. Mark McNiven - Mayo Clinic, Rochester, USA.
CD63-GFP	Dr Jyoti. Jaiswal - George Washington University, Washington D.C., USA.
GFP-clathrin	Dr Alexandre Benmerah - Institut Cochin, Paris, France.
dsRed-clathrin (rat light chain a)	Prof. Thomas Kirchausen - Harvard Medical School, Boston, MA, USA.
GFP-dynamin2(K44A)	Prof. Mark McNiven - Mayo Clinic, Rochester, USA
dynamin2aa-GFP	Prof. Mark McNiven - Mayo Clinic, Rochester, USA
EH29-GFP	Dr Alexandre.Benmerah -Institut Cochin, Paris, France.
pECFP-Mem	Clontech - BD Biosciences Clontech, Palo Alto, CA.
pEGFP-N1	Clontech - BD Biosciences Clontech, Palo Alto, CA.
NPY-mRFP	Dr Jyoti. Jaiswal - George Washington University, Washington D.C., USA.
GFP-occludin	Prof. Tianyi Wang - Department of Infectious Diseases and Microbiology, University of Pittsburgh, USA.
GFP-occludin(DelE2)	Prof. Tianyi Wang - Department of Infectious

	Diseases and Microbiology, University of Pittsburgh, USA.
PKD(K618N)-GFP	Prof. Vivek Malhotra - The Centre for Genomic Regulation, Barcelona, Spain.
GFP-Rab4(S22N)	Prof. Mary McCaffery – University College Cork, Cork, Ireland.
GFP-Rab5	Dr Marino Zerial - Max Planck, Dreseden.
Rab11-GFP	Dr J. Norman - The Beatson Institute of Cancer research, Glasgow, U.K.
Rab11(S25N)-GFP	Dr Frances Barr - University of Liverpool, Liverpool, UK
Rab25-GFP	Dr J. Norman - The Beatson Institute of Cancer research, Glasgow, U.K.

2.2 Cell culture

MDCK cells were cultured and maintained in culture medium (supplementary methods (S.M.1)) in humid conditions at 37ºC with 5% CO_2. Cells were cultured in plastic T75 flasks (Corning). During cell passage, cells were washed in 5ml of PBS (Lonza), followed by a 2ml wash with trypsin (S.M.2). Cells were then incubated with 2ml of trypsin for 12-15 minutes at 37ºC with 5% CO_2 until the cells were dissociated from the plastic. They were then plated in media as described above.

2.3 Bacterial transformation

1µg of DNA (as stated in table in section 2.1) was added to 50µl of MAX Efficiency DH5α Competent Cells (Invitrogen) and incubated on ice for 30 minutes. The bacteria were then heat shocked in a water bath at 42ºC for 45

seconds and then transferred back to ice for a further 2 minutes. 500µl of Luria Broth (LB) (Sigma) (S.M.3) was added to the bacteria, and the cells were incubated in a shaking incubator at 37ºC for 1.5 hours. 125µl of bacterial mix was spread onto an LB agar (Sigma) plate (13cm) containing either kanamycin or ampicillin (S.M.4) using a flaming loop. Plates were incubated inverted overnight at 37ºC. For each bacterial transformation, 2 non-touching colonies were picked with a pipette tip and placed in 14ml dual-position snap cap round bottomed tube (Falcon) containing 2ml LB broth plus kanamycin/ampicillin (final concentration of 50µg/ml or 100µg/ml, respectively) depending on the plasmid bacterial resistance gene expressed. The bacterial mix was then incubated in a shaking incubator at 37ºC for 6-8 hours. 200µl of bacterial mix was then removed and added to 100ml LB broth (containing antibiotics at previously stated concentrations) in a conical flask covered with aluminium foil. The flasks were then incubated in a shaking incubator at 37ºC for 6-8 hours. The flask contents were then split into 2x 50ml plastic centrifuge tubes (Falcon) centrifuged at 5000rpm at 4ºC using a Heraeus Labofuge 400R centrifuge (Thermo Scientific). The supernatant was aspirated and the pellets either lysed immediately for purification or stored at -20ºC prior to use. DNA was purified with a Qiagen Plasmid Maxi Kit (Qiagen) following manufacturer's instructions and using all kit reagents. Purified DNA was re-dissolved in 1ml ultrapure water. DNA concentration was measured using a U1800 model Spectrophotometer (Digilab Hitachi). DNA was stored at -20ºC.

2.4 MDCK cell transfection

MDCK cells were seeded onto either 35mm glass bottomed MatTek dishes (No. 1.5 glass thickness and 20mm glass diameter used throughout) (MatTek Corporation) or onto 24x24 mm glass coverslips (VWR) in plastic 35mm dishes (Corning) or onto 13mm glass coverslips (VWR) in a 24 well plate (Corning) (as stated in text) at ~75% confluence. Cells were transiently transfected 24h post-plating with the constructs listed in section 2.1, using Lipofectamine 2000 (Invitrogen). To increase transfection efficiency, the ratio of Lipofectamine 2000 to DNA was doubled in all experiments. In experiments where a single construct was expressed 4µg DNA, 20µl Lipofectamine 2000 and 500µl of serum free DMEM (SFM) were used per dish, in studies where the cells were co-expressing two constructs; 3µg of each DNA, 30µl Lipofectamine 2000 and 500µl of SFM were utilised per dish. Per dish; 250µl of serum free media was incubated with Lipofectamine 2000 (volume as stated above) for 5 minutes at room temperature (RTP). DNA was diluted in 250µl of SFM (as stated previously). The Lipofectamine 2000 and DNA mix were then combined and incubated for 15 minutes at RTP. 500µl of the transfection mix was then added to each dish. Transfected cells were incubated at 37ºC, 5% CO_2 in high humidity for 24 or 48 hours depending on the construct being expressed. The volume and quantity of reagents were scaled as manufacturer recommends for cells plated in 24 well plates.

2.5 Rate of migration in a wound healing assay

MDCK cells were seeded onto MatTek dishes. Cells were transfected as stated in section 2.4. The monolayer was then wounded with a yellow pipette tip forming a 1-2mm wound from the top to the bottom of the dish. The media was removed and replaced with 2ml cell imaging media (CIM) (S.M.5). Alternatively, non-transfected cells were treated with 2ml of 80µM Dynasore (80mM stock dissolved in dimethyl sulfoxide (DMSO)) (Sigma) or 1µl/ml DMSO (Fisher Scientific) in cell culture media for 30 minutes, wounded and maintained in 2ml Dynasore or DMSO containing CIM for the duration of wound healing. Cells were imaged as stated in section (2.13). For Dynasore-treated cells, the percentage of wound area covered after 6 hours was calculated with OpenLab 5 (Improvision, Coventry, UK). This was performed for 2 dishes per treatment and repeated 3 times. For cells expressing GFP-tagged mutant constructs, the rate of cell migration was calculated in OpenLab 5 using the calliper tool by following the mid-point of a transfected cell located within 50µm of the wound edge over the 6 hour period. To measure cell polarisation in cells expressing the GFP-tagged constructs or GFP alone the elliptical factor was calculated. Using the calliper tool, the longest axis of the cell was measured; the width of the cell was then calculated by measuring a line halfway along and perpendicular to the longest axis. A total of ~10 cells per group were analysed from 3 or 4 independent experiments and the mean rate of migration calculated. All data was then logged into Excel and a Student's t-test was performed to identify statistical significance.

2.6 Cholera Toxin B and DiI-LDL uptake assay

MDCK cells were plated onto glass coverslips in a 24 well plate. Cells were transfected as described in section 2.4. For the Cholera Toxin Subunit B uptake assay: the cells were incubated in 500µl 10ng/ml Cholera Toxin Subunit B conjugated to Alexa Fluor 555 (CTxB-AF555) (Invitrogen) in SFM, at 37°C, 5% CO_2 for 30 minutes. For the DiI-LDL uptake assay: the cells were incubated in 500µl 20µg/ml DiI-LDL (Invitrogen) in the aforementioned conditions for 15 minutes. Cells were washed 3 times in 1ml PBS, fixed in 4% paraformaldehyde (PFA) (S.M.6), washed again 3 times and mounted onto glass slides using Hydromount mounting media (Fisher Scientific). Images were acquired as stated in section 2.13. Using the region of interest (ROI) selection tool in ImageJ a region was drawn around the cell membrane and the average CTxB-AF555 intensity within the cell was measured and recorded in Excel. The background average area was measured and subtracted from the average CTxB-AF555 intensity.

For validation of Dynasore as an inhibitor of dynamin-dependent caveolar and clathrin-mediated endocytosis, MDCK cells were plated as previously described, treated with 2ml 80µM Dynasore or 1µl/ml DMSO for 30 minutes in SFM then treated with CTxB-AF555 or DiI-LDL as above, fixed, imaged and analysed as stated previously. For each experiment 3 separate repeats were performed. A Student's t-test was performed to ascertain statistical significance.

2.7 Neuropeptide-Y cargo trafficking assay

MDCK cells were plated onto glass coverslips in a 35mm plastic tissue culture dish at approximately 80% confluence. Cells were co-transfected as described in section 2.4. The cells were washed 3 times in 2ml PBS, fixed in 2ml 4% PFA in PBS, the washes repeated and the coverslips mounted onto glass slides as stated in section 2.6. Cells were imaged using epifluorescence microscopy (as described in section 2.13) and the intensity of the NPY-mRFP fluorescence signal in cells also expressing GFP/PKD(K618N)-GFP was measured using MetaMorph software, again the ROI tool was used to outline the cell cytosol. The average intensity within the ROI measured as in section 2.6 the average background intensity was subtracted from the NPY-mRFP average intensity values. Results are from 3 independent experiments and a Student's t-test was used to identify statistical significance.

2.8 Polarised trafficking assay

MDCK cells were seeded onto MatTek dishes and transfected as in section 2.4. 4-6 hours post-transfection the confluent monolayer was wounded as in section 2.5, 18 hours after wounding the media was removed and replaced with 2ml of 37ºC pre-warmed CIM. Cells at the wound edge displaying a fully polarised phenotype and obvious lamellipodia were imaged as detailed in section 2.13 at 37ºC. In observations of polarised caveolar endocytosis the cell footprint was outlined using the pECFP-mem image and divided into 2 regions; the lamellipodia and cell rear. This outline was then superimposed over the

caveolin1-mCherry image. The average caveolin1-mCherry intensity was then quantified for both the entire cell and each region. The average intensity per region was normalised against the average intensity of the whole cell volume. A Student's t-test was performed to quantify statistical significance from the 3 separate experiments.

In observations of polarised exocytosis of cargo from the Rab11- and Rab25-dependent pathway exocytic fusion events were analysed using methods previously described by Schmoranzer et al., 2000. The initial stage of identification was to run the video and identify potential fusion events, this is identifiable as the observation of a vesicle approaching the plasma membrane (thus intensity increases) followed by a characteristic "flash" as the vesicle fuses with the plasma membrane and fluorescently labelled proteins diffuse laterally within the plasma membrane. However it can be difficult to distinguish these events from events were vesicles approach the plasma membrane but do not fuse. Thus, two analytical methods were used to identify a true fusion event. The first method utilised NIS Elements line scan analysis tool; a line scan was drawn through the potential fusion event (the length of the line was the maximum diameter of the fusion event observed). The intensity values across the line scan were measured in each frame in which the fusion event took place. The values were logged in Excel and a graph produced, plotting intensity per pixel. A true fusion event was demonstrated by the line scan graph showing a narrow central peak (during the initial fusion event), this is followed by a reduction in the peak intensity value and the curve broadening during consecutive time frames (due to lateral diffusion). The second method of

analysis utilised the ROI tool. A circle was drawn around the fusion event (again through the frames the event took place) and the total intensity and area was recorded and logged in Excel. The confirmation of a fusion event also had to satisfy the second analysis method; in this method a true fusion event was confirmed as one where the total intensity remained static but the area of the circle increased (again confirming lateral diffusion). True fusion events were counted using the NIS elements count tool. The cell was divided again into lamellipodial region and cell rear and the areas measured. All true fusion events were normalised against the region area and a Student's t-test used to identify a significant difference between the leading and lagging edge of the cell. In both the Rab25-GFP and Rab11-GFP studies, fusions in 5 cells were measured from a minimum of 3 independent experiments.

2.9 Immunocytochemistry (IC)

MDCK cells were plated onto glass coverslips in 6 well plates. The cells were transfected as stated in section 2.4. In studies where IC was performed during wound healing the confluent monolayer was wounded as described in section 2.5 and the cells were allowed to migrate for 5, 15 or 60 minutes. IC experiments in non-treated cells were performed on a confluent MDCK monolayer. In experiments where observations of co-localisation between lysosomal compartments and occludin were measured, a confluent monolayer of cells were treated with 2ml of either 250nM Bafafilomycin A (BafA) (Calbiochem) (made from 10µg/100µl BafA stock dissolved in DMSO)) or 1.53µl/ml DMSO (control) diluted in cell culture media (S.M.1) for 3 hours in

humid conditions at 37ºC with 5% CO_2 prior to IC. In all experiments the cells were then washed 3 times in 2ml of PBS, fixed in 2ml of 4% PFA, the washes repeated then the cells were permeabilised for 7.5 minutes in 2ml of permeabilisation buffer (S.M.7) then the washes repeated. Cells were then blocked for 1 hour in 2ml of goat serum (GS)/bovine serum albumin (BSA) blocking buffer (S.M.8). The lid of the 6 well plate was covered with Parafilm (Alcan Packaging). Primary antibodies were diluted as stated in S.M.30 in GS-BSA block buffer to produce a final volume of 250µl per coverslip. A 250µl spot of primary antibody mix was pipetted onto the Parafilm (one spot per coverslip). The coverslips were then removed from the well and placed cell-side down in the spot. The coverslips were incubated in a sealed moist box in the dark for 1 hour. The coverslips were removed and placed back in their original wells and washed 3 times in 2ml of PBS. The lid from the 6 well plate was re-covered with Parafilm and spotted with 250µl of secondary antibody mix (secondary antibodies were diluted as stated in S.M.30 in GS-BSA block buffer to produce a final volume of 250µl per coverslip). Coverslips were removed and incubated as stated previously for 1 hour. Cells were washed 3 times in PBS and mounted onto glass slides as detailed above using Vectashield with DAPI (Vector Labs). Cells were imaged as described in section 2.13.

Image analysis in IC studies:

Occludin and ZO1 localisation during wound healing

Occludin and ZO1 localisation was quantified in NIS-Elements by placing four equally spaced points across the width of the lamellipodium. Line scan analysis was made at each of these points from the lamellipodium-cell boundary to the

leading edge. Data was transferred to Microsoft Excel and analysed by subtracting the background (lowest) pixel intensity from the pixel of the highest intensity. 15 cells from 3 independent experiments were analysed.

Co-localisation between Rab5-GFP and occludin

In studies examining co-localisation of endogenous occludin with Rab5 positive endosomal compartments analysis was performed in NIS elements using the automated ROI tool to outline the region of maximal intracellular Rab5 staining, apart from the entire cytosol. Subsequently a Pearson's coefficient comparing the Rab5 and occludin signals in the region was obtained. A minimum of 20 cells for each condition were analysed from 3 separate experiments.

Co-localisation between CD63-GFP and occludin

Occludin co-localisation with CD63-GFP in the presence of either BafA or DMSO was quantified as follows: the Z-stack slice containing the most intracellular punctate occludin stained structures was analysed using the automated ROI tool in NIS Elements to select the entire cytosol excluding the cell-cell junction staining. Subsequently a Pearson's coefficient comparing the CD63-GFP and occludin signals in the region were obtained. A total of 19 cells were analysed from 3 independent experiments.

Co-localisation between NPY-mRFP and occludin

Occludin co-localisation with NPY-mRFP was analysed using NIS Elements as follows: from the NPY-mRFP channel 20 punctate structures from each cell

were outlined using the ROI function. These outlines were then superimposed over the occludin stained image. The number of NPY-mRFP outlines which co-localise with occludin positive regions were counted. For the control, these regions were moved from NPY-mRFP puncta and again co-localisation with occludin was counted. A total of 13 cells from 3 independent experiments were analysed. In all of the aforementioned experiments the results were logged into Microsoft Excel and a Student's t-test was performed to assess statistical significance.

2.10 Localisation of GFP-occludin and GFP-occludin(DelE2) in migrating MDCK cells

MDCK cells were plated onto glass coverslips in 35mm plastic dishes. Cells were transfected as in section 2.4. The confluent monolayer was wounded as described in section 2.5. Following 1 hour of migration, the wounded monolayer was washed 3 times in 2ml of PBS, fixed in 2ml of 4% PFA in PBS and mounted with Hydromount mounting media. Cells were imaged as detailed in section 2.13. GFP-occludin and GFP-occludin(DelE2) localisation was quantified as described in section 2.9. Results obtained from 3 independent experiments.

2.11 BafA inhibition of lysosomal acidification and co-localisation of LysoTracker with CD63-GFP

MDCK cells were plated onto 35mm MatTek dishes. To observe co-localisation between markers of late endosome/lysosomal compartments with LysoTracker cells were transfected as stated in section 2.4 prior to experimentation. In both studies, 24 hours post-plating media was removed and replaced with 2ml cell culture media (S.M.1) plus 75nM LysoTracker Red DND-99 (in lysosomal acidification assays 250nM BafA or 1.53µl/ml DMSO was added to the LysoTracker media mix). The cells were incubated for 2 hours in humid conditions at 37ºC with 5% CO_2. The media was removed and the cells washed 3x2ml in 37ºC CIM. Cells were maintained at 37ºC in CIM and imaged as described in section 2.13).

2.12 Co-localisation of focal adhesions with caveolin1 and clathrin

MDCK cells were plated onto 35mm MatTek and co-transfected as described in section 2.4. The confluent monolayer was wounded as stated in section 2.5 18 hours prior to imaging and maintained at 37ºC, 5% CO_2 in humid conditions. Just before imaging, media was removed and replaced with CIM (pre-warmed to 37ºC). Single still images of transfected cells at the wound edge were acquired as described in section 2.13. Image analysis was performed in Nikon NIS-Elements AR. For the quantitative analysis, the cells were divided into front, middle and back regions in the direction of migration. All FAs in each region were outlined using the ROI function. These ROIs were transferred into the caveolin/clathrin channel and the percentage of ROIs that co-localised with

the endocyosis markers was calculated. For the control to check for random alignment of the markers, the same ROIs used to outline FAs were moved to areas of the cell were no FAs were detected and the presence of caveolin1/clathrin/dynamin in the ROIs was scored. A total of 10 cells from 3 independent experiments were analysed for each condition. A Student's t-test was used to determine statistically significant co-localisation.

2.13 Image acquisition

Wound healing (section 2.5), CTxB-AF555 and DiI-LDL internalisation (section 2.6) and NPY-mRFP cargo trafficking assays (section 2.7) were imaged using an inverted Nikon TE300 epifluorescence microscope (Nikon). Wound healing studies were imaged with a 10x CFI Plan Apo Lambda (0.45 NA) air objective (Nikon), and CTxB-AF555, DiI-LDL and and NPY-mRFP trafficking assays were imaged with a 60x CFL Plan Apo (1.40 NA) oil objective. The microscope system was placed in an Okolab incubation chamber set at 37°(Okolab). Using a Red/Green/Blue multiband emission filter with excitation toggled between red and green with a Ludl filter wheel. In wound healing assays a brightfield and fluorescence image was taken every 10 minutes for 6 hours. For CTxB-AF555, DiI-LDL and NPY-mRFP trafficking studies, brightfield and fluorescence images were taken of live cells (CTxB-AF555 and DiI-LDL) or fixed cells (NPY-mRFP). Acquisition and editing software used was Openlab 5.0 and ImageJ 1.42q (National Institute of Health).

TIRF microscopy was used to image polarised trafficking studies (section 2.8) and co-localisation between FAs and markers of endocytosis (section 2.12). Cells were imaged using a Nikon A1 TIRF confocal system with the Nikon Eclipse Ti inverted microscope utilising illumination through the microscope objective (CFL Plan Apo 60x NA 1.49, Nikon). The microscope system was placed within an enclosed microscope incubator (Okolab) set at 37°C for live cell imaging. For imaging polarised caveolar endocytosis and co-localisation between FA markers and markers of endocytosis, single TIRF and brightfield single images were taken of live cells. In studies where polarised exocytosis was imaged, cells were imaged as described previously by Schmoranzer et al., 2000 and Lampson et al., 2001; taking TIRF images every 100-200 ms for 15 minutes.

In all IC (section 2.9), occludin localisation (section 2.10) and LysoTracker experiments (section 2.11) confocal imaging was used. This was also performed on the A1R inverted confocal microscope using the microscope objective (CFL Plan Apo 60x NA 1.49, Nikon). In studies where co-localisation between endogenous occludin and GFP-Rab5/CD63-GFP/NPY-mRFP was measured a Z-stack with 500nm increments was performed on each cell imaged. In all other confocal experiments a brightfield and confocal image were taken of each cell.

For both TIRF and confocal microscopy all GFP constructs and Alexa Fluor 488 conjugated secondary antibodies were imaged following excitation with the 488nm line of an Argon-Ion laser 457-514nM, pECFP-mem and DAPI were imaged after excitation with a Violet Diode laser 400-405nm. All RFP

constructs, dsRed-clathrin, Alexa Fluor 568 conjugated secondary antibodies, and LysoTracker Red DND-99 probes were imaged after excitation with Green Diode 561nm laser. The camera utilised to acquire images was a 12-bit CCD (Ixon 1M EMCCD camera controlled by NIS Elements).

TIRF and confocal systems were controlled by Nikon Elements AR version 3.1/3.2. Analysis of time lapse sequences and still frames was completed using NIS-Elements AR version 3.1 (Nikon), Elements AR version 3.2 (Nikon), ImageJ 1.42q and Microsoft Excel.

2.14 Western blot protocol

Western bots were performed using the Mini-Protean Tetra Electrophoresis System (BioRad) all acrylamide gel details, running, transfer and TBST buffer recipes are as listed in the supplementary figures. Acrylamide gels were mixed to percentage as stated in relevant section (recipe S.M.9). Before use all combs, glass spacer plates and short glass plates (all BioRad) were cleaned in 70% ethanol (Fisher Scientific). The plates were inserted into the clamping frame (BioRad) then placed in the casting frame (BioRad). The combs were inserted and a marker line was drawn 2cm below the bottom of the comb, to mark where the resolving gel should be poured to. Approximately 7ml of 10% resolving gel was then poured to this line, 70% ethanol was poured on top of the resolving gel to ensure the gel front is straight. Once this had solidified (approximately 20 minutes), the ethanol was removed and blotted off with filter paper. 5ml of 4% stacking gel was poured on top of the resolving gel and the

comb inserted. Gels were left at RTP for approximately one hour to ensure the gel was completely set, the lanes were rinsed in running buffer (S.M.10) using a 50ml syringe and needle; any lanes that needed straightening were straightened with a gel loading tip. The gel/gels were then inserted into the electrode chamber so that the wells faced inwards, if only one gel was being run the buffer dam (BioRad) was used to form the chamber. The inside of the chamber and the outside of the tank were then filled with running buffer (S.M.10). To each gel 15µl of PageRuler Plus Prestained Protein Ladder (Fermentas), was loaded into a lane using gel loading tips. The samples were then loaded as stated specifically in text. The gels were run at 180V for approximately 1.5 hours using a PowerPac Basic Power Supply (BioRad) power pack. Once the dye front had reached the bottom of the gel, gels were removed from the tank, opened and the stack cut off. 0.5µm Immobilon-P PVDF Membrane (Millipore) was cut to size and activated with 100% methanol (Fisher Scientific) for 30 seconds. The blotting filter paper and sponges were soaked in ice cold transfer buffer (S.M.11). The blotting cassette from the Mini Trans-Blot Cell (BioRad) was immersed in transfer buffer, clear plastic side down and sandwiched as follows: sponge, filter paper, PVDF membrane, gel, filter paper and sponge, a plastic centrifuge tube was then rolled over the sandwich to remove bubbles before the black other half of the blotting cassette was closed. The cassette/cassettes were then inserted into the Mini Trans-Blot Cell (BioRad) (black side of the cassette facing black wall of the cell) the cell was filled with ice cold transfer buffer as recommended by manufacturer. The entire tank was set on ice and transferred for 1 hour at 400mA using the PowerPac

Basic Power Supply. After transfer, membranes were incubated in 5ml of Ponceau S Stain (Thermo Scientific) for 30 seconds to see the protein bands (confirmation of transfer of protein onto the PVDF membrane) then washed in 50ml TBST (S.M.12) on a rocker 2x 2minutes. The membrane/membranes were then blocked in 20ml TBST-Marvel block buffer (S.M.13) for 1 hour and probed with primary and secondary antibody as specifically stated in figure legends. Membrane/membranes were washed 4x5minutes in TBST after both the primary and secondary incubations. The membrane/membranes were blotted dry with tissue in preparation for chemiluminescent detection of proteins.

Detection reagents 1 and 2 from ECL Western Blotting Substrate Kit (Pierce) were mixed in a 1:1 ratio, making up a total volume of 2ml per membrane. The membrane\membranes were incubated in the ECL reagent for 2.5 minutes on each side of the membrane, and the excess reagent blotted from the membranes using tissue. The membranes were wrapped in cling film and taped into a developing cassette so that the protein side faces outward. X Ray film (Scientific Laboratory Supplies) was inserted into the developing cassette and exposed to the membranes for exposure times varying from 1 second to 6 minutes to ensure correct levels of exposure. The film was developed using a CURIX 60 XoGraph machine (AGFA).

2.15 Cell-surface biotinylation assay

MDCK cells were plated into a 6 well plate (Corning). In studies where plasma membrane localised endogenous occludin and GFP-occludin was measured cells were transfected as described in section 2.4 and serum starved in 2ms

SFM for 1 hour prior to the assay. In experiments where occludin localisation at the plasma membrane was measured in the presence of inhibitors of protein biosynthesis, cells were incubated for 0, 30, 60, 120 or 240 minutes in 2mls SFM containing either 1µl/ml DMSO (control) or 10µM cycloheximide (CHX) (stock 10mg/ml dissolved in DMSO) (Sigma). In treatments 0, 30 and 60 minutes the cells were pre-incubated in 2ml SFM so that in these conditions 2 hours serum starvation occurred before biotinylation.

In both studies cells were then washed in ice cold PBS. The reagents were prepared according to the manufacturer's instructions (Pierce). The cells were incubated with 1ml of Sulfosuccinimidyl-2-(biotinamido)-ethyl-1,3'-dithiopropionate (Sulfo-NHS-SS-Biotin) solution on a rotating stage (2x 30 minute incubations, with Sulfo-NHS-SS-Biotin removed between incubations). Cells were quenched in 0.5ml of quenching buffer (5 minutes at 4ºC on a rotating stage) (Pierce) then washed 3 times in ice cold PBS. 200µl of ice cold 1% Triton-X100 lysis buffer (S.M.14) was added to each well, the cells were scraped using a cell scraper and transferred into ice chilled plastic microfuge tubes. The lysates were vortexed and lysed on ice for 1 hour (vortexing every 15 minutes). The lysates were then centrifuged at 14,000g in a 5417R centrifuge (Eppendorf) (used in all plastic microfuge tube and spin column centrifugation steps) at 4ºC for 15 minutes. The supernatant was aspirated and transferred to fresh plastic microfuge tubes. 20µl of the lysate was removed for a whole cell lysate control; 10µl of 3X Sample buffer (S.M.15) was added and the samples were heated at 95ºC for 15 minutes using a digital tubetests heater (Palintest). Spin columns (Pierce) were prepared by adding 100 µl of

NeutrAvidin beads (Pierce) using a yellow pipette tip with the tip end cut off. The beads were spun at 1000g for 1 minute (all centrifugation steps with beads were spun for at 1000g for 1 minute), to remove all suspension liquid. 300µl of ice cold wash buffer (Pierce) was added to the columns and the columns then centrifuged, this wash was repeated and the spin column capped at the bottom. The lysates were added to the spin columns containing the NeutrAvidin beads incubated for 16-18 hours on a rotating mixer at 4ºC. The columns were then uncapped and centrifuged as previously stated. The beads were then washed 3 times in 300µl of ice cold wash buffer plus Complete-mini protease inhibitor (1 tablet per 10ml) (Roche), then the column bottom re-capped. The NeutrAvidin beads were incubated with rotational mixing in 3X Sample buffer containing 50mM dithiothreitol (DTT) for 1 hour. The spin column was then placed in a fresh plastic microfuge tube the top uncapped then the bottom, the tubes centrifuged and the eluate collected. 15µl of the whole cell lysates and post-biotinylation eluate were run on a SDS-PAGE acrylamide (10% gel with 4% stack (S.M.9)). Western blot protocol was then followed as described in section 2.14. This experiment was repeated 3 times the Western blot films were scanned and quantified using NIS Elements. To measure band intensity the ROI selection tool was used to draw a box around the band and the average intensity was measured. The average background intensity was measured using the same ROI box moved to a non-band region in the same lane as the band being measured. To remove background intensity, the average band intensity was then subtracted from average band intensity.

In the study where plasma membrane levels of GFP-occludin were measured and compared to endogenous occludin the difference between GFP-occludin average intensity was quantified relative to endogenous occludin average intensity.

Experiments where endogenous plasma membrane localised occludin was measured in the presence of cycloheximide, the values were background subtracted as described above. The band intensity value was normalised against the time 0 band intensity for either the control or treated cells. In both experimental proceedures the values were obtained from 3 separate experiments and a Student's t-test was performed to determine statistical significance.

2.16 Occludin recycling biotinylation assay and Western blot analysis

For the recycling biotinylation assay MDCK cells were plated onto a 6 well plate. 24h post-plating the confluent monolayer was serum starved for 1 hour in 2ml SFM in the presence of either 1.53µl/ml DMSO (control) or 250nM BafA in humid conditions at 37ºC with 5% CO_2. All reagents were prepared according to the manufacturer's instructions (Pierce). After serum starvation, the cells were washed in ice cold PBS 3x2ml. The cells were incubated with 1ml of Sulfo-NHS-SS-Biotin (2x 30 minute incubations, with Sulfo-NHS-SS-Biotin removed between incubations) at 4ºC on a rotating stage. Cells were washed 3x in 2ml of ice cold PBS, transferred to 2ml SFM pre-warmed to 37ºC containing either 250nM BafA or 1.53µl/ml DMSO incubated in humid conditions

at 37ºC with 5% CO_2 for 0, 5, 15, 30, 60 or 120 minutes. After the designated time points the cells were washed 3x in 2ml ice cold PBS, followed by 3x2ml washes with pH 8.6 biotinylation wash buffer (S.M.28). Cell-surface Sulfo-NHS-SS-Biotin was then removed by 30 minute incubation at 4ºC with 1ml of biotinylation reducing buffer (S.M.29). The total amount of plasma membrane biotinylated occludin, was measured using 2 dishes which were kept on ice post-biotinylation and washing, undergoing neither the internalisation period or cell-surface reduction. All treatments were then washed in 3x2ml ice cold PBS, the cells were lysed as described in section 2.15. All further treatment (incubation with NeutrAvidin beads, Western Blot etc) was repeated as described in section 2.15.

Western blot films were analysed as described in section 2.15 and the band average intensity value was normalised against the average value for the total plasma membrane occludin sample for each condition. Each experiment was analysed 3 times and a Student's t-test performed to identify statistical significance.

2.17 Direct coupling of protein G-Sepharose beads to antibodies

Protein G-Sepharose beads (Sigma) were washed in 10ml of PBS (post-washing at all stages was followed by centrifugation at 4ºC for 1 minute at 3000g using a Heraeus Labofuge 400R (Thermo Scientific) and the supernatant aspirated) and resuspended in PBS in a 1:1 ratio. Per 10cm diameter cell culture dish of MDCK cells, 90µl of the G-Sepharose (1:1 PBS resuspended) beads plus 9µg of either control rabbit IgG (Upstate) or rabbit anti-occludin

antibody was used; these values were scaled depending upon the surface area used to grow the cells upon. The beads were resuspended in 5ml of PBS mixed with antibody and incubated overnight at 4ºC with rotational mixing. The beads were washed twice with 10ml of 0.2M sodium borate (Sigma) pH 9.0 (S.M.16) (preheated to 37ºC as the sodium borate can precipitate out of solution). The beads were resuspended in 10ml of 0.2M sodium borate pH 9.0. Fresh dimethylpimelimidate (DMP) (Pierce) was added to the beads to give a final concentration of 5mg/ml and was mixed by rotation for 30 minutes at room temperature. The cross-linking reaction was stopped by washing the beads once with 10ml 0.2M ethanolamine pH 8.0 (Sigma) (S.M.17). 10ml of 0.2M ethanolamine pH 8.0 was added to the beads and again rotated for 2 hours at room temperature. The beads were washed in 10ml of PBS, followed by three washes with 10ml 0.1M glycine (Fisher Scientific) pH 3.0 (S.M.18) (to remove non-covalently linked antibody from the beads), three further washes in PBS were performed and the beads resuspended 1:1 in PBS. The beads were stored at 4ºC and used within 24 hours.

2.18 SILAC Labelling

MDCK cells were plated onto 10cm plastic cell culture dishes. The cells were cultured in an amino acid deficient DMEM (Thermo) containing 10% dialyzed FBS (Thermo), 0.5mg/mL proline (Sigma), 2 mM L-glutamine, 0.1mg/mL streptomycin, 0.2U/ml penicillin and either “light” 0.1mg/mL isotopically normal (R0K0) L-arginine and L-lysine (Sigma), “medium” (R6K4) $^{13}C_6$L-arginine and L-lysine-D4 or “heavy” (R10K8) $^{13}C_6{}^{15}N_4$L-arginine and $^{13}C_6$L$^{15}N_2$-lysine (Goss

Scientific). Cells were grown for at least six doubling times prior to use so that the MDCK cells fully incorporated the labelled amino acids.

2.19 Bradford Protein Quantification Assay

A set of protein standards were produced using the Quick Start Bovine Serum Albumin Standards (BioRad) 2mg/ml. Dilutions were made in distilled H_2O producing BSA protein standards of 25µg/ml, 20µg/ml, 15µg/ml, 10µg/ml, 5µg/ml, 2.5µg/ml. As the blank control distilled H_2O was used. 150µl of each protein standard was added to a 96 well plate (3 repeats of each). The cell lysates being quantified were diluted in distilled H_2O at 1:100, 1:250, 1:500 and 1:800 (a total sample volume of 0.6ml was made). 150µl of each dilution was added to the plate (3 repeats of each dilution). 150µl of Bradford Reagent (BioRad) was added to wells containing protein standard/cell lysate dilutions. The plate was then read using an EMax Precision Microplate Reader (Molecular Devices) controlled by SoftMax Version 2.3 for MacOS. The protein concentration of the unknown was calculated from the average values obtained from the 1:100 and 1:250 values for greater accuracy.

2.20 Immunoprecipitation of occludin for SILAC

MDCK cells previously labelled in either “light”, “medium” or “heavy” SILAC media were plated into 9x10cm tissue culture dishes (3x each SILAC media treated condition). DMSO was added to 15ml of “light” and “heavy” cell culture media to give a concentration of 1.53µl/ml. A 250nM concentration of BafA was made using “medium” media (made from 10µg/100µl BafA stock (dissolved in

DMSO)). All media treatments were pre-warmed to 37ºC prior to use. Cells were washed in 10ml PBS. 5ml of SILAC media plus DMSO/BafA was added to the correspondingly plated dishes e.g. “light” media plus DMSO was added to the “light” isotope cultured dishes. Cells were incubated with treatment for 2 hours in humid conditions at 37ºC and 5% CO_2. DMSO and BafA were made up in serum free “light”, “medium” or “heavy” SILAC media as described for the 2 hour treatment and pre-warmed to 37ºC. The cells were washed in 10ml PBS then 5ml of serum free SILAC media containing DMSO or BafA were then added to the cells (again as described previously to corresponding SILAC media cultured cells), and incubated for 1 hour in humid conditions at 37ºC and 5% CO_2. Cells were washed 3 times in 10ml of ice cold PBS. 1ml of ice cold 0.5% NP40 lysis buffer (S.M.19) was added to each dish of cells. The cells were scraped and pipetted into ice chilled plastic microfuge tubes, sonicated using a 200W probe sonicator (LABNET) for 10 seconds and lysed for 45 minutes. The cells were spun at 4ºC and 14,000g for 15 minutes using an 5417R Eppendorf centrifuge. The supernatant was aspirated and transferred to an ice chilled plastic microfuge tube. A Bradford assay was performed to quantify protein (detailed in section 2.19). Once the amount of protein was quantified, the samples were diluted in minimal volumes of 0.5% NP40 lysis buffer so that the “light”, “medium” and “heavy” samples were all of equal protein concentration. 1.5ml of lysates from the “light”, “medium” and “heavy” cultured cells were immunoprecipitated (IP) with 270µl of covalently coupled G-Sepharose beads (described fully in section 2.17) as follows: the “light” DMSO treated cells were mixed with rabbit IgG covalently linked beads, both the

“medium” BafA treated cells and the “heavy” DMSO treated cells were mixed with rabbit anti-occludin covalently linked beads. The tubes were then incubated with rotational mixing at 4ºC overnight, the beads were centrifuged as stated previously to pellet the beads. 1ml of ice cold PBS was added to the tubes containing the beads. The contents of each tube was removed and mixed together in a 15ml plastic centrifuge tube. The empty tubes were washed out with 1ml of ice cold PBS to ensure all beads were removed and again added to the 15ml plastic centrifuge tube. The mixed beads were centrifuged as previously stated, the supernatant aspirated and washed a further 2x with 2ml of PBS. The beads were resuspended in 0.5ml of PBS and transferred to an ice chilled plastic microfuge tube and again centrifuged and the supernatant removed. Proteins were eluted from the mixed beads by adding 100µl of 3x sample buffer, vortexing and boiling the beads 95ºC for 15 minutes. The mixed bead eluate was then centrifuged as previously stated and the supernatant collected. Prior to running the samples a pre-poured NuPAGE Bis-Tris 1.5mm, 10 well 4-12% gradient gel (Invitrogen) was prepared, removing one division from between two lanes to make one large lane. 1X NuPAGE Bis-Tris running buffer (Invitrogen) was prepared (S.M.20). All handling of the gel, gel running, preparation of buffers, staining and washing was undertaken in a laminar flow hood to minimise keratin contamination. The gel was inserted into an XCell SureLock gel electrophoresis tank (Invitrogen) opposite a buffer dam. The running buffer was added following manufacturer instructions. The gel was loaded using gel loading tips with 15µl PageRuler Plus Prestained Protein Ladder (Fermentas) in the lanes either side of the enlarged lane. The enlarged

lane was loaded with 60µl of the collected mixed bead eluate. The gel was run at 125V for 1.5hr using a PowerPac Basic Power Supply (BioRad) power pack. Once the dye front had reached the bottom of the gel, the gel was cracked open, the stacking gel removed and the remaining gel was placed in a new clean wash tub and washed in ultrapure H_2O 3 times for 5 minutes on a rocker (the wash tub only opened in the hood). All H_2O was removed and the gel was incubated in 20ml of Imperial Protein Stain (Thermo Scientific) for one hour on the rocker. After the hour, the stain was removed and the gel was de-stained in ultrapure H_2O for 2 hours, changing the H_2O every 15 minutes. Once the gel had been de-stained the lane containing the mixed bead eluate was divided into 5 sections. Using a new disposable scalpel for each gel section and the ladder as a guide, the lane was divided into sections containing proteins 250-130kDa, 130-70kDa, 70-35kDa, 35-15kDa and 15kDa-gel bottom. The gel plugs were then sent for in-gel digestion by The University of Birmingham Proteomic Unit and subsequent mass spectrometry analysis.

2.21 In-gel digestion (performed by The University of Birmingham Proteomic Unit)

The excised gel samples were sliced into 2 mm^3 cubes, and placed in a 96 well plate. The plate was then centrifuged at 1000g for 3 minutes to pellet all of the gel plugs. To ensure accuracy the washes and addition of reagents was performed by a Qiagen Biorobot 3000 controlled by Qiasoft4 (both Qiagen). acetonitrile (Fisher Scientific), 100mM ammonium bicarbonate (Sigma) (S.M.21) and 10mM DTT (Sigma) (S.M.22) (left capped) were added to the

corresponding well of the Biorobot and the machine loaded with 300µl tips. The 96 well plate containing the plugs was placed on the Biorobot and instructions followed on the pre-programmed software. The first stage was to de-stain the gel; 60µl of acetonitrile was added to each plug, shaken for 5 minutes, the waste was then drawn from the well. 50µl of ammonium bicarbonate solution was added to each well again and shaken for 15 minutes, the waste was then removed. The gel plugs were washed twice in 50µl of ammonium bicarbonate solution. This cycle was repeated if necessary until gel pieces were de-stained. The next step was to dehydrate the samples, to each plug 10µl acetonitrile was added followed by shaking for 15 minutes, and the waste removed. 50µl of ammonium bicarbonate solution was added, shaken for 10 minutes and the waste removed again. 10µl acetonitrile was added to each well and the samples shaken for 15 minutes and the waste removed. The plate was then transferred to an R3000 Rotovap evaporator (Buchi) set at 45ºC and the samples dehydrated for 15 minutes. The plate was placed back on the Biorobot and the DTT cap was removed. The samples were reduced in 25µl DTT solution, placed on a heating block and heated at 60ºC for 15 minutes. 50mM 2-iodoacetamide (S.M.23) was kept covered in foil, placed in the correct well of the Biorobot and uncapped. The plate was placed back in the Biorobot and allowed to cool before alkylation. The waste was taken and 25µl iodoacetamide solution was added to each sample and the plate incubated at RTP in the dark for 45 minutes. The plate was placed back on the Biorobot and the waste removed. The sample was washed in 25µl of ammonium bicarbonate and the waste removed. The samples were then dehydrated by adding 10µl

acetonitrile, shaking for 15 minutes the waste removed then rehydrated in 50µl ammonium bicarbonate, shaken for 10 minutes and the waste taken. A final stage of dehydration was performed; 5µl of acetonitrile was added, shaken for 15 minutes then the waste removed and the plate then taken back to the Rotovap, where the sample was dried completely at 45ºC. Trypsin (Progold) was then made as in S.M.24 and placed in the correct well of the Biorobot. The plate was placed back on the Biorobot and 20µl of the trypsin solution was added to each sample then shaken for 20 minutes. 20µl of ammonium bicarbonate solution was then added to the sample to neutralise the trypsin. The plate was removed, covered with a Qiagen plate cover (Qiagen) and hydrolysis allowed to occur as the plate was incubated at 37ºC overnight. A new plate was placed in the left hand part of the BioBot shaker and the original plate in the right hand part area, and extraction solution A (S.M.25) added to the correct well. 30µl of extraction solution A was added to each original well then shaken for 30 minutes. 23µl of sample from the original plates was transferred into the corresponding well of the new plate. Extraction solution B (S.M.26) was then added to the correct well of the Biorobot, 12µl of extraction solution B and 12µl of acetonitrile was added to the original wells and shaken for 30 minutes. Again 23µl was transferred from each original well to the corresponding well in the new plate. The new plate was removed and the samples dried at 45ºC with the Rotovap (approximately 15 minutes). Resuspension buffer (S.M.27) was added to the correct well of the Biorobot, and the new plate containing the dried samples was placed back on the Biorobot shaker. The samples were then

resupended in 10µl of resuspension buffer. The plate was then covered with a Qiagen plate cover and stored at -80º until mass spectrometry analysis.

2.22 Liquid Chromatography mass spectrometry

5µl of each gel sample (after In gel digestion) were run twice as follows: UltiMate® 3000 HPLC series (Dionex) was used for peptide concentration and separation. Samples were trapped on uPrecolumn Cartridge, Acclaim PepMap 100 C18, 5 um, 100A 300um i.d. x 5mm (Dionex) and separated in Nano Series™ Standard Columns 75 µm i.d. x 15 cm, packed with C18 PepMap100, 3 µm, 100Å (Dionex). The gradient used was from 3.2% to 44% solvent B (0.1% formic acid in acetonitrile) (Fisher Scientific) for 30 minutes. Peptides were eluted directly (~ 300 nL min^{-1}) via a Triversa Nanomate nanospray source (Advion Biosciences) into a LTQ Orbitrap Velos ETD mass spectrometer (ThermoFisher Scientific). The data-dependent scanning acquisition was controlled by Xcalibur 2.7 software. The mass spectrometer alternated between a full FT-MS scan (m/z 380 – 1600) and subsequent collision-induced dissociation (CID) MS/MS scans of the 7 most abundant ions. Survey scans were acquired in the Orbitrap with a resolution of 30000 at m/z 400 and automatic gain control (AGC) $1x10^6$. Precursor ions were isolated and subjected to CID in the linear ion trap with AGC $1x10^5$. Collision activation for the experiment was performed in the linear trap using helium gas at normalized collision energy to precursor m/z of 35% and activation Q 0.25. The width of the precursor isolation window was 2 m/z and only multiply-charged precursor ions were selected for MS/MS.

The Mass spectra were quantified with MaxQuant version 1.0.12.31 software. Data was searched using the peptide search engine Andromeda against the Canis lupus familiaris IPI database. The database was further supplemented with common contaminants such as BSA, keratin and trypsin and the reverse-sequenced versions of the same database. The search parameters were set to cleavage enzyme trypsin/P, maximum 2 missed cleavages, maximum 5 modifications per peptide, maximum charge 7, peptide tolerance 20ppm for first search and 6ppm for main search and mass tolerance 0.5 Da. Cysteine carbamidomethylation (C) was set as a fixed modification, the variable protein modifications were set as oxidation (M), acetylation (Protein N-term), S/T phosphorylation (ST), Y phosphorylation (Y) and ubiquitination (gly/gly). The appropriate SILAC labels were selected and the maximum labelled amino acids was set to 3. The results of the database search were further processed and statistically evaluated using MaxQuant. Proteins with at least 2 peptides (with one unique the protein sequence) were considered as valid identifications. Ratio alterations were considered a “hit” when the values deviated from the median range (identified by a plot of all ratio values). The “hit” classification ratio value were as follows: “heavy” to “light” and “medium” to “light” conditions ≥1.8. In comparing “heavy” to “medium” treated cells a value ≤ 0.5 identifies proteins which IP with increased frequency in “medium” treatment whilst proteins with a ratio value ≥1.4 exhibits increased IP in “light” conditions.

CHAPTER 3

THE ROLE OF VESICLE TRAFFICKING IN EPITHELIAL CELL MIGRATION

3.1 Introduction

Directed cell migration is involved in many pathological and physiological processes, and one of the least studied models of cell migration is epithelial wound healing. Ineffective wound healing poses a significant clinical problem. Incorrectly repaired tissue can severely affect gas and solute exchange as well as the barrier function of the damaged tissue, leading to increased likelihood of secondary infection. *In vivo,* the final stage of re-epithelialisation is collective epithelial cell migration to close the wound. *In vitro*, this can be modelled by mechanical damage to a monolayer of cultured cells.

Regulation of directed cell migration is complex and involves numerous cellular processes (Ridley et al., 2003) (explained in detail in chapter 1). One way in which these processes may be regulated is through vesicle trafficking. Vesicle trafficking represents a key co-ordinator of both the initial morphological changes associated with migration followed by maintenance of this phenotype for persistent migration (Fletcher & Rappoport, 2010; Fletcher & Rappoport, 2009).

Many hypotheses have been suggested as to how vesicle trafficking may regulate cell migration ranging from trafficking of cell adhesion components (Camand et al., 2012; Caswell & Norman, 2006; Chao & Kunz, 2009; Du et al., 2010; Ezratty et al., 2009; Jekely et al., 2005), to recycling of chemoattractant receptors (Bailly et al., 2000; Hopkins et al., 1994) and as means of modulating signalling (de Kreuk et al., 2011; Sorkin, 2001).

Many previous studies have sought to determine a function for specific trafficking pathways in cell migration, and have used disparate assay systems and cell lines; however, due to cell-cell variability and differing migratory stimuli these findings cannot be extrapolated into general understanding (reviewed in Fletcher & Rappoport, 2010; Fletcher & Rappoport, 2009). Therefore the aim of this chapter was to produce a single cohesive model to identify a role for vesicle trafficking in epithelial cell migration during wound healing. The vesicle trafficking pathways examined in this chapter were the dynamin-dependent pathways (CME and caveolar endocytosis), the Rab4- and Rab11-mediated recycling pathways and finally the biosynthetic secretory pathway (Figures 1.5 and 1.6).

The findings of this study demonstrate inhibition of dynamin-dependent internalisation pathways using Dynasore and a dominant negative mutant of dynamin2 (Dyn2(K44A)) significantly inhibited epithelial cell migration. Interestingly, both CME and caveolar endocytosis inhibition by dominant negative mutants reduced the rate of cell motility, however only CME inhibition affected the ability of cells to generate a polarised migratory phenotype. Specific inhibition of the Rab4- and Rab11-dependent recycling pathways

mediated a small but statistically significant reduction in the rate of MDCK migration, with no significant effect on the ability of the cells to polarise. Intriguingly, inhibition of post-Golgi biosynthetic secretory trafficking had no effect on either the rate of cell motility or cellular morphology. These results indicate an important role for both endocytosis and recycling during epithelial cell migration; yet the biosynthetic secretory pathway appears to have minimal function during collective motility.

3.2 Results

In all studies, the MDCK epithelial cell line was used as an epithelial model and directed migration was initiated by wounding a confluent monolayer of MDCK cells plated onto glass. MDCK cells are an excellent model for epithelial wound healing as they have been demonstrated to heal the denuded region by collective directed migration, rather than via cell proliferation or actin-mediated contraction of the wound edge (Fenteany, Janmey, & Stossel, 2000). Furthermore, the scratch wound assay in MDCK cell monolayers is extremely well characterised (Castor, 1968; Rappoport & Simon, 2003).

Transient transfection was used throughout this work. Therefore initial studies to optimise transfection efficiency and cell viability were performed; altering transfection reagent and ratio of transfection reagent to DNA. Using the transfection reagent Lipofectamine 2000 and increasing DNA concentration (as stated in section 2.4), augmented transfection efficiency to 60-80% whilst still maintaining cell viability (data not shown).

Preliminary studies were also performed examining cell migration throughout the wounded region (comparing the migration of cells 0-100μm from the wound edge), it was found that cells within 50μm of the wound edge migrated significantly faster than those outside this region (data not shown). Therefore in studies where transient expression of dominant negative mutants was utilised, only cells within this 50μm region (which did not undergo mitosis or leave the field of view) were measured. The rate of migration of individual fluorescently labelled cells was measured for 6 hours or until the wound closed. Cellular polarisation was measured at time end and the elliptical factors were calculated as the length of the cell divided by the width halfway along the longest axis (Grande-Garcia et al., 2007).

3.3 Inhibition of dynamin-dependent endocytosis significantly reduces the rate of epithelial cell migration

Dynamin is a GTPase localised to the neck of budding vesicles that mediates membrane scission upon GTP hydrolysis (Chappie et al., 2010). Both CME and caveolar endocytosis are dynamin-dependent internalisation pathways however there are other pathways in which dynamin may have a role (Figure 1.4) (Doherty & McMahon, 2009). Multiple studies have implicated dynamin-dependent internalisation in regulation of cell migration in various cell types and migratory models (Bruzzaniti et al., 2005; Chao & Kunz, 2009; Kawada et al., 2009; Macia et al., 2006; Shieh et al., 2011). Work by Kruchten and McNiven (2006), suggest an alternative function for dynamin in cell migration, acting to facilitate membrane expansion, retraction and deformation as well as actin

polymerisation (Kruchten & McNiven, 2006). A useful tool, which has been widely validated as a small molecule inhibitor of dynamin-dependent endocytosis, is Dynasore (Macia et. al., 2006). Dynasore functions by inhibiting GTP hydrolysis, thus preventing membrane scission of budding vesicles (Macia, et al., 2006). Dynasore has greatly facilitated the analysis of endocytosis in a variety of systems (Macia et al., 2006, Chen et al., 2009). Furthermore, it has been previously shown that Dynasore treatment inhibited cell migration (Macia et al., 2006).

To examine the role of dynamin-dependent internalisation during epithelial wound healing, cells were treated with Dynasore or as a control, DMSO (Dynasore was dissolved in DMSO). The monolayer was wounded after pre-treatment and the cells were allowed to migrate in the presence of DMSO/Dynasore for 6 hours. As depicted in Figure 3.1a and 3.1b, MDCK cells incubated with Dynasore show a significant reduction (42%) in the percentage area of the field of view covered with cells in comparison to DMSO treated control cells. To ensure Dynasore was inhibiting dynamin-dependent internalisation pathways, cargo uptake assays were performed using cargo known to undergo endocytosis via either CME or caveolar endocytosis pathways (both dynamin-dependent). To demonstrate the ability of Dynasore to inhibit CME, a low density lipoprotein (LDL) uptake assay was performed. LDL is a lipoprotein which binds to LDL receptors and has been demonstrated to undergo internalisation specifically via CME (Brodsky, 1988; Chen, Goldstein, & Brown, 1989) and has been used widely as a marker of clathrin coated pits

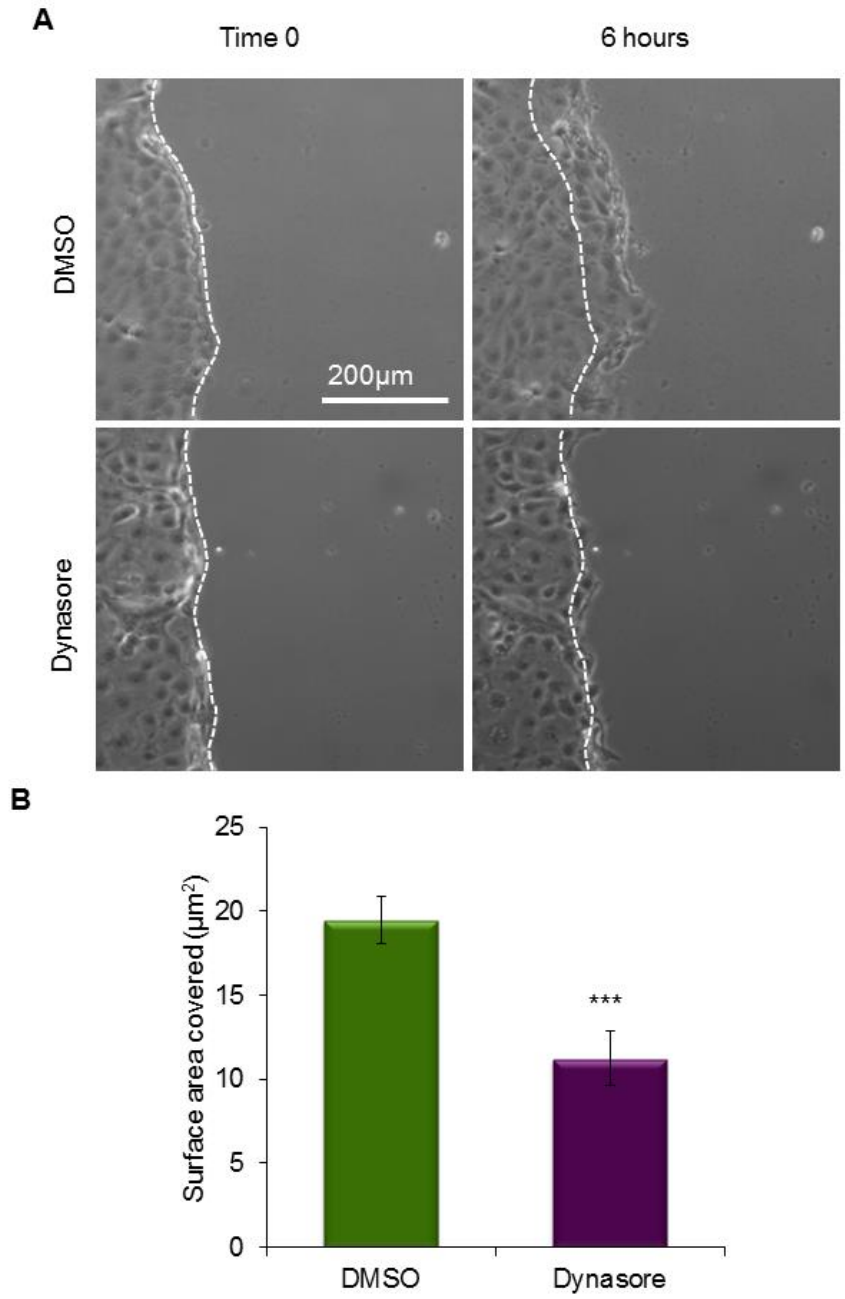

Figure 3.1. Inhibition of dynamin-dependent endocytosis reduces the rate of MDCK epithelial cell migration. MDCK cells were pre-incubated with 80µM Dynasore or 1µl/ml DMSO for 30 minutes, wounded and imaged, a brightfield image was taken every 10 minutes for 6 hours. (A) A brightfield image of control and Dynasore treated cells in a wound healing assay (white line indicates wound edge at time 0). (B) Quantification of Dynasore effect on wound healing (n=3 repetitions). Dynasore significantly inhibited cell migration rates relative to control ($p<0.001$).

(Ehrlich et al., 2004; Keyel et al., 2006). In this study LDL receptor internalisation was imaged using LDL conjugated to a DiI fluorescent probe.

To validate Dynasore as in inhibitor of caveolar endocytosis, a Cholera Toxin B subunit (CTxB) uptake assay was performed. CTxB binds to the GM_1 ganglioside localised in caveolae (Orlandi & Fishman, 1998; Singh et al., 2003). CTxB has been shown to undergo internalisation preferentially by caveolar endocytosis (Orlandi & Fishman, 1998) and has been used widely as a marker of caveolar endocytosis (Ferrari et al., 2003). To examine CTxB internalisation by microscopy; CTxB conjugated to Alexa Fluor 555 was utilised. Internalisation of both CTxB and LDL was quantified by drawing an ROI around the plasma membrane and measuring the average fluorescent intensity within the cell body. A large number of intracellular punctate structures of CTxB and LDL are observed within the DMSO treated control cells, however upon incubation with Dynasore there was a reduction in the number of these structures (Figure 3.2). When the average intensity within the cell body was measured a significant reduction in both DiI-LDL and CTxB-AF555 intensity was observed (32% and 65% respectively), proving Dynasore to be an inhibitor of the clathrin-mediated and caveolar, dynamin-dependent pathways.

The function for dynamin in regulation of epithelial directed migration was further validated by transient expression of a constitutively GDP-bound dynamin2 dominant negative mutant Dyn2(K44A) (Damke et al., 1994). This Dyn2(K44A) mutant has been specifically associated with inhibition of

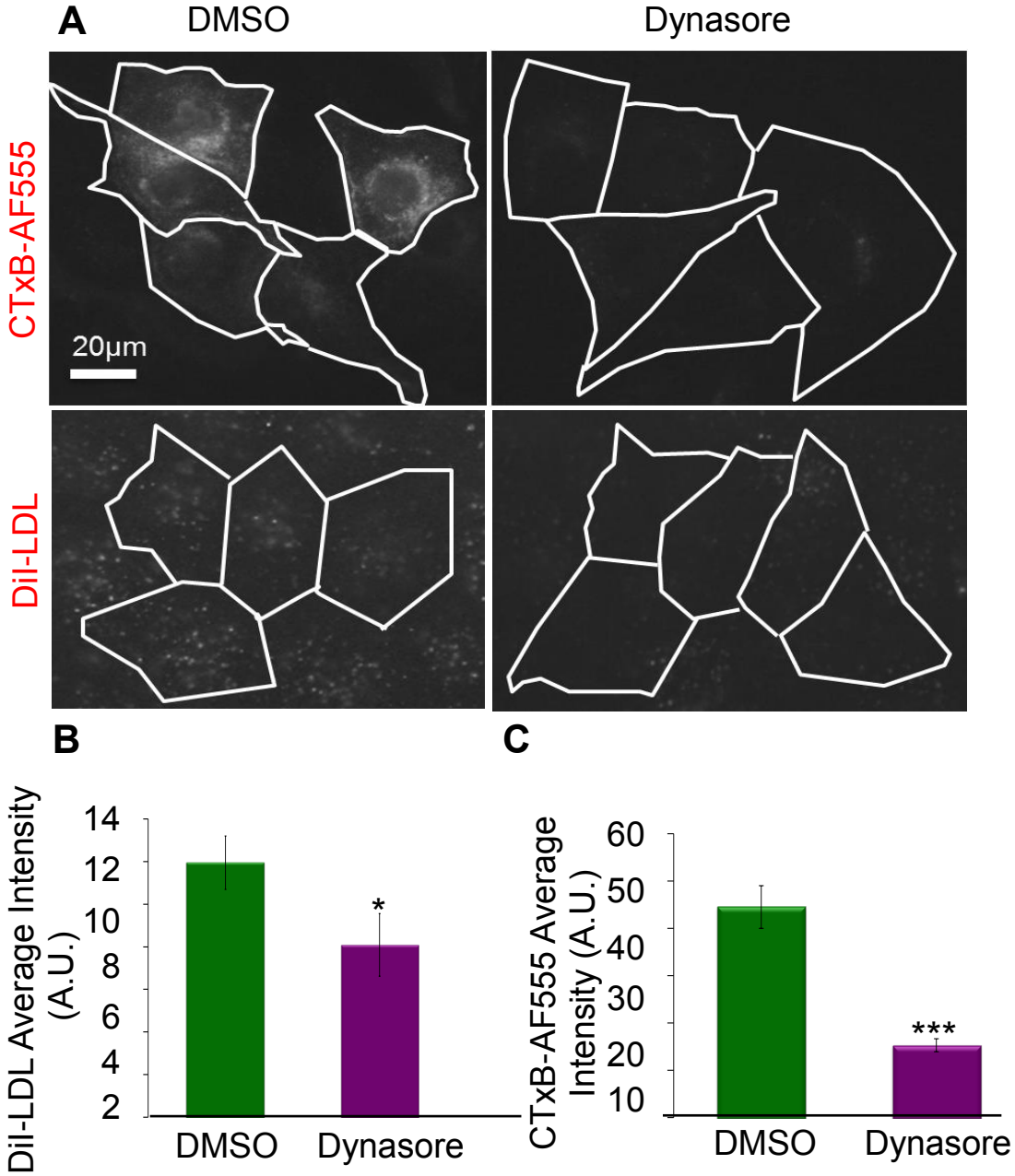

Figure 3.2. Dynasore inhibits caveolar and clathrin-mediated endocytosis. MDCK cells were pre-incubated with 80µM Dynasore or 1µl/ml DMSO for 30 minutes. Cells were then incubated with either 10ng/ml CTxB-AF555 (30 minutes) or 20µg/ml DiI-LDL (15 minutes). Single still brightfield and epifluorescence images were taken. (A) Epifluorescence image of intracellular CTxB-AF555 and DiI-LDL in cells treated with DMSO/Dynasore. The cell outline is depicted in white. (B) Quantification of average DiI-LDL intensity (marker for CME) in MDCK cells treated with Dynasore shows a significant inhibition of DiI-LDL entry compared to DMSO treated control cells ($p < 0.05$; n=74 DMSO control cells and n=63 Dynasore treated cells). (C) Quantification of average CTxB-AF555 intensity (a marker for caveolar endocytosis) in MDCK cells treated with Dynasore shows a significant inhibition of CTxB entry compared to DMSO control cells ($p < 0.001$; n=79 DMSO control cells and n=81 Dynasore treated cells). All cell numbers were taken from 3 independent experiments.

endocytosis in a wide variety of systems (Shieh et al., 2011), including in MDCK cells (Altschuler et al., 1998). In this study a confluent monolayer of MDCK cells expressing Dyn2(K44A)-GFP or GFP (control) was wounded and the cells allowed to migrate for 6 hours. The rate of migration and elliptical factor of individual fluorescently labelled cells was measured. Similarly to Dynasore treated cells, Dyn2(K44A) expressing cells exhibited a significant 27% reduction in the rate of migration in comparison to GFP expressing cells (Figure 3.3a). Furthermore, there was no significant effect of expression of Dyn2(K44A) on elliptical factor in comparison to GFP expressing cells (Figure 3.3b).

3.4 Inhibition of clathrin-mediated endocytosis significantly reduces the rate of epithelial cell migration and reduces polarised migratory morphology

Work by previous groups has implicated a role for CME in cell migration indicating it as an integral function in both disassembly of membrane-substrate interactions in HT1080 fibrosarcoma cells and retraction of the uropod in migrating T-cells (Chao & Kunz, 2009; Samaniego et al., 2007). Recent work both *In vivo* and *In vitro* by Sheih et al., (2011) has also suggested a role for CME in translocation of neurons (Shieh et al., 2011). Several groups have found specific integrin heterodimers undergo internalisation via CME (Ezratty et al., 2009; Chao and Kunz, 2009; Ramsay et al., 2007; Sancey et al., 2009; Upla et al., 2004), again suggesting CME as a critical regulator of cell adhesion and migration. Therefore the effects of CME inhibition on directed

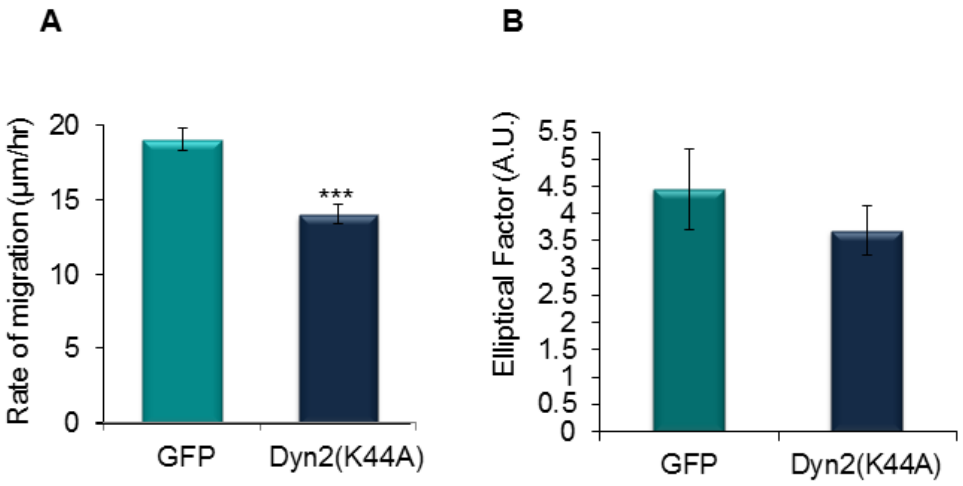

Figure 3.3. Expression of Dyn2(K44A)-GFP significantly reduced the rate of MDCK epithelial cell migration. MDCK cells were transiently transfected with either GFP or Dyn2(K44A)-GFP, wounded and imaged using brightfield and epifluorescence every 10 minutes for 6 hours. (A) Quantification of cell migration during a scratch wound assay in cells expressing either GFP or Dyn2(K44a)-GFP. Cells expressing Dyn2(K44A)-GFP exhibit a significantly reduced rate of migration in comparison to control GFP expressing cells. (B) Quantification of elliptical factor of MDCK cells transfected with Dyn2(K44A)-GFP or GFP DNA, show little alteration in elliptical factor in comparison to control cells. (160 cells of either GFP or Dyn2(K44A)-GFP quantified from 4 individual experiments $p < 0.001$).

migration was observed during epithelial wound healing. CME was inhibited by transient expression of an Eps15 mutant. This mutant is a deletion mutant lacking its third EH (Eps15-homolgogy) domain (Benmerah et al., 1998; Benmerah et al., 1999). This deletion affects the ability of Eps15 and AP-2 to localise to clathrin coated pits and has been shown to inhibit CME (Benmerah et al., 1999). MDCK cells transiently expressing either Eps15(EH29)-GFP demonstrated a significant 37% reduction in the rate of migration during wound healing assays than GFP expressing control cells (Figure 3.4). In addition to inhibiting the rate of migration, EH29-GFP also caused a small but significant decrease in the elliptical factor of cells by 13%. Thus cells on the wound edge transfected with Eps15(EH29)-GFP had a somewhat more rounded and less polarised morphology than control cells (Figure 3.4b).

These results implicate a role for CME in both the initial morphological change responsible for generation of a polarised phenotype but also in maintenance of this phenotype for continued of migration. Although the Eps15(EH29) mutant has been widely validated previously, an LDL uptake assay was performed and analysed as described in section 3.3. Cells expressing Eps15(EH29)-GFP demonstrated a significant reduction in intracellular LDL positive punctate structures in comparison to GFP expressing cells. Quantification of the intracellular average intensity demonstrated a significant 49% reduction in LDL intensity in Eps15(EH29) expressing cells in comparison to control cells (Figure 3.5). Therefore these data indicate the Eps15(EH29) mutant is inhibiting CME and decreasing LDL internalisation.

Figure 3.4. Inhibition of clathrin-mediated endocytosis significantly reduces the rate of epithelial cell migration and reduces polarised migratory morphology. MDCK cells were transiently transfected with either GFP or Eps15(EH29)-GFP and the monolayer was wounded. Cells were imaged by epifluorescence and brightfield every 10 minutes for 6 hours. (A) Epifluorescence image of MDCK cells expressing GFP or Eps15(EH29)-GFP migrating in response to wound formation. The white arrow indicates direction and distance of cell migration, the blue line = wound edge at time 0, red line = wound edge at time end. Scale bars denote 100μm. (B) Enlarged epifluorescence image of cells migrating on the wound edge seen in (A), observation of elliptical factor in cells expressing either GFP or Eps15(EH29)-GFP DNA, the white outline borders the cell membrane. (C) Quantification of rate of migration of MDCK cells transfected with Eps15(EH29)-GFP DNA or GFP DNA. Cells expressing Eps15(EH29)-GFP exhibit a significantly reduced rate of migration in comparison to control GFP expressing cells. (D) Quantification of elliptical factors of MDCK cells transfected with Eps15(EH29)-GFP or GFP DNA, showing a significant decrease in elliptical factor in MDCK cells expressing Eps15(EH29)-GFP. * P-value ≤0.05, *** P-value.

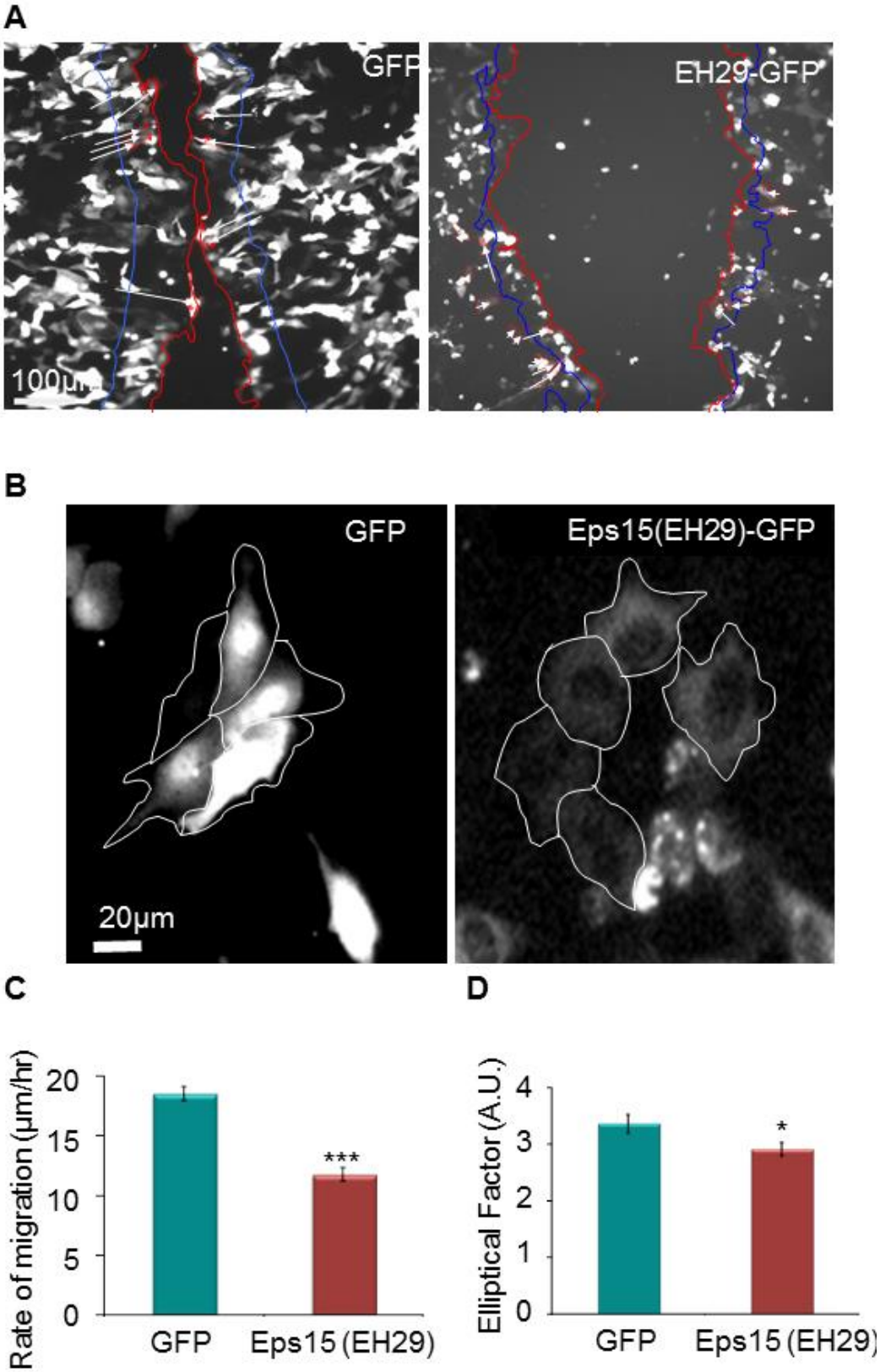
A
GFP
EH29-GFP
100μm
B
GFP
Eps15(EH29)-GFP
20μm
C
Rate of migration (μm/hr)
20
15
10
5
0
***
GFP
Eps15 (EH29)
D
Elliptical Factor (A.U.)
4
3
2
1
0
*
GFP
Eps15 (EH29)

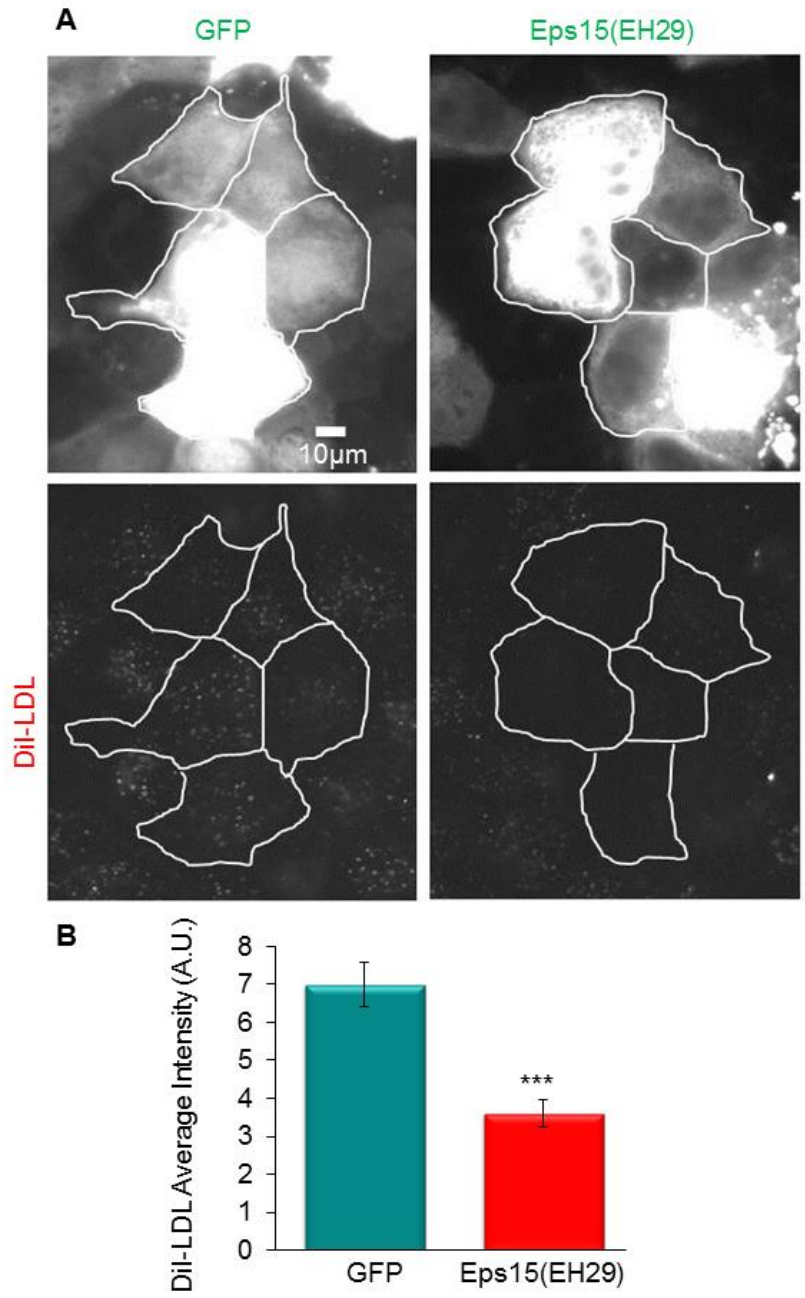

Figure 3.5. Expression of Eps15(EH29-GFP) significantly inhibits CME. MDCK cells were transiently transfected with either Eps15(EH29)-GFP or GFP DNA. Cells were then incubated in 20μg/ml DiI-LDL for 15 minutes then imaged using epifluorescence. (A) Epifluorescence image of intracellular DiI-LDL (a marker for CME) in cells expressing either Eps15(EH29)-GFP or GFP DNA. The cell outline is depicted in white. (B) Quantification of average DiI-LDL intensity in MDCK cells expressing Eps15(EH29)-GFP or GFP. Results show a significant reduction in internalised DiI-LDL in MDCK cells expressing Eps15(EH29)-GFP. ($p < 0.001$; at least 60 cells from 3 separate experiments).

3.5 Inhibition of caveolar endocytosis affects epithelial cell migration but has no effect on generation of a polarised phenotype

In this study the function for caveolar endocytosis in collective epithelial cell migration was examined. Several groups have investigated the role of caveolar endocytosis in regulation of cell migration, however results have been different as it has been implicated as both a positive and negative regulator of cell migration (Galvez et al., 2004; Zhang et al., 2000; Zhou et al., 2004; Kwik et al., 2003; Vassilieva et al., 2008). However, these studies all utilised different cell lines and adopted various methodological strategies to initiate migration. Therefore, this study examined the role for caveolar endocytosis in epithelial cell migration.

To inhibit caveolar endocytosis specifically, a previously published dominant negative caveolin1(Y14F)-GFP mutant was utilised (Orlichenko et al., 2006). This mutant is unable to undergo tyrosine phosphorylation at position 14 (required for caveolar biogenesis) (Orlichenko et al., 2006). Transient expression of caveolin1(Y14F)-GFP in MDCK cells subjected to the scratch wound assay significantly decreased directed migration by 16% in comparison to GFP expressing controls (Figure 3.6a). When the elliptical factor was quantified no significant difference in polarised morphology was observed between cells transfected with GFP or caveolin1(Y14F)-GFP (Figure 3.6b). Therefore these data suggest caveolar endocytosis plays a role in epithelial wound healing, however not for generation of a motile phenotype.

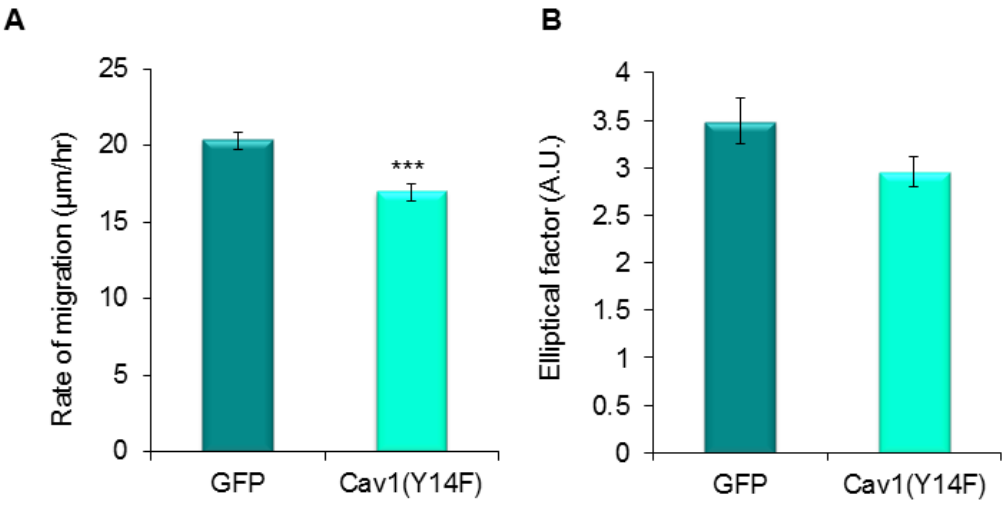

Figure 3.6. Inhibition of caveolar endocytosis significantly reduces the rate of epithelial cell migration. MDCK cells were transiently transfected with either GFP or caveolin1(Y14F)-GFP (cav1(Y14F)), wounded and imaged using brightfield and epifluorescence every 10 minutes for 6 hours. (A) Quantification of cell migration during a scratch wound assay in cells expressing either GFP or cav1(Y14F)-GFP. Cells expressing cav1(Y14F)-GFP exhibit a significantly reduced rate of migration in comparison to control GFP expressing cells. (B) Quantification of elliptical factor of MDCK cells transfected with cav1(Y14F)-GFP or GFP DNA show no alteration in elliptical factor in comparison to control cells. *** P-value ≤0.001. 160 GFP and 143 cav1(Y14F)-GFP cells counted from 4 separate experiments.

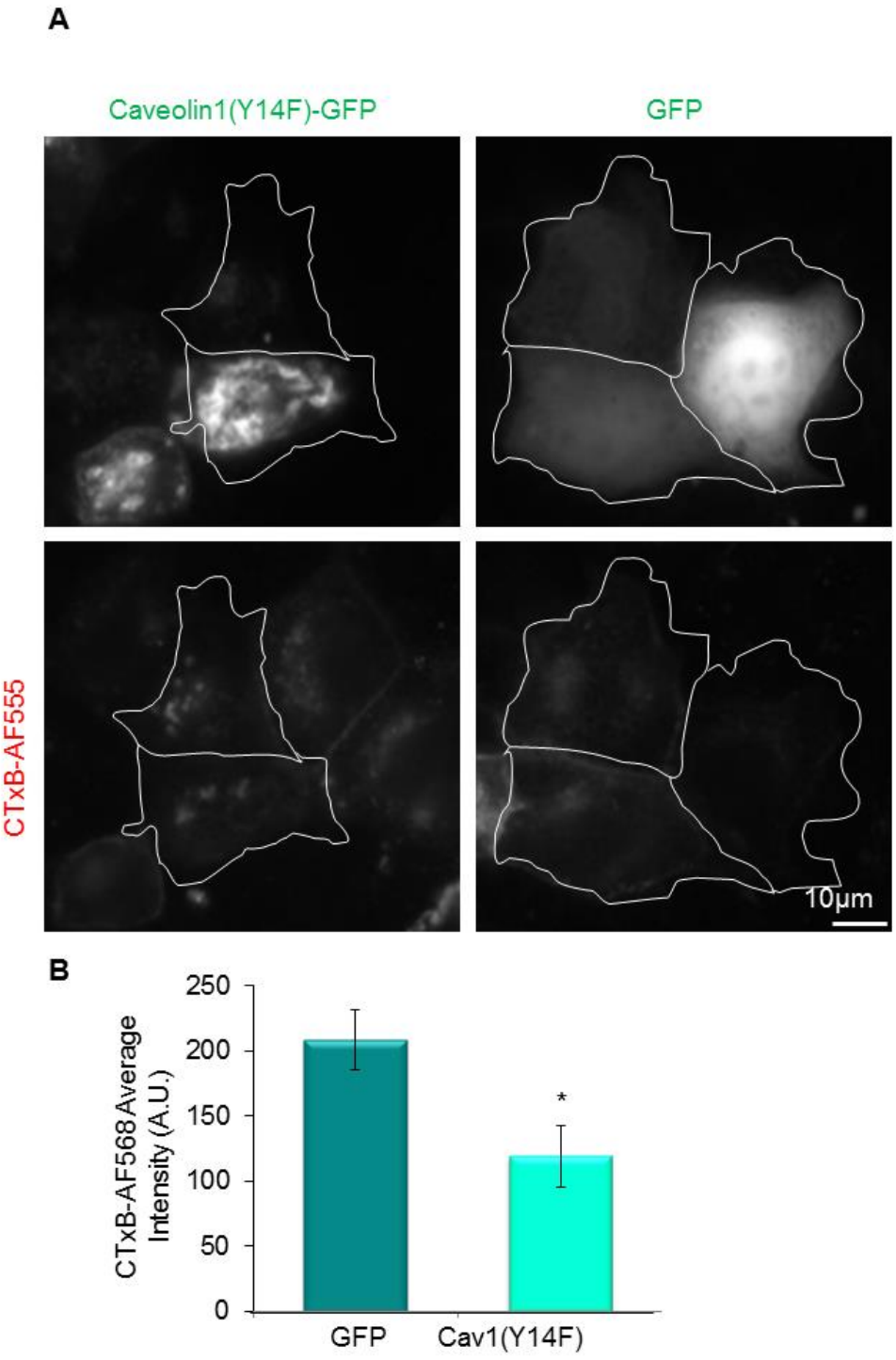

Figure 3.7. Expression of caveolin1(Y14F)-GFP significantly inhibits caveolar endocytosis in MDCK cells. MDCK cells were transiently transfected with either cav1(Y14F)-GFP or GFP DNA. Cells were then incubated in 10ng/ml CTxB-AF555 for 30 minutes, then imaged using epifluorescence. (A) Epifluorescence image of intracellular CTxB-AF555 (a marker for caveolar endocytosis) in cells expressing either cav1(Y14F)-GFP or GFP DNA. The cell outline is depicted in white. (B) Quantification of average CTxB-AF555 intensity in MDCK cells expressing cav1(Y14F)-GFP or GFP. Results show a significant reduction in internalised CTxB-AF555 in MDCK cells expressing cav1(Y14F)-GFP. ($p < 0.05$; at least 60 cells from 3 separate experiments).

It was important to validate caveolin1(Y14F) as an inhibitor of caveolar endocytosis. Despite the caveolin1(Y14F) mutant being previously validated (Orlichenko et al., 2006), the functionality of this mutant to inhibit caveolar endocytosis was assessed by performing a CTxB uptake assay as described in section 3.3. A punctate intracellular distribution of CTxB was observed in both control (GFP) and caveolin1(Y14F) expressing cells, however there was a reduction in the number of these structures in cells expressing caveolin1(Y14F). Analysis of the average intracellular intensity of CTxB demonstrates a statistically significant 43% decrease in intracellular intensity in cells expressing caveolin1(Y14F) as shown in Figure 3.7. These data indicate caveolin1(Y14F) does inhibit caveolar endocytosis.

3.6 Inhibition of post-Golgi biosynthetic trafficking does not affect the rate of epithelial cell migration or polarised migratory morphology

The biosynthetic secretory pathway has also been widely implicated as an important mechanism in cell migration. Work by Bershadsky & Futerman, (1994) found disruption of the Golgi by brefeldin A led to the inability of Swiss 3T3 fibroblasts to generate a motile polarised morphology and decreased directed migration on a planar 2D surface. This result was further corroborated in the same cell line in studies by Prigozhina and Waterman-Storer (2004). This group identified decreased lamellipodial activity and migration upon expression of mutant PKD (PKD(K618N)-GFP) (Prigozhina & Waterman-Storer, 2004). PKD(K618N)-GFP is a kinase dead mutant of PKD which has been demonstrated to inhibit membrane fission and production of vesicles from the

trans-Golgi-network (TGN) (Liljedahl et al., 2001). From work by Prigozhina & Waterman-Storer, (2004) a connection has been formed between fibroblast migration and trafficking of newly synthesised proteins to the plasma membrane. Therefore this study investigated the role of the biosynthetic secretory pathway during epithelial wound healing. This study utilised the kinase dead PKD(K618N) mutant expressed in migrating MDCK cells to inhibit post-Golgi trafficking. Transient expression of PKD(K618N)-GFP for 24 hours and repetition of our previous experimental parameters demonstrated no significant alteration in either the rate of migration or the ability of cells to polarise (Figure 3.8) (experiments performed and analysed by Elizabeth Haining). This experiment was also repeated with extended expression (48 hours) of PKD(K618N)-GFP and again no alteration in migratory phenotype was observed (data not shown). This study indicated that there was a minimal role for the biosynthetic secretory pathway in regulation of epithelial cell migration. As no effect on migratory phenotype was observed upon expression of PKD(K618N), the functionality of this mutant in inhibition biosynthetic secretion was measured. A cargo trafficking assay was performed; co-transfecting MDCK cells with secretory cargo Neuropeptide Y labelled with a red fluorescent protein tag (NPY-mRFP) and either GFP (control) or PKD(K618N)-GFP. As NPY is a soluble secretory protein which does not undergo recycling, all intracellular mRFP fluorescence signal is from newly synthesised NPY-mRFP protein. Thus any inhibition of Golgi secretion should lead to retention of NPY-mRFP within the Golgi and increased NPY-mRFP intensity. Average intracellular NPY intensity was quantified as in previously described cargo

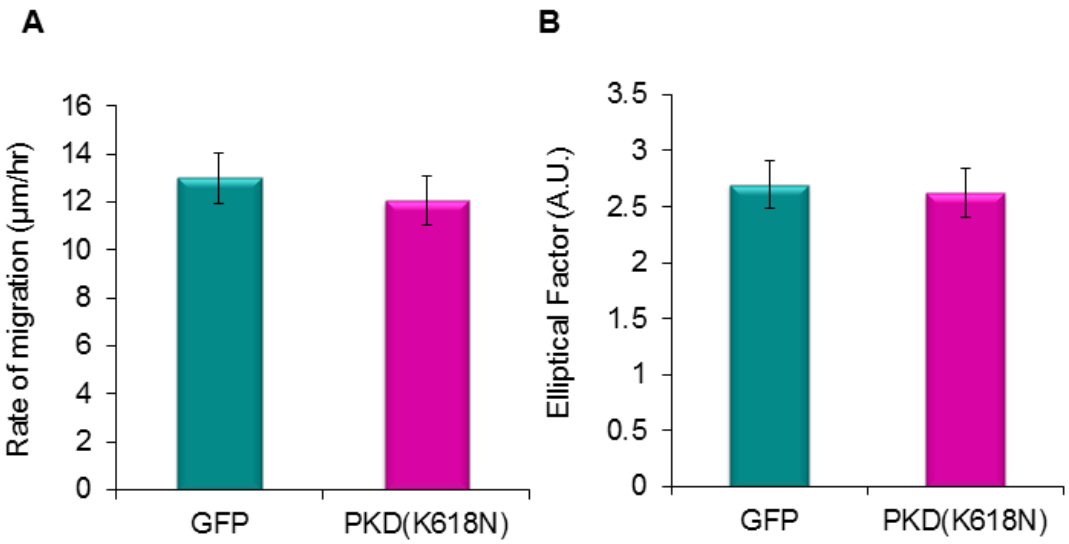

Figure 3.8. Inhibition of post-Golgi biosynthetic trafficking does not affect the rate of MDCK epithelial cell migration or polarised migratory morphology. MDCK cells were transiently transfected with either GFP or PKD(K618N)-GFP, wounded and imaged using brightfield and epifluorescence every 10 minutes for 6 hours. (A) Quantification of cell migration during a scratch wound assay in cells expressing either GFP or PKD(K618N)-GFP. Cells expressing PKD(K618N)-GFP exhibit no significant alteration in the rate of migration in comparison to control GFP expressing cells. (B) Quantification of elliptical factor of MDCK cells transfected with PKD(K618N)-GFP or GFP DNA, show no significant alteration in elliptical factor in comparison to control cells. 157 GFP expressing cells and 143 PKD(K618N)-GFP expressing cells were analysed from 4 separate experiments.

trafficking assays (sections 3.4 and 3.5).

In cells transfected with PKD(K618N) there was an observable increase in NPY-mRFP localised to globular structures adjacent to the nucleus (likely to be the TGN). Although these structures were observed in the GFP expressing cells, they did not appear enlarged (as seen in the PKD mutant expressing cells). When average NPY intensity was quantified, a significant 40% increase in NPY fluorescence was demonstrated in cells expressing PKD(K618N)-GFP (Figure 3.9). These data confirm functionality of PKD(K618N)-GFP as an inhibitor of the biosynthetic secretory pathway.

3.7 Inhibition of endosomal recycling significantly reduces the rate of epithelial cell migration and affects polarised migratory morphology

The process of endosomal recycling has widely been accepted as a critical requirement for cell migration (Jones, Caswell, & Norman, 2006; Nabi, 1999). Several hypotheses have been formed to its exact role, with suggestions varying from recycling of bulk membrane to recycling of individual cell adhesion molecules and chemotaxis receptors (Bretscher, 1984; Sheetz et al., 1999). However, the function of endosomal vesicle trafficking may be modified in response to various migratory stimuli (Fletcher & Rappoport, 2009). The two pathways under examination in this section are the Rab4- and Rab11-mediated recycling pathways (Figure 1.5 and 1.6). One way in which Rab4-mediated recycling may regulate cell migration is through trafficking of cell adhesion molecules (Roberts et al., 2001; Woods et al., 2004).

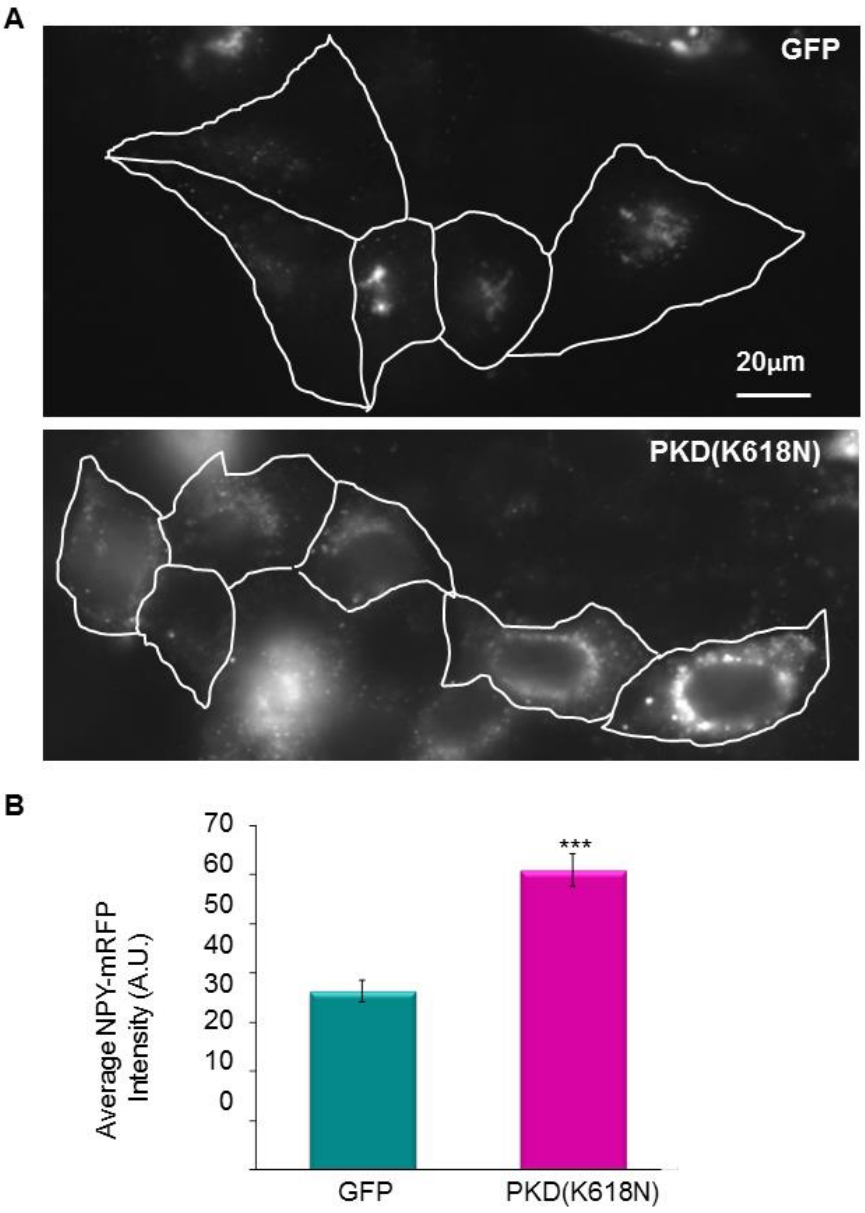

Figure 3.9. PKD(K618N)-GFP significantly inhibits post-Golgi biosynthetic trafficking in MDCK cells. MDCK cells were transiently co-transfected with either PKD(K618N)-GFP or GFP and NPY-mRFP DNA. Single still epifluorescence and brightfield images of cells were taken. (A) Epifluorescence image of intracellular NPY-mRFP (a marker for the biosynthetic secretory pathway) in cells expressing either PKD(K618N)-GFP or GFP DNA. The cell outline is depicted in white. The average intensity of NPY-mRFP in cells expressing either GFP or PKD(K618N)-GFP. (B) Quantification of average NPY-mRFP intensity in MDCK cells expressing PKD(K618N)-GFP or GFP. Results show a significant increase in intracellular NPY-mRFP in MDCK cells expressing PKD(K618N)-GFP. *** P-value ≤0.001 n=3. (190 GFP expressing cells and 226 PKD(K618N)-GFP expressing cells analysed from 4 separate experiments).

In studies where Rab4-dependant recycling was inhibited in fibroblasts, cells displayed increased migratory tortuosity potentially due to effects on integrin recycling (White, Caswell, & Norman, 2007). As a function for Rab4-mediated trafficking has been demonstrated in fibroblast cell lines, this study examined the function of this pathway during epithelial wound healing. To specifically inhibit Rab4-dependent recycling a Rab4 mutant unable to bind GTP, Rab4(S22N)-GFP (Mohrmann et al., 2002) was utilised. This mutant has previously been shown to decrease recycling of transferrin, and facilitate its accumulation in a perinuclear compartment (McCaffrey et al., 2001).

Transient expression of Rab4(S22N)-GFP in MDCK cells followed by initiation of directed migration in the scratch wound assay, produced a migratory phenotype which was significantly slower than GFP expressing control cells, inhibiting migration by 20% (Figure 3.10a). No alteration in the ability of Rab4(S22N)-GFP expressing cells to initiate development of a polarised phenotype was observed (Figure 3.10b). These data suggest that Rab4-mediated trafficking has a function during directed epithelial wound healing.

The other trafficking pathway implicated in cell migration is the Rab11-mediated recycling pathway. The function of this trafficking pathway is cell line specific and has been suggested to regulate trafficking via the PNRC in BHK and CHO cells, or the apical recycling compartment in polarised MDCK cells (Maxfield & McGraw, 2004; Ullrich et al., 1996; Weisz & Rodriguez-Boulan, 2009). A function for this pathway has been established in cell migration studies. Experiments in PtK1 epithelial cells demonstrated expression of dominant

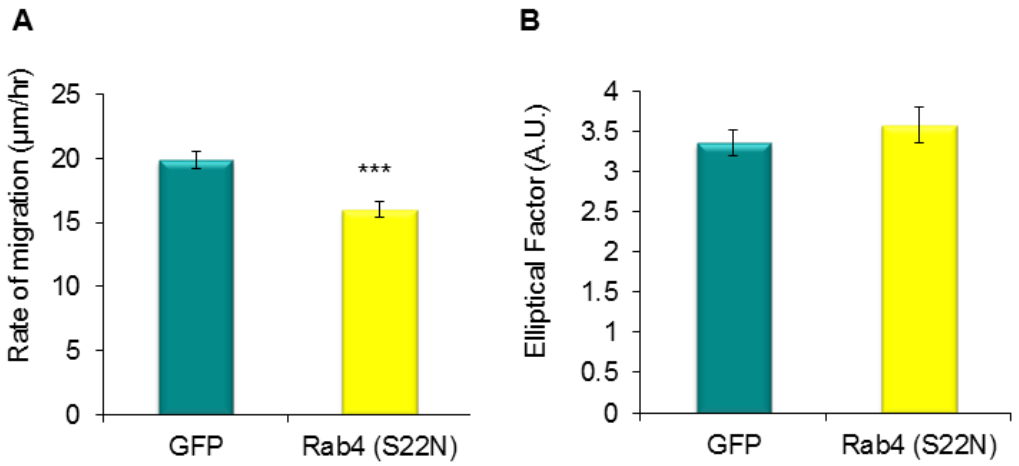

Figure 3.10. Inhibition of Rab4-mediated endosomal recycling significantly reduces the rate of MDCK epithelial cell migration. MDCK cells were transiently transfected with either GFP or Rab4(S22N)-GFP, wounded and imaged using brightfield and epifluorescence every 10 minutes for 6 hours. (A) Quantification of cell migration during a scratch wound assay in cells expressing either GFP or Rab4(S22N)-GFP. Cells expressing Rab4(S22N)-GFP exhibit a significantly reduced rate of migration in comparison to control GFP expressing cells. (B) Quantification of the elliptical factor of MDCK cells transfected with Rab4(S22N)-GFP or GFP DNA show no significant alteration in elliptical factor in comparison to control cells. *** P-value ≤0.001. (160 GFP expressing cells and 160 Rab4(S22N)-GFP expressing cells analysed from 4 separate experiments).

negative Rab11b severely affected cell migration (Prigozhina & Waterman-Storer, 2006). This study investigated the role of Rab11-mediated recycling during epithelial wound healing. A GFP tagged Rab11a mutant unable to bind GTP, (Rab11a(S25N)-GFP (Ren et al., 1998)), was transiently expressed in MDCK epithelial cells (Prigozhina & Waterman-Storer, 2006). Cell migration and elliptical factors were measured as previously described. Expression of Rab11a(S25N)-GFP significantly reduced rates of epithelial migration by 13% in comparison to GFP expressing control cells (Figure 3.11a). Alterations in polarised phenotype were also observed in MDCK cells expressing Rab11a(S25N)-GFP, with cells displaying a slightly elongated phenotype which was not observed in control cells (Figure 3.11b). Although this elongation was only nearing statistical significance, it is consistent with observations in other cell lines where difficulties retracting the lagging edge were seen (Prigozhina & Waterman-Storer, 2004). These data may indicate a function for Rab11a in retraction of the cell rear aiding in maintenance of continued migration.

3.8 Discussion

The findings from this study, the first systematic analysis of the role of several vesicle trafficking pathways in directed epithelial cell migration, indicate a key function for trafficking in epithelial cell motility. For the first time the function of specific vesicle trafficking pathways has been observed in a single epithelial wound healing model assessing both the ability of cells to generate a polarised morphology and in maintenance of steady-state motility.

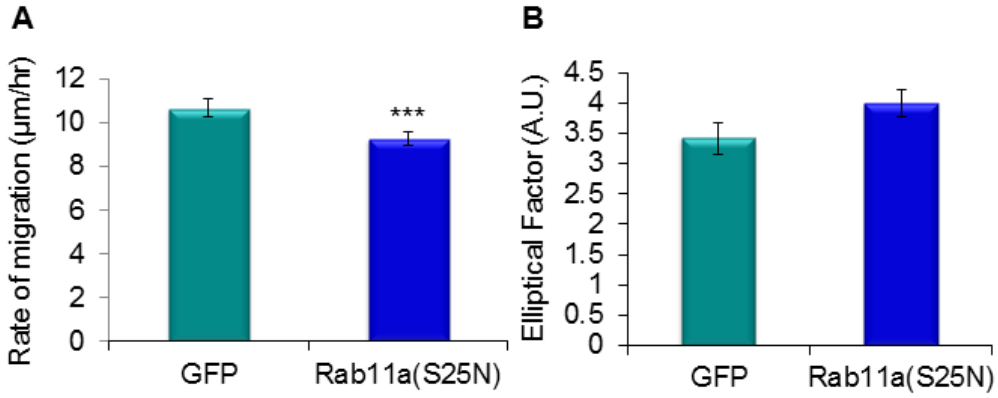

Figure 3.11. Inhibition of Rab11-mediated endosomal recycling significantly reduces the rate of epithelial cell migration and affects polarised migratory morphology. MDCK cells were transiently transfected with either GFP or Rab11a(S25N)-GFP, wounded and imaged using brightfield and epifluorescence every 10 minutes for 6 hours. (A) Quantification of cell migration during a scratch wound assay in cells expressing either GFP or Rab11a(S25N)-GFP. Cells expressing Rab11a(S25N)-GFP exhibit a significantly reduced rate of migration in comparison to control GFP expressing cells. (B) Quantification of elliptical factor of MDCK cells transfected with Rab11a(S25N)-GFP or GFP DNA show a small but not statistically significant elongation in comparison to control cells. *** P-value ≤0.001. (160 GFP expressing cells and 157 Rab11a(S25N)-GFP expressing cells analysed from 4 separate experiments).

The results from this study demonstrate that within the MDCK epithelial wound healing model, dynamin-dependent internalisation pathways have an important function during epithelial cell migration. Furthermore, upon analysis of specific dynamin-dependent pathways, it was observed CME was required for both generation of a motile phenotype and steady-state migration. Caveolar endocytosis on the other hand, is required only for continued epithelial cell migration. In contrast, exocytosis of newly synthesised cargo from the Golgi via the biosynthetic secretory pathway plays minimal role in either development of the motile phenotype or continued migration. However, exocytosis of cargo undergoing recycling via the Rab4- and Rab11-dependent endosomal recycling pathways were not essential for generation of a polarised phenotype but were required for effective cell migration.

The findings in this chapter and in research from other groups suggest dynamin-dependent internalisation pathways are a requirement for effective cell migration. As described previously, dynamin is required for both CME and caveolar endocytosis and has been implicated in both pinocytosis and flotillin-dependent internalisation (Damke et al., 1994; Doherty & McMahon, 2009; Payne et al., 2007). As observed in this study, migratory defects upon inhibition of dynamin-dependent internalisation have been observed by several groups. These groups utilised a variety of tools (dominant negative dynamin mutants, siRNA against dynamin and pharmacological dynamin inhibition) to identify an important function for dynamin in regulation of cell migration (Bruzzaniti et al., 2005; Chao & Kunz, 2009; Kawada et al., 2009; Macia et al., 2006; Shieh et al., 2011). This chapter further identified the function of specific dynamin-

dependent internalisation pathways (CME and caveolar endocytosis) during epithelial motility. CME and caveolar endocytosis were inhibited by expression of dominant negative mutants to selectively inhibit each pathway.

As stated in section 3.4, specific inhibition of CME decreased both the ability of MDCK cells to generate a polarised phenotype and maintain steady state migration. Effects on cell migration have been observed upon CME inhibition in other migratory models. In fibroblast derived cell lines undergoing random migration and T lymphocytes undertaking basal and CXCL12 induced migration, CME inhibition severely abrogated cell translocation (Chao & Kunz, 2009; Samaniego et al., 2007). Similar studies in the SVZa neuronal cell line where CME was inhibited by monodansyl cadaverine and DN-Hub (encodes the Hub region of clathrin heavy chain preventing clathrin coat formation) showed decreased invasion into Matrigel but did not affect neuronal morphology (Shieh et al., 2011). Both the findings in this chapter and findings of previous groups suggest an important role for CME in cell migration, however the exact mechanism through which CME may be regulating cell migration is currently unknown and requires further investigation.

Like CME, caveolar endocytosis is a dynamin-dependent internalisation pathway which has also been widely implicated in regulation of cell migration. As described in detail in chapter 1, many groups have linked caveolar endocytosis as a regulator of cell migration. Also the migratory defects demonstrated upon inhibition of caveolar endocytosis correspond with previous research (Grande-Garcia et al., 2007). Observations of cell migration in caveolin1 knockout mouse embryonic fibroblasts (MEFs) identified a reduction

in the rate of migration and a rounded morphology in wound healing assays. Interestingly, this rounded phenotype was not observed in MDCK cells upon inhibition of caveolar endocytosis. This may be a cell specific variant as both the MDCK cell line used in this study and caveolin knock out MEFs were undergoing migration in response to loss of contact inhibition. Furthermore, work by Podar et al., (2004) suggests a role for caveolae in VEGF induced Multiple Myeloma cell migration; cells treated with β-cyclodextrin or expressing antisense full-length caveolin1 mRNA (under the influence of an inducible promoter), showed decreased migration in a Boyden chamber (Podar et al., 2004). Similarly, in primary human astrocytes; caveolin1 siRNA inhibited chemotaxis towards monocyte chemoattractant protein 1 in a transwell migration assay (Ge & Pachter, 2004). The data obtained in this chapter and from other groups demonstrate an important function for caveolae in cell migration. It is unknown exactly how caveolae regulate cell migration and is a question which is further complicated by other non-endocytosis functions for caveolae.

Caveolae are home to many signalling molecules, therefore caveolae may act to coordinate and organise signalling pathways from caveolar compartments (Isshiki et al., 2002a; Isshiki et al., 2002b). However, an alternative role for caveolae has emerged suggesting that caveolae may regulate plasma membrane tension by responding to mechanical stress. Caveolae have been proposed to act as a “membrane reserve” flattening and disassembling during increased mechanical strain (Sinha et al., 2011). Work by Isshiki et al., (2002a) also suggests a role for caveolae in sensing/regulating mechanical stress as

cells grown under laminar stress showed a redistribution of caveolae (Isshiki et al., 2002a). Thus inhibition of caveolar biogenesis by caveolin1(Y14F), could also affect epithelial wound healing via effects on signalling and regulation of mechanical stress, as well as through trafficking of cell-surface proteins and lipids.

As endocytosis appears to have such an important functioning during epithelial wound healing, the next aim of the chapter was to examine the function of exocytosis in regulation of collective cell migration, firstly examining the biosynthetic secretory pathway. This study demonstrated that selective inhibition of the biosynthetic secretory pathway had no effect on either the generation of a motile phenotype or its maintenance in persistent cell motility in MDCK cells; contrasting with previous findings in fibroblast derived cell lines (Prigozhina & Waterman-Storer, 2004). When the PKD(K681N) mutant was expressed in NIH3T3 cells a significant reduction in cell migration was recorded. Later research from this same group contained an unpublished observation that expression of the PKD(K618N) mutant in migrating PtK1 epithelial cells caused no discernible migratory phenotype, corroborating the findings in this chapter (Prigozhina & Waterman-Storer, 2006). This indicates the biosynthetic secretory pathway is critical for migration in some cell types but appears to be dispensable in epithelial cells, again highlighting the importance of a systematic study in a single cellular model. Yet, these data imply that if trafficking of proteins synthesised de-novo to the plasma membrane is not important for cell migration then perhaps recycling of “ready-made” proteins may play a more important role in epithelial wound healing. Therefore, the function for Rab4- and

Rab11-mediated recycling pathways in regulation of collective migration was also examined.

Inhibition of Rab4-dependent recycling during wound closure showed a significant decreased in the rate of epithelial cell migration. These findings corroborate with recent studies by Linford et al., (2012) in the A459 human alveolar adenocarcinoma epithelial derived cell line where Rab4 siRNA reduced the rate of migration in a scratch wound assay (Linford et al., 2012). This finding was further supported by recent *in vivo* studies performed by Kawauchi et al., (2010) who found inhibition of Rab4-mediated recycling by expression of Rab4(S22N) affected migration of cortical neurons (Kawauchi et al., 2010). However it must be noted; although migration was altered, the migratory defect was not statistically significant.

Evidently a function for Rab4-mediated recycling exists during MDCK migration, therefore the Rab11-dependent trafficking pathway was also investigated for a potential role during epithelial wound healing. Inhibition of Rab11 in MDCK cells demonstrated a reduction in the rate of epithelial cell migration suggesting an important function during epithelial wound healing. Moreover it also showed a nearly statistical significant alteration in polarised phenotype, with cells becoming elongated and apparently having problems retracting their lagging edge. This correlates with previous data detailed by Linford et al., (2012). Again siRNA was used to inhibit Rab11 in A459 cells during a wound healing assay and a decrease in the ability to close the wound was recorded (Linford et al., 2012). Interestingly studies performed by Prigozhina and Waterman-Storer (2006), show a range of migratory defects depending upon transient/stable

dominant negative Rab11b expression and migratory stimulus (Prigozhina & Waterman-Storer, 2006). When small “islands” of PtK1 epithelial derived cells were transiently transfected with Rab11b(S25N), the cells exhibited increased velocity (opposite to observations made in section 3.7), with cells exhibiting an increased likelihood to migrate away from the island and a more elongated morphology then control cells. This phenotype is consistent with results obtained in section 3.7 where transient expression of Rab11a(S25N) led to MDCK cells displaying a more polarised phenotype and appeared to have problems detaching from the substrate. Recent work by Kessler et al., 2012 has also suggested a role for Rab11 in HeLa cell stretching, where expression of Rab11(S25N) lead to an increase in the ability of HeLa cells to stretch on both glass and fibronectin which may explain the slight elongation observed in chapter 3.7. (Kessler et al., 2012). This work also demonstrates expression of Rab11(S25N) significantly decreased the ability of MDA-MB231 breast cancer cells to maintain a single direction during random migration, but again no alteration in velocity was observed similar to the findings of the Waterman-Storer group. However in stable Rab11b expressing PtK1 cells undergoing directed migration in a scratch wound assay, wound healing defects were observed as seen in MDCK cells in section 3.7 (Prigozhina & Waterman-Storer, 2006). This was suggested to be due to cells developing a more tortuous migratory pattern, rather than a reduced rate of motility (Prigozhina & Waterman-Storer, 2006). Although no effect on directionality has been observed in MDCK cells expressing Rab11a(S25N) (section 3.7), and a decrease in the rate of migration was observed rather than an increase; this

could be due to either cell-cell variability or a role for Rab11b in cell directionality whilst Rab11a somehow regulates rate of migration.

Utilising the findings in this chapter, a new model for how vesicle trafficking may regulate cell migration in epithelial cells undergoing directed migration has arisen. This model suggests that endocytosis of cargo via the dynamin-dependent pathways (clathrin-mediated and caveolar endocytosis) occurs and is transported back to the plasma membrane, potentially by Rab4- and Rab11-mediated recycling. This is a departure from earlier models where protein biosynthesis and exocytosis of newly formed proteins have been implicated in cell migration (Prigozhina & Waterman-Storer, 2006; Yadav et al., 2009). How this model facilitates cell migration is yet to be ascertained, dynamin-dependent endocytosis may aid in cell migration via release of cell adhesion molecules from the substrate and their subsequent internalisation. Moreover, certain specific integrin subunits and heterodimers have already been identified as undergoing internalisation and trafficking via specific pathways (Altankov & Grinnell, 1995; Chao & Kunz, 2009; De Deyne et al., 1998; Ramsay et al., 2007; Sancey et al., 2009; Upla et al., 2004). The Rab4- and Rab11-mediated recycling pathways have been widely implicated as a key requirement for trafficking of several integrin subunits (Roberts et al., 2001; White, Caswell, & Norman, 2007; Woods et al., 2004) reviewed fully in (Fletcher & Rappoport, 2009; Fletcher & Rappoport, 2010). Furthermore, endocytosis and vesicle trafficking of cell-cell adhesion molecules may play a role in regulation of epithelial cell migration (Camand et al., 2012; Du et al., 2010; Kawauchi et al.,

2010). Taken together this study identifies a key function for several vesicle trafficking pathways during epithelial wound healing.

3.9 Key chapter findings

- CME is required for MDCK cell migration and generation of a polarised phenotype.
- Caveolar endocytosis, Rab4- and Rab11-mediated recycling are required during epithelial wound healing but not for development of a motile phenotype.
- The biosynthetic secretory pathway has minimal role during directed epithelial migration.

3.10 Conclusion

As the first systematic study utilising a single epithelial cell line in a physiologically relevant migratory assay system, this research confirms the critical role for several trafficking pathways in both generation of a motile phenotype and for subsequent migration. CME is required for both the initial development of the migratory phenotype and for continued migration while caveolar endocytosis is required for steady-state migration only. Furthermore, this study confirmed the Rab4- and Rab11-mediated vesicle recycling pathway has a key function in epithelial cell migration, while the biosynthetic secretory is dispensable during epithelial wound healing.

CHAPTER 4

POLARISED TRAFFICKING IN MIGRATING EPITHELIAL CELLS

4.1 Introduction

Vesicle trafficking has been established as a major regulator of cell migration and polarisation as shown in chapter 3 (Fletcher et al., 2012, Fletcher & Rappoport, 2010; Fletcher & Rappoport, 2009). In the previous chapter, dynamin-dependent, clathrin-mediated and caveolar endocytosis were demonstrated to be required for collective epithelial cell migration, along with the Rab4 and Rab11 recycling pathways. Interestingly, abrogation of the biosynthetic secretory pathway did not affect MDCK cell migration.

Evidently, vesicle trafficking is a vital regulator of MDCK cell migration, yet the extent to which these trafficking pathways are polarised during epithelial wound healing is less well understood. Data in other cell types from groups suggest polarised trafficking occurs during cell migration (reviewed in Fletcher & Rappoport, 2010). As described in section 1.6 there are three proposed mechanisms through which polarised trafficking may regulate cell migration; the "rear to front trafficking model" (Sheetz et al., 1999), the "bulk membrane flow model" (Bretscher, 1984) and finally polarised receptor recycling during

chemotaxis (Bailly et al., 2000). Recent advancements in microscopy and live cell imaging have enabled researchers to accurately visualise and further elucidate the role of vesicle trafficking in cell migration (reviewed in Fletcher & Rappoport, 2009). One recently developed technique is TIRF microscopy. TIRF microscopy provides the ability to selectively illuminate fluorophores associated with the adherent plasma membrane, avoiding contamination of images from out-of-focus cytosolic signal (Axelrod, 1981). This makes TIRF microscopy an ideal platform to examine the potential for polarisation of vesicle trafficking pathways in migrating cells (Rappoport et al., 2003). Previous work using TIRF microscopy has already shown CME polarised to the front of migrating MDCK cells (Rappoport & Simon, 2003).

Therefore, in this chapter a systematic analysis of the potential for polarisation of other vesicle trafficking pathways in migrating MDCK cells was performed using TIRF microscopy. Although much data has examined localised trafficking of specific cargo molecules (Bailly et al., 2000; Kamimura et al., 2008; Roberts et al., 2001; Roberts et al., 2004; Sheetz et al., 1999; White, Caswell, & Norman 2007; Woods et al., 2004) little research has investigated polarisation of specific recycling pathways during migration, particularly in epithelial cell lines. Through application of fluorescently labelled marker proteins and TIRF microscopy, the potential for polarised caveolar endocytosis, Rab11- and Rab25-mediated recycling was examined. These pathways were selected as their inhibition had been shown to effect epithelial migration in chapter 3. Moreover, previous observations have identified polarisation of caveolar endocytosis, yet its localisation to the cell front or rear has been disputed (Galvez et al., 2004;

Isshiki et al., 2002a; Parat, Anand-Apte, & Fox, 2003). Conversely, no literature exists on polarisation of the Rab11 trafficking pathway; therefore this study sought to be the first to identify polarisation of caveolar endocytosis events and Rab11 trafficking in migrating epithelial cells. Examination of Rab25 recycling was also investigated as minimal research has been performed to identify the function of this epithelial cell specific member of the Rab11 family during cell migration (Goldenring et al., 1993). However, Rab25 has been demonstrated to localise to the apical recycling compartment with Rab11 in polarised MDCK cells (Casanova et al., 1999) (Figure 1.6) and may function in regulating cell migration via integrin trafficking (Caswell et al., 2007; Cheng et al., 2004). Therefore its epithelial specificity, similarity to Rab11 and role in migration makes Rab25 an interesting candidate to assess for polarised trafficking during epithelial wound healing.

The results of this study, utilising transient expression of caveolin1-mRFP as a marker of caveolar endocytosis identifies polarisation of caveolar endocytosis to the rear of migrating MDCK cells. However, expression of Rab11-GFP or Rab25-GFP and thorough examination of exocytic events via these pathways show polarised fusion of recycling endosomes does not occur during collective cell motility. In summary, this study suggests that polarised endocytosis, but not exocytosis regulates epithelial wound healing.

4.2 Results

4.3 Caveolar endocytosis is polarised to the rear of migrating epithelial cells

In the past decade many groups have examined the function of clathrin-independent endocytosis pathways in cell migration. One such pathway is caveolar endocytosis. Caveolae are flask-shaped invaginations rich in cholesterol and sphingolipids and densely populated with many signalling molecules (de Laurentiis, 2007). Recently, research from multiple groups suggested caveolar endocytosis may be required for internalisation of specific integrin heterodimers, linking caveolar endocytosis with turnover of substratum attachments in migrating cells (Shi & Sottile, 2008; Tayeb et al., 2005). Furthermore, polarisation of caveolar endocytosis to the cell rear during 2D migration may support the back-to-front recycling hypothesis (Galvez et al., 2004; Isshiki et al., 2002a; Parat, Anand-Apte, & Fox, 2003; Sheetz et al., 1999). Therefore this study examined polarisation of caveolar endocytosis during collective epithelial migration.

To label caveolae this study utilised caveolin1-mRFP fluorescent protein. Caveolin1 is a hairpin protein localised to caveolae and required for caveolar biogenesis (Fra et al., 1995; Hayer et al., 2010). As a marker of the adherent plasma membrane "footprint" ECFP-mem a palmitoylated enhanced cyan fluorescent protein was utilised (Jiang & Hunter, 1998). A monolayer of MDCK cells transfected with caveolin1-mRFP and ECFP-mem was wounded with a yellow pipette tip and the cells were allowed to migrate for 18 hours. Utilising

TIRF microscopy, cells at the wound edge displaying various caveolin1-mRFP expression levels and a fully polarised phenotype were imaged and caveolin1-mRFP localisation measured (Figure 4.1a). As expected, ECFP-mem provided a homogenous representation of the adherent plasma membrane (Figure 4.1a). Utilising the outline of the ECFP-mem signal, cells were divided into two regions associated with the migratory trajectory, the leading edge (which contained the lamellipodia) and the retracting edge (the region behind the lamellipodia) (Figure 4.1a). The overlaying regions drawn in Figure 4.1a were superimposed over the caveolin1-mRFP image and the distribution of caveolin1-mRFP within the two regions quantified by measurement of the average intensity. Intensity values were normalised against the average intensity of the entire cell footprint. Increased caveolin1-mRFP fluorescence was observed in the retracting edge of the cell relative to the leading lamella (Figure 4.1b). Thus, utilising TIRF microscopy, this study confirms caveolae are preferentially localised to the rear of MDCK cells undergoing planar directed migration, and are excluded from the lamellipodium.

4.4 Rab11-mediated recycling is not polarised in migrating epithelial cells

As described in chapter 3, the Rab11-dependent recycling pathway has an important function during steady state epithelial cell migration. Several studies have implicated the polarised recycling model in regulation of cell migration, where cargo undergoes internalisation and is transported through endosomal compartments (including the Rab11 positive recycling compartment) to the

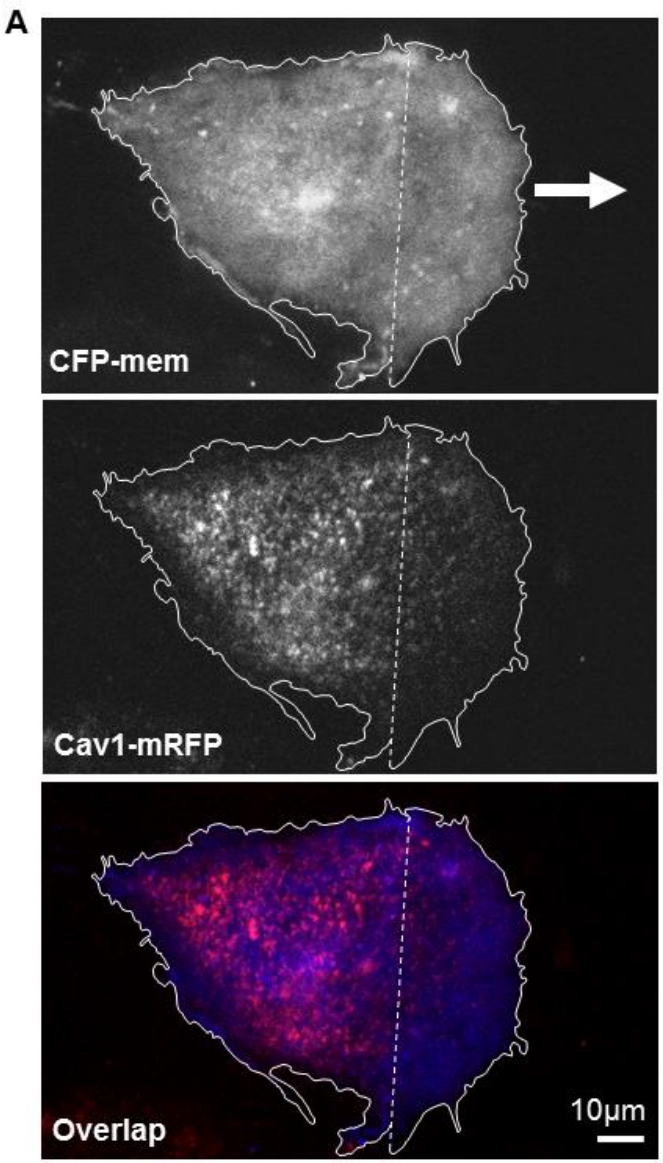

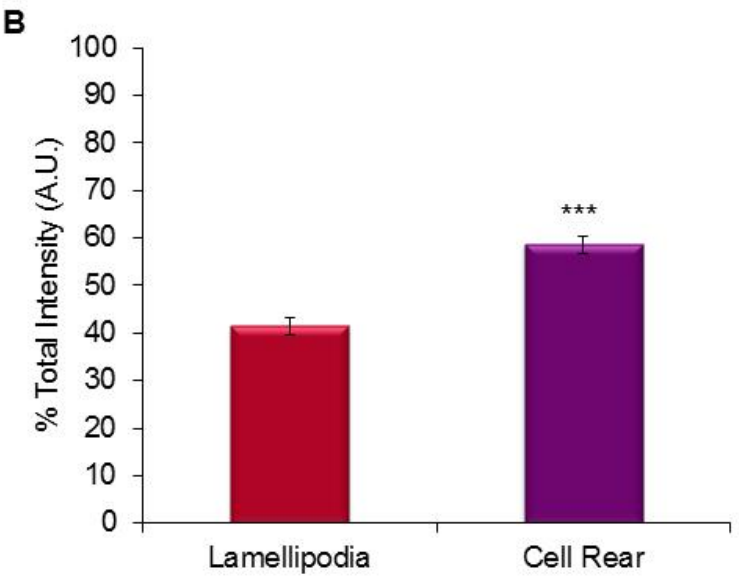

Figure 4.1. Caveolae are polarised away from the leading lamella in migrating MDCK cells. MDCK cells were co-transfected with caveolin1-mRFP and pECFP-Mem, wounded and allowed to migrate for 18 hours before taking single still brightfield and TIRF images at 37ºC. (A) TIRF microscopy image of a migrating MDCK cell expressing pECFP-mem with apparent migratory direction (white arrow), the adherent surface border (white line) and the leading and lagging edge separated by the dotted border. TIRF microscopy image of the same cell expressing caveolin1-mRFP with the same border overlying. Overlay of both CFP-mem (blue) and caveolin1-mRFP (red) images. (B) The quantification of the relative caveolin1-mRFP fluorescence intensity per unit area within the two regions along the migrating axis of the cell showing increased caveolae localised to the cell rear. The average from 38 cells was plotted from 3 independent experiments. *** P-value ≤0.001.

leading edge (Caswell & Norman, 2006; Sheetz, et al., 1999; Ullrich et al., 1996). Although polarisation of the Rab11-dependent pathway itself has not been examined (Fletcher & Rappoport, 2009; Fletcher & Rappoport, 2010); multiple studies have reported polarised trafficking of cargo via the Rab11-dependent pathway. Polarised trafficking of the α_5 and β_1-integrin subunits to the lamellipodial region has been observed in migrating fibroblast cells (Laukaitis et al., 2001; Palecek et al., 1996). Whilst in motile neutrophils polarised trafficking of α_5 and $\alpha_v\beta_3$-integrin to the leading edge was seen (Lawson & Maxfield, 1995; Pierini et al., 2000).

Therefore, this study sought to identify polarisation of the Rab11-dependent pathway in the adherent plasma membrane during epithelial wound healing. Previously, Rab11 has been demonstrated to remain associated with recycling vesicles during exocytic fusion (Ward et al., 2005). Therefore, TIRF microscopy was utilised to image Rab11-GFP positive fusion events. Fusion events were validated using quantitative criteria previously described by Schmoranzer et al., 2000 and shown in Figure 4.2 (Schmoranzer et al., 2000). Two analysis methods verified fusion events. Firstly, the area of the fusion was outlined and the total intensity measured within this region (Figure 4.2a). This was repeated for consecutive frames; a true fusion exhibits increased total intensity as the Rab11a-GFP containing vesicle approaches and fuses with the plasma membrane. This rise in total intensity is due to increased Rab11a-GFP excitation as the vesicle enters the TIRF evanescent wave. Intensity increases as the vesicle pushes and flattens against the plasma membrane and a fusion pore is created (Schmoranzer et al., 2000). Once fusion has occurred, the

Rab11a-GFP protein then freely diffuses laterally in the plane of the membrane (Ward et al., 2005). Thus the total fluorescence will initially be maintained, then start to decline as fusion area increases with each consecutive frame until the signal returns to background level (Figure 4.2c). The second method employed a “line scan” analysis (Figure 4.2b), a single pixel thick line was drawn through the centre of the fusion event allowing measurement of the fluorescent intensity of each pixel along the line. With each consecutive timeframe, as diffusion through the plasma occurs the fluorescent intensity should spread laterally, whilst intensity at the centre of the fusion region decreases.

In this study, a confluent monolayer of MDCK cells transiently expressing Rab11a-GFP was wounded and the cells were allowed to migrate for 18 hours. Cells on the wound edge, displaying a polarised morphology were imaged every 100-200ms for 15 minutes at 37°C, producing a time-lapse video. The cell footprint was outlined, and based upon the cells migratory trajectory the cell was divided into the leading edge (lamellipodia) and the cell rear. Each potential fusion event was quantified using the 2 methods stated previously and only events which were confirmed as true fusion events in both experimental parameters were considered definite fusions. The number of true fusions per region were counted and normalised to the region area. As can be seen in Figure 4.3 there is no significant difference between the number of Rab11-GFP fusions per area in either the lamellipodia region or the cell rear. Furthermore, division of the adherent plasma membrane longitudinally in the direction of migration into equal length front, middle and rear sections, demonstrated no significant difference in normalised number of fusions (data not shown).

Figure 4.2. Observation of fusion events in the adherent plasma membrane using GFP labelled Rab GTPase proteins and TIRF microscopy. MDCK cells were either transfected with Rab11-GFP or Rab25-GFP and allowed to migrate for 18 hours before imaging taking images every 100-200ms at 37ºC using TIRF microscopy. (A) TIRF microscopy image showing the initial vesicle fusion event and subsequent diffusion throughout the plasma membrane. The outline of the fusion event was circled in white to enable quantification of total membrane intensity. (B) TIRF microscopy image as shown in (A) (white dotted arrow denotes line scan area). (C) Quantification of the total intensity of spot and spot area in consecutive time frames, showing as the area increases (300-500ms), the total intensity remains relatively static confirming fusion. (D) Line scan measurements showing intensity per pixel across the length of a line annotated through the center of the fusion event.

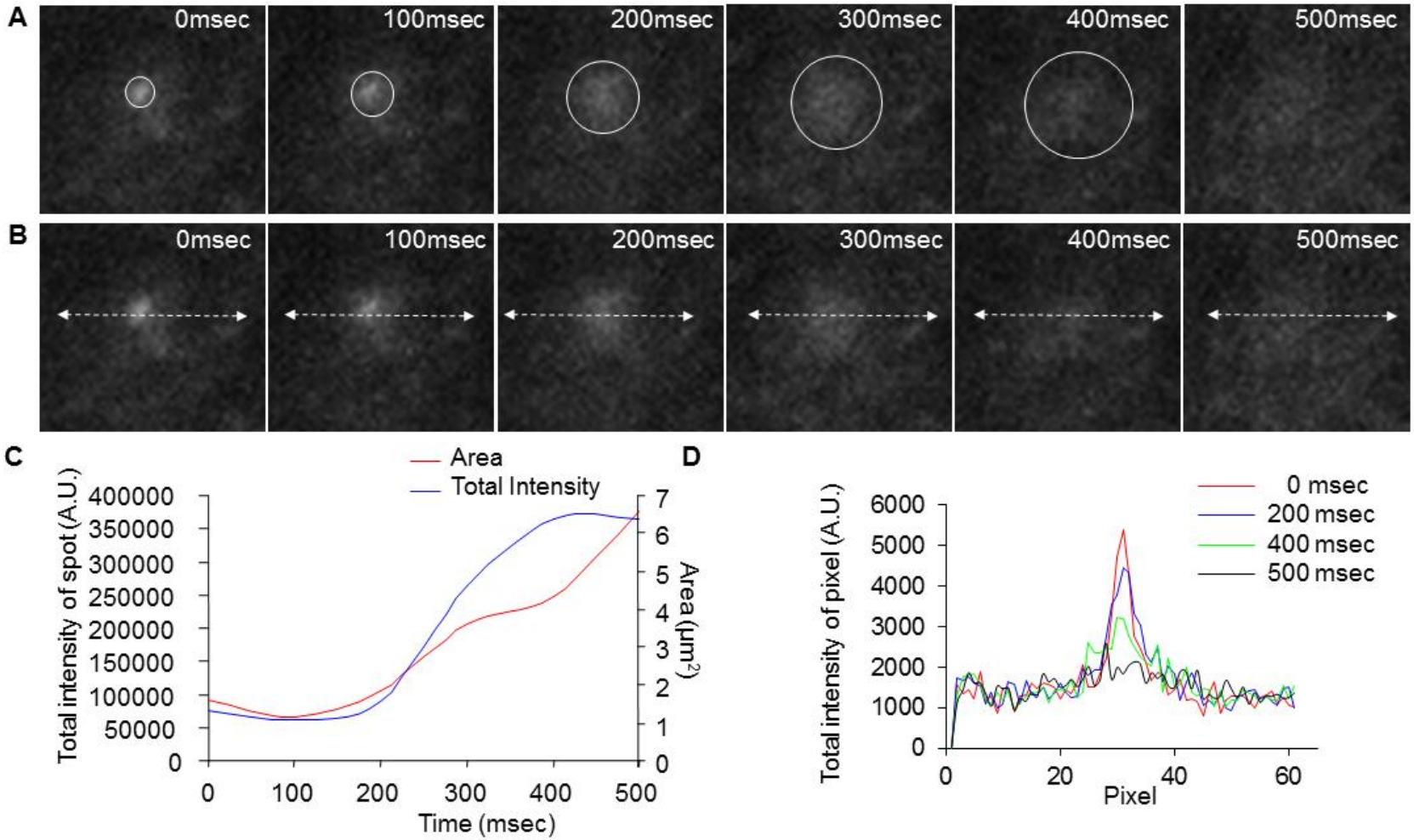
A
0msec
100msec
200msec
300msec
400msec
500msec
B
0msec
100msec
200msec
300msec
400msec
500msec
C
Area
Total Intensity
Total intensity of spot (A.U.)
Area (μm²)
Time (msec)
D
0 msec
200 msec
400 msec
500 msec
Total intensity of pixel (A.U.)
Pixel

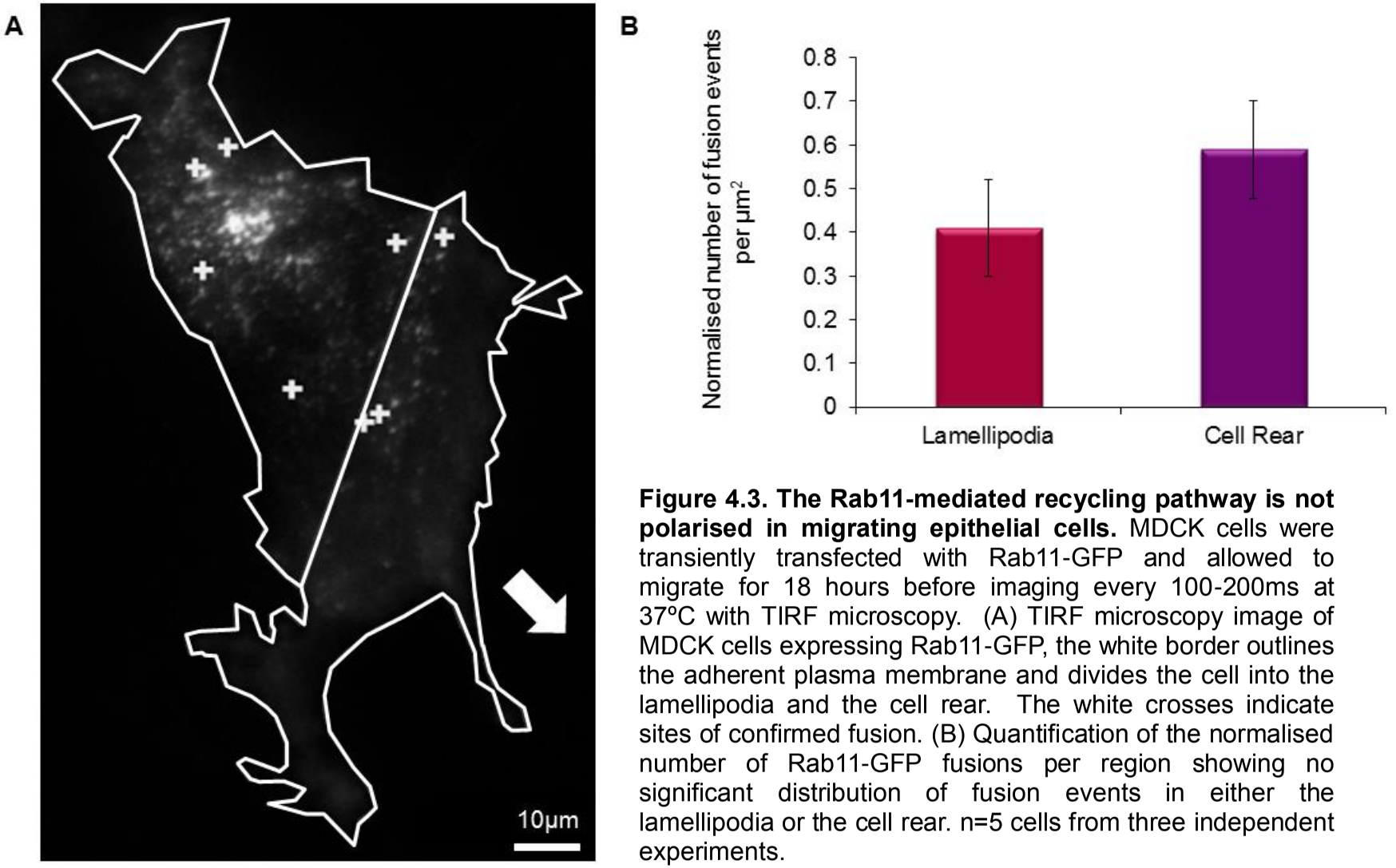

Figure 4.3. The Rab11-mediated recycling pathway is not polarised in migrating epithelial cells. MDCK cells were transiently transfected with Rab11-GFP and allowed to migrate for 18 hours before imaging every 100-200ms at 37ºC with TIRF microscopy. (A) TIRF microscopy image of MDCK cells expressing Rab11-GFP, the white border outlines the adherent plasma membrane and divides the cell into the lamellipodia and the cell rear. The white crosses indicate sites of confirmed fusion. (B) Quantification of the normalised number of Rab11-GFP fusions per region showing no significant distribution of fusion events in either the lamellipodia or the cell rear. n=5 cells from three independent experiments.

Therefore these data indicate that within migrating MDCK cells, Rab11-dependent trafficking is not polarised.

4.5 Rab25-mediated recycling is not polarised in migrating epithelial cells

Although recycling via Rab11a is not polarised, there is another epithelial cell specific member of the Rab11 family, Rab25 (Goldenring et al., 1993). Recent studies have linked over-expression of Rab25 with increased tumour invasiveness both in-vivo and in-vitro (Caswell et al., 2007; Cheng et al., 2004). Therefore, this study identified whether the Rab25-dependent trafficking pathway was polarised in migrating MDCK cells. However, the first stage was to determine whether like Rab11, Rab25 remained associated with exocytic vesicles which had traversed the Rab25-dependent recycling pathway. Observation of fusion events using TIRF microscopy demonstrated that transient expression of Rab25-GFP in migrating cells lead to fusion events with similar dynamics to those observed with Rab11-GFP (data not shown). To determine whether the Rab25 derived trafficking pathway was polarised within migrating MDCK cells, cells were transfected with Rab25-GFP, wounded and allowed to migrate for 18 hours before TIRF microscopy imaging. Fusions were quantified and confirmed as true fusions as stated in section 4.4. As demonstrated in Figure 4.4 no significant difference between the normalised number of fusion events was observed between the lamellipodial region and the cell rear. Furthermore, as described in section 4.4, migrating cells were divided into leading edge, middle and cell rear, the number of fusion events per region

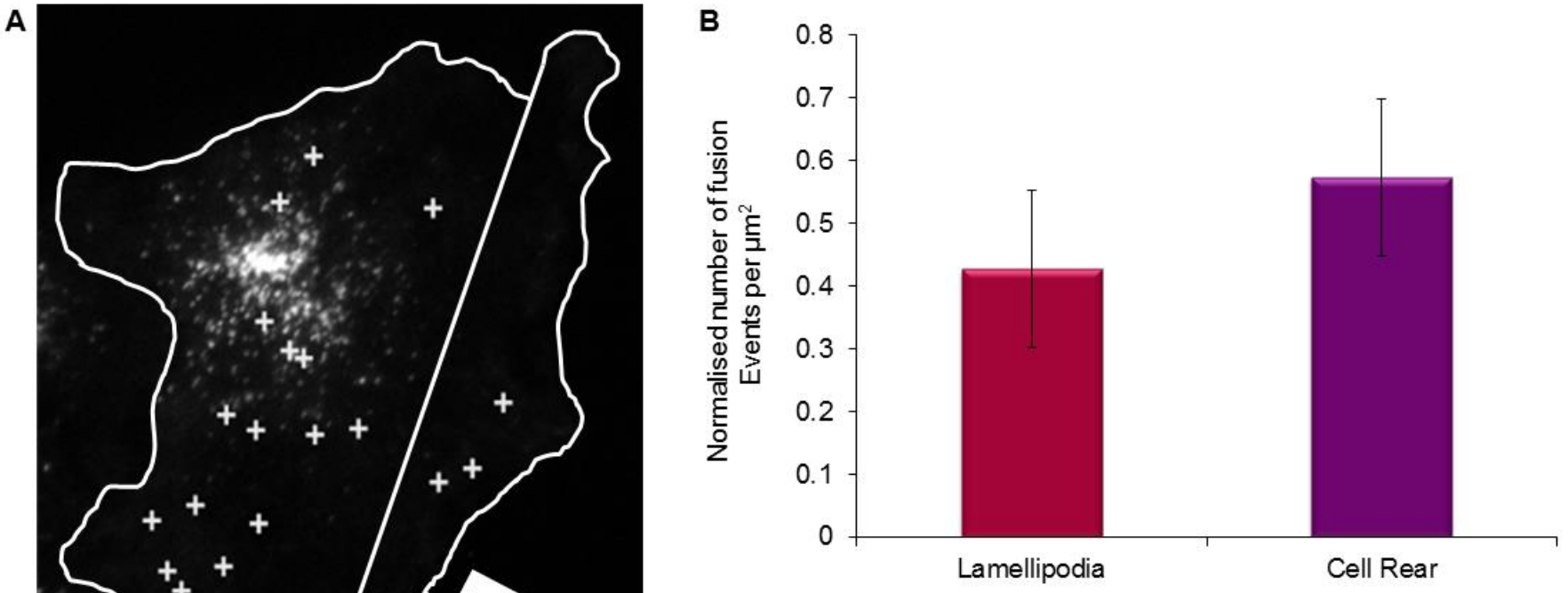

Figure 4.4. The Rab25-mediated recycling pathway is not polarised in migrating epithelial cells. MDCK cells were transiently transfected with Rab25-GFP and allowed to migrate for 18 hours before imaging every 100-200ms at 37ºC with TIRF microscopy. (A) TIRF microscopy image of MDCK cells expressing Rab25-GFP, the white border outlines the adherent plasma membrane and divides the cell into the lamellipodia and the cell rear. The white crosses indicate sites of confirmed fusion. (B) Quantification of the normalised number of Rab25-GFP fusions per region showing no significant distribution of fusion events in either the lamellipodia or the cell rear. n=5 cells from three independent experiments.

were re-analysed but no difference in the number of fusions was seen (data not shown). Therefore these data show that polarised Rab25-dependent trafficking does not occur during epithelial wound healing.

4.6 Discussion

This study represents the first systematic study examining polarised exocytosis and endocytosis in a single migratory model. In this chapter the potential for polarised distribution of caveolar endocytosis, Rab11a and Rab25 endosomal recycling events was examined during epithelial wound healing. Published observations from this study (Fletcher et al., 2012) and previous data (Rappoport & Simon, 2003) show that within the MDCK epithelial cell scratch wound model, CME is excluded from the rear of the cell. Conversely, caveolae are polarised away from the leading edge. In contrast, neither Rab11- nor Rab25-mediated recycling were polarised.

Through application of TIRF microscopy these data show that caveolae are preferentially localised to the rear of epithelial cells migrating on 2D surfaces as previously demonstrated in ECs (Galvez et al., 2004; Isshiki et al., 2002a; Parat, Anand-Apte, & Fox, 2003). Furthermore, Parat et al., (2003) identified initial caveolin1 distribution at the cell rear in 2D migrating ECs, however during invasion through Transwell filter pores, caveolin1 was released from rear caveolae structures and re-localised to a cytoplasmic distribution polarised to protruding cell front (Parat, Anand-Apte, & Fox, 2003). These data indicate that migratory stimulus and mode of migration (2D crawling or 3D invasion) can alter

polarisation and localisation of vesicle trafficking pathways, but also emphases the importance of studying a variety of pathways in a single model.

However it must be noted, although data presented in this chapter predicts increased caveolar endocytosis at the rear of the migrating epithelial cell, actual endocytosis events were not examined. Importantly, functions other than caveolar endocytosis have been proposed for both caveolae and caveolin1, which may explain the mechanism by which polarised caveolae regulate cell migration (reviewed fully in Navarro, Anand-Apte, & Parat, 2004). Many signalling molecules are compartmentalised into caveolae, thus caveolae may act as a platform for co-ordination of signalling pathways required for cell migration. Work by Labrecque et al., (2003) demonstrated vascular endothelial growth factor receptor-2 (VEGFR-2) localisation to caveolae and interaction with caveolin1 was required for regulation of VEGFR-2-mediated ERK signalling and EC migration (Labrecque et al., 2003). Furthermore, caveolin1 has been shown to perturb Rac and CDC42 activity but increase Rho activity by inhibition of the Src p190RhoGAP pathway (Grande-Garcia et al., 2007; Joshi et al., 2008). Rho is required for regulation of actomysin stress fibres and endosomal trafficking (Heasman & Ridley, 2008). Moreover, Rho has exhibited rear localisation in migrating fibroblasts during wound healing (Goulimari et al., 2005) thus the spatial polarisation of caveolin1 to the cell rear observed in this chapter may be required for effective regulation of Rho GTPases.

An alternate role for caveolae has been shown to exist in response to mechanical stress. Recent findings from the laboratory of Christoph Lamaze, have demonstrated that in cells undergoing mechanical stress and increased

membrane tension due to hyperosmotic shock, caveolae flatten and undergo disassembly (Sinha, et al., 2011). Many studies have shown alterations in membrane tension during cell migration (Tan et al., 2003; Dembo & Wang, 1999). Potentially, the rear localisation of caveolae could act as a membrane reserve during cell migration buffering alterations in membrane tension. Alternatively, increased membrane tension in the lamellipodium could restrict the presence of caveolae in this region. Results from chapter 3, establish a clear function for caveolae in cell migration (Figure 3.6). Whilst, expression of caveolin(1Y14F)-GFP inhibits caveolar endocytosis (Figure 3.7) this mutant also abrogates caveolar biogenesis (Orlichenko et al., 2006). Thus, the migratory defects observed upon expression of caveolin1(Y14F) may be due to any of the previously proposed mechanisms ranging from effects on signalling, response to mechanical stress or uptake of cell adhesion molecules. However, in this chapter it is confirmed that caveolae are polarised to the rear of migrating MDCK cells. Yet, the requirement for this caveolar polarisation is unknown.

This chapter also examined polarisation of Rab11- and Rab25-mediated endosomal recycling. Using TIRF microscopy to only excite Rab11-GFP/Rab25-GFP near the adherent plasma membrane, fusion events of Rab11 and Rab25 positive vesicles were observed (Ward et al., 2005). This study confirmed the Rab11 and Rab25 vesicle trafficking pathways were not polarised in the adherent surface of migrating MDCK epithelial cells. The exact role of Rab11 and Rab25 in regulating membrane trafficking in migrating epithelial cells is currently unknown (as described in section 1.10). However, inferences can be drawn from examining trafficking in polarised MDCK cells. Work by

Casanova et al., (1999) identified both Rab11 and Rab25 localisation to the apical recycling endosome (See Figure 1.6) (Casanova et al., 1999). In studies by Casanova et al., (1999) overexpression of Rab25 in MDCK cells affected basolateral to apical transcytosis, but had no effect on apical or basolateral recycling (See Figure 1.6). Whilst, inhibition of Rab11a by a GTP binding-deficient and GTPase deficient mutants had no effect on basolateral recycling, but affected apical recycling and transcytosis to varying extents (Casanova et al., 1999; Wang et al., 2000). Recent work by the Lencer laboratory has further established the role of Rab25 in transcytosis and Rab11a in basolateral recycling (Tzaban et al., 2009). Evidently in polarised MDCK cells both Rab11 and Rab25 trafficking pathways have a specific function in polarised trafficking of cargo both locally and across apical and basolateral membranes. However, in migrating MDCK cells basolateral and apical polarity no longer exists, instead cells develop a front-rear axis of polarity. In non-apically basolaterally polarised cells, Rab11 is required for “long-loop” trafficking via the PNRC (Ullrich et al., 1996; Zeng et al., 1999) (Figure 1.5). Yet, in non-polarised MDCK cells grown on glass, Rab11 localises to an organelle similar to the apical recycling endosome, however this organelle is not required for transferrin recycling thus is not comparable to the PNRC (Brown et al., 2000). This suggests Rab11 functions in disparate pathways in cells capable of apical basolateral polarisation to those unable to polarise. In the previous chapter, a clear role for Rab11 in MDCK cell migration was observed (Figure 3.11), this function is unknown but this current study has established exocytosis of vesicles from the Rab11 trafficking pathway is not polarised during epithelial cell migration.

Unlike Rab11, no studies have been performed in examining Rab25 function and endosomal localisation in non-polarised MDCK cells, yet results from this chapter have established exocytosis of Rab25 positive vesicles are not polarised during epithelial wound healing.

Combining the results from this chapter with those of the previous chapter has enabled further development of an overall model for the role of vesicle trafficking in epithelial cell migration. In this model, CME occurs in middle to front regions of the adherent plasma membrane (Rappoport & Simon, 2003), whilst caveolar endocytosis occurs towards the rear of the adherent surface of migrating epithelial cells. Upon internalisation of cargo from the plasma membrane, this cargo is then recycled via Rab11-mediated trafficking in a non-polarised fashion (Figure 4.5.). This model represents a departure from earlier models which suggest cell migration requires endocytosis at the trailing edge and polarised exocytosis at the leading edge (Bretscher, 1996; Palecek et al., 1996; Sheetz et al., 1999).

4.7 Key chapter findings

- During epithelial wound healing caveolae are polarised to the rear of the adherent plasma membrane.
- Exocytosis of cargo from the Rab11- and Rab25-mediated trafficking pathways is not polarised in migrating MDCK cells.

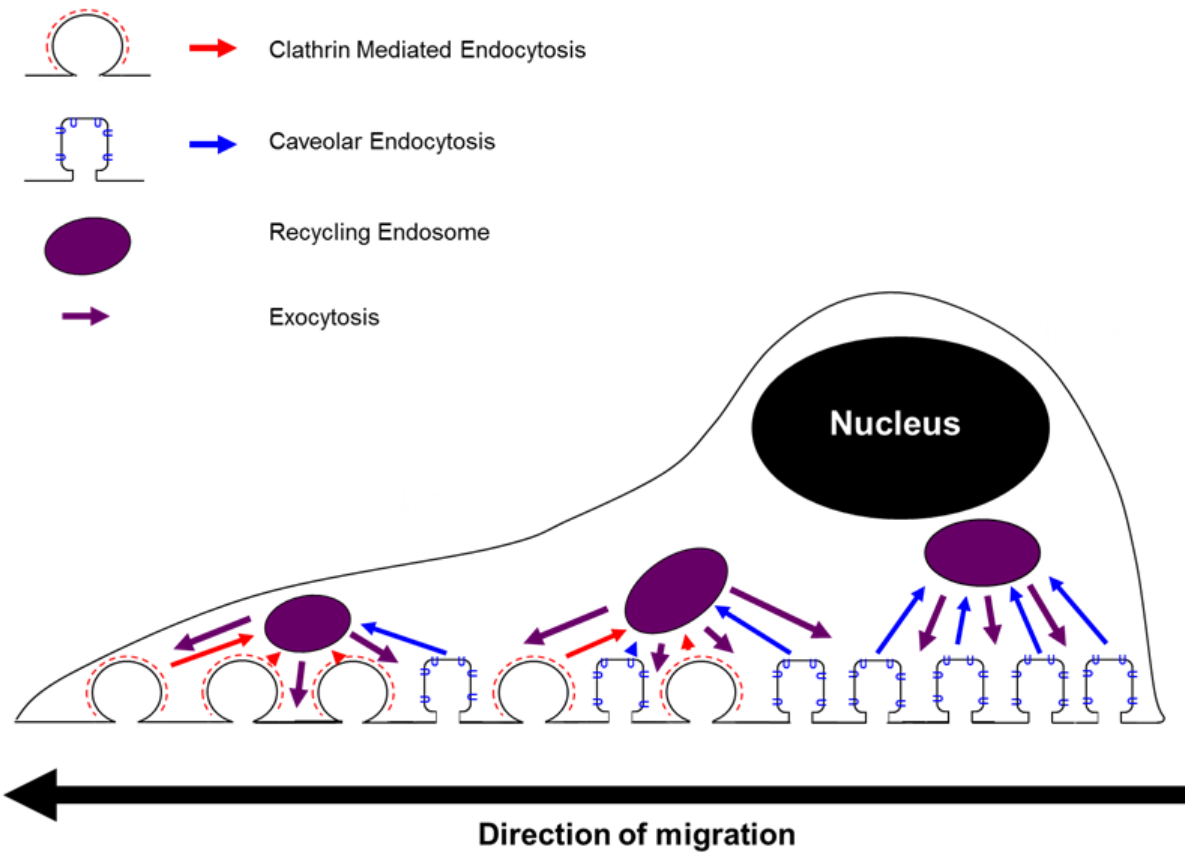

Figure 4.5. Schematic diagram showing polarised trafficking in migrating epithelial cells. Diagram demonstrating CME polarised to the front and caveolar endocytosis polarised to the rear of migrating MDCK cells. This model also shows exocytosis of cargo from the Rab11 and Rab25 recycling pathways is not polarised in migrating MDCK cells.

4.7 Conclusion

As one of the first studies to systematically evaluate the role of vesicle trafficking using a single migratory model, this study confirms caveolae are polarised to the cell rear and are required for steady-state migration (chapter 2). Whilst exocytosis of Rab11 positive vesicles is not polarised, however is a requirement for effective MDCK cell migration (chapter 2). This study also identified that exocytosis of cargo from the Rab25-dependent recycling pathway is also not polarised during epithelial wound healing.

CHAPTER 5

TRAFFICKING OF ADHESION COMPLEXES DURING EPITHELIAL CELL MIGRATION

5.1 Introduction

In the past decades, much work has been performed examining the dynamics of cell adhesions. Cell adhesions are vital structures, functioning to anchor cells both to an ECM and to neighbouring cells. The most widely studied adhesive structures are FAs. FAs form in both 2D and 3D culture systems and attach the cell via its cytoskeleton to the ECM. During cell migration these attachments undergo assembly, maturation and disassembly, a process integral for successful cellular translocation (Caswell et al., 2009; Lauffenburger & Horwitz, 1996; Valdembri et al., 2009). Another type of adhesion structure are intercellular adhesions. Re-modelling of these adhesions is required for collective cell migration and their disassembly has been implicated in EMT where cells develop a more migratory and invasive phenotype (Zavadil & Bottinger, 2005). Evidently, regulation of adhesive structure dynamics is implicated in cell migration.

One mechanism through which cell adhesion structures may be regulated is through trafficking of adhesion complex components. FAs and cell-cell

adhesions have a highly similar structural organisation. They are multi-protein complexes consisting of transmembrane proteins, signalling molecules (which regulate adhesion turnover) and scaffolding molecules which couple transmembrane proteins to the cell cytoskeleton (Brennan et al., 2010; Mitra, Hanson, & Schlaepfer, 2005; Niessen, 2007; Petit & Thiery, 2000). In the case of FAs the ectodomain of the transmembrane proteins bind the ECM, while in cell-cell junctions these extracellular domains polymerise with the extracellular regions of homologous proteins in neighbouring cells. The cytoplasmic domains of the transmembrane components of adhesive structures have been confirmed as cargo for endocytosis and trafficking in many studies (Camand et al., 2012; Caswell & Norman, 2006; Ivanov, Nusrat & Parkos, 2004; Marchiando et al., 2010; Roberts et al., 2001; Stamatovic et al., 2009; White, Caswell, & Norman, 2007; Woods et al., 2004; Xia et al., 2009). One of the most widely researched transmembrane components of FAs are integrins. Integrins bind immobilised ligands in the ECM, and via scaffolding proteins (paxillin, vinculin, talin, etc) are linked to the actin cytoskeleton. Integrins also function in signalling during FA formation and disassembly (reviewed in Scales & Parsons, 2011). Integrins have been identified to undergo internalisation via many endocytosis pathways (summarised in Fletcher & Rappoport, 2010) and have been linked to regulation of migration, cell spreading and maintenance of cell directionality (Caswell & Norman, 2006; Roberts et al., 2001; White, Caswell, & Norman, 2007; Woods et al., 2004). Like FAs, some cell-cell adhesion components have been shown to undergo endocytosis during disassembly of the adhesive structure. One such adhesion structure are TJs and the

transmembrane protein occludin. Occludin has been demonstrated to undergo endocytosis by both clathrin-mediated and caveolar endocytosis during disassembly of TJs in a manner dependent on stimulus (Ivanov, Nusrat, & Parkos, 2004; Marchiando et al., 2010; Stamatovic et al., 2009; Xia et al., 2009). Occludin has been implicated in regulation of cell migration as loss of occludin from TJs and TJ disassembly is observed during EMT where cells become more migratory (Grande et al., 2002). Additionally, occludin has been shown to interact with several polarity complexes both at the TJ and the leading edge (during wound healing) (Du et al., 2010). These complexes mediate effects on cell migration facilitating actin polymerisation and membrane protrusion at the leading edge via activation of Rac and Cdc42 (Dow et al., 2007; Du et al., 2010; Ozdamar et al., 2005; Shin, Wang, & Margolis, 2007). Thus, occludin is a protein which undergoes internalisation and may function in cell motility, however the extent to which specific vesicle trafficking pathways regulate migration via occludin is currently unknown.

Therefore, in this study the aim was to examine the potential for dynamin-dependent internalisation pathways in regulation of adhesion complexes during collective epithelial cell migration. Chapters 3 and 4 have previously described the potential for endocytosis and trafficking in regulation of epithelial cell migration, this section will now identify the function of these pathways in FA and TJ turnover. This study is of particular importance as most of the work previously examining the role of FA turnover/integrin trafficking has been performed in fibroblasts, ECs and leukocytes (e.g. neutrophils) (Fletcher & Rappoport, 2010; Fletcher & Rappoport, 2009). Therefore, this study is the first

to examine the potential for endocytosis in regulation of FA dynamics in cells with significant cell-cell junctions. Furthermore, this chapter will examine the potential for endocytosis of the TJ protein occludin in modulation of collective epithelial cell migration.

The results from this study found markers of clathrin-mediated and caveolar endocytosis do not co-localise with FA components during epithelial cell migration. Combined with evidence from Fletcher et al., 2012, demonstrating inhibition of the aforementioned pathways did not affect FA dynamics during wound healing, these data suggest dynamin-dependent endocytosis has little role in regulating FA turnover in motile epithelial cells. Instead this work implicates CME of occludin from the wound edge to Rab5 positive endosomal compartments as a novel mechanism for regulating epithelial wound healing. Additionally, this redistribution of occludin from the wound edge was required for effective epithelial cell migration. Finally, the second extracellular loop of occludin is required for its effective removal from the leading edge.

5.2 Results

Prior to assessing the role of endocytosis in regulation of FAs during epithelial cell migration, fluorescent exogenous FA markers had to be verified to confirm correct FA localisation. Exogenously expressed GFP-tagged β_3-integrin and mRFP-paxillin have both been previously utilised as FA markers (Parsons et al., 2008; Tsuruta et al., 2002). β_3-integrin is a transmembrane protein (previously shown to be expressed endogenously in MDCK cells (Schoenenberger et al.,

1994)), which localises to FAs and may represent a potential cargo for endocytosis during FA disassembly. To mark any non β_3-integrin containing FAs, Paxillin-mRFP, a scaffolding protein present at all stages of FA turnover was used (Deakin & Turner, 2008). IC using antibodies which identify pFAK was used as an endogenous FA marker (Ezratty et al., 2005; Huveneers & Danen, 2009). A high level of co-localisation between both exogenous and endogenous FA markers was observed suggesting overexpression of these proteins did not cause miss-localisation to non-FA structures or affected FA morphology (shown in Fletcher et al., 2012).

As a second control study to validate the method of analysis used to determine co-localisation between FA and endocytosis markers, co-localisation between the Src family kinase member Fyn and the FA marker paxillin-mRFP was analysed during epithelial wound healing (shown in Fletcher et al., 2012). SFKs have been implicated in regulation of disassembly of FAs during migration (Buettner et al., 2008; Dumont et al., 2009; Milano et al., 2009; Pichot et al., 2009; Webb et al., 2004), and in particular Fyn has been demonstrated to bind FA components (Li et al., 1996) and co-localise with FAs (Reddy, Smith, & Plow, 2008). A significant level of co-localisation was observed between Fyn and paxillin-mRFP, validating analysis strategies used in this study.

5.3 Markers of clathrin-mediated endocytosis do not co-localise with focal adhesions

As described previously, dynamin is required for both clathrin-mediated and caveolar endocytosis. Recent studies have also suggested dynamin may be required for effective microtubule-induced FA disassembly as well as internalisation of specific integrin heterodimers (Chao & Kunz, 2009; Ezratty et al., 2009). Preliminary studies were performed to examine the function of dynamin-dependent internalisation in regulation of FAs during epithelial wound healing. These studies used exogenously expressed dynamin2-GFP and paxillin-mRFP to identity co-localisation between dynamin and FAs. Additionally the Dyn2(K44A) mutant was expressed alongside FA markers to examine alterations in FA turnover (quantifying FA size and distribution) upon inhibition of dynamin-dependent endocytosis. These studies found no significant level of co-localisation between dynamin and FAs, and expression of Dyn2(K44A) had no effect on FA turnover in MDCK cells during epithelial wound healing (data shown in Fletcher et al., 2012).

Although no significant role for dynamin in regulation FA dynamics in migrating epithelial cells was identified in the aforementioned study, the function of specific dynamin-dependent pathways in FA dynamics was examined further. Specifically a function for clathrin-mediated endocytosis. Recent studies have implicated clathrin-mediated endocytosis of integrins as a mechanism involved in disassembly of FAs (Chao & Kunz, 2009; Ezratty et al., 2009). However, these observations were performed in fibroblast derived cell lines, and no previous work has examined CME in regulation of FAs in epithelial cell lines.

MDCK cells were transiently transfected with the previously validated FA marker β_3-GFP (Fletcher et al., 2012) and dsRed-clathrin (light chain) a widely used marker of CME (Rappoport et al., 2008; Saffarian, Cocucci, & Kirchhausen, 2009) to assess co-localisation. Cells were imaged as they underwent collective migration to heal a scratch to the epithelial monolayer performed 18 hours previously, and imaged using TIRF microscopy. As can be seen in Figure 5.1a there was no observable co-localisation between β_3-GFP and dsRed-clathrin. Data were analysed by outlining each β_3-GFP containing FA, and counting co-localisation between these FAs and dsRed-clathrin. As the control, the outlined regions were moved to nearby β_3-GFP negative regions and co-localisation with dsRed-clathrin measured. Initial observations showed no significant co-localisation between β_3-GFP and dsRed-clathrin in the adherent plasma membrane of migrating MDCK cells (data not shown).

Therefore, the cells were divided into regions, as region specific co-localisation between FAs and endocytosis markers has been observed (Ezratty et al., 2009). Each cell was divided into 3 equal length sections in the direction of migration (front, middle and back) and again co-localisation between β_3-GFP and dsRed-clathrin analysed. Once more no significant co-localisation between FAs and clathrin was observed in any region of the adherent plasma membrane during epithelial monolayer migration. This evidence was further supported in data from Fletcher et al., 2012 where time lapse imaging demonstrated that at no point during FA formation and disassembly did dsRed-clathrin co-localise

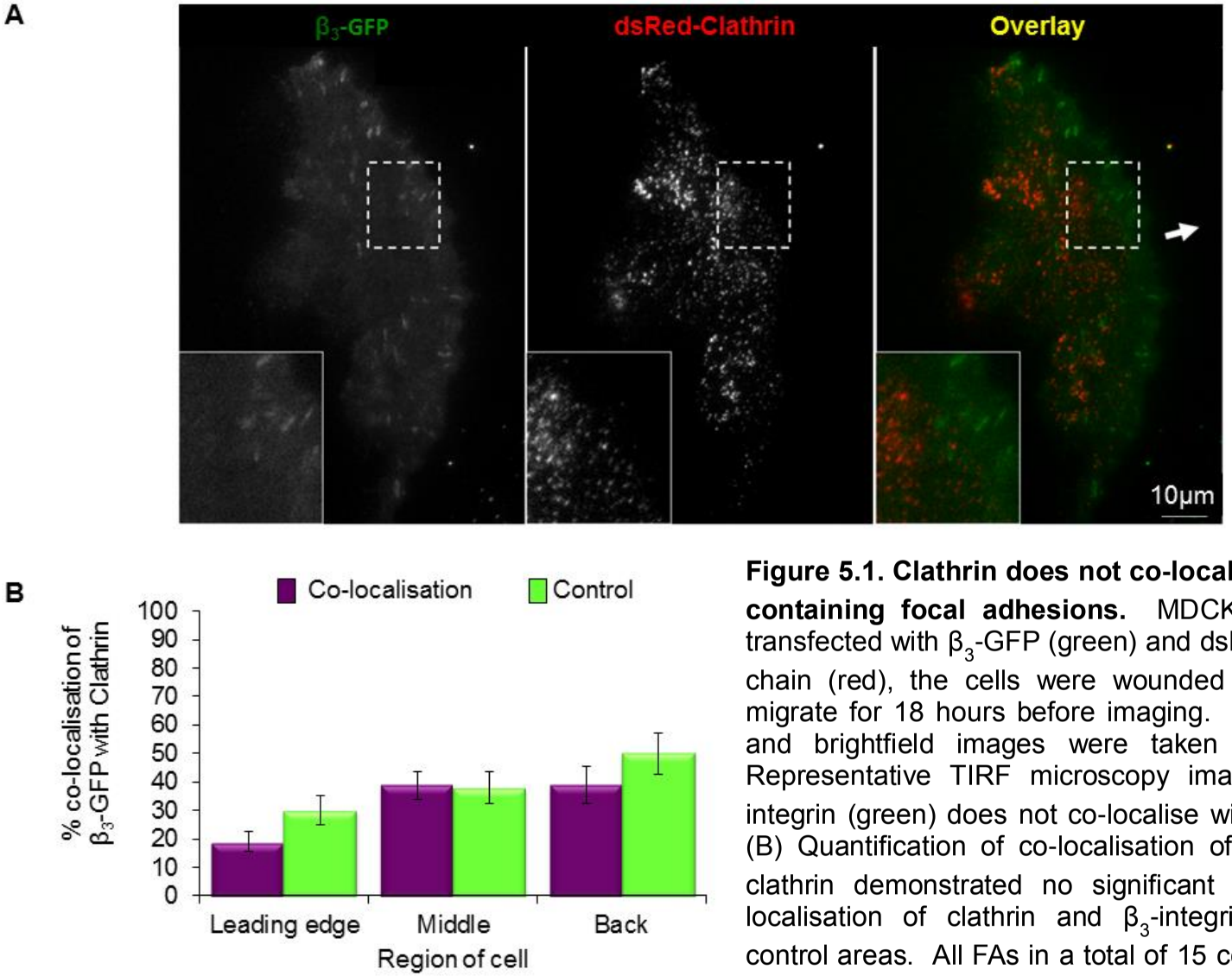

Figure 5.1. Clathrin does not co-localise with β_3-GFP containing focal adhesions. MDCK cells were co-transfected with β_3-GFP (green) and dsRed-clathrin light chain (red), the cells were wounded and allowed to migrate for 18 hours before imaging. Single still TIRF and brightfield images were taken at 37ºC. (A) Representative TIRF microscopy image showing β_3-integrin (green) does not co-localise with clathrin (red). (B) Quantification of co-localisation of β_3-integrin with clathrin demonstrated no significant increase in co-localisation of clathrin and β_3-integrin compared to control areas. All FAs in a total of 15 cells taken from 3 independent experiments were analysed. White arrow denotes direction of migration.

with β_3-GFP in migrating MDCK cells. Additionally inhibition of clathrin-mediated endocytosis by the previously validated (Figure 3.5) Eps15(EH29) mutant had no effect on FA distribution or size (data not shown, Fletcher et al., 2012). Together the data suggests CME has a minimal function in regulation of FA dynamics during epithelial wound healing.

5.4 Markers of caveolar endocytosis do not co-localise with focal adhesions

Another well researched dynamin-dependent internalisation pathway is caveolar endocytosis. Caveolar endocytosis has recently come to light as a pathway which may regulate FA dynamics. Several lines of research have implicated caveolar endocytosis in internalisation of specific integrin heterodimers (reviewed fully in Fletcher & Rappoport, 2010). Using the same experimental and analysis parameters as in section 5.3, this study utilised β_3-GFP as a FA marker and caveolin1-mRFP as a marker of caveolae (as seen in section 4.3) and co-localisation between caveolar endocytosis and FAs was assessed. As shown in Figure 5.2, there was no significant co-localisation between β_3-GFP containing FAs and caveolin1-mRFP during epithelial migration in either the entire adherent plasma membrane (data not shown), or the adherent membrane when divided into 3 regions. Again this conclusion was confirmed by further studies. In time lapse studies of migrating MDCK cells; β_3-GFP containing FAs undergoing assembly/disassembly failed to co-localise with caveolin1-mRFP (data not shown, Fletcher et al., 2012). Additionally inhibition of caveolar endocytosis by the previously validated caveolin1(Y14F) (Figure 3.7) had no

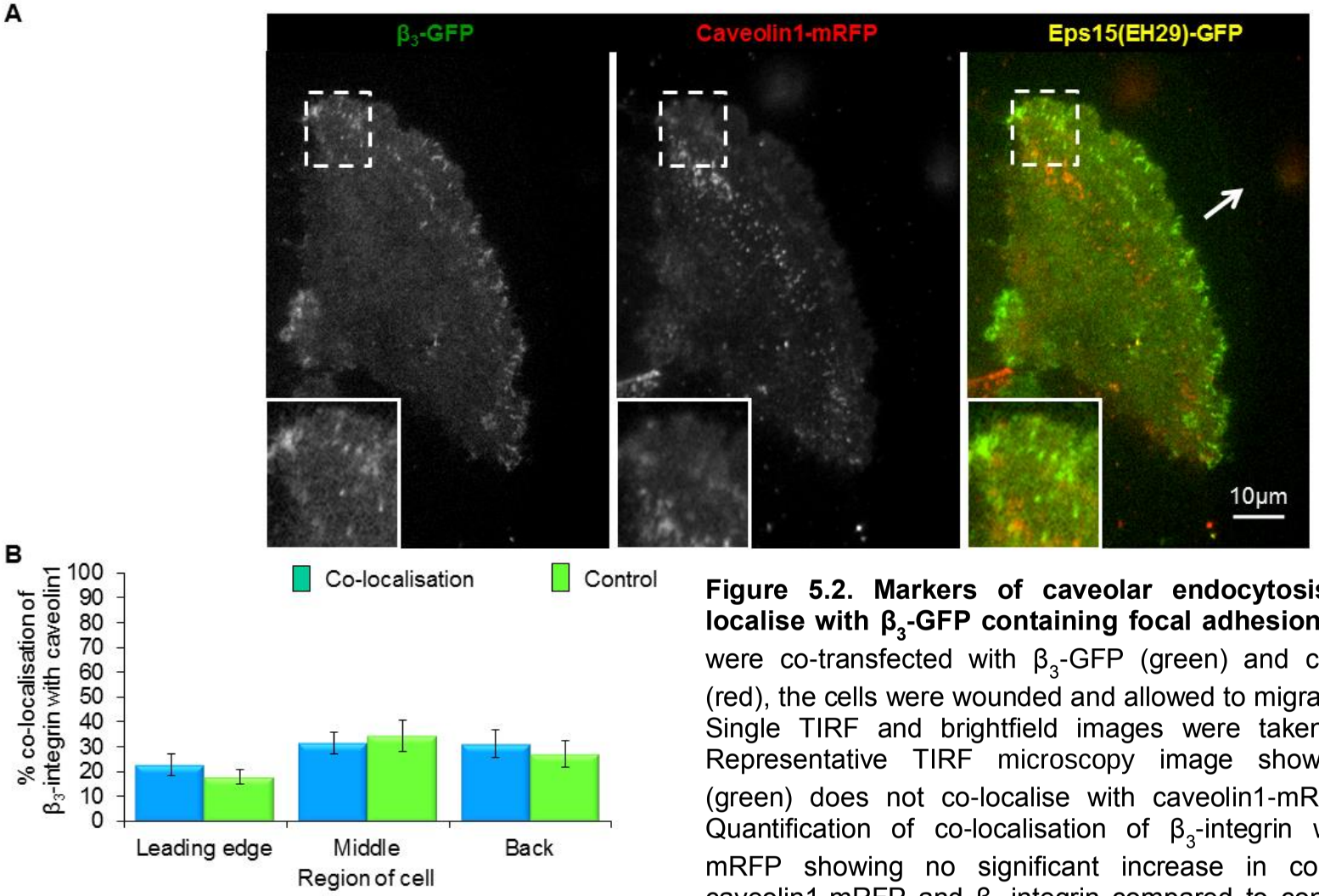

Figure 5.2. Markers of caveolar endocytosis do not co-localise with β_3-GFP containing focal adhesions. MDCK cells were co-transfected with β_3-GFP (green) and caveolin1-mRFP (red), the cells were wounded and allowed to migrate for 18 hours. Single TIRF and brightfield images were taken at 37ºC. (A) Representative TIRF microscopy image showing β_3-integrin (green) does not co-localise with caveolin1-mRFP (red). (B) Quantification of co-localisation of β_3-integrin with caveolin1-mRFP showing no significant increase in co-localisation of caveolin1-mRFP and β_3-integrin compared to control areas. All FAs in a total of 15 cells taken from 3 independent experiments were analysed. White arrow denotes direction of migration.

effect on either FA size or distribution (data not shown Fletcher et al., 2012). Together the data demonstrate caveolar endocytosis has a minimal function in regulation of FA dynamics during collective epithelial cell migration.

5.5 Wound formation stimulates occludin redistribution from the leading edge to Rab5-GFP positive early endosomes

Observations in sections 5.2-5.4 suggest CME, caveolar or dynamin-dependent endocytosis does not regulate collective epithelial migration via FA turnover. However, as documented in section 3.3-3.5, these pathways are integral for effective MDCK cell migration. Therefore, this chapter examined one of the main physiological differences between epithelial and non-epithelial cells; the role of intercellular adhesive structures during epithelial wound healing. In particular this work focused on TJs as well as trafficking and localisation of the TJ protein occludin. Localisation of endogenous occludin was investigated during the initial stages of development of a motile phenotype and during steady state migration. A confluent monolayer of MDCK cells expressing Rab5-GFP as an early endosomal marker (Maxfield and McGraw, 2004), was wounded and the cells allowed to migrate for 5, 15 or 60 minutes before fixation and IC (staining endogenous occludin) was performed. Confocal microscopy was utilised to image occludin localisation during wound healing. As demonstrated in Figure 5.3, occludin distribution at lateral membranes adjacent to neighbouring cells remains unchanged up to 60 minutes after wounding. However, redistribution of occludin from the plasma membrane at the wound

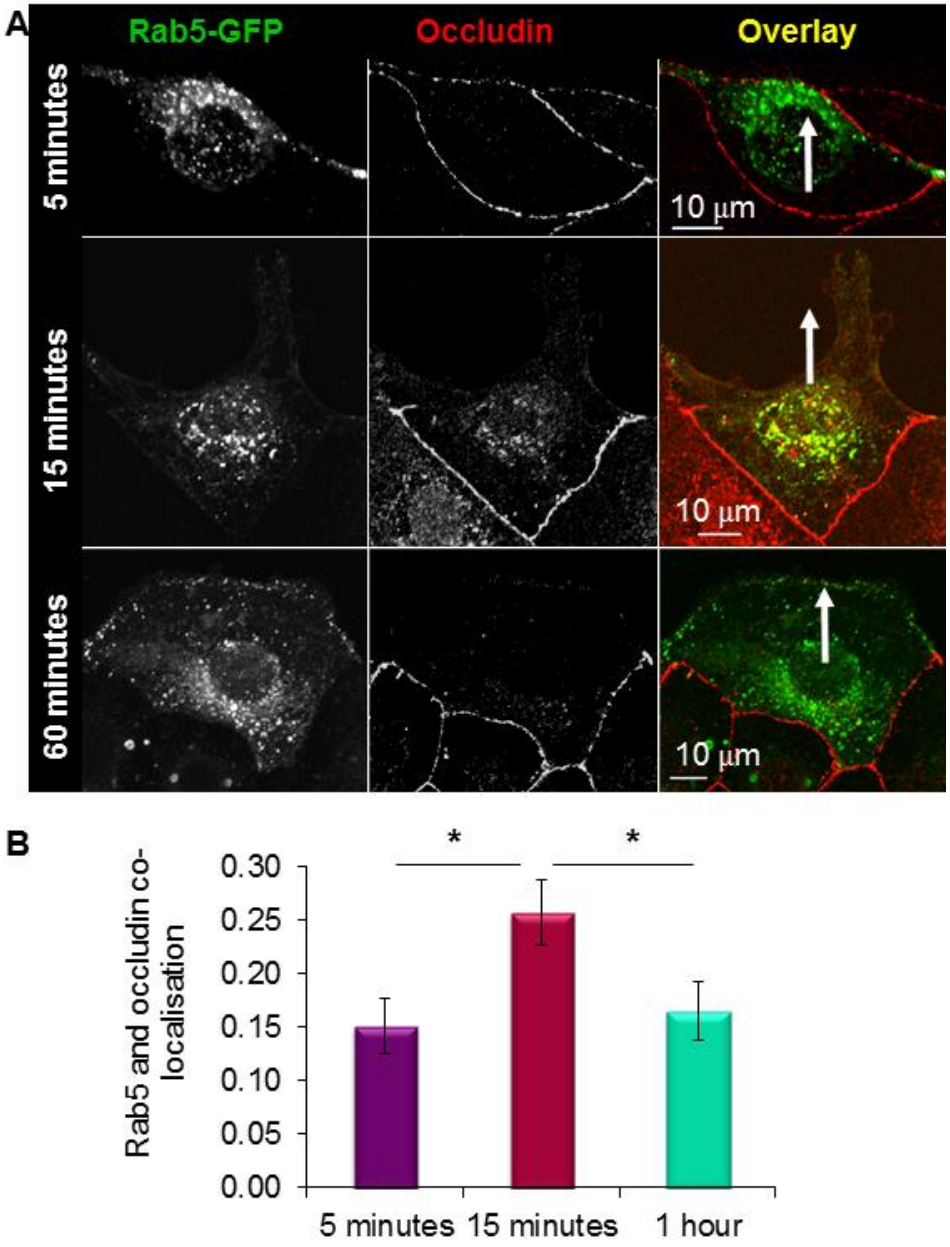

Figure 5.3. During epithelial wound healing endogenous occludin redistributes from the leading edge to Rab5 positive early endosomes. MDCK cells were transfected with Rab5-GFP (green), the confluent monolayer was wounded and the cells allowed to migrate for 5, 15 or 60 minutes before fixation and immuno-localisation using rabbit anti-occludin (1:250 dilution) and donkey anti-rabbit-Alexa Fluor 568 (1:200 dilution) (red). (A) Confocal microscopy showed redistribution of occludin from the wound edge and increased occludin and Rab5-GFP co-localisation at 15 minutes. (B) Quantification of co-localisation of Rab5-GFP and Occludin. * $p \leq 0.05$, n=3 repetitions, at least 20 cells analysed per time point. White arrow denotes direction of migration.

edge is observed 15 minutes post-wounding (Figure 5.3). This lack of occludin at the wound edge is still apparent 60 minutes post-wounding; by one hour post-wounding a migratory phenotype with a well spread leading lamella can be observed.

In order to determine whether the redistribution of occludin from the wound edge occurs via endocytosis; co-localisation between endogenous occludin and the endosomal marker Rab5 was measured in Rab5-GFP expressing cells. Co-localisation was measured using a Pearson's Correlation Coefficient in automatically selected ROIs. As identified in Figure 5.3a, at 5 minutes there is minimal co-localisation between Rab5-GFP and occludin. However this co-localisation was significantly increased by 15 minutes. Interestingly, by 1 hour co-localisation of occludin with Rab5 positive endosomes was reduced. Therefore these data suggest that upon wound formation, occludin is internalised from the leading edge to early endosomal compartments, suggesting that monolayer wounding can serve as a stimulus for occludin endocytosis.

5.6 Occludin redistribution from the leading edge is dynamin-dependent

To further elucidate the mechanism mediating occludin internalisation from the leading edge, a role for dynamin-dependent endocytosis in this process was examined. For this we utilised Dynasore to inhibit dynamin-dependent endocytosis (validated in Figure 3.2). MDCK cells expressing GFP were treated with DMSO (control) or Dynasore, wounded and allowed to migrate for 15

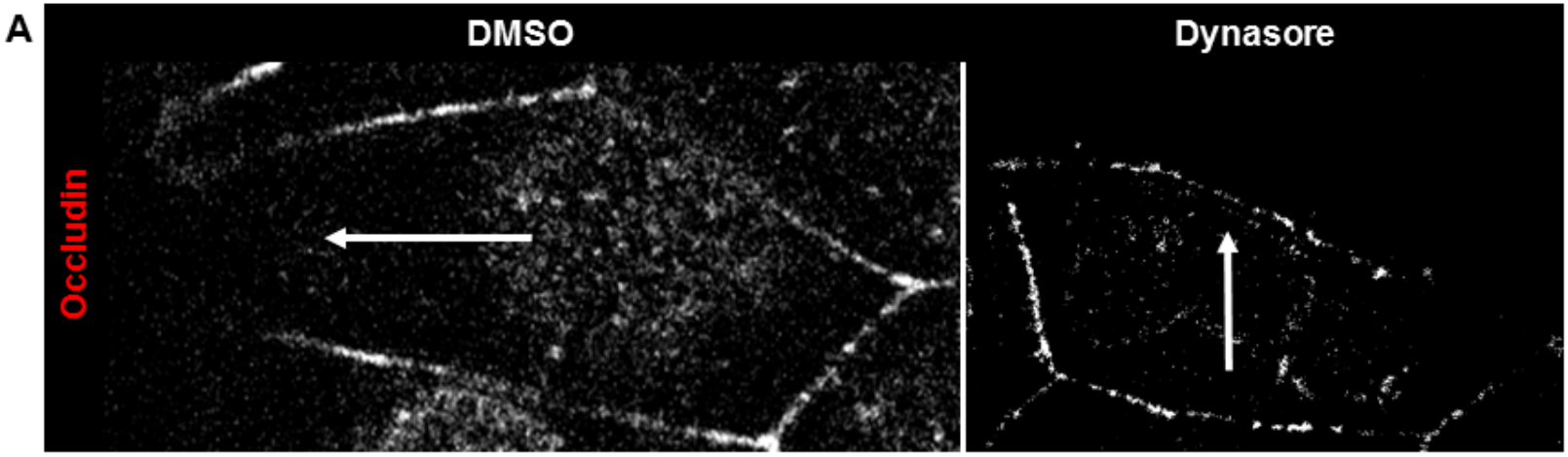

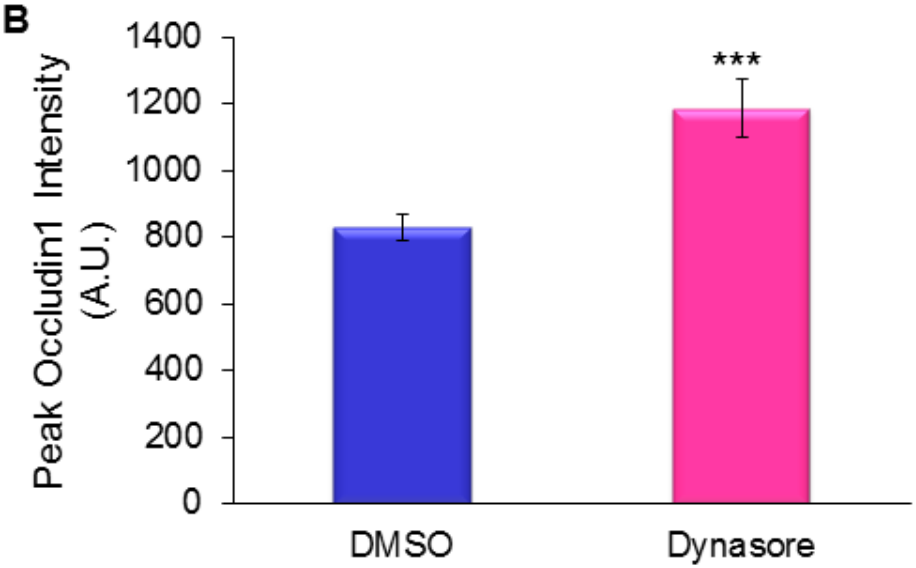

Figure 5.4. Inhibition of dynamin-dependent endocytosis prevents redistribution of occludin from the wound edge. MDCK cells were transfected with GFP, the cells were incubated for 30 minutes in either DMSO (1µl/ml) or 80 µM Dynasore. The confluent monolayer was wounded and the cells allowed to migrate for 15 minutes before fixation and immuno-localisation using rabbit anti-occludin (1:250 dilution) and donkey anti-rabbit-Alexa Fluor 568 (1:200 dilution). (A) Confocal microscopy image showing inhibition of dynamin-dependent endocytosis prevents redistribution of occludin from the wound edge in comparison to DMSO treated control cells. (B) Quantification showing increased occludin intensity at the leading edge in cells treated with Dynasore. *** p≤0.001, n=3 repetitions, 15 cells analysed of each condition. White arrow denotes direction of migration.

minutes (15 minutes allowed complete occludin redistribution from the wound edge in Figure 5.3). Immunocytochemistry was performed and endogenous occludin imaged by confocal microscopy. The plasma membrane localisation of occludin at the wound edge was analysed using line scan analysis measuring peak intensity in the lamellipodial region. As observed in Figure 5.4, a 40% increase in occludin localisation at the wound edge was observed in cells treated with Dynasore in comparison to DMSO treated cells. These data suggest that dynamin-dependent endocytosis is required for occludin internalisation from the wound edge during epithelial wound healing.

5.7 Inhibition of clathrin-mediated endocytosis results in increased occludin behind the leading edge

As previously demonstrated and verified (Figure 3.2), Dynasore inhibits multiple endocytosis pathways including clathrin-mediated and clathrin-independent endocytosis (Doherty & McMahon, 2009). Therefore, the aim of this section was to specifically identify the dynamin-dependent endocytosis pathway required for internalisation of occludin from the leading edge during epithelial wound healing. For this, selective inhibition of CME and caveolar endocytosis was achieved by expression of Eps15(EH29)-GFP and caveolin1(Y14F)-GFP mutants respectively (Figures 3.5 and 3.7) (Benmerah et al., 1999; Orlichenko et al., 2006). Directed migration was initiated by wounding a confluent monolayer of cells expressing the aforementioned constructs. The cells were allowed to migrate for 1 hour before fixation and immunocytochemistry, staining

Figure 5.5. Inhibition of CME prevents redistribution of occludin from the wound edge. MDCK cells were transfected with GFP, Eps15(EH29)-GFP or caveolin1(Y14F)-GFP DNA (green), the monolayer was wounded and the cells allowed to migrate for 60 minutes before fixation and immuno-localisation using rabbit anti-occludin (1:250 dilution) and donkey anti-rabbit-Alexa Fluor 568 (1:200 dilution) (red). (A) Confocal microscopy image showing inhibition of CME prevents redistribution of occludin from the wound edge whilst inhibition of caveolar endocytosis did not alter the redistribution phenotype. (B) Quantification showing increased occludin intensity at the leading edge of cells expressing Eps15(EH29)-GFP. (C) Quantification showing overexpression of Eps15(EH29)-GFP and caveolin1(Y14F)-GFP did not affect lamellipodial formation when the ratio of cell body to cell lamellipodia was measured. *** $p \leq 0.001$, n=3 repetitions, 15 cells of each expression condition were measured. White arrow denotes direction of migration.

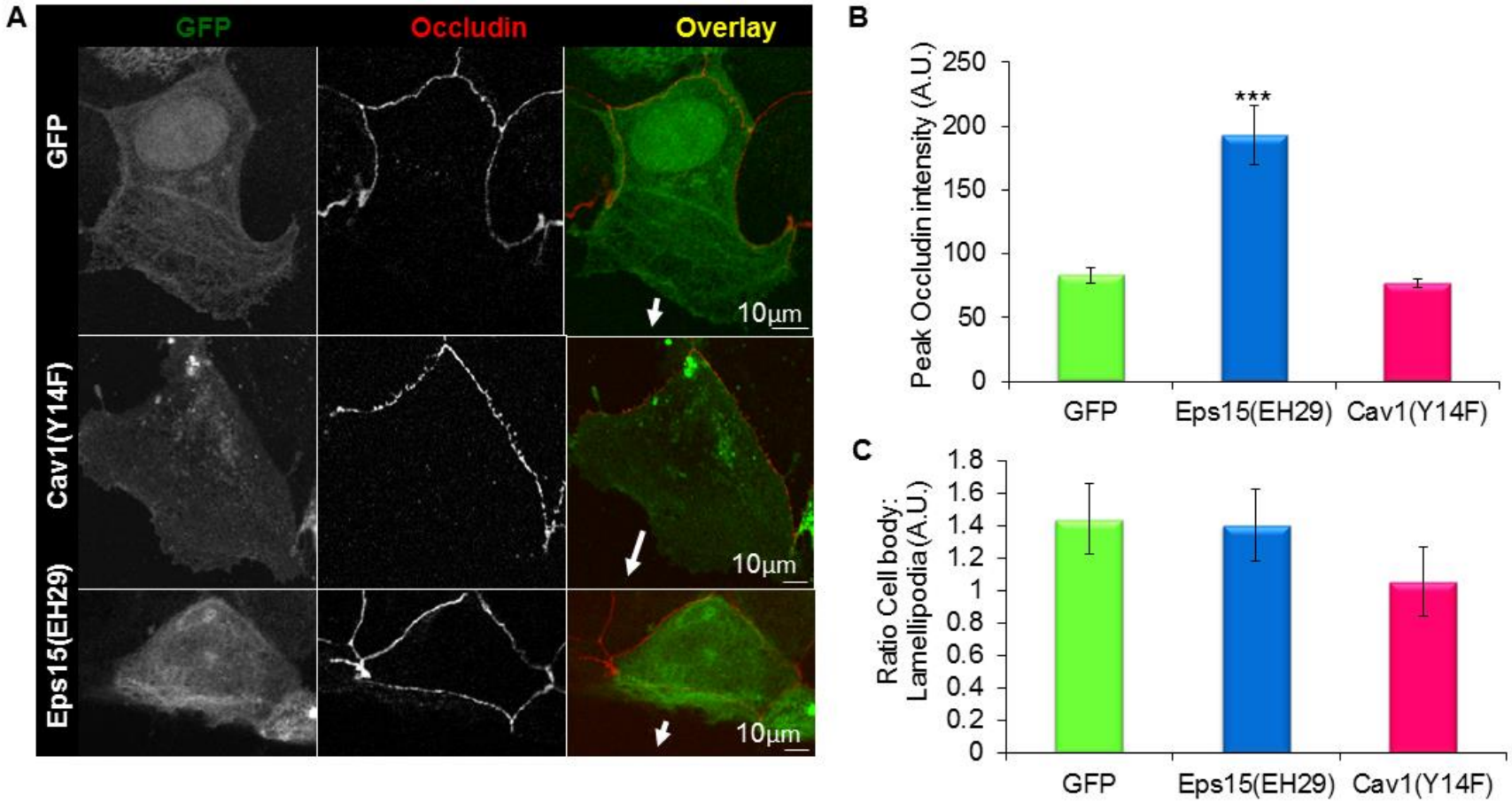
A
GFP
Occludin
Overlay
GFP
Cav1(Y14F)
Eps15(EH29)
10µm
10µm
10µm
B
Peak Occludin intensity (A.U.)
250
200
150
100
50
0
***
GFP
Eps15(EH29)
Cav1(Y14F)
C
Ratio Cell body: Lamellipodia (A.U.)
1.8
1.6
1.4
1.2
1
0.8
0.6
0.4
0.2
0
GFP
Eps15(EH29)
Cav1(Y14F)

endogenous occludin. Upon inhibition of these pathways, occludin localisation at the plasma membrane bordering the wound edge was quantified as in section 5.6. As depicted in Figure 5.5 in cells expressing GFP, 1 hour post-wounding the leading edge was completely devoid of occludin staining and a broad lamellipodia was formed. In cells were caveolar endocytosis was inhibited, all occludin had been internalised from the wound edge, as observed in GFP expressing cells. However, as demonstrated in Figure 5.5, in cells where CME was inhibited occludin remained at the wound edge 1 hour after wounding. Occludin was localised to a band posterior to the leading edge plasma membrane. In all three conditions, lateral membrane occludin localisation remained unaltered. It was also shown that inhibition of CME and caveolar endocytosis had no effect on the ability of cells to generate lamellipodia, with cell body area:lamellipodia area remaining similar in all three conditions (Figure 5.5c). Therefore these data suggest that clathrin-mediated endocytosis, not caveolar endocytosis is required for redistribution of occludin from the leading edge. However failure to achieve this redistribution did not affect generation of a lamellipodia in migrating MDCK cells.

5.8 Inhibition of clathrin-mediated endocytosis does not affect ZO1 localisation

In order to determine whether leading edge occludin present after inhibition of endocytosis remained as part of a TJ complex, the experiment performed in section 5.7 was repeated and localisation of endogenous ZO1 observed. ZO1 is a scaffolding protein which is localised to TJs, functioning to link occludin to

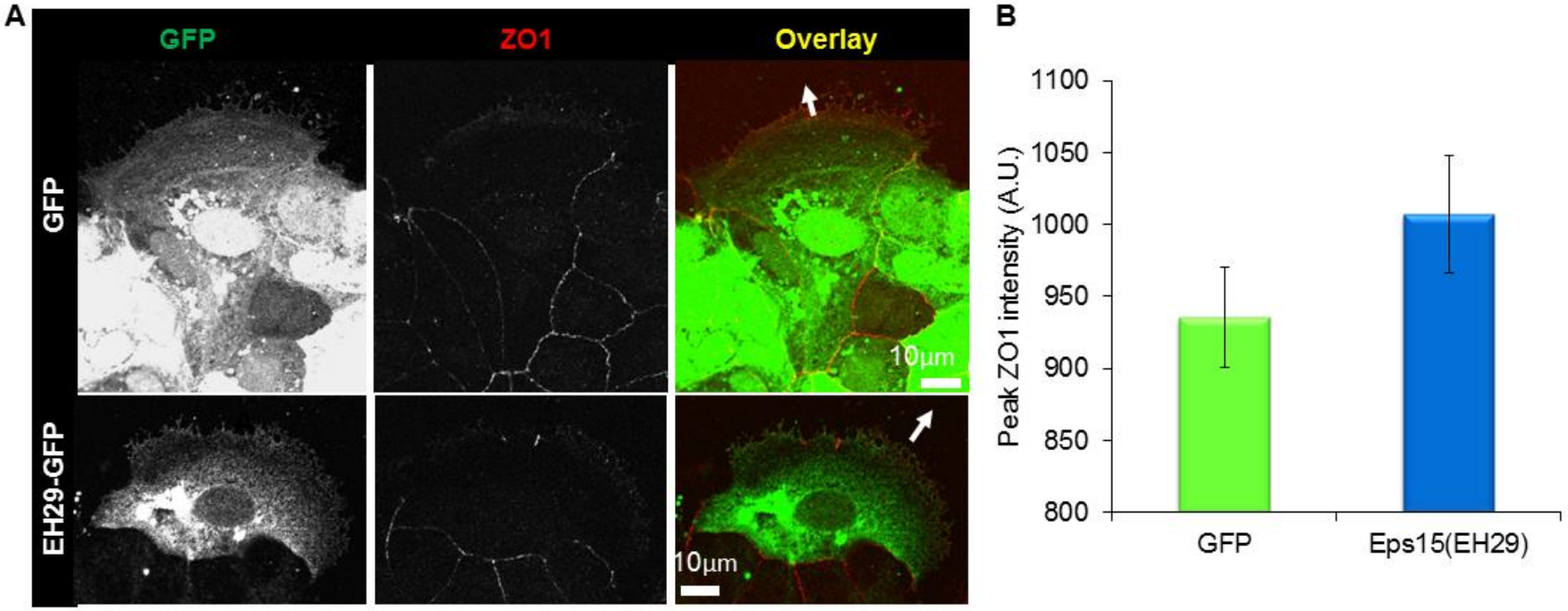

Figure 5.6. Inhibition of CME does not affect ZO1 localisation. MDCK cells were transfected with GFP or Eps15(EH29)-GFP (green), the monolayer was wounded and the cells allowed to migrate for 60 minutes before fixation and immuno-localisation using rabbit anti-ZO1 (1:250 dilution) and donkey anti-rabbit-Alexa Fluor 568 (1:200 dilution) (red). (A) Confocal microscopy image showing inhibition of CME has no effect on ZO1 localisation at the leading edge. (B) Quantification showing no alteration in ZO1 intensity at the leading edge of cells expressing Eps15(EH29)-GFP. n=3 repetitions, 15 cells of each expression condition were measured. White arrow denotes direction of migration.

the actin cytoskeleton (Steed, Balda, & Matter, 2010). CME was inhibited by expression of Eps15(EH29)-GFP and cells were probed for ZO1 1 hour post-wounding and imaged by confocal microscopy. As observed in Figure 5.6, ZO1 is clearly localised to the lateral membranes of migrating MDCK cells. To measure ZO1 localisation at the leading edge, cells were analysed as in section 5.7 and peak ZO1 intensity recorded. Figure 5.6 demonstrates in GFP expressing cells, ZO1 is absent from the area behind the forming leading edge. Inhibition of CME had no effect on ZO1 localisation and upon expression of Eps15(EH29)-GFP, ZO1 remained absent from the plasma membrane at the wound edge. Therefore, these data suggests inhibition of occludin endocytosis does not lead to retention of full TJ complexes at the forming leading edge.

5.9 Overexpression of GFP-occludin localises to the plasma membrane including the leading edge and decreases MDCK cell migration

Previous observations in this chapter have led to development of the hypothesis that clathrin-mediated endocytosis of occludin from the wound edge, into an early endosomal compartment, is stimulated by monolayer wounding. In numerous cases over-expression of membrane proteins has resulted in increased plasma membrane localisation. Similarly inhibition of endocytosis often causes the density of cargo to increase in the cell-surface, often with functional consequences (Butterworth et al., 2009; Gumpert et al., 2008; Hirsch, Varella-Garcia, & Cappuzzo, 2009; Liu et al., 2010; Lu et al., 2004; Volchuk et al., 1998). Thus, this study examined the hypothesis that increased plasma membrane localised occludin will lead to saturation of the mechanism which

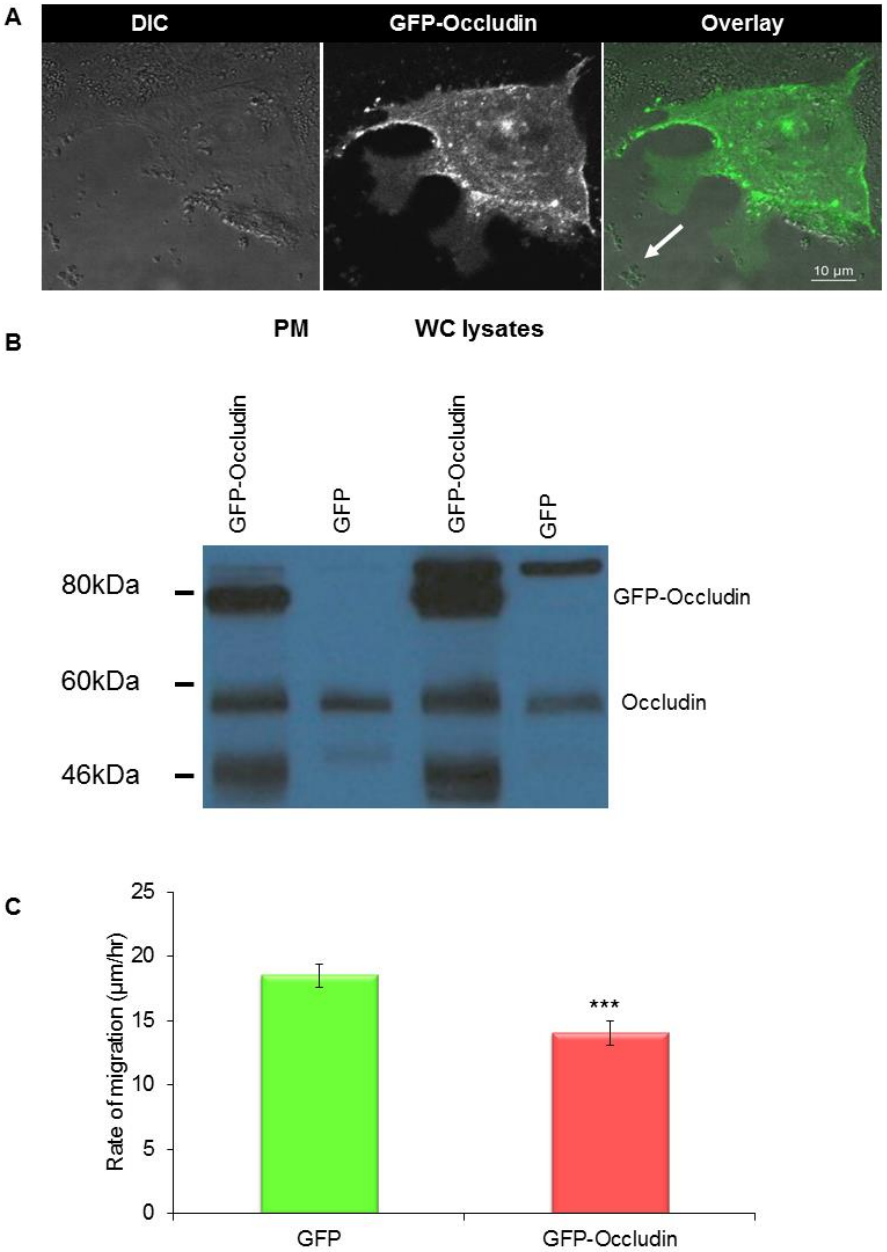

Figure 5.7. Over-expression of GFP-occludin leads to increased plasma membrane localised occludin, enrichment of occludin at the leading edge and decreased MDCK cell migration. MDCK cells were transfected with GFP-occludin, the monolayer was wounded and the cells allowed to migrate for 60 minutes before confocal imaging. (A) Brightfield and confocal image showing increased GFP-occludin at the wound edge. (B) Cell-surface biotinylation and Western blot analysis demonstrating increased occludin in the plasma membrane of cells expressing GFP-occludin compared to GFP control (n=3). The membranes were probed with primary rabbit anti-occludin antibody (diluted 1:500) and secondary anti-rabbit-HRP antibody (diluted 1:10000). (C) MDCK cells were transfected with GFP or GFP-occludin, the monolayer was wounded and imaged by epifluorescence and brightfield every 10 minutes for 6 hours. MDCK cells expressing GFP-occludin had significantly slower migration rates in comparison to GFP expressing controls. ***=p ≤0.001, n=160 cells from each condition measured from 4 independent experiments.

mediates redistribution of occludin from the wound edge, resulting in migratory defects. Therefore, this study utilised over expression of a previously described GFP-tagged occludin construct (Liu et al., 2010) at the plasma membrane and identified alterations in MDCK cell migration.

As is demonstrated in Figure 5.7b, in MDCK cells expressing GFP-occludin, Western blotting shows a band at 80kDa indicating GFP-occludin is present in over expressed whole cell lysate samples. Furthermore, in a cell-surface biotinylation assay (where only biotinylated plasma membrane proteins are pulled down by NeutrAvidin beads), GFP-occludin is observed at the plasma membrane. Also, the cell-surface biotinylation Western blot showed GFP-occludin was incorporated into the plasma membrane at approximately a threefold higher level than endogenous occludin (a band seen in all samples at ~58kDa). A band is observed in all lanes at approximately 46kDa, the identity of this band is unknown but may be a degradation product of occludin. Observations, of GFP-occludin localisation in live cells undergoing steady state migration show enrichment of occludin at the leading edge (Figure 5.7a). In 74% of cells assessed (14/19) occludin was seen at the cell-lamellipodium boundary, similar to what is observed following inhibition of endocytosis. As shown in Figure 5.7c, overexpression of GFP occludin led to a significant reduction in the rate of migration of MDCK cells relative to GFP control cells. This confirms that increasing the amount of occludin in the plasma membrane specifically at the wound edge, is sufficient to reduce the rate of epithelial cell migration during wound healing.

5.10 Deletion of the second extracellular loop of occludin leads to increased localisation at the wound edge

To further analyse the role of vesicle trafficking in redistribution of occludin from the wound edge, a mutant variant of occludin (previously shown to localise to the plasma membrane, but not present in a dynamin containing protein complex) (Liu et al., 2010) was utilised.

This occludin mutant, GFP-occludin(EL2), has had the second extracellular loop deleted (Liu et al., 2010). As depicted in Figure 5.8a and quantified in 5.8b, peak occludin fluorescence at the leading edge (measured as described in section 5.7) shows that localisation of the DelE2 occludin mutant is significantly increased in the forming lamellipodia following monolayer wounding relative to GFP-occludin. A wound healing assay was also performed on cells expressing either GFP-occludin or GFP-occludin(EL2). Figure 5.8c demonstrated there was no significant difference in the rate of migration of cells expressing either GFP-occludin or GFP-occludin(EL2). As observed previously (Figure 5.7c), overexpression of GFP-occludin decreased migration, potentially further inhibition of occludin endocytosis by deletion of the second extracellular loop may have no further migratory effect due to complete saturation of the occludin endocytosis pathway upon wild type overexpression. Therefore, occludin incorporation into a dynamin containing protein complex may be required for occludin endocytosis and when this does not occur redistribution of occludin following wounding is further perturbed. Taken together, these results support the hypothesis that endocytosis regulates epithelial cell migration during

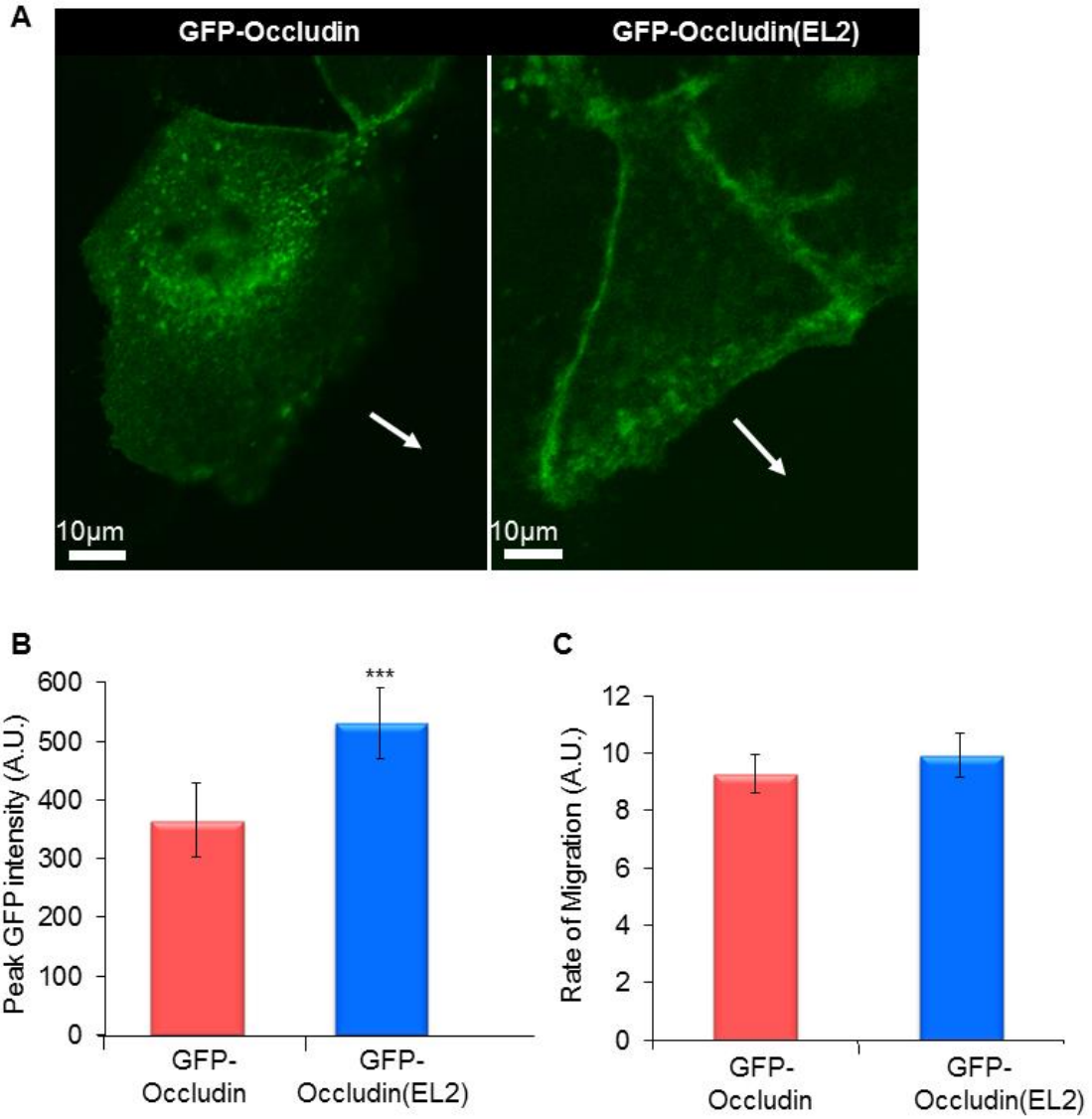

Figure 5.8. Deletion of the second extracellular loop of occludin leads to increased localisation of occludin at the cell edge bordering the wound. (A-B) MDCK cells were transfected with GFP-occludin or GFP-occludin(EL2)-GFP. The monolayer was wounded and the cells allowed to migrate for 1 hour before confocal imaging. (A) Confocal image showing increased localisation of GFP-occludin at the leading edge upon deletion of the second extracellular loop of occludin. (B) Quantification showing increased GFP-occludin(EL2) localisation at the leading edge in comparison to GFP-occludin. (C) MDCK cells were transfected with GFP-occludin or GFP-occludin(EL2)-GFP, the monolayer was wounded and imaged by epifluorescence and brightfield every 10 minutes for 6 hours. There was no alteration in the rate of migration between MDCK cells expressing GFP-occludin and GFP-occludin(EL2). ***=p ≤0.001, n=160 cells from each condition measured from 4 independent experiments

wound healing through redistribution of occludin from the site of leading lamella formation.

5.11 Discussion

The hypothesis that vesicle trafficking has a significant function in cell migration has gained increased credence since initial reports in the early 1980s where trafficking of membrane lipid to the extending leading lamella was implicated in cell migration (Bretscher, 1984). Currently, several potential mechanistic roles for endocytosis and trafficking during cell migration have been proposed including trafficking of cell adhesion molecules, activated growth factor receptors, and polarised exocytosis of proteases during invasion (Bailly et al., 2000; Bretscher, 1996; Caldieri et al., 2012; Caswell & Norman, 2006; Fletcher & Rappoport, 2010; Sheetz et al., 1999). It is now becoming apparent, that the role for a specific vesicle trafficking pathway may be cell-line specific and vary dependent upon migratory stimulus (Fletcher & Rappoport, 2010; Gu et al. 2011). This is demonstrated in chapter 3, where inhibition of the biosynthetic secretory pathway had no effect on MDCK cell migration, however the same mechanism of inhibition in a fibroblast cell lines caused significant migratory defects (Prigozhina & Waterman-Storer, 2004). Data from chapters 3 and 4 indicate the role of vesicle trafficking in epithelial cell migration may be significantly different from other cell types. Therefore, this study has sought to identify the role of vesicle trafficking in regulation of cell-cell matrix and cell-cell adhesion structures.

Data from this chapter indicates that during collective epithelial migration in response to a scratch wound, FAs dynamics are not regulated by CME, caveolar or dynamin-dependent endocytosis. However, upon wound formation the TJ protein occludin is internalised from the wound edge to a Rab5 positive early endosomal compartment in a manner dependent on CME. Furthermore, this redistribution of occludin from the leading edge was required for effective cell epithelial migration.

The results obtained in chapter 3 demonstrated that inhibition of dynamin, caveolar and clathrin-mediated endocytosis all had a significant effect on epithelial cell migration. Furthermore, previous research (Rappoport & Simon, 2003) and findings in chapter 4 showed that caveolar endocytosis and CME are polarised to different regions of the adherent plasma membrane in migrating MDCK cells, with caveolar endocytosis polarised to the rear, and CME localised to the cell front. Together these data may indicate a role for polarised CME or caveolar endocytosis in FA regulation during MDCK cell migration. This hypothesis is based upon evidence derived from studies in fibroblast cell lines. Work from Gregg Gundersen's lab has demonstrated that clathrin-mediated endocytosis plays an important role in FA disassembly (Ezratty et al., 2009). This evidence has been supported in studies by Chao and Kunz (2009), where inhibition of CME impaired FA disassembly and cell migration (Chao & Kunz, 2009). Furthermore, caveolar endocytosis has also been implicated in FA disassembly in work by Upla et al, (2004) where the integrin heterodimer $\alpha_2\beta_1$ was demonstrated to undergo internalisation by caveolar endocytosis in a manner dependent upon PKC in osteosarcoma cell lines (Upla et al., 2004).

However it is important to clearly delineate whether there is localised endocytosis of integrins from disassembling FAs, something no previous studies have directly demonstrated. Therefore this chapter addressed the potential role of the dynamin-dependent internalisation pathways (CME and caveolar endocytosis) in regulation of FA turnover during epithelial wound healing.

Preliminary work was performed to identify a suitable marker for FAs in MDCK cells (Fletcher et al., 2012). Although several fluorescently labelled constructs were demonstrated to localised to FAs (Fletcher et al., 2012), the studies performed is chapter 5 utilised β_3-integrin fluorescently labelled with GFP as a FA marker. β_3 is expressed endogenously in MDCK cells and has also been widely validated, is fully functional, capable of activation and is incorporated into FA structures (Schoenenberger et al., 1994; Tsuruta et al., 2002). Co-localisation analysis between FAs and markers of dynamin-dependent, caveolar and clathrin-mediated endocytosis was then performed during MDCK wound healing. In this chapter, contrasting with results observed previously (Chao & Kunz, 2009; Ezratty et al., 2009; Ezratty, Partridge, & Gundersen. 2005; Upla et al., 2004) no co-localisation between FA markers and these dynamin-dependent endocytosis pathways was observed in single still TIRF images taken during epithelial wound healing. Additionally, time-lapse studies examining co-localisation between markers of endocytosis and FAs during FA assembly, maturation and disassembly, demonstrated markers of CME or caveolar endocytosis did not co-incident with β_3-GFP (data not shown Fletcher et al., 2012). Further experiments examining effects of endocytosis pathway

inhibition on FA morphology during epithelial wound healing also showed no effect on either FA size or distribution in comparison to control cells (data not shown Fletcher et al., 2012). Importantly, the assays were verified as capable of identifying co-localisation with FAs and alterations in FA distribution or structure (data not shown Fletcher et al., 2012). Therefore, data obtained in sections 5.3-5.4 and published in Fletcher et al., 2012, indicate a minimal role for the dynamin-dependent, clathrin-mediated and caveolar endocytosis pathways in modulation of FA turnover during MDCK cell migration.

Although there is apparently little role for dynamin-dependent endocytosis in regulation of FA turnover during epithelial cell migration, more evidence is emerging of non-dynamin, clathrin-independent mechanisms of FA component endocytosis. Recent work by Gu et al, 2011 suggested that in fibroblasts stimulated with PDGF, β_3-integrins are internalised by large dorsal circular ruffles (Gu et al., 2011). This has been demonstrated further where internalisation of β_1-integrin has been shown to occur via membrane ruffles dependent upon R-Ras activity (Conklin et al., 2010). Therefore, data from this chapter suggests in epithelial cells undergoing 2D planar directed migration, FA turnover is independent of caveolar, clathrin-mediated and dynamin-dependent endocytosis, however other internalisation pathways may play a role in regulation of FA dynamics.

In migrating epithelial cells, a key physiological difference in comparison to other cell lines is the presence of significant cell-cell adhesions maintained throughout the “sheet-like” migration process. These structures require constant remodelling to ensure collective migration as a single epithelial

monolayer. In this study, regulation of the tight-junction protein occludin by endocytosis was examined during epithelial wound healing. Work by other groups has identified that occludin undergoes endocytosis when subject to a variety of stimuli. Factors such as calcium depletion and growth factor/cytokine treatment promotes internalisation of occludin into EE (Harhaj & Antonetti, 2002; Ivanov, Nusrat & Parkos, 2004; Stamatovic et al., 2009; Su et al., 2010). Furthermore, the endocytosis pathway through which occludin has been suggested to occur is dependent upon stimulus (Ivanov, Nusrat & Parkos, 2004; Marchiando et al., 2010; Stamatovic et al., 2009; Xia et al., 2009).

This chapter proposes epithelial wound healing as a novel mechanism which stimulates endocytosis of occludin from the leading edge to Rab5 positive compartments shortly after wound formation. Selective inhibition of dynamin demonstrated dynamin-dependent endocytosis of occludin is required for redistribution of occludin from the leading edge. This is particularly interesting as work by Liu et al, (2010) suggests that occludin forms a complex with dynamin2 (Liu et al., 2010). Whether this complex is formed and required for occludin endocytosis or whether dynamin2 has an alternative function at TJs is unknown. Further dissection of the dynamin-dependent endocytosis pathways required for occludin redistribution from the leading edge indicated occludin is internalised by CME. Although inhibition of CME prevented redistribution of occludin from the wound edge, other TJ proteins did not remain, the scaffolding protein ZO1 was absent from the leading edge upon CME inhibition (as seen in control treated cells), suggesting the entire TJ complex was not retained at the leading edge upon CME inhibition. As occludin redistribution from the leading

edge occurred during epithelial wound healing, the hypothesis that removal of occludin from the wound edge was required to promote epithelial cell migration was established. The findings described in this chapter suggest expression of GFP-occludin in MDCK cells leads to a similar occludin localisation to that observed when dynamin-dependent endocytosis was inhibited. Furthermore that overexpression of occludin at the wound edge significantly reduced the rate of epithelial cell migration in comparison to control GFP expressing cells, therefore removal of occludin from the wound edge may be a pre-requisite for effective MDCK cell migration. This finding is further supported in recent work by Du et al., (2010). Their findings suggest that 6 hours post-wounding occludin is re-localised to the leading edge and is required for recruitment of aPKC-Par3 and PatJ polarity complexes to the leading edge stimulating membrane localised PI3 kinase activity and promoting membrane protrusions (Du et al., 2010). Therefore the initial internalisation of occludin from the leading edge observed in this study may be required prior to the redistribution of occludin to the lamellipodial edge. Thus re-localisation of occludin to the leading edge could occur via polarised endosomal recycling and may be required for stabilisation of polarity complexes at the leading edge facilitating membrane expansion and cell migration. Moreover, it appears that the ability of dynamin to form a complex with occludin is required for effective endocytosis from the plasma membrane. Cells expressing an occludin mutant lacking the second extracellular loop were unable to form a complex with dynamin (Liu et al., 2010) and show a significant increase in wound edge localisation in comparison to cells expressing wild type occludin (section 5.10). Interestingly, overexpression

of the dynamin binding deficient mutant had no effect on migration in comparison to over expression of wild type occludin, although both exhibited a reduction in migration in comparison to GFP expressing cells. This suggests the endocytosis mechanism may already be saturated upon wild type occludin expression, therefore further endocytosis defects do not affect the rate of migration during epithelial wound healing.

5.12 Key chapter findings

- FA turnover is not regulated by dynamin-dependent, clathrin-mediated or caveolar endocytosis during epithelial wound healing.
- Wound healing stimulates endocytosis of occludin from the wound edge to EEs shortly after wounding, in a manner dependent on clathrin-mediated endocytosis.
- Overexpression of occludin reduces MDCK cell migration.
- Deletion of the second extracellular loop of occludin leads to increased localisation at the wound edge of migrating MDCK cells.

5.13 Conclusion

These results include independent and novel findings. While CME is required for effective epithelial cell migration, it does not act via regulation of FAs but through internalisation of occludin from the wound edge. This chapter provides further evidence for differences in the mechanisms linking vesicle trafficking and cell migration between epithelial and non-epithelial cells. Additionally, this study

demonstrates another physiologically relevant stimulus for occludin endocytosis and identifies the specific pathway responsible.

CHAPTER 6

STEADY-STATE OCCLUDIN TRAFFICKING

6.1 Introduction

The previous chapter demonstrated the stimulated trafficking of the TJ protein occludin from the plasma membrane at the wound edge during MDCK wound healing (Fletcher et al., 2012). It also showed that after internalisation, occludin was transported to Rab5 positive EEs. Endocytosis and trafficking of occludin has also been observed by other groups upon stimulated TJ disassembly (Ivanov, Nusrat, & Parkos, 2004; Marchiando et al., 2010; Stamatovic et al., 2009; Xia et al., 2009). However, little work has been performed examining occludin trafficking under steady-state conditions. Work previously has implicated occludin in both formation and maintenance of TJs (Balda et al., 1996; Furuse et al., 1996; Saitou et al., 2000), yet little is known about how occludin is regulated at the plasma membrane.

Several lines of evidence suggest occludin turnover at the plasma membrane may be regulated by vesicle trafficking. As mentioned previously, many groups have observed endocytosis of occludin under stimulated TJ disassembly (Ivanov, Nusrat, & Parkos. 2004; Marchiando et al., 2010; Stamatovic et al., 2009; Xia et al., 2009). However a function for vesicle trafficking in regulation of

occludin trafficking has been observed in non-stimulated conditions in data from the laboratory of Takuya Sasaki who demonstrated in both fibroblastic BHK cells (transiently expressing occludin) and MTD-1A epithelial cells (endogenously expressing occludin); that occludin undergoes continuous endocytosis via CME and recycling back to the plasma membrane in a manner dependent on Rab13 (Morimoto et al., 2005).

Additionally, occludin trafficking may be further regulated by post-translational modification. A recent review by Dörfel and Huber (2012), has highlighted the importance of post-translational modification of occludin in its plasma membrane localisation (Dörfel & Huber, 2012). Occludin phosphorylation (directly or downstream) by Src, FAK, Rho kinase, MAP kinases, PKC, casein kinases and phosphatidylinositol-3-kinase have all been demonstrated to regulate occludin distribution at TJs (reviewed fully in Dorfel & Huber, 2012). Furthermore, occludin has been shown to undergo ubiquitination dependent upon phosphorylation at Serine 490, which is required for its endocytosis and trafficking upon VEGF induced TJ disassembly (Murakami et al., 2009) suggesting post-translational modification may be a key factor in regulation of occludin trafficking.

One of the main aims of this chapter was to identify proteins which may function in regulation of occludin trafficking and maintenance of plasma membrane occludin homeostasis in a confluent monolayer of non-stimulated MDCK cells. For this, a quantitative proteomics approach called stable-isotope labelling by amino acids in cell culture (SILAC) combined with mass spectrometry was

utilised. SILAC enables incorporation of amino acids with substituted stable isotopic nuclei into cellular proteins. This is achieved by incubation with media containing either “light” (isotypically normal L-arginine and L-lysine), “medium” ($^{13}C_6$L-arginine and L-lysine-D4) or “heavy” ($^{13}C_6{}^{15}N_4$L-arginine and $^{13}C_6$L$^{15}N_2$-lysine) amino acids through several rounds of cell division. As there is minimal chemical difference between the labelled and natural amino acid isotopes, several experimental parameters can be examined with no difference to control isotypically normal cells. This technique enables quantitative measurement of alterations in protein abundance (treatment in comparison to control). SILAC also removes experimental bias between samples as after lysis samples are combined (thus subject to the same processing). Pairs or triplets of identical peptides can be differentiated by mass spectrometry due to their mass difference as a result of incorporation of different isotopes. Recently, IP techniques have been applied alongside SILAC to identify interaction partners and proteins which form the components of multi-protein complexes which co-immunopurify with the protein of interest (Trinkle-Mulcahy et al., 2006). Thus, in this chapter a combination of IP, SILAC and high-resolution mass spectrometry were utilised to identify potential occludin binding partners/multi-protein complexes which may regulate occludin trafficking in non-stimulated MDCK cells.

Alongside attempting to identify specific occludin binding proteins which may regulate occludin trafficking, a second aim for this chapter was to identify the pathways through which occludin may traverse. Although occludin has been shown to undergo continuous recycling (Morimoto et al., 2005) the exact

endosomal compartments through which occludin is transported is unknown. In this study, confocal imaging and co-localisation analysis between fluorescently labelled endosomal compartment markers and endogenous occludin were utilised to determine its trafficking route. Furthermore, the function of these pathways in regulation of occludin plasma membrane localisation and endosomal trafficking was verified biochemically using several Sulfo-NHS-SS-Biotin based recycling assay systems.

The findings of this chapter demonstrate under steady state conditions in MDCK cells that the majority of plasma membrane-associated occludin is internalised within 30 minutes, similar to results obtained in studies by Morimoto et al., 2005. However, by 2 hours the amount of intracellular occludin which has been internalised from the plasma membrane has significantly reduced. Lysosomal degradation of occludin was verified by repetition of biotinylation experiments in the presence of the lysosomal acidification inhibitor BafA, leading to increased abundance of internalised occludin. Furthermore, treatment with BafA led to a significant increase in co-localisation between endogenous occludin and CD63-GFP (late endosome/lysosomal marker).

SILAC proteomic analysis combined with IP and mass spectrometry to identify occludin binding partners in the presence of DMSO (control) or BafA, yielded several unexpected results. Firstly, none of the expected binding partners of occludin such as members of the ZO family (Furuse et al., 1994; Itoh, Morita, & Tsukita, 1999) were found to bind occludin under either experimental condition. Furthermore, no proteins which are involved in protein trafficking were identified

as definite “hits” during the mass spectrometry screen. However, grouping of these data into protein function groups identified a large proportion of the proteins which did bind occludin were proteins involved in biosynthesis, suggesting occludin may undergo constant synthesis rather than recycling. This was further confirmed by performing cell-surface biotinylation assays in the presence of CHX (inhibitor of protein synthesis). A significant reduction in the level of plasma membrane localised occludin was observed four hours post-CHX treatment in comparison to DMSO treated control cells. Also, a high level of co-localisation was observed between markers of the secretory pathway (NPY) and endogenous occludin. Therefore, the data from this chapter indicates occludin is undergoing a constant cycle of endocytosis, degradation and biosynthesis to maintain plasma membrane occludin homeostasis in a confluent monolayer of MDCK cells.

6.2 Results

6.3 The majority of plasma membrane occludin internalised is targeted for degradation or recycling

There is little data examining occludin trafficking under steady state non-stimulated conditions. Therefore this study utilised a Sulfo-NHS-SS-Biotin based recycling assay (Roberts et al., 2001) to measure occludin internalisation and trafficking dynamics in a non-migrating confluent MDCK cell monolayer. This assay utilised a cell-impermeant, cleavable biotinylation reagent (Sulfo-NHS-SS-Biotin) to biotin label all cell-surface proteins at 4ºC (to inhibit

endocytosis and vesicle trafficking). The cells were warmed back to 37ºC to permit trafficking for a designated time, the temperature reduced to 4ºC and all remaining cell-surface Sulfo-NHS-SS-Biotin-labelled proteins were cleaved using a cell-impermeant reducing agent. This method enabled quantitative measurement of Sulfo-NHS-SS-Biotin-labelled proteins internalised from the plasma membrane (only biotinylated proteins within the cell body were protected from reduction). All biotinylated proteins were then pulled down using NeutrAvidin beads. Results from this assay, as demonstrated in Figure 6.1a show a steady increase in the abundance of internalised occludin between 0 minutes and peaking at 30 minutes. A reduction in the level of internalised intracellular occludin is observed after 30 minutes and by 2 hours this occludin pool was reduced significantly. These data were normalised against the total plasma membrane level of biotinylated occludin (lane 1 Figure 6.1a), and plotted in Figure 6.1b. Figure 6.1b shows the majority of plasma membrane localised occludin is internalised by 30 minutes and is likely to be undergoing either degradation or recycling back to the plasma membrane by 120 minutes.

6.4 Under non-stimulated conditions a large proportion of internalised occludin undergoes lysosomal degradation

Figure 6.1, demonstrates that post-internalisation the level of internalised intracellular occludin decreases dramatically, suggesting this pool of occludin is undergoing recycling or degradation. This study examined the potential for

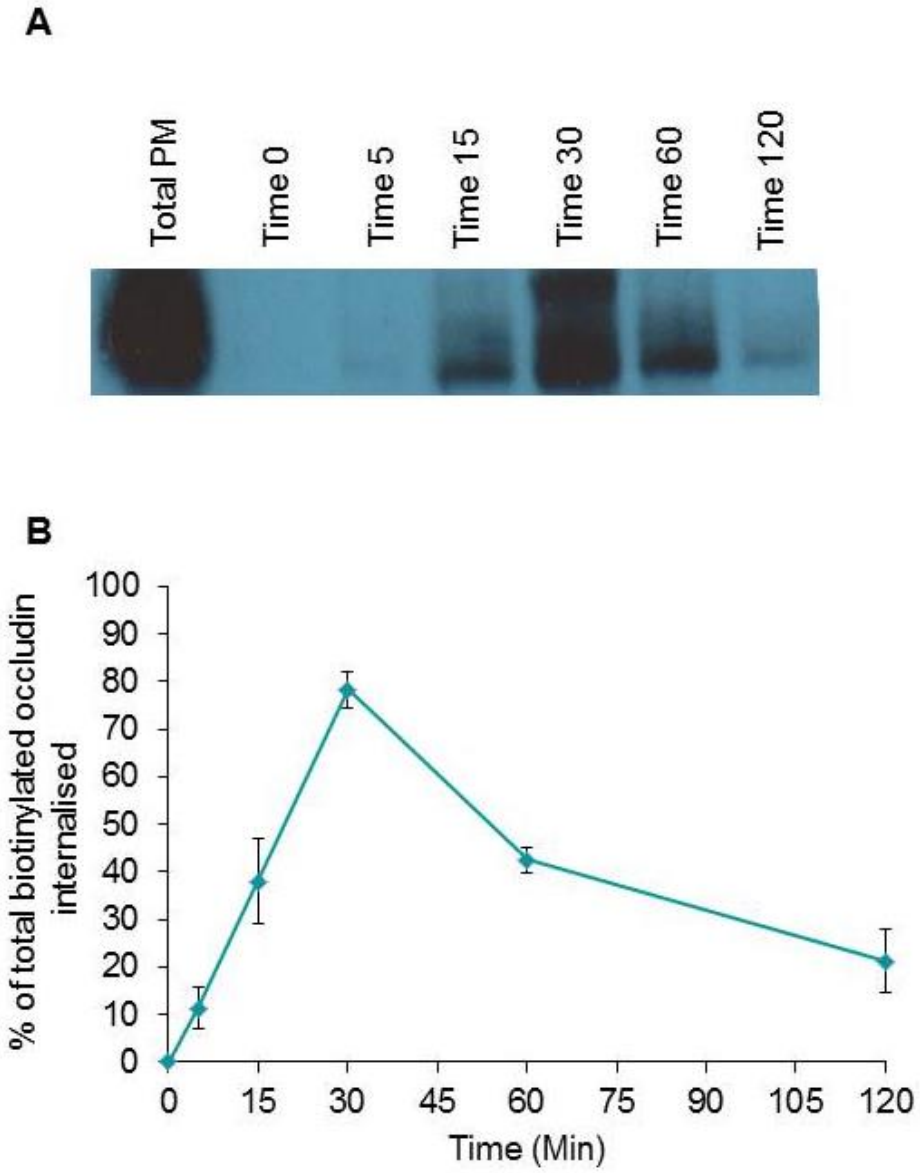

Figure 6.1. Steady state internalisation and endosomal trafficking of occludin. A confluent monolayer of MDCK cells were serum starved for 1 hour. Cell-surface proteins were biotinylated at 4ºC and warmed to 37ºC for designated time points. Cell-surface biotinylated proteins were reduced, enabling only proteins within the cell body to remain biotinylated. Cells were lysed and biotinylated proteins pulled down with NeutrAvidin beads. Protein abundance was quantified by Western blot analysis. The membranes were probed with primary rabbit anti-occludin antibody (diluted 1:500) and secondary anti-rabbit-HRP antibody (diluted 1:10000). (A) A biochemical trafficking assay demonstrates that occludin undergoes continuous rapid endocytosis, and that the internalised pool of occludin is subsequently lost. (B) Quantification of 3 repeats of the experiments shown in (A).

occludin degradation after internalisation as a mechanism through which occludin plasma membrane homeostasis is regulated. To test this hypothesis, the macrolide antibiotic BafA was utilised to inhibit lysosomal degradation. BafA acts on V-ATPases to inhibit lysosomal acidification (Yoshimori et al., 1991). To confirm lysosomal acidification was inhibited by BafA, MDCK cells were incubated with LysoTracker in the presence of either DMSO or BafA. LysoTracker probes are widely published, weakly basic amine probes, coupled to various fluorescent dyes which selectively accumulate in acidic compartments (Boya et al., 2003). As can be observed in confocal images in Figure 6.2a, in the presence of DMSO (control) there is a punctate intracellular distribution of LysoTracker-Red DND-99 positive lysosomes. In cells treated with BafA, no punctate lysosomal structures were seen. To quantify retention of LysoTracker within Lysosomes, the intracellular LysoTracker intensity was quantified by drawing an ROI around the cell cytosol and measuring the average intensity within this region. The LysoTracker intensity in BafA treated cells demonstrated a highly significant (98.8%) reduction in average LysoTracker Red DND-99 intensity in comparison to control cells (Figure 6.2b). These data demonstrate BafA is inhibiting lysosomal acidification, as LysoTracker has not accumulated in lysosomal structures.

Once BafA treatment had been verified as an inhibitor of lysosomal acidification, the biotinylation recycling protocol performed in section 6.3 was repeated in the presence of BafA to assess degradation of internalised occludin in an MDCK cell monolayer. As shown in Figure 6.3a and b, BafA treatment had little effect on occludin internalisation dynamics, the level of occludin

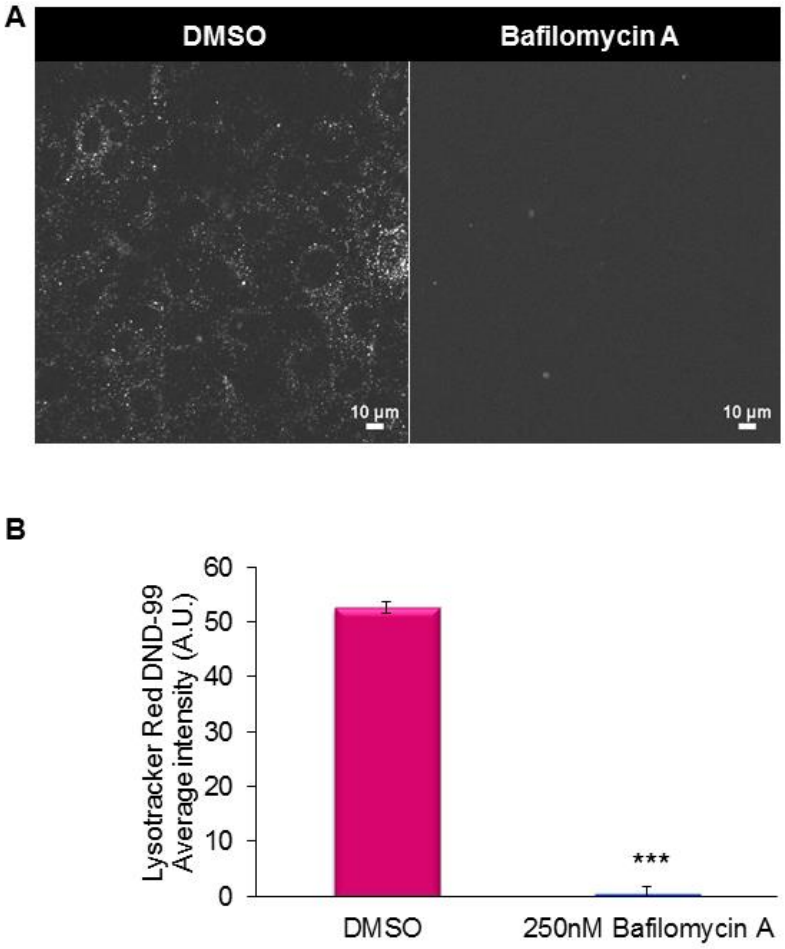

Figure 6.2. BafA inhibits lysosomal acidification. A confluent monolayer of MDCK cells were incubated with 75nM LysoTracker Red DND-99 plus either 1.53µl/ml DMSO or 250nm BafA for 2 hours. Live cells were imaged using confocal microscopy. (A) Confocal image demonstrating accumulation of LysoTracker in acidic compartments in the presence of DMSO. No accumulation of LysoTracker was observed in cells incubated with BafA. (B) Quantification of 3 repeats of the experiments shown in (A) a minimum of 18 cells from each condition were measured. *** $p \leq 0.001$,

internalised from the membrane still peaked at 30 minutes however occludin began to build up at 15 minutes. In both the BafA and DMSO treated samples a decrease in the level of occludin internalised from the plasma membrane is observed after 30 minutes. However, at 2 hours there is an accumulation of internalised occludin in cells treated with BafA not observed in control cells (Figure 6.1). This is confirmed in Figure 6.3c, a 63% reduction in degradation of occludin internalised from the plasma membrane was observed in cells treated with BafA. These data demonstrate a large proportion of occludin undergoes endocytosis followed by lysosomal degradation. However it must be noted, a reduction between peak (time 30) and internalised intracellular occludin levels at 60 and 120 minutes is still observed in the presence of BafA potentially indicating occludin recycling back to the plasma membrane.

6.5 BafA treatment increases co-localisation between endogenous occludin and late endosome/lysosomal compartments

As demonstrated in the previous section, BafA treatment inhibits degradation of internalised occludin in a non-stimulated epithelial monolayer, leading to increased intracellular occludin levels. This section aimed to identify the localisation of intracellular endogenous occludin in a non-stimulated MDCK cell monolayer. MDCK cells transiently expressing fluorescently labelled endosomal markers were assessed for co-localisation with endogenous occludin during either DMSO or BafA treatment. Preliminary results examining co-localisation between occludin and Rab5-GFP (EE marker), Rab11-GFP and Rab25-GFP (recycling endosome markers) demonstrated minimal co-

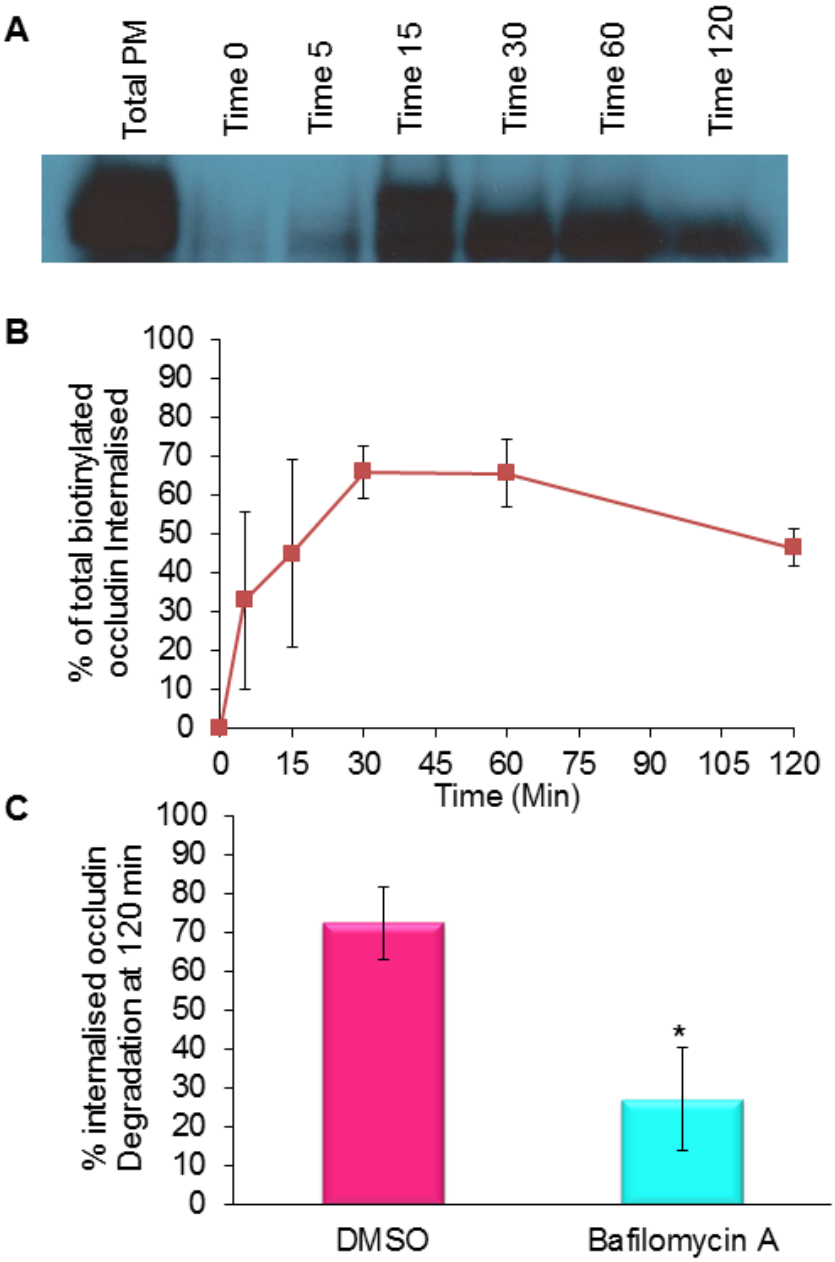

Figure 6.3. Steady-state degradative trafficking of occludin. A confluent monolayer of MDCK cells were serum starved for 1 hour in the presence of either 1.53 µl/ml DMSO or 250nm BafA. Cell-surface proteins were biotinylated at 4ºC and warmed to 37ºC for designated time points in the presence of DMSO or BafA. Cell-surface biotinylated proteins were reduced, enabling only proteins within the cell body to remain biotinylated. Cells were lysed and biotinylated proteins pulled down with NeutrAvidin beads. Protein abundance was quantified by Western blot analysis. The membranes were probed with primary rabbit anti-occludin antibody (diluted 1:500) and secondary anti-rabbit-HRP antibody (diluted 1:10000). (A) Treatment with BafA (inhibitor of lysosomal degradation), attenuates the decrease in occludin signal following endocytosis. (B) Quantification of 3 repeats of the experiments shown in (A). (C) Quantification of the decrease in occludin signal between 30 and 120 minutes comparing control to BafA treatment. * $p \leq 0.05$,

localisation between recycling endosomal compartments and occludin in DMSO treated cells (data not shown). No alteration of this phenotype was observed upon treatment with BafA (data not shown). Together, these data suggest occludin undergoes minimal recycling in epithelial monolayers. Therefore, co-localisation between lysosomes and endogenous occludin was observed.

To fluorescently label the late endosomal/lysosomal compartments, CD63-GFP was expressed in MDCK cells (Metzelaar et al., 1991). CD63-GFP was verified as a marker of the late endosomal/lysosomal pathway by incubation of CD63-GFP expressing MDCK cells with LysoTracker and examining co-localisation by confocal microscopy. As shown in Figure 6.4, CD63-GFP and LysoTracker positive structures are co-incident, making CD63-GFP a suitable late endosome/lysosomal marker. Therefore, co-localisation analysis was performed examining endogenous occludin localisation in CD63-GFP expressing cells.

As demonstrated in Figure 6.5a under control conditions (DMSO) CD63-GFP positive puncta were observed throughout the cytosol with a slight clustering in a juxtanuclear position. However upon treatment with BafA an increase in CD63-GFP vesicle clustering was seen adjacent to the nucleus. Under control conditions intracellular occludin puncta co-localise with CD63-GFP positive structures. This level of co-localisation significantly increased in the presence of BafA (Figure 6.5a). A Pearson's Correlation Coefficient was performed on selected regions of interest and co-localisation between CD63-GFP and occludin was quantified and compared in DMSO and BafA treated cells. A significant 72% increase in co-localisation between occludin and CD63-GFP

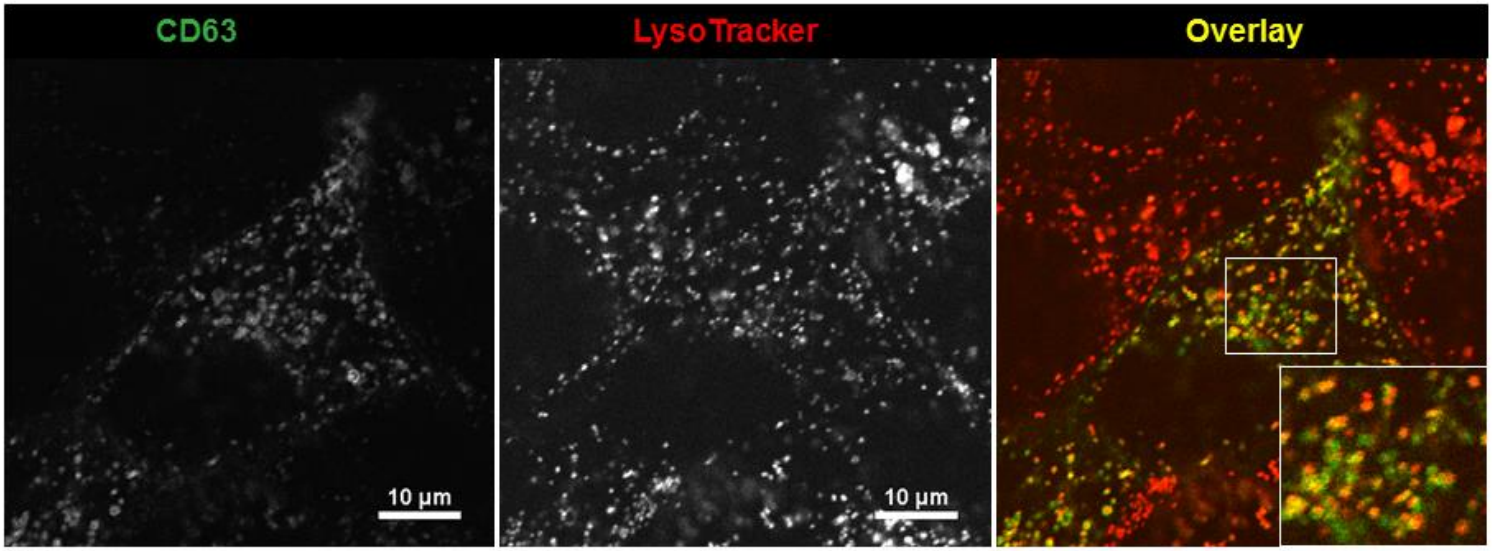

Figure 6.4. LysoTracker Red DND-99 co-localises with CD63-GFP. A confluent monolayer of MDCK cells transiently expressing CD63-GFP were incubated with 75nM LysoTracker Red DND-99 for 2 hours. Live cells were imaged using confocal microscopy. A high level of co-localisation was observed between CD63-GFP and LysoTracker positive structures (n=1).

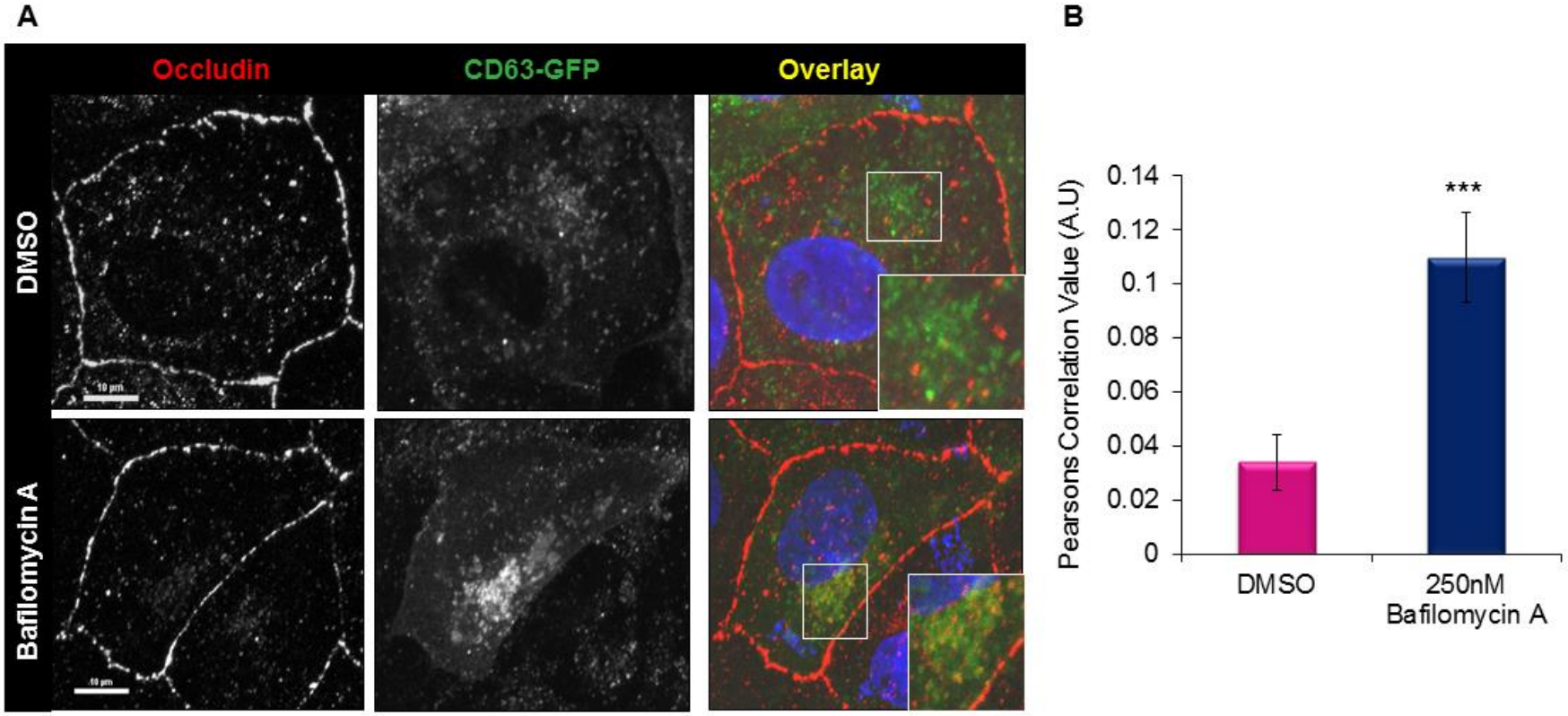

Figure 6.5. Intracellular occludin positive puncta co-localise with late endosome/lysosomal structures. Incubation with BafA increases co-localisation between occludin and CD63-GFP. A confluent monolayer of MDCK cells transiently expressing CD63-GFP were incubated with 1.53 µl/ml DMSO or 250nm BafA for 2 hours, before fixation and immuno-localisation with primary mouse anti-occludin antibody (diluted 1:100) and secondary anti-mouse-AlexaFluor568 antibody (1:100). Cells were imaged by confocal microscopy. (A) Confocal image showing co-localisation between occludin and CD63-GFP in the presence of DMSO or BafA. (B) Quantification of 3 repeats of the experiments shown in (A) with a minimum of 12 cells analysed of each condition. *** $p \leq 0.001$.

was observed in cells incubated with BafA (Figure 6.5b). Therefore, data from this section further corroborates the findings described in section 6.4, with endogenous occludin demonstrating minimal co-localisation between recycling endosomal compartments and a high level of co-localisation between late endosome/lysosomal compartments, suggesting occludin is predominantly degraded rather than recycled in epithelial monolayers.

6.6 Quantitative proteomic analysis of occludin binding proteins suggest a high level of occludin biosynthesis

As has been demonstrated in section 6.3 and throughout chapter 5, occludin is a protein which undergoes endocytosis in MDCK cells. Chapter 5 also showed occludin internalisation from the wound edge to Rab5 positive EEs was mediated by dynamin-dependent clathrin-mediated endocytosis (Fletcher et al., 2012). Furthermore, work from several other groups has suggested occludin undergoes endocytosis and trafficking via several trafficking pathways including caveolar endocytosis and clathrin-mediated endocytosis (Ivanov, Nusrat, & Parkos 2004; Marchiando et al., 2010; Morimoto et al., 2005; Murakami, Felinski, & Antonetti, 2009; Stamatovic et al., 2009; Xia et al., 2009). In many of the aforementioned studies, cells were stimulated with growth factors, cytokines, calcium depletion or as described in chapter 5, wound formation to examine occludin internalisation. Few studies have examined occludin trafficking under non-stimulated conditions, until this current study. Therefore, to further examine the endocytosis mechanisms and trafficking pathways

involved in regulation of steady state occludin trafficking, SILAC in combination with IP and mass spectrometry was performed. In this study a triple SILAC protocol was used to identify proteins which may either bind directly or form multi-protein complexes with occludin to regulate its trafficking. A triple SILAC experiment enabled examination of occludin binding proteins in three conditions. The first “light” SILAC condition consisted of cells treated with DMSO, and the IP was performed with rabbit IgG conjugated G-Sepharose beads. This condition was the control to remove proteins binding non-specifically from the screen. In the “medium” SILAC condition cells were treated with BafA to maximise intracellular occludin levels (potentially increasing occludin binding trafficking proteins); the IP was performed with rabbit anti-occludin conjugated beads. The final “heavy” condition acted as a control for the “medium” treated cells. “Heavy” cells were treated with DMSO and IP performed with rabbit anti-occludin beads.

Once the IP method had been validated, analysis by mass spectrometry and processing of files in MaxQuant, generated a total of 386 proteins identified in the screen. MaxQuant analysis provides a quantitative value of changes in protein abundance between two samples in the form of a ratio value. This ratio value enables establishment of a median range of values, which are considered “non-hits” as the majority of proteins which fall in this category have no or an insignificant change in abundance upon condition variation. “Hits” are classified as proteins whose ratios do not lie within this median range, instead they have a particularly high/low ratio indicating a change in protein abundance. Obviously the median value range exhibits a high level of experimental variation, so the

Figure 6.6. Distribution of ratios obtained after SILAC labelling and mass spectrometry analysis. "Light" and "heavy" cells were incubated with corresponding SILAC media containing 1.53µl/ml DMSO, whilst "medium" cells were incubated with medium SILAC media containing 250nM BafA, all cells were treated for 2 hours. The cells were then serum starved, "light" and "heavy" cells were incubated with serum free SILAC media containing DMSO or "medium" serum free SILAC media containing 250nM BafA for 2 hours, then lysed. Immunoprecipitations were performed: "light" samples were incubated with Rabbit IgG conjugated beads whilst "medium" and "heavy" samples were incubated with Rabbit anti-occludin conjugated beads (all samples incubated 1:10 antibody to G-Sepharose beads). Samples were run on SDS-PAGE, the lane containing the samples was excised, and subject to mass spectrometry analysis. (A) A data plot comparing "heavy" to "light" ratio "hits" (proteins showing increased pull down in "heavy" conditions than "light" treated cells) were classed as those with a ratio above 1.6. (B) A data plot comparing "medium" to "light" ratio "hits" (proteins showing increased pull down in "medium" conditions then in "light" treated cells) were classed as those with a ratio above 1.8. (C) A data plot comparing "heavy" to "medium" ratio "hit" proteins showing increased pull down in "heavy" conditions then in "medium" treated cells were classed as those with a ratio above 1.4. "hit" proteins showing increased pull down in "medium" conditions then in "heavy" treated cells were classed as those with a ratio below 0.5. "hits" in "heavy" treated cells. "hits" in "medium" treated cells.

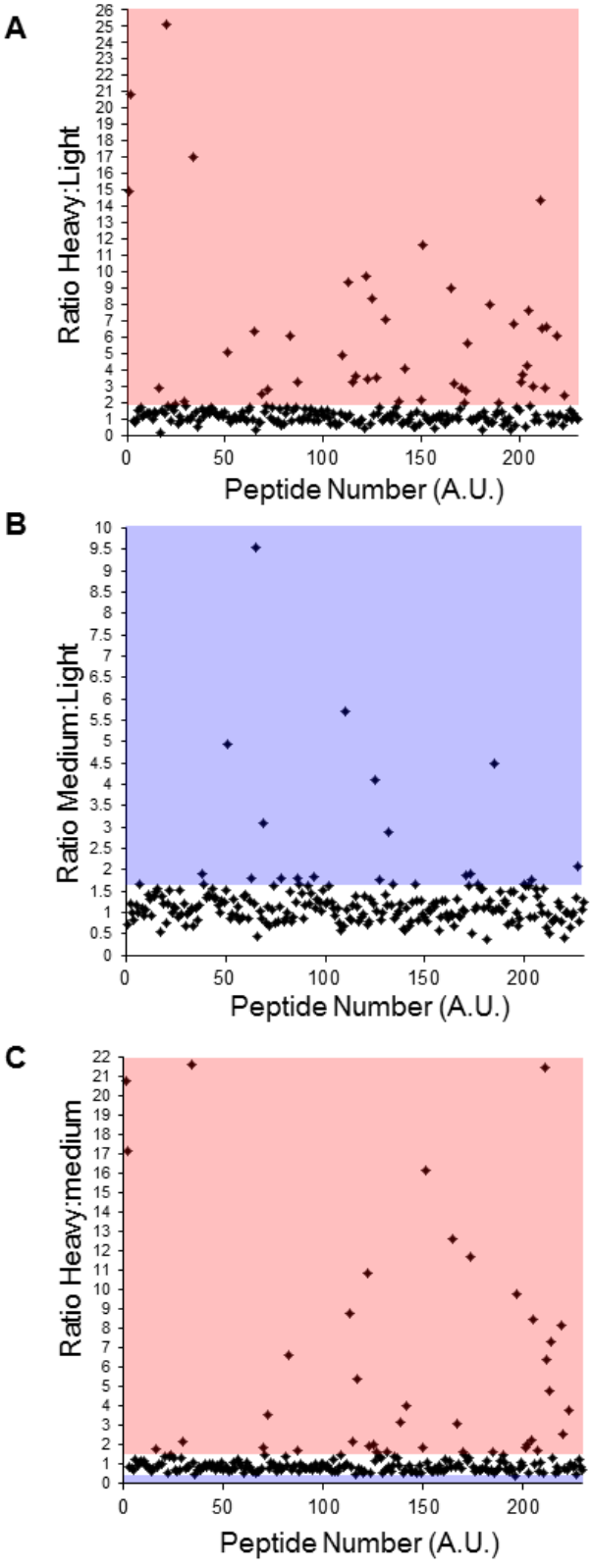
A
Ratio Heavy:Light
Peptide Number (A.U.)
B
Ratio Medium:Light
Peptide Number (A.U.)
C
Ratio Heavy:medium
Peptide Number (A.U.)

parameters must be changed after examination of ratio distribution. Before distribution plots of protein ratio were performed, proteins with a unique peptide score of less than 2 or whose ratios were expressed as non-applicable numbers were removed from the sample as they were unlikely to be valid “hits”, leaving a total of 231 proteins. Figure 6.6a shows the distribution of ratios in “heavy” to “light” conditions, the majority of ratio values fall into the median range of 0.4-1.8. Proteins within this range are ones which IP similarly with both IgG and rabbit anti-occludin coupled beads, thus are likely to be binding non-specifically and can be discounted. Proteins with a value of <0.4 are demonstrating increased pull down with the IgG coupled beads so are also likely to be binding non-specifically. Therefore, only proteins with a value above 1.8 are classed as occludin interacting “hit” proteins.

This data plot was repeated comparing “medium” (cells treated with BafA and IP performed with rabbit anti-occludin conjugated beads) to “light” (cells treated with DMSO and IP performed with rabbit IgG conjugated beads) treated samples. Figure 6.6b demonstrates the majority of ratio values fall between 0.6 and 1.8. Ratio values for proteins which fall within the median range or below 0.6, are likely to be binding non-specifically to the IgG beads, however proteins with values above 1.8 showed increased IP under “medium” conditions.

Finally, Figure 6.6c compares the ratio of “heavy” to “medium” treated cells to identify proteins which IP with rabbit anti-occludin beads but display altered abundance in either DMSO or BafA conditions. Figure 6.6c shows the majority of proteins are within the 0.5-1.4 median range, proteins within this range show no alteration in abundance during either DMSO or BafA treatment. A value of

Table 6.1. Proteins with increased SILAC ratios in DMSO treated cells incubated with anti-occludin conjugated beads in comparison to IgG coupled control beads.

Protein IDs	Protein Descriptions	Unique Peptides	Sequence Coverage [%]	Ratio H/L
GI 73981533	Histone 2 H2ac	2	31.1	25.069
GI 74004213	H2B histone family member F	2	33.5	20.806
GI 74004215	Germinal histone H4 gene	6	10.1	16.977
GI 74004189	Histone H2A.l	2	30.1	14.864
GI 73966009	DNA topoisomerase II alpha isozyme isoform 3	4	5	11.614
GI 73953311	Nucleolar RNA helicase II	5	8.5	9.715
GI 73948346	Fibrillarin	5	20.1	9.3128
GI 73971330	H2A histone family, member Y isoform 3	7	22.6	9.008
GI 73954339	Brix domain containing protein 2	2	8.3	8.3265
GI 73984025	MKI67 FHA domain interacting nucleolar phosphoprotein	3	15.2	8.0048
GI 73998783	RRP5 protein homolog	3	1.4	7.6057
GI 73959105	Ribosomal L1 domain containing protein 1	3	8.2	7.0978
GI 73990502	DNA topoisomerase II, beta isozyme	2	2.4	6.7911
GI 74004254	Histone H1.5 (Histone H1a)	2	25.1	6.6429
GI 74003979	Histone H1.2 (H1d)	3	23.5	6.5236
GI 7407643	occludin 1B	2	6.4	6.3419
GI 73977788	SWI/SNF related matrix associated actin dependent regulator of chromatin subfamily A member 5	3	2.7	6.0769
GI 74005181	Nucleolar protein NOP5	4	8.8	6.0628
GI 73977348	Chromatin-specific transcription elongation factor large subunit isoform 1	4	4.6	5.6526
GI 73984472	RuvB-like protein 1 isoform 1	9	28	5.0575
GI 73948016	RuvB-like 2	11	27.9	4.8849
GI 73997745	Proliferating-cell nucleolar antigen p120	3	3.4	4.266

Protein IDs	Protein Descriptions	Unique Peptides	Sequence Coverage [%]	Ratio H/L
GI 73961765	Desmoglein-2 precursor	4	4.2	4.0472
GI 73996579	Keratin, type II cytoskeletal 7	10	39.5	3.6864
GI 73950644	Basement membrane-specific heparan sulfate proteoglycan core protein precursor	3	1.5	3.5738
GI 73955265	Myb-binding protein 1A isoform 3	4	3.4	3.5166
GI 73953440	Nucleophosmin 1 isoform 1	6	37.1	3.4267
GI 73948956	Vimentin isoform 1	20	48.7	3.2573
GI 73996298;	Keratin, type I cytoskeletal 18	14	43.1	3.256
GI 73996455	Keratin, type II cytoskeletal 8	6	39.4	3.2473
GI 73973308	Alpha 1 type XII collagen long isoform precursor isoform 1	6	2.5	3.1931
GI 73974720	Plectin 1 isoform 1 isoform 6	89	23.3	2.9232
GI 157060706	Keratin 19	2	77.6	2.8605
GI 74004041	Desmoplakin isoform II	12	5.5	2.8499
GI 73990618	Heterogeneous nuclear ribonucleoprotein G	2	4.6	2.7862
GI 73977327	isoform 19	7	22.8	2.7428
GI 50979166	Endoplasmin precursor	5	7.2	2.528
GI 74006345	Myeloid cell nuclear differentiation antigen	3	9.1	2.4229
GI 73965906	Junction plakoglobin isoform 4	4	6	2.1948
GI 73960920	Lamin A/C	17	30.4	2.1085
GI 327532722	Matrin-3	3	6	2.0889
GI 73974852	Epiplakin 1	6	10.7	1.9419
GI 73986955	Heterogeneous nuclear ribonucleoprotein M isoform a isoform 2	8	15.3	1.9394
GI 307133722	Splicing factor, arginine/serine-rich 7	2	12.6	1.8651

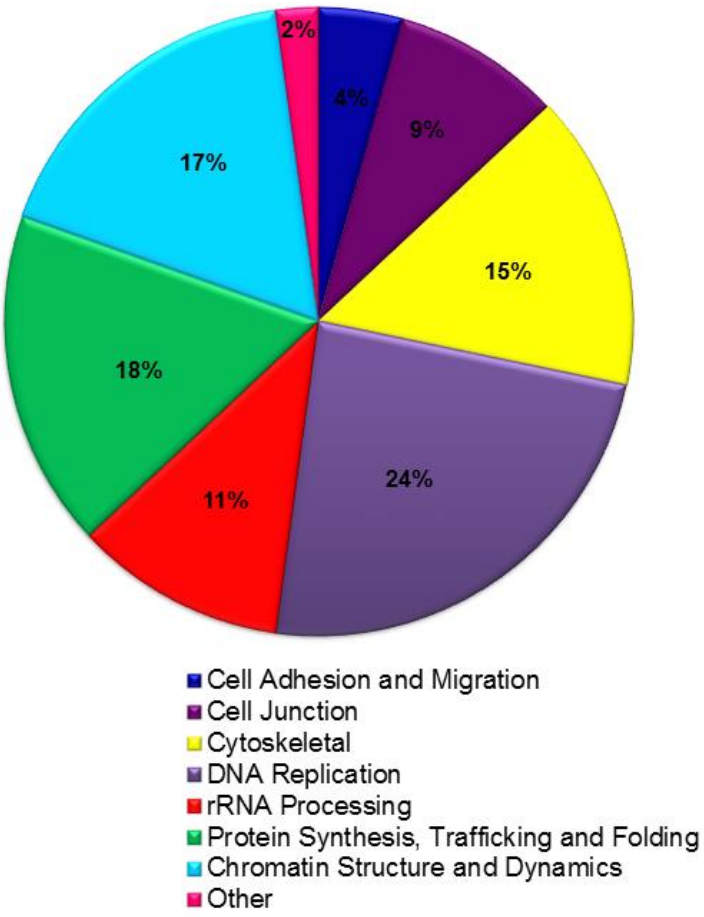

Figure 6.7. Pie chart showing the functional groups of proteins with increased SILAC ratios in "heavy" (DMSO treated cells incubated with anti-occludin beads) compared to "light" (DMSO treated cells incubated with IgG beads) treated cells. The proteins with increased SILAC ratio in "heavy" to "light" treated cells were assessed for their functionality and assembled into groups, the percentage of proteins per group was calculated from the total number of "hits".

less than 0.5 identifies proteins which IP with increased frequency after BafA treatment whilst proteins with a ratio value above 1.4 exhibit increased IP after control DMSO incubation.

Once median ratio ranges had been established probable “hits” were identified as stated above and the function of the protein examined. As shown in Table 6.1 comparing “heavy” to “light” SILAC conditions (comparing ratios of cells treated with DMSO and subject to rabbit anti-occludin IP to those treated with DMSO and rabbit IgG IP), there were 45 potential “hit” proteins with SILAC ratios above 1.8. Of these potential hit proteins a large proportion of these proteins were nuclear/involved in DNA transcription, whilst 18% of proteins were involved in biosynthesis and folding (Figure 6.7). In this category only one protein was identified which has a role in protein trafficking, the endoplasmin precursor protein, a heat shock protein localised to the endoplasmic reticulum (Koch, Macer, & Wooding, 1988). Interestingly, cell-cell junction proteins such as desmoplakin II and junction plakoglobin 4 (Pigors et al., 2011; Virata et al., 1992) and the protein human basement membrane heparin sulfate proteoglycan core protein (HSPG), required for regulation of integrity of basement membranes, angiogenesis, metastasis and tissue repair (Sher et al., 2006) were identified in the screen. Of the remaining proteins, 15% were cytoskeletal and 2% had an unidentified function.

This analysis was repeated to compare “medium” to “light” treated cells (comparing ratios of cells treated with BafA and subject to rabbit anti-occludin IP to those treated with DMSO and rabbit IgG IP). As exhibited in Table 6.2, there were 31 potential “hit” proteins with SILAC ratios above 1.8. Figure 6.8 shows

Table 6.2. Proteins with increased SILAC ratios in BafA treated cells incubated with anti-occludin conjugated beads in comparison to DMSO treated cells incubated with IgG coupled control beads.

Protein IDs	Protein Descriptions	Unique Peptides	Sequence Coverage [%]	Ratio M/L
GI 7407643	Occludin 1B	2	6.4	9.5392
GI 73948016	RuvB-like 2	11	27.9	5.7055
GI 73984472	RuvB-like protein 1 isoform 1	9	28	4.9371
GI 73984025	MKI67 FHA domain interacting nucleolar phosphoprotein	3	15.2	4.4854
GI 73954339	Brix domain containing protein 2	2	8.3	4.1133
GI 50979166	Endoplasmin precursor	5	7.2	3.0834
GI 73959105	Ribosomal L1 domain containing protein 1	3	8.2	2.8788
GI 74007823	phosphoglycerate kinase 1 isoform 10	3	10.6	2.0802
GI 73968009	60S ribosomal protein L12 isoform 4	6	51.5	1.9251
GI 73977327	isoform 19	7	22.8	1.8907
GI 73974720	Plectin 1 isoform 1 isoform 6	89	23.3	1.8877
GI 57113163	Ribosomal protein L30 isoform 1	2	24.3	1.8433
GI 57086947	Ribosomal protein L13 isoform 1	5	23.2	1.8057
GI 57103532	Ribosomal protein L14	3	15.7	1.7963
GI 50978796	60S ribosomal protein L27	3	31.1	1.7939
GI 73955265	Myb-binding protein 1A isoform 3	4	3.4	1.7613
GI 73997745	Proliferating-cell nucleolar antigen p120	3	3.4	1.7524
GI73980235	Activating signal cointegrator 1 complex subunit 3-like 1 isoform 6	2	0.9	1.6732
GI 73996298	Keratin, type I cytoskeletal 18	14	43.1	1.6593
GI 73959552	60S ribosomal protein L5 isoform 1	2	13	1.6582
GI 4506609	60S ribosomal protein L19	2	13.3	1.6538
GI 73994631	60S ribosomal protein L6	4	25	1.6516

Protein IDs	Protein Descriptions	Unique Peptides	Sequence Coverage [%]	Ratio M/L
GI 13592009	60S ribosomal protein L10a	4	20.7	1.6494
GI 57108289	Ribosomal protein L4 isoform 1	4	14.2	1.6457
GI 73996455	Keratin, type II cytoskeletal 8	6	39.4	1.6449
GI 57036383	Ribosomal protein L18	3	20.7	1.6251
GI6981488	40S ribosomal protein S26	2	20.9	1.6185
GI 73996579	Keratin, type II cytoskeletal 7	10	39.5	1.6136
GI 73974852	Epiplakin 1	6	10.7	1.6128

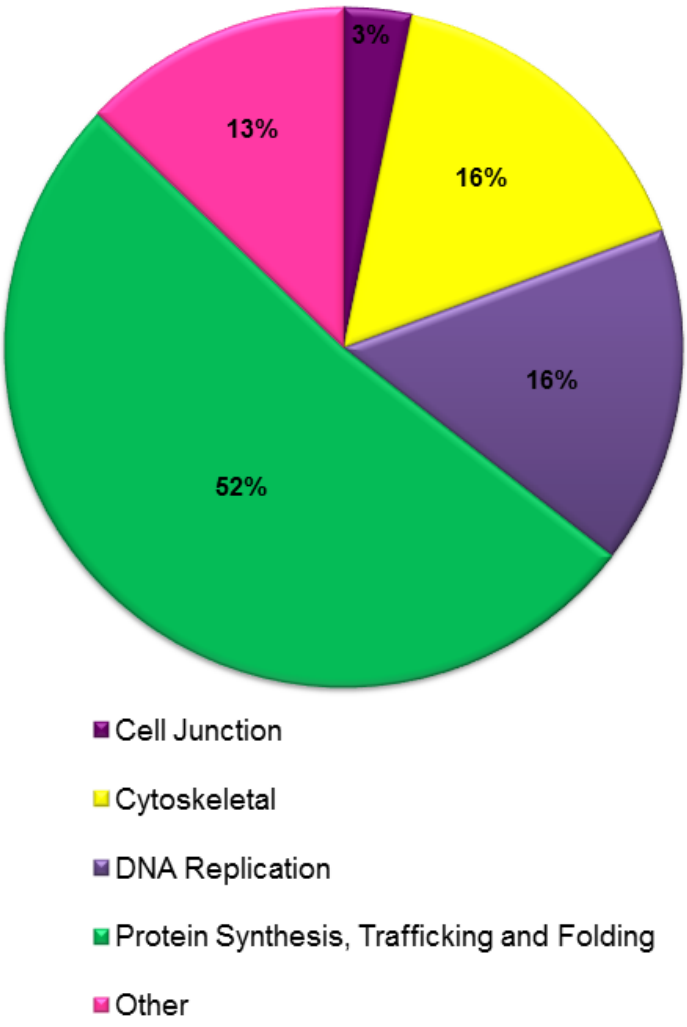

Figure 6.8. Pie chart showing the functional groups of proteins with increased SILAC ratios in "medium" (BafA treated cells incubated with anti-occludin beads) compared to "light" (DMSO treated cells incubated with IgG beads) treated cells. The proteins with increased SILAC ratio in "medium" to "light" treated cells were assessed for their functionality and assembled into groups, the percentage of proteins per group was calculated from the total number of "hits".

the functional groups of proteins identified as “hits” within the screen. 52% were proteins involved in protein biosynthesis, 16% were cytoskeletal proteins and 16% were nuclear proteins involved in DNA replication. Of the remaining proteins their function was unknown or related to glycolysis. Occludin was the only cell-cell adhesion molecule identified in the screen.

Finally, a direct comparison of occludin binding proteins in the presence of DMSO or BafA was made by comparing “heavy” and “medium” condition cells. Table 6.3 shows 51 potential “hits” were identified, which demonstrate increased IP in the presence of DMSO than in BafA. Conversely only 2 “hits” were identified which showed increased abundance in IP samples incubated with BafA, one protein had an unknown function whilst the other was a kinase protein involved in signalling (Figure 6.9). When the functional groups for proteins identified in table 6.3 were examined (Figure 6.10), these results echo those stated previously with a large proportion of hits (30%) involved in biosynthesis and 44% of proteins were localised to the nucleus and involved in either DNA replication or chromatin structure; 12% of proteins were cytoskeletal proteins. Other proteins identified include: the desmosomal proteins desmoplakin II and desmoglein (Virata, et al., 1992), the cell adhesion molecules alpha 1 type XII collagen long isoform precursor isoform 1 and fibronectin 1 (Kato et al., 2000; Steffens et al., 2012), and basement membrane regulating HSPG protein (Sher et al., 2006). Interestingly, the proteins desmoplakin II, alpha 1 type XII collagen and HSPG protein were shown as “hits” when comparing “heavy” and “light” samples. Although potential interactions between occludin and other junctional and migratory proteins were

A

Protein IDs	Protein Descriptions	Unique Peptides	Sequence Coverage [%]	Ratio H/M
GI 74007823	Phosphoglycerate kinase 1 isoform 10	3	10.6	0.47153
GI 73989473	Hypothetical protein XP_863466	2	3.7	0.41086

B

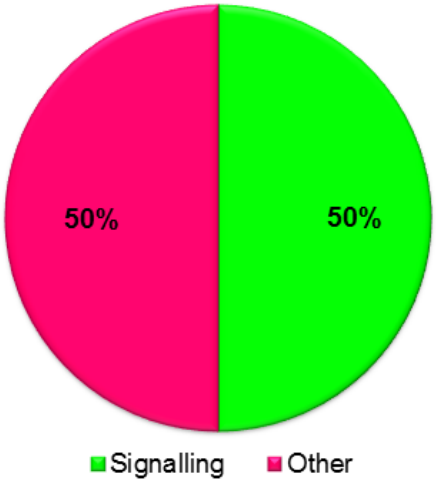

Figure 6.9. Proteins with decreased SILAC ratios in BafA treated cells incubated with anti-occludin conjugated beads in comparison to cells incubated in DMSO with anti-occludin coupled beads.
(A) Table showing "hit" proteins with a decreased "heavy" to "medium" ratio. (B) Pie chart showing the functional groups of proteins with decreased SILAC ratios in "heavy" to "medium" treated cells were assessed for their functionality and assembled into groups, the percentage of proteins per group was calculated from the total number of "hits".

Table 6.3. Proteins with increased SILAC ratios in DMSO treated cells incubated with anti-occludin conjugated beads in comparison to BafA treated cells incubated with anti-occludin beads

Protein IDs	Protein Descriptions	Unique Peptides	Sequence Coverage [%]	Ratio H/M
GI 73981533	Histone 2, H2ac	2	31.1	27.204
GI 74004215	germinal histone H4 gene	6	10.1	21.622
GI 74003971	Histone 1, H2ai	5	32.4	21.444
GI 74004189	Histone H2A.l	2	30.1	20.82
GI 74004213	H2B histone family, member F	2	33.5	17.134
GI 73966011	DNA topoisomerase II, alpha isozyme isoform 3	4	5	16.207
GI 73971330	H2A histone family, member Y isoform 3	7	22.6	12.66
GI 57093467	H/ACA ribonucleoprotein complex subunit 2	2	12.4	12.093
GI 73977348	Chromatin-specific transcription elongation factor large subunit isoform 1	4	4.6	11.745
GI 73953311	Nucleolar RNA helicase II	5	8.5	10.877
GI 73990502	DNA topoisomerase II, beta isozyme	2	2.4	9.7529
GI 73948346	Fibrillarin	5	20.1	8.7995
GI 73998783	RRP5 protein homolog	3	1.4	8.5085
GI 74005181	Nucleolar protein NOP5	4	8.8	8.165
GI 74004254	Histone H1.5	2	25.1	7.3481
GI 73977788	SWI/SNF related matrix associated actin dependent regulator of chromatin subfamily A member 5	3	2.7	6.6488
GI 74003979	Histone H1.2 (H1d)	3	23.5	6.4242
GI 73950644	Basement membrane-specific heparan sulfate proteoglycan core protein precursor	3	1.5	5.4148
GI 74004041	Desmoplakin isoform II	12	5.5	4.7982
GI 57110429	Histone H1.5 (Histone H1a)	2	22.5	4.2902

Protein IDs	Protein Descriptions	Unique Peptides	Sequence Coverage [%]	Ratio H/M
GI 73961765	Desmoglein-2 precursor	4	4.2	4.0297
GI 74006345	Myeloid cell nuclear differentiation antigen	3	9.1	3.8163
GI 73990618	Heterogeneous nuclear ribonucleoprotein G	2	4.6	3.5716
GI 74004189	Histone H2A.l	2	30.1	20.82
GI 74004213	H2B histone family, member F	2	33.5	17.134
GI 73966011	DNA topoisomerase II, alpha isozyme isoform 3	4	5	16.207
GI 73971330	H2A histone family, member Y isoform 3	7	22.6	12.66
GI 57093467	H/ACA ribonucleoprotein complex subunit 2	2	12.4	12.093
GI 73977348	Chromatin-specific transcription elongation factor large subunit isoform 1	4	4.6	11.745
GI 73953311	Nucleolar RNA helicase II	5	8.5	10.877
GI 73990502	DNA topoisomerase II, beta isozyme	2	2.4	9.7529
GI 73948346	Fibrillarin	5	20.1	8.7995
GI 73998783	RRP5 protein homolog	3	1.4	8.5085
GI 74005181	Nucleolar protein NOP5	4	8.8	8.165
GI 74004254	Histone H1.5	2	25.1	7.3481
GI 73977788	SWI/SNF related matrix associated actin dependent regulator of chromatin subfamily A member 5	3	2.7	6.6488
GI 74003979	Histone H1.2 (H1d)	3	23.5	6.4242
GI 73950644	Basement membrane-specific heparan sulfate proteoglycan core protein precursor	3	1.5	5.4148
GI 74004041	Desmoplakin isoform II	12	5.5	4.7982
GI 57110429	Histone H1.5 (Histone H1a)	2	22.5	4.2902
GI 73961765	Desmoglein-2 precursor	4	4.2	4.0297
GI 74006345	Myeloid cell nuclear differentiation antigen	3	9.1	3.8163
GI 73990618	Heterogeneous nuclear ribonucleoprotein G	2	4.6	3.5716

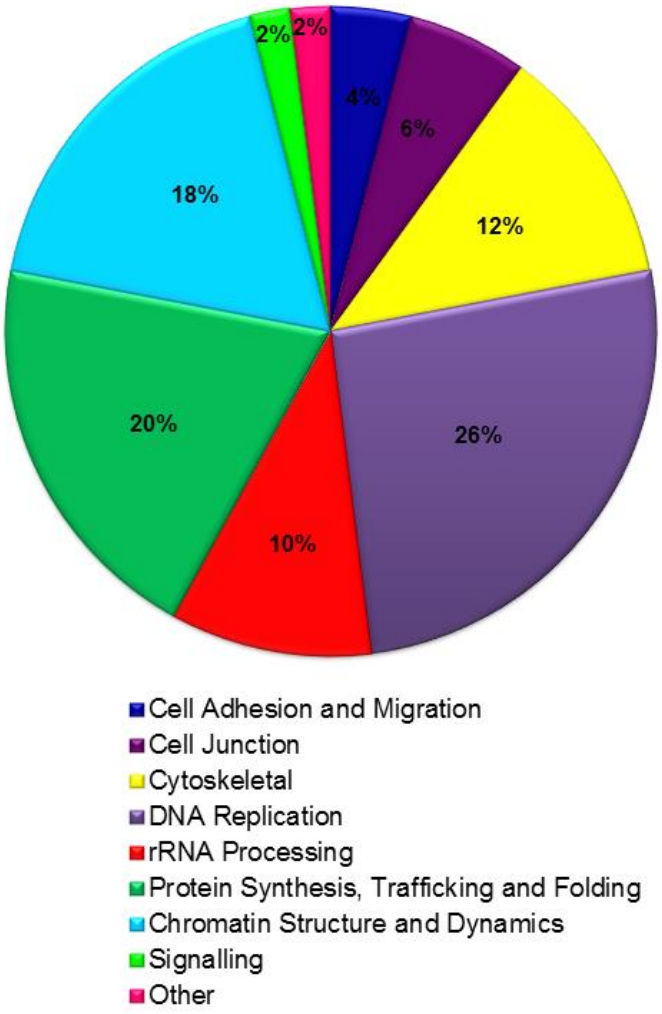

Figure 6.10. Pie chart showing the functional groups of proteins with increased SILAC ratios in "heavy" (DMSO treated cells incubated with anti-occludin beads) to "medium" (BafA treated cells incubated and anti-occludin beads) treated cells. The proteins with increased SILAC ratio in "heavy" to "medium" treated cells were assessed for their functionality and assembled into groups, the percentage of proteins per group was calculated from the total number of "hits".

identified within the screen, no proteins with endocytosis/endosomal trafficking functions were discovered. However, a large proportion of proteins identified were involved in biosynthesis including entire ribosomal subunits, chaperone molecules required for correct folding and trafficking and proteins involved in rRNA processing. These data suggest occludin is a molecule which undergoes a high level of biosynthesis rather than recycling under steady state conditions.

6.7 Inhibition of protein biosynthesis decreases the abundance of occludin in the plasma membrane

In the previous section, SILAC coupled with mass spectrometry and IP was utilised to identify potential occludin binding partners or complexes which may regulate occludin trafficking in an unstimulated MDCK cell monolayer. Although no proteins involved in trafficking were identified in this screen, findings did indicate occludin may be a protein undergoing constant biosynthesis. Coupling this observation to those seen in section 6.4 where the majority of occludin internalised from the plasma membrane is targeted for degradation may imply occludin undergoes a constant cycle of internalisation, degradation and synthesis to maintain occludin equilibrium at the plasma membrane. Therefore this study tests this hypothesis, examining the role of protein synthesis in regulation of plasma membrane occludin levels. This study utilised a cell-surface biotinylation assay, where all cell-surface proteins were biotinylated at 4ºC in the presence of either DMSO or the protein synthesis inhibitor CHX (Schneider-Poetsch et al., 2010), to examine the abundance of occludin at the plasma membrane upon inhibition of protein synthesis. Figure 6.11a and b

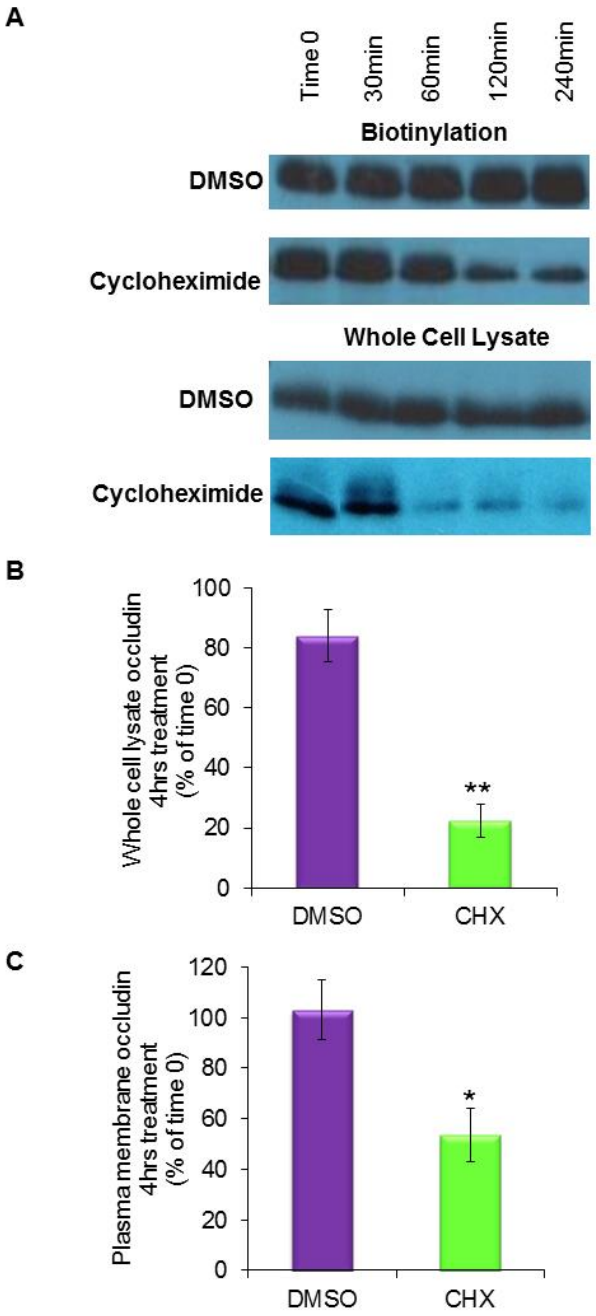

Figure 6.11. Inhibition of protein synthesis reduces the amount of plasma membrane localised occludin. MDCK cells were serum starved for 2 hours before incubation with 10μM CHX or 1μl/ml DMSO for varying time points. Cell-surface proteins were then biotinylated, quenched, lysed and pulled down with NeutrAvidin beads. Plasma membrane abundance of occludin was quantified by Western blot analysis. Membranes were probed with primary rabbit anti-occludin antibody (diluted 1:500) and secondary anti-rabbit-HRP antibody (diluted 1:10000). (A) Incubation with CHX reduces both whole cell lysate and plasma membrane occludin levels. (B) Quantification of 3 independent experiments measuring whole cell lysate levels of occludin 4 hours post-CHX treatment normalised to Time 0. (C) Quantification of 3 independent experiments measuring plasma membrane levels of occludin 4 hours post-CHX treatment normalised to Time 0. $p \leq 0.05$ and ** $p \leq 0.01$,

demonstrates a reduction in the whole cell lysate occludin levels by 62% in cells incubated with CHX, in comparison to DMSO treatment alone. This indicates that for maintenance of cellular occludin levels, a high level of occludin synthesis is required. Furthermore, Figure 6.11a and c demonstrate that 4 hours post-CHX treatment a 49% reduction in cell-surface occludin was observed. These data may suggest that one way through which plasma membrane occludin levels are regulated is via constitutive exocytosis of newly synthesised occludin to the plasma membrane.

6.8 Endogenous occludin co-localises with markers of the biosynthetic secretory pathway

As evidence to further support the hypothesis of constitutive occludin exocytosis in maintenance of plasma membrane occludin equilibrium. Co-localisation studies were performed between markers of the biosynthetic secretory pathway and endogenous occludin. As a marker of the biosynthetic secretory pathway the cargo peptide NPY was utilised (described in chapter 3). Cells were transfected with NPY-mRFP and immunocytochemistry was performed to stain endogenous occludin. Co-localisation was measured by drawing ROIs around individual occludin positive vesicles and counting vesicles which co-localised with NPY-mRFP structures. As a control, random co-localisation with NPY-mRFP was measured by moving the ROI regions to occludin negative regions and again vesicles which co-localised where counted. As shown in Figure 6.12, there was a significant level of co-localisation observed between NPY-mRFP and endogenous occludin. Therefore these data further support a role for

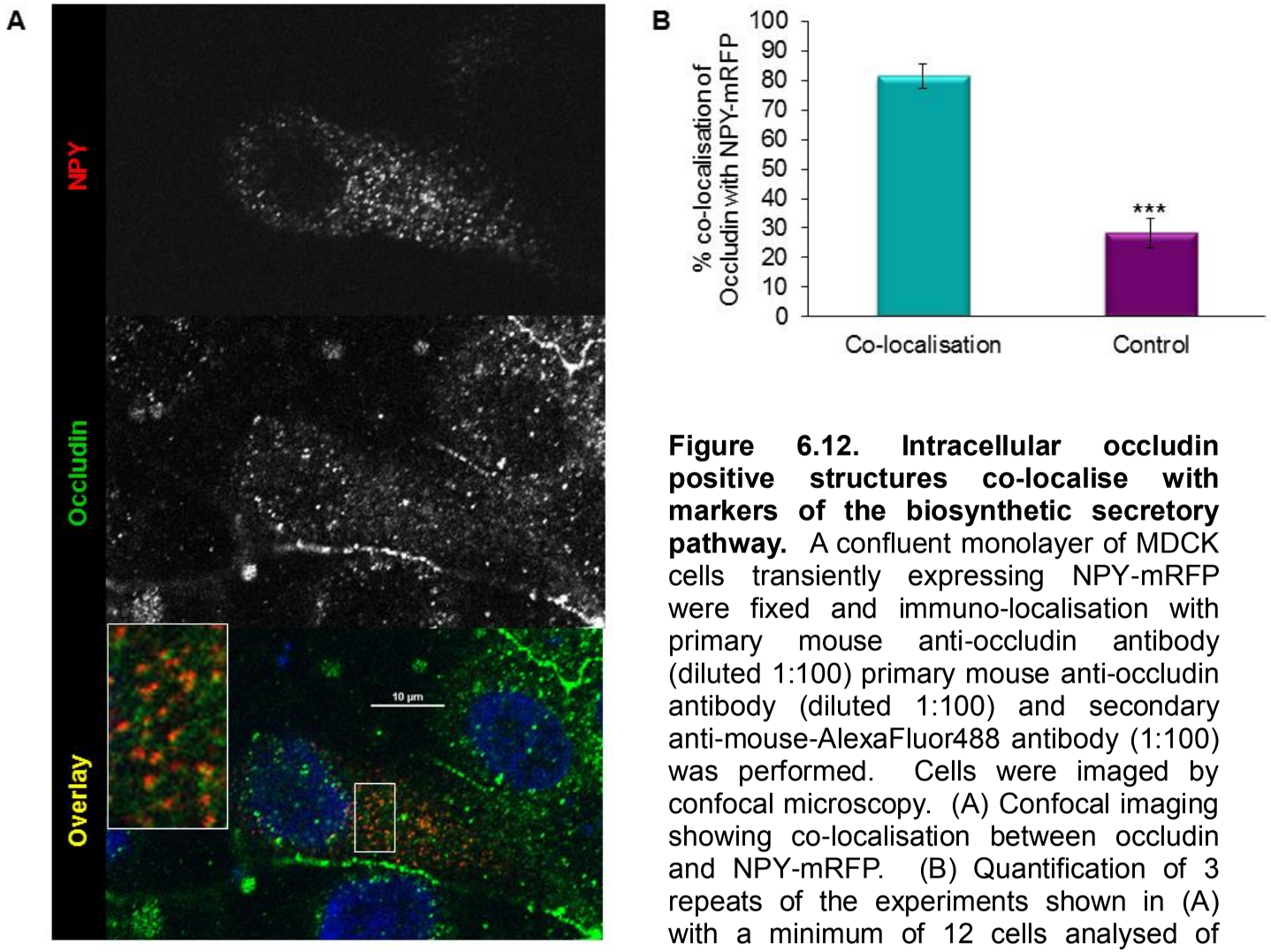

Figure 6.12. Intracellular occludin positive structures co-localise with markers of the biosynthetic secretory pathway. A confluent monolayer of MDCK cells transiently expressing NPY-mRFP were fixed and immuno-localisation with primary mouse anti-occludin antibody (diluted 1:100) primary mouse anti-occludin antibody (diluted 1:100) and secondary anti-mouse-AlexaFluor488 antibody (1:100) was performed. Cells were imaged by confocal microscopy. (A) Confocal imaging showing co-localisation between occludin and NPY-mRFP. (B) Quantification of 3 repeats of the experiments shown in (A) with a minimum of 12 cells analysed of each condition. *** $p \leq 0.001$.

biosynthetic secretion of occludin in regulation of plasma membrane occludin levels.

6.9 Discussion

TJs are essential for many processes, such as regulation of paracellular permeability, maintenance of apical basolateral polarity and they also provide structural support for epithelial monolayers. Deregulation of TJs can lead to several pathological conditions including Crohn's disease and nonsyndromic recessive deafness (Wilcox et al., 2001; Zeissig et al., 2007), however loss of TJs is also observed in the pathology of conditions such as cystic fibrosis and polycystic kidney disease (Wilson, 1997). In particular occludin is emerging as a regulator of numerous physiological and pathological processes both within the TJ complex and through other mechanisms (Du et al., 2010). Thus, TJ regulation under steady state, non-stimulated conditions is highly physiologically relevant. Therefore this chapter investigated the role of vesicle trafficking in regulation of occludin in a confluent monolayer of MDCK cells.

Importantly, this study was the first to examine occludin trafficking in non-stimulated cells, and yielded highly interesting results. Quantitative, biochemical analysis of occludin trafficking utilising cell-surface biotinylation recycling techniques (Roberts et al., 2001) identified the majority of the plasma membrane pool of occludin was internalised within 30 minutes, where peak internalised intracellular occludin was observed. After 30 minutes, internalised intracellular occludin was reduced and lost from detection by 2 hours.

This study utilised BafA to determine that the reduction in intracellular occludin was due to lysosomal occludin degradation. This hypothesis was further confirmed by immunocytochemistry studies where endogenous occludin was found to co-localise with late endosome/lysosomal marker CD63 (Metzelaar, et al., 1991) under control conditions. Increased co-localisation between occludin and CD63-GFP was observed in the presence of BafA. Interestingly, proteomic analysis and mass spectrometry failed to identify any proteins involved in endocytosis/trafficking which co-IP with occludin either under control conditions or in the presence of BafA. However a large proportion of proteins required for correct biosynthesis were identified within the screen, suggesting new occludin protein may be constantly synthesised. This hypothesis was tested by pharmacological inhibition of protein synthesis. Under these conditions a significant reduction in whole cell lysate and plasma membrane occludin abundance was observed, suggesting trafficking of newly synthesised occludin to the plasma membrane was required to maintain occludin plasma membrane homeostasis. The data obtained in this chapter implicate a continuous cycle of internalisation, degradation and synthesis acting in equilibrium is required to regulate plasma membrane occludin localisation (Figure 6.13).

The results observed in this chapter vary to those made previously by Morimoto et al., (2005) whose data obtained from fibroblast and epithelial derived cell lines suggested occludin undergoes a constant cycle of rapid internalisation and recycling back to the plasma membrane (Morimoto et al., 2005). However, this paper fails to correctly validate their recycling hypothesis, and the results observed may potentially be due to effects on lysosomal degradation instead.

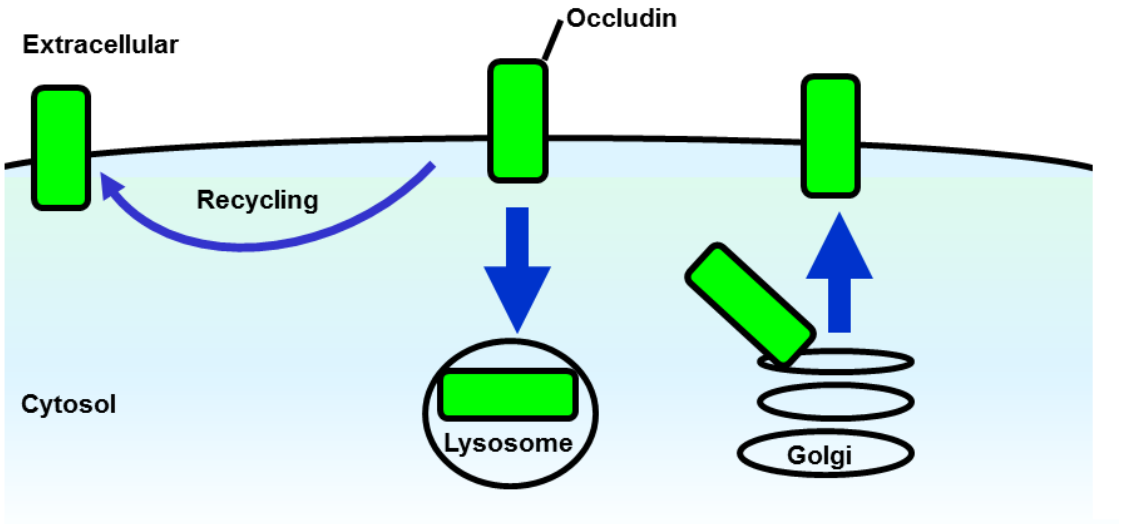

Figure 6.13. Schematic diagram showing constitutive endocytosis and lysosomal degradation of occludin coupled to biosynthetic secretion and low-level recycling.

For example their biotinylation recycling assay demonstrates increased intracellular occludin signal followed by a signal reduction (as described in section 6.3) was suggested to be due to recycling back to the plasma membrane, however this could also be due to occludin degradation. Interestingly, BafA was utilised to inhibit trafficking, which although has been suggested to affect recycling this effect has been highly cell line specific (Presley et al., 1997). Although the group did observed defects in transferrin recycling upon BafA treatment in the fibroblast BHK cell line, they failed to repeat the experiment in the MTD-1A epithelial model. This is critical as not only where different cell lines used but also occludin was overexpressed in the BHK model whilst endogenous occludin was observed in MTD-1A cells. These differences between expression type and cell line prevent extrapolation of findings from one model to the other. Thus it cannot be determined whether the increased intracellular occludin signal observed upon addition of BafA was due to inhibitory effects on lysosomal degradation or trafficking in the more physiologically relevant MTD-1A epithelial model. Moreover, the group also utilised a reduction in temperature to 18ºC to inhibit recycling however this treatment has also been shown to inhibit lysosomal degradation (Ahlberg et al., 1985). Immunocytochemistry experiments also fail to validate the occurrence of occludin recycling as suggested by Morimoto et al., (2005). As observed in section 6.5 and demonstrated by Morimoto et al., (2005) no co-localisation was seen between endogenous occludin and Rab4/Rab11 recycling compartments (suggesting recycling does not occur via these compartments), instead co-localisation was observed with Rab13 (required for TGN to recycling endosome

trafficking (Morimoto et al., 2005; Nokes et al., 2008). The co-localisation of occludin with Rab13 might instead suggest a proportion of newly synthesised occludin is transported to recycling endosomes, a pathway observed in polarised MDCK cells (Figure 1.6) (Weisz & Rodriquez-Boulin, 2009). Taken together, the data from Morimoto et al, (2005) may actually further support the hypothesis proposed in this chapter; that a large percentage of intracellular occludin undergoes lysosomal degradation rather than recycling in non-stimulated epithelial cells in the MDCK cell model (Morimoto et al., 2005). One way in which occludin degradation may be regulated is via ubiquitination (Murakami, Felinski, & Antonetti, 2009).

Ubiquitination of proteins is a versatile mechanism through which addition a of single ubiquitin molecule (monoubiquitination) or whole chain of ubiquitin molecules (polyubiquitination) occurs via a covalent bond to a lysine residue and can signal for down regulation and lysosomal degradation of plasma membrane proteins (reviewed in Hicke, 1997). Occludin has been demonstrated to undergo ubiquitination upon stimulation with VEGF (Murakami, Felinski, & Antonetti, 2009), furthermore this group identified interaction of occludin with trafficking proteins Eps15 and Hrs. To further understand occludin trafficking, a quantitative SILAC proteomics study coupled to IP and high resolution mass spectrometry was utilised to identify candidate proteins which bind occludin directly or as part of a multi-protein complex to regulate trafficking such as that described by Murakami, Felinski, & Antonetti (2009). Unfortunately, no candidate trafficking proteins were identified, either under control conditions or during BafA treatment. However, other interesting

molecules were found. The cell-cell adhesion proteins desmoglein, desmoplakin II and junction plakoglobin 4 were identified within the screen. Desmogleins are transmembrane members of the cadherin family, whilst plakoglobin (armadillo family member) binds to the cytoplasmic domains of cadherins facilitating binding of desmoplakin, linking the desmosomal structures to the actin cytoskeleton (Green & Simpson, 2007). The identification of the entire desmosomal complex associated with occludin may indicate that in confluent MDCK cells, a proportion of TJs may associate with desmosomal structures. It has previously been identified that members of the desmosomal complex can also be localised to non-desmosomal junctions such as adherens and GAP junctions (Franke et al., 2006). Another interesting protein identified was the HSPG cell basement membrane regulating protein. HSPG has been implicated in effective wound healing in KO mice (Zhou et al., 2004), perhaps this interaction with occludin is required for regulation of migration during epithelial wound healing (Fletcher et al., 2012). As few interesting candidate molecules were identified, the proteins were grouped into functional groups. Upon grouping, a large percentage of the proteins identified were localised to the nucleus. The literature demonstrates no known localisation or function for occludin at the nucleus, however this particular batch of antibodies utilised for IP, were observed to localise to nuclear regions and TJs in immunocytochemistry experiments (Western blot analysis confirmed rabbit anti-occludin binding occludin with a similar affinity to previous batches). Therefore identification of nuclear proteins is probably due to non-specific binding of the anti-occludin antibody. Another large functional group of proteins identified

within the screen were cytoskeletal proteins, this is unsurprising as occludin has been shown to be bound to the cytoskeleton. Finally, many proteins involved in the screen were those required for protein biosynthesis suggesting occludin undergoes a high level of biosynthesis. This finding is highly important, in sections 6.4 and 6.5 it is demonstrated a large majority of the plasma membrane pool of occludin is internalised rapidly and continuously then subject to lysosomal degradation. Obviously, to maintain occludin levels new occludin protein must be synthesised to compensate for the loss by degradation. The presence of many proteins functioning in biosynthesis in the screen suggest this is a likely explanation. However to confirm this hypothesis a cell-surface biotinylation assay was performed, enabling quantification of cell-surface levels of occludin in the presence of CHX to inhibit protein synthesis. In comparison to control cells there was a significant reduction in whole cell lysate in cells incubated with CHX, this reduction in occludin levels was also observed at the plasma membrane. These data support the hypothesis that occludin undergoes constant synthesis and trafficking to the plasma membrane to maintain occludin equilibrium. Furthermore, to support this hypothesis a high level of co-localisation was observed between markers of the biosynthetic pathway and endogenous occludin. Therefore, taken together the results from this chapter demonstrate that under steady state non-stimulated conditions, occludin undergoes a continuous cycle of endocytosis and degradation which is matched by biosynthetic exocytic trafficking (Figure 6.13).

6.10 Key chapter findings

- In a non-stimulated epithelial monolayer the majority of plasma membrane localised occludin undergoes rapid internalisation from the plasma membrane within 30 minutes and by 2 hours most internalised occludin has undergone lysosomal degradation.
- Inhibition of lysosomal degradation leads to retention of internalised occludin within the cell, with cells demonstrating increased co-localisation with late endosome/lysosomal markers.
- Occludin is a protein which undergoes constant biosynthesis. A high level of co-localisation was observed between markers of the biosynthetic secretory pathway and endogenous intracellular occludin. Also inhibition of protein synthesis lead to a significant reduction in plasma membrane localised occludin.

6.11 Conclusion

The mechanistic analysis of occludin trafficking at steady-state is relevant for many reasons. TJs are critical in the connections between cells and for the maintenance of apical basolateral polarity (Steed, Balda, & Matter, 2010; Yu & Turner, 2008). Although several groups have investigated stimulated occludin trafficking, constitutive trafficking has not been as well studied (Fletcher et al., 2012; Ivanov, Nusrat & Parkos, 2004; Marchiando et al., 2010; Stamatovic et al., 2009; Xia et al., 2009). These results are important for two reasons: steady-state trafficking is the baseline upon which physiologically relevant alterations must be built. Furthermore, occludin has already been shown to

function in a role beyond TJ formation (Du et al., 2010; Fletcher et al., 2012; Liu et al., 2010; Meredith et al., 2012). Therefore, the analysis of the steady state trafficking of occludin represents a key step in understanding the role of this interesting and important protein in numerous physiological and pathological contexts.

CHAPTER 7

FINAL DISCUSSION AND FUTURE DIRECTIONS

7.1 Final Discussion

Epithelial cells are specialised cells forming barriers across which molecules are selectively transported. They differ from other cell types as they are held together laterally by TJs which regulate epithelial polarity and restrict paracellular permeability. Epithelial cells also have an important function in protection of underlying tissue from injury. However, epithelial layers can be damaged by wounding and healing is required to prevent secondary infection, to maintain tissue integrity and prevent fibrosis of surrounding tissues.

This PhD has examined both the role of vesicle trafficking and the extent to which vesicle trafficking is polarised during epithelial wound healing. Furthermore, endocytosis and trafficking of cell adhesion molecules was examined to further investigate mechanisms which may regulate collective cell migration.

Evidence from many groups has suggested an important function for vesicle trafficking in regulation of cell migration (extensively reviewed in Fletcher & Rappoport, 2010; Fletcher & Rappoport, 2009). Chapter 3 focused on the function of specific vesicle trafficking pathways during directed epithelial

migration. Pharmacological inhibition and expression of dominant negative mutants were utilised to specifically inhibit trafficking pathways during MDCK wound healing. The findings of chapter 3 demonstrate inhibition of dynamin-dependent internalisation pathways, CME and caveolar endocytosis significantly reduced the rate of cell motility; however only CME inhibition affected the ability of cells to generate a migratory phenotype. Inhibition of the Rab4- and Rab11-dependent recycling pathways both significantly decreased the rate of MDCK migration, however no effect on the ability of the cells to polarise was observed. Interestingly, inhibition of post-Golgi biosynthetic secretory trafficking had no effect on either the rate of cell motility or cellular morphology as has been observed previously (Prigozhina & Waterman-Storer, 2004). These results indicate an important role for both endocytosis and recycling during epithelial cell migration. The extent to which these pathways were polarised during wound healing was examined in chapter 4.

Transient expression of fluorescent labelled markers of caveolar endocytosis, Rab11- and Rab25-mediated trafficking were imaged in the adherent plasma membrane by TIRF microscopy. The results of this study demonstrate polarisation of caveolar endocytosis to the rear of migrating MDCK cells. Detailed fusion analysis also confirmed exocytosis of vesicles derived from the Rab11- and Rab25-dependent pathways were not polarised during collective epithelial cell motility. Due to the importance of vesicle trafficking during epithelial wound healing and identification of polarised caveolar endocytosis and CME (Rappoport & Simon, 2003); the potential for these pathways in regulation of FA and TJ dynamics was examined.

Several groups have suggested an important function for trafficking of adhesion complexes in regulation of cell migration (Chao & Kunz, 2009; Du, et al., 2010; Ezratty et al., 2009). Chapter 5 demonstrates dynamin-dependent, clathrin and caveolar endocytosis has little role in regulating FA turnover in motile epithelial cells. Instead, this work implicates CME of the TJ protein occludin from the wound edge to Rab5 positive endosomal compartments as a mechanism for regulating epithelial wound healing. This study also identified redistribution of occludin from the wound edge was required for effective epithelial cell migration. Chapter 5 demonstrates wound healing is a novel mechanism through which occludin endocytosis from the wound edge regulates MDCK cell motility.

However, little work has examined steady state occludin trafficking in non-stimulated cells, therefore chapter 6 focused on base-line occludin trafficking in MDCK cell monolayers as well as identification of potential binding partners which may regulate occludin trafficking. This chapter utilised Sulfo-NHS-SS-Biotin-based recycling assays, immunocytochemistry and confocal imaging to demonstrate that under steady state conditions occludin is internalised continuously and rapidly from the plasma membrane and undergoes constitutive degradation. This is coupled to continual occludin biosynthesis to maintain plasma membrane occludin levels.

The findings from this thesis have a high level of physiological relevance. Failure of wounds to correctly heal can lead to the formation of fibrotic scar tissue. This not only has cosmetic implications but can severely affect gas and solute exchange when fibrosis occurs in the lung and kidney. Furthermore,

inability to correctly heal wounds can lead to an increased likelihood of secondary infection. Moreover, occludin functions as a receptor for the Hepatitis C Virus (HCV), thus increased understanding of how occludin is trafficked may shed light on the mechanism of HCV infection. Additionally, one of the functions of TJs is to maintain apical basolateral polarity, numerous human diseases such as cystic fibrosis, have been demonstrated to involve loss of epithelial polarity. Therefore, further information regarding TJ regulation potentially via occludin trafficking is of clinical importance. The findings of this study could potentially aid in development of therapeutic interventions in diseases which affect epithelial polarity and wound healing.

To summarise, this thesis is the first work of its kind to examine various trafficking pathways in a single migratory model. It is also the first time caveolar endocytosis has been demonstrated to be excluded from the lamellipodial regions of migrating MDCK cells. Furthermore, it shows a novel function for occludin endocytosis from the wound edge as a mechanism through which directed cell migration is regulated. This study is also the first to demonstrate that under non-stimulated conditions, occludin undergoes a cycle of internalisation, degradation and synthesis.

7.2 Future Studies

Occludin is a key regulator of epithelial function and wound healing, the trafficking of occludin has not been well characterised, either in the context of apical-basolateral polarity or during epithelial wound healing. Prior to this thesis there was very little knowledge regarding the trafficking of occludin during

epithelial wound healing or under steady-state conditions. Future studies would make use of well characterised cellular models and techniques to combine biochemical and cellular analyses with cutting edge quantitative imaging and development of previously used proteomics approaches. This would enable identification of mechanisms which regulate generation, maintenance and repair of polarised epithelia. Although this thesis has examined trafficking in non-polarised but confluent MDCK cell monolayers, a future study would be to determine the specific biosynthetic, degradative and recycling pathways that regulate occludin localisation in cultured, fully polarised epithelial monolayers. MDCK cells are an excellent model for such studies as MDCK cells cultured on TransWell permeable supports facilitate epithelial polarisation.

Furthermore, the role of occludin in generation of apical basolateral polarisation could potentially be investigated. In work by Fletcher et al., (2012) it was demonstrated that over-expression of GFP-tagged occludin led to saturation of the mechanisms which regulate occludin internalisation from the wound edge, resulting in decreased wound healing (Fletcher et al., 2012). Similarly, RNAi studies performed by Du et al., (2010) report effects on epithelial cell motility and reduced localisation of polarity proteins (e.g. the Par3-aPKC complex) at the leading edge (Du et al., 2010). To further identify the function of occludin during apical basolateral polarisation, knock down and over expression studies could be performed to compare their effects on the ability of the MDCK cells to polarise. The effects of occludin over-expression and silencing could be evaluated using previously published reagents (Fletcher et al., 2012; Liu et al., 2010) and techniques to assess generation of apical-basolateral polarity in

epithelial monolayers such as trans-epithelial resistance measurements and imaging markers of apical basolateral polarisation. This method would also allow performance of knock-down and rescue studies. However, there is potential for GFP-occludin expression levels de-regulating occludin trafficking, thus the Tet-On regulated expression system would allow precise control of occludin levels.

To further define the mechanisms involved in regulation of occludin trafficking, developments in SILAC, IP and mass spectrometry techniques need to be made. A key factor in this development would involve screening several anti-occludin antibodies to ensure they are localising correctly, suitable for IP and recognising canine occludin protein. This should eradicate the large abundance of non-specifically binding nuclear proteins identified within the original screen. Furthermore, incubation with inhibitors of protein synthesis such as CHX would prevent co-immunoprecipitation of proteins involved in occludin biosynthesis. To further eradicate the presence of these proteins an antibody which binds to the N terminus of occludin could be used for IP. During protein synthesis the C terminus is formed first and the N terminus last; by utilising an antibody against the N terminus, only fully formed proteins would be pulled down during IP. Additionally, to maintain protein-protein interactions cross linking of protein complexes could be performed (Woodcock et al., 2009). These studies could be performed in fully polarised epithelial monolayers as well as during polarisation, to identify regulators of occludin trafficking throughout the stages of epithelial polarisation.

Alongside examination of steady state occludin trafficking, there is still the potential to investigate occludin trafficking during wound healing. In chapter 5 and Fletcher et al., (2012) it was shown that following monolayer wounding occludin undergoes rapid clathrin-mediated endocytosis from the wound edge into a Rab5 positive compartment (Fletcher et al., 2012). Whilst in work by Du et al., (2010) it was demonstrated that six hours following wounding occludin can be seen at the very leading edge of the migrating front (Du et al., 2010). However, the mechanism by which occludin redistributes to this location and regulates the morphology of the migratory cells has not been determined. Thus is could be suggested that either occludin is arriving at the leading edge through polarised endosomal recycling, or via biosynthetic secretory traffic specifically directed at the very front of the cell. Importantly, evidence for the existence of polarised exocytic trafficking in migrating cells exists (reviewed fully in Fletcher & Rappoport, 2010), thus either of these hypotheses could be correct. Therefore, by further analyses of the mechanisms regulating occludin trafficking in migrating cells the origin of the leading edge localised occludin could be determined and its implication regarding cell polarity examined. Furthermore, this system would also enable live-cell imaging of occludin trafficking to visualise the re-localisation of occludin following monolayer wounding, from the wound edge into the subsequent endosomal system, particularly if the Tet-On regulated expression system was utilised.

The combination of proteomics, live cell imaging and biochemical techniques, would enable generation of an overall mechanistic understanding of the regulation of occludin trafficking during wound healing, initial polarisation and in

a polarised monolayer. Moreover, there is definite potential to examine the role of occludin in both regulation of epithelial polarisation and wound healing in i*n vivo* models.

For example, methods already exist for the use of Zebrafish as a model for wound healing (Tawk, Joulie, & Vriz, 2000). Therefore the role of occludin in wound healing *in vivo* could be examined using these previously validated systems. This could be completed through analysis of the localisation of occludin following wounding, along with co-staining of compartment markers (e.g. Rab5), as well as the effects of endocytosis inhibitors (e.g. Dynasore) on redistribution of occludin from the wound edge. Similarly it could also be determined if occludin is present at the leading edge of the migrating front during wound healing, and whether it also co-localises with polarity proteins. Furthermore, a screen for factors specifically altering the localisation of occludin during steady state and wound healing could be performed by utilising a series of morpholinos to inhibit pathways identified in this thesis such as clathrin and dynamin. Transference of *in vitro* wound healing research into *in vivo* studies is integral for further understanding re-epithelialisation and also in development of pharmacological tools to aid in this process, making these *in vivo* studies invaluable.

CHAPTER 8

REFERENCE LIST

Ahlberg, J., Berkenstam, A., Henell, F., & Glaumann, H. 1985. Degradation of short and long lived proteins in isolated rat liver lysosomes. Effects of pH, temperature, and proteolytic inhibitors. *J.Biol Chem.*, 260(9), pp. 5847-5854.

Altankov, G. & Grinnell, F. 1995. Fibronectin receptor internalization and AP-2 complex reorganization in potassium-depleted fibroblasts. *Exp.Cell Res.*, 216(2), pp. 299-309.

Altschuler, Y., Barbas, S. M., Terlecky, L. J., Tang, K., Hardy, S., Mostov, K. E., & Schmid, S. L. 1998. Redundant and distinct functions for dynamin-1 and dynamin-2 isoforms. *The Journal of Cell Biology*, 143(7), pp. 1871-1881.

Axelrod, D. 1981. Cell-substrate contacts illuminated by total internal reflection fluorescence. *The Journal of Cell Biology*, 89(1), pp. 141-145.

Bahri, S., Wang, S., Conder, R., Choy, J., Vlachos, S., Dong, K., Merino, C., Sigrist, S., Molnar, C., Yang, X., Manser, E., & Harden, N. 2010. The leading edge during dorsal closure as a model for epithelial plasticity: Pak is required for recruitment of the Scribble complex and septate junction formation. *Development*, 137(12), pp. 2023-2032.

Bailly, M. & Condeelis, J. 2002. Cell motility: insights from the backstage. *Nat.Cell Biol.*, 4(12), pp. 292-294.

Bailly, M., Wyckoff, J., Bouzahzah, B., Hammerman, R., Sylvestre, V., Cammer, M., Pestell, R., & Segall, J. E. 2000. Epidermal growth factor receptor distribution during chemotactic responses. *Molecular Biology of the Cell*, 11(11), pp. 3873-3883.

Balda, M. S., Whitney, J. A., Flores, C., Gonzalez, S., Cereijido, M., & Matter, K. 1996. Functional dissociation of paracellular permeability and transepithelial electrical resistance and disruption of the apical-basolateral intramembrane diffusion barrier by expression of a mutant tight junction membrane protein. *J.Cell Biol*, 134(4), pp. 1031-1049.

Ballestrem, C., Hinz, B., Imhof, B. A., & Wehrle-Haller, B. 2001. Marching at the front and dragging behind: differential alphaVbeta3-integrin

turnover regulates focal adhesion behaviour. *J Cell Biol.*, 155(7), pp. 1319-1332.

Benmerah, A., Bayrou, M., Cerf-Bensussan, N., & Dautry-Varsat, A. 1999. Inhibition of clathrin-coated pit assembly by an Eps15 mutant. *Journal of Cell Science*, 112(9), pp. 1303-1311.

Benmerah, A., Lamaze, C., Begue, B., Schmid, S. L., Dautry-Varsat, A., & Cerf-Bensussan, N. 1998. AP-2/Eps15 interaction is required for receptor-mediated endocytosis. *The Journal of Cell Biology*, 140(5), pp. 1055-1062.

Bergmann, J. E., Kupfer, A., & Singer, S. J., 1983. Membrane insertion at the leading edge of motile fibroblasts. *Proceedings of the National Academy of Sciences of the United States of America*, 80(5), pp. 1367-1371.

Bershadsky, A. D. & Futerman, A. H., 1994. Disruption of the Golgi apparatus by brefeldin A blocks cell polarization and inhibits directed cell migration. *Proc.Natl.Acad.Sci.U.S.A*, 91(12), pp. 5686-5689.

Boucrot, E. & McMahon, H. T. 2011. [Nucleation of clathrin-coated pits - << membrane sculptors >> at work]. *Med.Sci.(Paris)*, 27(2), pp. 122-125.

Boya, P., Andreau, K., Poncet, D., Zamzami, N., Perfettini, J. L., Metivier, D., Ojcius, D. M., Jaattela, M., & Kroemer, G., 2003. Lysosomal membrane permeabilization induces cell death in a mitochondrion-dependent fashion. *Journal of Experimental Medicine*, 197(10), pp. 1323-1334.

Brennan, K., Offiah, G., McSherry, E. A., & Hopkins, A. M., 2010. Tight junctions: a barrier to the initiation and progression of breast cancer? *J.Biomed.Biotechnol.*, 2010, pp. 460607.

Bretscher, M. S., 1983. Distribution of receptors for transferrin and low density lipoprotein on the surface of giant HeLa cells. *Proceedings of the National Academy of Sciences of the United States of America*, 80(2), pp. 454-458.

Bretscher, M. S., 1984. Endocytosis: relation to capping and cell locomotion. *Science*, 224(4650), pp. 681-686.

Bretscher, M. S.. 1996. Moving membrane up to the front of migrating cells. *Cell*, 85(4), pp. 465-467.

Brodsky, F. M., 1988. Living with Clathrin - Its Role in Intracellular Membrane Traffic. *Science*, 242(4884), pp. 1396-1402.

Brown, P. S., Wang, E., Aroeti, B., Chapin, S. J., Mostov, K. E., & Dunn, K. W., 2000. Definition of distinct compartments in polarized Madin-

Darby canine kidney (MDCK) cells for membrane-volume sorting, polarized sorting and apical recycling. *Traffic*, 1(2), pp. 124-140.

Bruzzaniti, A., Neff, L., Sanjay, A., Horne, W. C., De, C. P., & Baron, R., 2005. Dynamin forms a Src kinase-sensitive complex with Cbl and regulates podosomes and osteoclast activity. *Molecular Biology of the Cell*, 16(7), pp. 3301-3313.

Buettner, R., Mesa, T., Vultur, A., Lee, F., & Jove, R., 2008. Inhibition of Src family kinases with dasatinib blocks migration and invasion of human melanoma cells. *Mol Cancer Res.*, 6(11), pp. 1766-1774.

Burridge, K. & Chrzanowska-Wodnicka, M., 1996. Focal adhesions, contractility, and signalling. *Annu.Rev.Cell Dev.Biol*, 12, pp. 463-518.

Butterworth, M. B., Edinger, R. S., Frizzell, R. A., & Johnson, J. P., 2009. Regulation of the epithelial sodium channel by membrane trafficking. *Am.J.Physiol Renal Physiol*, 296(1), pp. 10-24.

Calalb, M. B., Polte, T. R., & Hanks, S. K.,1995. Tyrosine phosphorylation of focal adhesion kinase at sites in the catalytic domain regulates kinase activity: a role for Src family kinases. *Mol.Cell Biol.*, 15(2), pp. 954-963.

Calderwood, D. A., 2004. Talin controls integrin activation. *Biochem.Soc.Trans.*, 32(3), pp. 434-437.

Caldieri, G., Capestrano, M., Bicanova, K., Beznoussenko, G., Baldassarre, M., & Buccione, R., 2012. Polarised apical-like intracellular sorting and trafficking regulates invadopodia formation and degradation of the extracellular matrix in cancer cells. *Eur.J.Cell Biol*. Epub ahead of print.

Camand, E., Peglion, F., Osmani, N., Sanson, M., & Etienne-Manneville, S., 2012. N-cadherin expression level modulates integrin-mediated polarity and strongly impacts on the speed and directionality of glial cell migration. *Journal of Cell Science*, 125(4), pp. 844-857.

Casanova, J. E., 2002. Epithelial cell cytoskeleton and intracellular trafficking V. Confluence of membrane trafficking and motility in epithelial cell models. *Am.J.Physiol Gastrointest.Liver Physiol*, 283(5), pp. 1015-1019.

Casanova, J. E., Wang, X., Kumar, R., Bhartur, S. G., Navarre, J., Woodrum, J. E., Altschuler, Y., Ray, G. S., & Goldenring, J. R., 1999. Association of Rab25 and Rab11a with the apical recycling system of polarized Madin-Darby canine kidney cells. *Molecular Biology of the Cell*, 10(1), pp. 47-61.

Castor, L. N., 1968. Contact regulation of cell division in an epithelial-like cell line. *J.Cell Physiol*, 72(3), pp. 161-172.

Caswell, P. T. & Norman, J. C., 2006. Integrin trafficking and the control of cell migration. *Traffic.*, 7(1), pp. 14-21.

Caswell, P. T., Spence, H. J., Parsons, M., White, D. P., Clark, K., Cheng, K. W., Mills, G. B., Humphries, M. J., Messent, A. J., Anderson, K. I., McCaffrey, M. W., Ozanne, B. W., & Norman, J. C., 2007. Rab25 associates with alpha5beta1 integrin to promote invasive migration in 3D microenvironments. *Dev.Cell*, 13(4), pp. 496-510.

Caswell, P. T., Vadrevu, S., & Norman, J. C., 2009. Integrins: masters and slaves of endocytic transport. *Nat.Rev.Mol.Cell Biol.*, 10(12), pp. 843-853.

Caswell, P. T. & Norman, J. C., 2006. Integrin Trafficking and the Control of Cell Migration. *Traffic*, 7(1), pp. 14-21.

Chao, W. T. & Kunz, J., 2009. Focal adhesion disassembly requires clathrin-dependent endocytosis of integrins. *FEBS Lett.*, 583(8), pp. 1337-1343.

Chappie, J. S., Acharya, S., Leonard, M., Schmid, S. L., & Dyda, F., 2010. G domain dimerization controls dynamin's assembly-stimulated GTPase activity. *Nature (London)*, 465 (7297), pp. 435-440.

Chen, W. J., Goldstein, J. L., & Brown, M. S., 1989. NPXY, a Sequence Often Found in Cytoplasmic Tails, Is Required for Coated Pit-mediated Internalization of the Low Density Lipoprotein Receptor. *The Journal of Biological Chemistry*, 265(6), pp. 3116-3123.

Chen, C, Hou1, W., Liu, I., Hsiao, G., Huang, S. & Huang, J., 2009. Inhibitors of clathrin-dependent endocytosis enhance TGFβ signaling and responses. *J. Cell Sci*., 122*,* pp*.* 1863-1871*.*

Cheng, K. W., Lahad, J. P., Kuo, W. L., Lapuk, A., Yamada, K., Auersperg, N., Liu, J., Smith-McCune, K., Lu, K. H., Fishman, D., Gray, J. W., & Mills, G. B., 2004. The RAB25 small GTPase determines aggressiveness of ovarian and breast cancers. *Nat.Med.*, 10(11), pp. 1251-1256.

Chou, J., Burke, N. A., Iwabu, A., Watkins, S. C., & Wells, A., 2003. Directional motility induced by epidermal growth factor requires Cdc42. *Exp.Cell Res.*, 287(1), pp. 47-56.

Conklin, M. W., da-Nguema, A., Parsons, M., Riching, K. M., & Keely, P. J., 2010. R-Ras regulates beta1-integrin trafficking via effects on membrane ruffling and endocytosis. *BMC.Cell Biol*, 11, pp. 14.

Dai, J. & Sheetz, M. P., 1995. Axon membrane flows from the growth cone to the cell body. *Cell*, 83(5), pp. 693-701.

Damer, C. K. & O'Halloran, T. J., 2000. Spatially Regulated Recruitment of Clathrin to the Plasma Membrane during Capping and Cell Translocation. *Molecular Biology of the Cell*, 11(6), pp. 2151-2159.

Damke, H., Baba, T., Warnock, D. E., & Schmid, S. L., 1994. Induction of mutant dynamin specifically blocks endocytic coated vesicle formation. *The Journal of Cell Biology*, 127(4), pp. 915-934.

Damke, H., Binns, D. D., Ueda, H., Schmid, S. L., & Baba, T., 2001. Dynamin GTPase domain mutants block endocytic vesicle formation at morphologically distinct stages. *Molecular Biology of the Cell*, 12(9), pp. 2578-2589.

Danen, E. H., van, R. J., Franken, W., Huveneers, S., Sonneveld, P., Jalink, K., & Sonnenberg, A., 2005. Integrins control motile strategy through a Rho-cofilin pathway. *The Journal of Cell Biology*, 169(3), pp. 515-526.

Daro, E., Van Der, S. P., Galli, T., & Mellman, I., 1996. Rab4 and cellubrevin define different early endosome populations on the pathway of transferrin receptor recycling. *Proc.Natl.Acad.Sci.U.S.A*, 93(18), pp. 9559-9564.

Davis, B. H., Walter, R. J., Pearson, C. B., Becker, E. L., & Oliver, J. M., 1982. Membrane activity and topography of F-Met-Leu-Phe-Treated polymorphonuclear leukocytes. Acute and sustained responses to chemotactic peptide. *Am.J.Pathol.*, 108(2), pp. 206-216.

De Deyne, P. G., O'Neill, A., Resneck, W. G., Dmytrenko, G. M., Pumplin, D. W., & Bloch, R. J., 1998. The vitronectin receptor associates with clathrin-coated membrane domains via the cytoplasmic domain of its beta5 subunit. *J Cell Sci*, 111(18), pp. 2729-2740.

de Kreuk, B. J., Nethe, M., Fernandez-Borja, M., Anthony, E. C., Hensbergen, P. J., Deelder, A. M., Plomann, M., & Hordijk, P. L., 2011. The F-BAR domain protein PACSIN2 associates with Rac1 and regulates cell spreading and migration. *Journal of Cell Science*, 124(14), pp. 2375-2388.

de Laurentiis, A., Donovan, L., Arcaro, A., (2007). Lipid rafts and caveolae in signalling by growth factor receptors. *Open Biochemsitry Journal*. 1, pp. 12-32.

Deakin, N. O. & Turner, C. E. 2008, "Paxillin comes of age", *Journal of Cell Science*, vol. 121, no. Pt 15, pp. 2435-2444.

Diabetes in the UK 2012 (2012). Avaliable online at <http://www.diabetes.org.uk/Documents/Reports/Diabetes-in-the-UK-2012.pdf.> [Accessed 22nd June 2012].

Dembo, M. & Wang, Y. L., 1999. Stresses at the cell-to-substrate interface during locomotion of fibroblasts. *Biophysical Journal*, 76(4), pp. 2307-2316.

Doherty, G. J. & McMahon, H. T., 2009. Mechanisms of endocytosis. *Annual Review of Biochemistry*, 78, pp. 857-902.

Dorfel, M. J. & Huber, O., 2012. Modulation of tight junction structure and function by kinases and phosphatases targeting occludin. *J.Biomed.Biotechnol.*, Epub ahead of print

Dow, L. E., Kauffman, J. S., Caddy, J., Zarbalis, K., Peterson, A. S., Jane, S. M., Russell, S. M., & Humbert, P. O., 2007. The tumour-suppressor Scribble dictates cell polarity during directed epithelial migration: regulation of Rho GTPase recruitment to the leading edge. *Oncogene*, 26(16), pp. 2272-2282.

Du, D., Xu, F., Yu, L., Zhang, C., Lu, X., Yuan, H., Huang, Q., Zhang, F., Bao, H., Jia, L., Wu, X., Zhu, X., Zhang, X., Zhang, Z., & Chen, Z., 2010. The tight junction protein, occludin, regulates the directional migration of epithelial cells. *Dev.Cell*, 18(1), pp. 52-63.

Dukes, J. D., Whitley, P., & Chalmers, A. D., 2011. The MDCK variety pack: choosing the right strain. *BMC.Cell Biol.*, 12, pp. 12-43.

Dumont, R. A., Hildebrandt, I., Su, H., Haubner, R., Reischl, G., Czernin, J. G., Mischel, P. S., & Weber, W. A., 2009. Noninvasive imaging of alphaVbeta3 function as a predictor of the antimigratory and antiproliferative effects of Dasatinib. *Cancer Research*, 69(7), pp. 3173-3179.

Ehrlich, M., Boll, W., Van Oijen, A., Hariharan, R., Chandran, K., Nibert, M. L., & Kirchhausen, T., 2004. Endocytosis by random initiation and stabilization of clathrin-coated pits. *Cell*, 118(5), pp. 591-605.

Ellenbroek, S. I., Iden, S., & Collard, J. G., 2012. Cell polarity proteins and cancer. *Semin.Cancer Biol.*, 22(3), pp. 208-215.

Etienne-Manneville, S., Manneville, J. B., Nicholls, S., Ferenczi, M. A., & Hall, A., 2005. Cdc42 and Par6-PKCzeta regulate the spatially localized association of Dlg1 and APC to control cell polarization. *The Journal of Cell Biology*, 170(6), pp. 895-901.

Ezratty, E. J., Bertaux, C., Marcantonio, E. E., & Gundersen, G. G., 2009. Clathrin mediates integrin endocytosis for focal adhesion

disassembly in migrating cells. *The Journal of Cell Biology*, 187(5), pp. 733-747.

Ezratty, E. J., Partridge, M. A., & Gundersen, G. G., 2005. Microtubule-induced focal adhesion disassembly is mediated by dynamin and focal adhesion kinase. *Nat.Cell Biol.*, 7(6), pp. 581-590.

Fabbri, M., Di Meglio, S., Gagliani, M. C., Consonni, E., Molteni, R., Bender, J. R., Tacchetti, C., & Pardi, R., 2005. Dynamic Partitioning into Lipid Rafts Controls the Endo-Exocytic Cycle of the {alpha}L/{beta}2 Integrin, LFA-1, during Leukocyte Chemotaxis. *Molecular Biology of the Cell*, 16(12), pp. 5793-5803.

Falanga, V., 2005. Wound healing and its impairment in the diabetic foot. *Lancet*, 366(9498), pp. 1736-1743.

Fenteany, G., Janmey, P. A., & Stossel, T. P., 2000. Signaling pathways and cell mechanics involved in wound closure by epithelial cell sheets. *Curr.Biol.*, 10(14), pp. 831-838.

Ferguson, M. L., Prasad, K., Boukari, H., Sackett, D. L., Krueger, S., Lafer, E. M., & Nossal, R., 2008. Clathrin triskelia show evidence of molecular flexibility. *Biophysical Journal*, 95(4), pp. 1945-1955.

Ferrari, A., Pellegrini, V., Arcangeli, C., Fittipaldi, A., Giacca, M., & Beltram, F., 2003. Caveolae-mediated internalization of extracellular HIV-1 tat fusion proteins visualized in real time. *Mol.Ther.*, 8(2), pp. 284-294.

Fletcher, S. J., Poulter, N. S., Haining, E. J., & Rappoport, J. Z., 2012. Clathrin-mediated endocytosis regulates occludin, and not focal adhesion, distribution during epithelial wound healing. *Biol.Cell*, 104(4), pp. 238-256.

Fletcher, S. J. & Rappoport, J. Z., 2010. Moving forward: polarised trafficking in cell migration. *Trends in Cell Biology*, 20(2), pp. 71-78.

Fletcher, S. J. & Rappoport, J. Z., 2009. The role of vesicle trafficking in epithelial cell motility. *Biochem.Soc.Trans.*, 37(5), pp. 1072-1076.

Ford, M. G., Mills, I. G., Peter, B. J., Vallis, Y., Praefcke, G. J., Evans, P. R., & McMahon, H. T., 2002. Curvature of clathrin-coated pits driven by epsin. *Nature (London)*, 419(6905), pp. 361-366.

Ford, M. G., Pearse, B. M., Higgins, M. K., Vallis, Y., Owen, D. J., Gibson, A., Hopkins, C. R., Evans, P. R., & McMahon, H. T., 2001. Simultaneous binding of PtdIns(4,5)P2 and clathrin by AP180 in the nucleation of clathrin lattices on membranes. *Science*, 291(5506), pp. 1051-1055.

Fra, A. M., Williamson, E., Simons, K., & Parton, R. G., 1995. De novo formation of caveolae in lymphocytes by expression of VIP21-caveolin. *Proceedings of the National Academy of Sciences of the United States of America*, 92(19), pp. 8655-8659.

Frank, P. G., Woodman, S. E., Park, D. S., & Lisanti, M. P., 2003. Caveolin, caveolae, and endothelial cell function", *Arterioscler.Thromb.Vasc.Biol.*, vol. 23, no. 7, pp. 1161-1168.

Franke, W. W., Borrmann, C. M., Grund, C., & Pieperhoff, S., 2006. The area composita of adhering junctions connecting heart muscle cells of vertebrates. I. Molecular definition in intercalated disks of cardiomyocytes by immunoelectron microscopy of desmosomal proteins. *Eur.J.Cell Biol*, 85(2), pp. 69-82.

Friedl, P., 2004. Prespecification and plasticity: shifting mechanisms of cell migration. *Curr.Opin.Cell Biol.*, 16(1), pp. 14-23.

Friedl, P., Borgmann, S., & Brocker, E. B., 2001. Amoeboid leukocyte crawling through extracellular matrix: lessons from the Dictyostelium paradigm of cell movement. *J.Leukoc.Biol.*, 70(4), pp. 491-509.

Friedl, P. & Wolf, K., 2003. Tumour-cell invasion and migration: diversity and escape mechanisms. *Nat.Rev.Cancer*, 3(5), pp. 362-374.

Furuse, M., Fujimoto, K., Sato, N., Hirase, T., Tsukita, S., & Tsukita, S. 1996. Overexpression of occludin, a tight junction-associated integral membrane protein, induces the formation of intracellular multilamellar bodies bearing tight junction-like structures. *Journal of Cell Science*, 109(2), pp. 429-435.

Furuse, M., Hirase, T., Itoh, M., Nagafuchi, A., Yonemura, S., Tsukita, S., & Tsukita, S., 1993. Occludin: a novel integral membrane protein localizing at tight junctions. *The Journal of Cell Biology*, 123(6;2), pp. 1777-1788.

Furuse, M., Itoh, M., Hirase, T., Nagafuchi, A., Yonemura, S., Tsukita, S., & Tsukita, S., 1994. Direct association of occludin with ZO-1 and its possible involvement in the localization of occludin at tight junctions. *J.Cell Biol*, 127,(6;1), pp. 1617-1626.

Galvez, B. G., Matias-Roman, S., Yanez-Mo, M., Vicente-Manzanares, M., Sanchez-Madrid, F., & Arroyo, A. G., 2004. Caveolae are a novel pathway for membrane-type 1 matrix metalloproteinase traffic in human endothelial cells. *Molecular Biology of the Cell*, 15(2), pp. 678-687.

Ge, S. & Pachter, J. S., 2004. Caveolin-1 knockdown by small interfering RNA suppresses responses to the chemokine monocyte chemoattractant

protein-1 by human astrocytes. *Journal of Biological Chemistry*, 279(8), pp. 6688-6695.

Geggel, H. S., Friend, J., & Thoft, R. A., 1984. Conjunctival epithelial wound healing. *Invest Ophthalmol.Vis.Sci.*, 25(7), pp. 860-863.

Gerst, J. E. 1999, "SNAREs and SNARE regulators in membrane fusion and exocytosis", *Cell Mol.Life Sci.*, vol. 55, no. 5, pp. 707-734.

Giannone, G., Ronde, P. Gaire, M., Haiech, J., Takeda, K., 2002. Calcium osscillations trigger focal adhesion disassembly in human U87 astroscytoma cells. *J. Biol. Chem.* 277, pp. 26364-26371.

Gingras, A. R., Bate, N., Goult, B. T., Patel, B., Kopp, P. M., Emsley, J., Barsukov, I. L., Roberts, G. C., & Critchley, D. R., 2010. Central region of talin has a unique fold that binds vinculin and actin. *Journal of Biological Chemistry*, 285(38), pp. 29577-29587.

Goldenring, J. R., Shen, K. R., Vaughan, H. D., & Modlin, I. M., 1993. Identification of a small GTP-binding protein, Rab25, expressed in the gastrointestinal mucosa, kidney, and lung. *Journal of Biological Chemistry*, 268(25), pp. 18419-18422.

Gotlieb, A. I., May, L. M., Subrahmanyan, L., & Kalnins, V. I., 1981. Distribution of microtubule organizing centers in migrating sheets of endothelial cells", *The Journal of Cell Biology*, 91(2;1), pp. 589-594.

Goulimari, P., Kitzing, T. M., Knieling, H., Brandt, D. T., Offermanns, S., & Grosse, R., 2005. Galpha12/13 is essential for directed cell migration and localized Rho-Dia1 function. *J.Biol Chem.*, 280(51), pp. 42242-42251.

Goult, B. T., Bate, N., Anthis, N. J., Wegener, K. L., Gingras, A. R., Patel, B., Barsukov, I. L., Campbell, I. D., Roberts, G. C., & Critchley, D. R., 2009. The structure of an interdomain complex that regulates talin activity. *Journal of Biological Chemistry*, 284(22), pp. 15097-15106.

Grande, M., Franzen, A., Karlsson, J. O., Ericson, L. E., Heldin, N. E., & Nilsson, M., 2002. Transforming growth factor-beta and epidermal growth factor synergistically stimulate epithelial to mesenchymal transition (EMT) through a MEK-dependent mechanism in primary cultured pig thyrocytes. *Journal of Cell Science*, 115(22), pp. 4227-4236.

Grande-Garcia, A., Echarri, A., de, R. J., Alderson, N. B., Waterman-Storer, C. M., Valdivielso, J. M., & del Pozo, M. A., 2007. Caveolin-1 regulates cell polarization and directional migration through Src kinase and Rho GTPases. *The Journal of Cell Biology*, 177(4), pp. 683-694.

Green, K. J. & Jones, J. C., 1996. Desmosomes and hemidesmosomes: structure and function of molecular components. *FASEB J.*, 10(8), pp. 871-881.

Green, K. J. & Simpson, C. L., 2007. Desmosomes: new perspectives on a classic. *J.Invest Dermatol.*, 127(11), pp. 2499-2515.

Grinnell, F., 1994. Fibroblasts, myofibroblasts, and wound contraction. *The Journal of Cell Biology*, 124, pp. 401-404.

Gu, Z., Noss, E. H., Hsu, V. W., & Brenner, M. B., 2011. Integrins traffic rapidly via circular dorsal ruffles and macropinocytosis during stimulated cell migration. *The Journal of Cell Biology*, 193(1), pp. 61-70.

Gumpert, A. M., Varco, J. S., Baker, S. M., Piehl, M., & Falk, M. M., 2008. Double-membrane gap junction internalization requires the clathrin-mediated endocytic machinery. *FEBS Lett.*, 582(19), pp. 2887-2892.

Hansen, C. G., Bright, N. A., Howard, G., & Nichols, B. J., 2009. SDPR induces membrane curvature and functions in the formation of caveolae. *Nat.Cell Biol.*, 11(7), pp. 807-814.

Harhaj, N. S., Barber, A. J., & Antonetti, D. A., 2002. Platelet-derived growth factor mediates tight junction redistribution and increases permeability in MDCK cells. *J.Cell Physiol*, 193(3), pp. 349-364.

Hayer, A., Stoeber, M., Ritz, D., Engel, S., Meyer, H. H., & Helenius, A., 2010. Caveolin-1 is ubiquitinated and targeted to intralumenal vesicles in endolysosomes for degradation. *The Journal of Cell Biology*, 191(3), pp. 615-629.

Heasman, S. J. & Ridley, A. J., 2008. Mammalian Rho GTPases: new insights into their functions from *in vivo* studies. *Nat.Rev.Mol Cell Biol*, 9(9), pp. 690-701.

Hershko, A. & Ciechanover, A., 1998. The ubiquitin system. *Annual Review of Biochemistry*, 67, pp. 425-479.

Hicke, L., 1997. Ubiquitin-dependent internalization and down-regulation of plasma membrane proteins. *FASEB J.*, 11(14) pp. 1215-1226.

Hicke, L. & Dunn, R., 2003. Regulation of membrane protein transport by ubiquitin and ubiquitin-binding proteins. *Annual Review of Cell and Developmental Biology,* 19, pp. 141-172.

Hill, M. M., Bastiani, M., Luetterforst, R., Kirkham, M., Kirkham, A., Nixon, S. J., Walser, P., Abankwa, D., Oorschot, V. M., Martin, S., Hancock, J. F., & Parton, R. G., 2008. PTRF-Cavin, a conserved cytoplasmic protein required for caveola formation and function. *Cell*, 132(1), pp. 113-124.

Hinshaw, J. E., 2000. Dynamin and its role in membrane fission. *Annual Review of Cell and Developmental Biology*, 16(1), pp. 483-519.

Hirsch, F. R., Varella-Garcia, M., & Cappuzzo, F., 2009. Predictive value of EGFR and HER2 overexpression in advanced non-small-cell lung cancer. *Oncogene*, 28(1), pp. 32-37.

Hopkins, C. R., Gibson, A., Shipman, M., Strickland, D. K., & Trowbridge, I. S., 1994. In migrating fibroblasts, recycling receptors are concentrated in narrow tubules in the pericentriolar area, and then routed to the plasma membrane of the leading lamella. *The Journal of Cell Biology*, 125(6), pp. 1265-1274.

Husnjak, K. & Dikic, I., 2006. EGFR trafficking: parkin' in a jam. *Nat.Cell Biol.*, 8(8), pp. 787-788.

Huttenlocher, A., Lakonishok, M., Kinder, M., Wu, S., Truong, T., Knudsen, K.A., & Horwitz, A.F. 2012, Integrin and Cadherin Synergy Regulates Contact Inhibition of Migration and Motile Activity. *The Journal of Cell Biology*, 141(2), pp. 515-526.

Huveneers, S. & Danen, E. H., 2009. Adhesion signaling - crosstalk between integrins, Src and Rho. *Journal of Cell Science*, 122(8), pp. 1059-1069.

Iglesias, P. A. & Devreotes, P. N., 2008. Navigating through models of chemotaxis. *Curr.Opin.Cell Biol.*, 20(1), pp. 35-40.

Ikenouchi, J., Furuse, M., Furuse, K., Sasaki, H., Tsukita, S., & Tsukita, S., 2005a. Tricellulin constitutes a novel barrier at tricellular contacts of epithelial cells. *The Journal of Cell Biology*, 171(6), pp. 939-945.

Ingber, D. E., 2003. Mechanosensation through integrins: cells act locally but think globally. *Proc.Natl.Acad.Sci.U.S.A*, 100(4), pp. 1472-1474.

Isshiki, M., Ando, J., Yamamoto, K., Fujita, T., Ying, Y., & Anderson, R. G., 2002a. Sites of Ca(2+) wave initiation move with caveolae to the trailing edge of migrating cells. *J Cell Sci*, 115(3), pp. 475-484.

Isshiki, M., Ying, Y. S., Fujita, T., & Anderson, R. G., 2002b. A molecular sensor detects signal transduction from caveolae in living cells. *Journal of Biological Chemistry*, 277(45), pp. 43389-43398.

Itoh, M., Morita, K., & Tsukita, S., 1999. Characterization of ZO-2 as a MAGUK family member associated with tight as well as adherens junctions with a binding affinity to occludin and alpha catenin. *J.Biol Chem.*, 274(9), pp. 5981-5986.

Ivanov, A. I., Nusrat, A., & Parkos, C. A., 2004. Endocytosis of epithelial apical junctional proteins by a clathrin-mediated pathway into a unique storage compartment. *Molecular Biology of the Cell*, 15(1), pp. 176-188.

Izzard, C. S. & Lochner, L. R., 1976. Cell-to-substrate contacts in living fibroblasts: an interference reflexion study with an evaluation of the technique. *Journal of Cell Science*, 21(1), pp. 129-159.

Jekely, G., Sung, H. H., Luque, C. M., & Rorth, P., 2005. Regulators of endocytosis maintain localized receptor tyrosine kinase signaling in guided migration. *Dev.Cell*, 9(2), pp. 197-207.

Jiang, W. & Hunter, T., 1998. Analysis of cell-cycle profiles in transfected cells using a membrane- targeted GFP. *BioTechniques*, 24(3), pp. 349-350.

Jones, M. C., Caswell, P. T., & Norman, J. C., 2006. Endocytic recycling pathways: emerging regulators of cell migration. *Curr.Opin.Cell Biol.*, 18(5), pp. 549-557.

Joshi, B., Strugnell, S. S., Goetz, J. G., Kojic, L. D., Cox, M. E., Griffith, O. L., Chan, S. K., Jones, S. J., Leung, S. P., Masoudi, H., Leung, S., Wiseman, S. M., & Nabi, I. R., 2008. Phosphorylated caveolin-1 regulates Rho/ROCK-dependent focal adhesion dynamics and tumor cell migration and invasion. *Cancer Research*, 68(20), pp. 8210-8220.

Kamiguchi, H. & Lemmon, V., 2000. Recycling of the cell adhesion molecule L1 in axonal growth cones. *Journal of Neuroscience*, 20(10), pp. 3676-3686.

Kamiguchi, H., Long, K. E., Pendergast, M., Schaefer, A. W., Rapoport, I., Kirchhausen, T., & Lemmon, V., 1998. The neural cell adhesion molecule L1 interacts with the AP-2 adaptor and is endocytosed via the clathrin-mediated pathway. *Journal of Neuroscience*, 18(14), pp. 5311-5321.

Kamimura, Y., Xiong, Y., Iglesias, P. A., Hoeller, O., Bolourani, P., & Devreotes, P. N., 2008. PIP3-independent activation of TorC2 and PKB at the cell's leading edge mediates chemotaxis. *Curr.Biol.*, 18(14), pp. 1034-1043.

Karjalainen, M., Kakkonen, E., Upla, P., Paloranta, H., Kankaanpää, P., Liberali, P., Renkema, G.H., Hyypiä, T., Heino, J. & Marjomäki, V., 2008. A Raft-derived, Pak1-regulated entry participates in alpha2beta1 integrin-dependent sorting to caveosomes. *Mol. Biol. Cell*, 19, pp. 2857–2869.

Kato, T., Nakayasu, K., Kanai, A., Nishiyama, T., Imamura, Y., & Hayashi, T., 2000. Distribution and isoform characterization of type XII collagen in bovine cornea. *Ophthalmic Res.*, 32(5), pp. 215-221.

Katoh, K., Kano, Y., Amano, M., Onishi, H., Kaibuchi, K., & Fujiwara, K., 2001. Rho-kinase--mediated contraction of isolated stress fibers", *The Journal of Cell Biology*, 153(3), pp. 569-584.

Kawada, K., Upadhyay, G., Ferandon, S., Janarthanan, S., Hall, M., Vilardaga, J. P., & Yajnik, V., 2009. Cell migration is regulated by platelet-derived growth factor receptor endocytosis. *Mol.Cell Biol.*, 29(16), pp. 4508-4518.

Kawauchi, T., Sekine, K., Shikanai, M., Chihama, K., Tomita, K., Kubo, K., Nakajima, K., Nabeshima, Y., & Hoshino, M., 2010. Rab GTPases-dependent endocytic pathways regulate neuronal migration and maturation through N-cadherin trafficking. *Neuron*, 67(4), pp. 588-602.

Kessler, D., Gruen, G. C., Heider, D., Morgner, J., Reis, H., Schmid, K. W., & Jendrossek, V., 2012. The action of small GTPases Rab11 and Rab25 in vesicle trafficking during cell migration. *Cell Physiol Biochem.*, 29(5-6), pp. 647-656.

Keyel, P. A., Mishra, S. K., Roth, R., Heuser, J. E., Watkins, S. C., & Traub, L. M., 2006. A single common portal for clathrin-mediated endocytosis of distinct cargo governed by cargo-selective adaptors. *Molecular Biology of the Cell*, 17(10) pp. 4300-4317.

Kiehart, D. P., 1999. Wound healing: The power of the purse string. *Curr.Biol.*, 9(16), p. 602-605.

Kirfel, G., Rigort, A., Borm, B., & Herzog, V., 2004. Cell migration: mechanisms of rear detachment and the formation of migration tracks. *Eur.J.Cell Biol.*, 83(11-12), pp. 717-724.

Klausner, R. D., Donaldson, J. G., & Lippincott-Schwartz, J., 1992, Brefeldin A: insights into the control of membrane traffic and organelle structure. *The Journal of Cell Biology*, 116, pp. 1071-1080.

Koch, G. L., Macer, D. R., & Wooding, F. B., 1988. Endoplasmin is a reticuloplasmin. *Journal of Cell Science*, 90(3), pp. 485-491.

Kolanus, W. & Seed, B., 1997. Integrins and inside-out signal transduction: converging signals from PKC and PIP3. *Curr.Opin.Cell Biol.*, 9(5), pp. 725-731.

Kolluru, G. K., Bir, S. C., & Kevil, C. G., 2012. Endothelial dysfunction and diabetes: effects on angiogenesis, vascular remodeling, and wound healing. *Int.J.Vasc.Med.*, 2012, I.D. 918267, 30 pages.

Krause G., Winkler, L., Mueller, S.L, Haseloff, R.F., Piontek, J., and Blasig, I.E., 2008. Structure and function of claudins. *Biochimica et Biophysica Acta (BBA) – Biomembranes.* 1778(3), pp. 631-645.

Krause, M., Dent, E.W., Bear, J.E., Loureiro, J.J. & Gertler, F.B., 2003. Ena/VASP proteins: regulators of the actin cytoskeleton and cell migration. *Annu Rev Cell Dev Biol.,* 19, pp. 541-564.

Kruchten, A. E. & McNiven, M. A., 2006. Dynamin as a mover and pincher during cell migration and invasion. *Journal of Cell Science*, 119(9), pp. 1683-1690.

Kublaoui, B., Lee, J., & Pilch. P.F., 1995. Dynamics of Signalling during Insulin-stimulated Endocytosis of Its receptor in Adipocytes. *The Journal of Biological Chemistry*, 270(1), pp. 59-65.

Kucik, D. F., Elson, E. L., & Sheetz, M. P., 1990. Cell migration does not produce membrane flow. *The Journal of Cell Biology*, 111(4), pp. 1617-1622.

Kwik, J., Boyle, S., Fooksman, D., Margolis, L., Sheetz, M. P., & Edidin, M., 2003. Membrane cholesterol, lateral mobility, and the phosphatidylinositol 4,5-bisphosphate-dependent organization of cell actin. *Proc.Natl.Acad.Sci.U.S.A*, 100(24), pp. 13964-13969.

Labrecque, L., Royal, I., Surprenant, D. S., Patterson, C., Gingras, D., & Beliveau, D., 2003. Regulation of Vascular Endothelial Growth Factor Receptor-2 Activity by Caveolin-1 and Plasma Membrane Cholesterol. *Molecular Biology of the Cell*, 14(1), pp. 334-347.

Lampe, P. D. & Lau, A. F., 2004. The effects of connexin phosphorylation on gap junctional communication. *Int.J.Biochem.Cell Biol.*, 36(7), pp. 1171-1186.

Lampugnani, M. G., 1999. Cell migration into a wounded area in vitro. *Methods Mol.Biol.*, 96, pp. 177-182.

Lauffenburger, D. A. & Horwitz, A. F., 1996. Cell migration: a physically integrated molecular process. *Cell*, 84(3), pp. 359-369.

Laukaitis, C. M., Webb, D. J., Donais, K., & Horwitz, A. F., 2001, Differential dynamics of alpha 5 integrin, paxillin, and alpha-actinin during formation and disassembly of adhesions in migrating cells. *J Cell Biol.*, 153(7), pp. 1427-1440.

Lawson, M. A. & Maxfield, F. R., 1995. Ca(2+)- and calcineurin-dependent recycling of an integrin to the front of migrating neutrophils. *Nature (London)*, 377(6544), pp. 75-79.

Le, R. C. & Wrana, J. L., 2005. Clathrin- and non-clathrin-mediated endocytic regulation of cell signalling. *Nat.Rev.Mol.Cell Biol.*, 6(2), pp. 112-126.

Lee, J., Gustafsson, M., Magnusson, K. E., & Jacobson, K., 1990. The direction of membrane lipid flow in locomoting polymorphonuclear leukocytes. *Science*, 247(4947), pp. 1229-1233.

Li, J., Avraham, H., Rogers, R. A., Raja, S., & Avraham, S., 1996. Characterization of RAFTK, a novel focal adhesion kinase, and its integrin-dependent phosphorylation and activation in megakaryocytes. *Blood*, 88(2), pp. 417-428.

Li, L., Okura, M., & Imamoto, A., 2002. Focal adhesions require catalytic activity of Src family kinases to mediate integrin-matrix adhesion. *Mol.Cell Biol.*, 22(4), pp. 1203-1217.

Li, Y., Fanning, A. S., Anderson, J. M., & Lavie, A., 2005. Structure of the conserved cytoplasmic C-terminal domain of occludin: identification of the ZO-1 binding surface. *Journal of Molecular Biology*, 352(1), pp. 151-164.

Liljedahl, M., Maeda, Y., Colanzi, A., Ayala, I., Van, L. J., & Malhotra, V., 2001. Protein kinase D regulates the fission of cell surface destined transport carriers from the trans-Golgi network. *Cell*, 104(3), pp. 409-420.

Linford, A., Yoshimura, S., Nunes, B. R., Langemeyer, L., Gerondopoulos, A., Rigden, D. J., & Barr, F. A., 2012. Rab14 and its exchange factor FAM116 link endocytic recycling and adherens junction stability in migrating cells. *Dev.Cell*, 22(5), pp. 952-966.

Liu, S., Kuo, W., Yang, W., Liu, W., Gibson, G. A., Dorko, K., Watkins, S. C., Strom, S. C., & Wang, T., 2010. The second extracellular loop dictates Occludin-mediated HCV entry. *Virology*, 407(1), pp. 160-170.

Liu, Y., Nusrat, A., Schnell, F. J., Reaves, T. A., Walsh, S., Pochet, M., & Parkos, C. A., 2000. Human junction adhesion molecule regulates tight junction resealing in epithelia. *Journal of Cell Science*, 113(13), pp. 2363-2374.

Lu, H., Sun, T. X., Bouley, R., Blackburn, K., McLaughlin, M., & Brown, D., 2004. Inhibition of endocytosis causes phosphorylation (S256)-independent plasma membrane accumulation of AQP2. *Am.J.Physiol Renal Physiol*, 286(2), pp. 233-243.

Macia, E., Ehrlich, M., Massol, R., Boucrot, E., Brunner, C., & Kirchhausen, T., 2006. Dynasore, a cell-permeable inhibitor of dynamin. *Dev.Cell*, 10(6), pp. 839-850.

Madin, S. H., & Darby Jr, N. B., 1958. Established kidney cell lines of normal adult bovine and ovine origin. *Proc.Soc.Exp.Biol.Med.*, 98(3), pp. 574-576.

Mammoto, A., Ohtsuka, T., Hotta, I., Sasaki, T., & Takai, Y., 1999. Rab11BP/Rabphilin-11, a downstream target of rab11 small G protein implicated in vesicle recycling. *Journal of Biological Chemistry*, 274(36), pp. 25517-25524.

Marchiando, A. M., Shen, L., Graham, W. V., Weber, C. R., Schwarz, B. T., Austin, J. R., Raleigh, D. R., Guan, Y., Watson, A. J., Montrose, M. H., & Turner, J. R. 2010, Caveolin-1-dependent occludin endocytosis is required for TNF-induced tight junction regulation *in vivo*. *The Journal of Cell Biology*, 189(1), pp. 111-126.

Marcus, P. I., 1962. Dynamics of surface modification in myxovirus-infected cells. *Cold Spring Harb.Symp.Quant.Biol.*, vol. 27, pp. 351-365.

Marti, G., Ferguson, M., Wang, J., Byrnes, C., Dieb, R., Qaiser, R., Bonde, P., Duncan, M. D., & Harmon, J. W., 2004. Electroporative transfection with KGF-1 DNA improves wound healing in a diabetic mouse model. *Gene Ther.*, 11(24), pp. 1780-1785.

Martin-Belmonte, F. & Mostov, K., 2008. Regulation of cell polarity during epithelial morphogenesis. *Curr.Opin.Cell Biol.*, 20(2), pp. 227-234.

Maxfield, F. R. & McGraw, T. E., 2004. Endocytic recycling", *Nat.Rev.Mol.Cell Biol.*, 5(2), pp. 121-132.

McCaffrey, M. W., Bielli, A., Cantalupo, G., Mora, S., Roberti, V., Santillo, M., Drummond, F., & Bucci, C., 2001. Rab4 affects both recycling and degradative endosomal trafficking. *FEBS Lett.*, 495(1-2), pp. 21-30.

McNeely, M. J., Boyko, E. J., Ahroni, J. H., Stensel, V. L., Reiber, G. E., Smith, D. G., & Pecoraro, R. F., 1995. The independent contributions of diabetic neuropathy and vasculopathy in foot ulceration. How great are the risks?. *Diabetes Care*, 18(2), pp. 216-219.

Meredith, L. W., Wilson, G. K., Fletcher, N. F., & McKeating, J. A., 2012. Hepatitis C virus entry: beyond receptors. *Rev.Med.Virol.*, 22(3), pp. 182-193.

Metzelaar, M. J., Schuurman, H. J., Heijnen, H. F., Sixma, J. J., & Nieuwenhuis, H. K., 1991. Biochemical and immunohistochemical characteristics of CD62 and CD63 monoclonal antibodies. Expression of GMP-140 and LIMP-CD63 (CD63 antigen) in human lymphoid tissues. *Virchows Arch.B Cell Pathol.Incl.Mol Pathol.*, 61(4), pp. 269-277.

Milano, V., Piao, Y., LaFortune, T., & de, G. J., 2009. Dasatinib-induced autophagy is enhanced in combination with temozolomide in glioma. *Mol Cancer Ther.*, 8(2), pp. 394-406.

Mitra, S. K., Hanson, D. A., & Schlaepfer, D. D., 2005. Focal adhesion kinase: in command and control of cell motility. *Nat.Rev.Mol.Cell Biol.*, 6(1), pp. 56-68.

Mohrmann, K., Leijendekker, R., Gerez, L., & Van Der, S. P., 2002. Rab4 regulates transport to the apical plasma membrane in Madin-Darby canine kidney cells. *Journal of Biological Chemistry*, 277(12), pp. 10474-10481.

Monier, S., Parton, R. G., Vogel, F., Behlke, J., Henske, A., & Kurzchalia, T. V., 1995. VIP21-caveolin, a membrane protein constituent of the caveolar coat, oligomerizes *in vivo* and *in vitro*. *Molecular Biology of the Cell*, 6(7), pp. 911-927.

Morimoto, S., Nishimura, N., Terai, T., Manabe, S., Yamamoto, Y., Shinahara, W., Miyake, H., Tashiro, S., Shimada, M., & Sasaki, T., 2005. Rab13 mediates the continuous endocytic recycling of occludin to the cell surface. *Journal of Biological Chemistry*, 280(3), pp. 2220-2228.

Morita, K., Furuse, M., Fujimoto, K., & Tsukita, S., 1999. Claudin multigene family encoding four-transmembrane domain protein components of tight junction strands. *Proc.Natl.Acad.Sci.U.S.A*, 96(2), pp. 511-516.

Mukherjee, S., Tessema, M., & Wandinger-Ness, A., 2006. Vesicular trafficking of tyrosine kinase receptors and associated proteins in the regulation of signaling and vascular function. *Circ.Res.*, 98(6), pp. 743-756.

Murakami, T., Felinski, E. A., & Antonetti, D. A., 2009. Occludin phosphorylation and ubiquitination regulate tight junction trafficking and vascular endothelial growth factor-induced permeability. *Journal of Biological Chemistry*, 284(31), pp. 21036-21046.

Murata, M., Peranen, J., Schreiner, R., Wieland, F., Kurzchalia, T. V., & Simons, K., 1995. VIP21/caveolin is a cholesterol-binding protein. *Proceedings of the National Academy of Sciences of the United States of America*, 92(22), pp. 10339-10343.

Nabi, I. R., 1999. The polarization of the motile cell. *Journal of Cell Science*, 112(12), pp. 1803-1811.

Nam, S., Kim, D., Cheng, J. Q., Zhang, S., Lee, J. H., Buettner, R., Mirosevich, J., Lee, F. Y., & Jove, R., 2005. Action of the Src family kinase inhibitor, dasatinib (BMS-354825), on human prostate cancer cells. *Cancer Research*, 65(20), pp. 9185-9189.

Navarro, A., Anand-Apte, B., & Parat, M. O., 2004. A role for caveolae in cell migration. *FASEB J*, 18(15), pp. 1801-1811.

Ng, T., Shima, D., Squire, A., Bastiaens, P.I., Gschmeissner, S., Humphries, M.J. & Parker, P.J., 1999. PKCalpha regulates beta1 integrin-dependent cell motility through association and control of integrin traffic. *EMBO J*., 18, pp. 3909–3923.

Niessen, C. M., 2007. Tight junctions/adherens junctions: basic structure and function. *J.Invest Dermatol.*, 127(11), pp. 2525-2532.

Nishimura, T. & Kaibuchi, K., 2007. Numb controls integrin endocytosis for directional cell migration with aPKC and PAR-3. *Dev.Cell*, 13(1), pp. 15-28.

Nokes, R. L., Fields, I. C., Collins, R. N., & Folsch, H., 2008. Rab13 regulates membrane trafficking between TGN and recycling endosomes in polarized epithelial cells. *J.Cell Biol*, 182(5), pp. 845-853.

Nuzzi, P. A., Senetar, M. A., & Huttenlocher, A., 2007. Asymmetric localization of calpain 2 during neutrophil chemotaxis. *Molecular Biology of the Cell*, 18(3), pp. 795-805.

Oh, P., McIntosh, D. P., & Schnitzer, J. E., 1998. Dynamin at the neck of caveolae mediates their budding to form transport vesicles by GTP-driven fission from the plasma membrane of endothelium. *The Journal of Cell Biology*, 141(1), pp. 101-114.

Orlandi, P. A. & Fishman, P. H., 1998. Filipin-dependent inhibition of cholera toxin: evidence for toxin internalization and activation through caveolae-like domains. *The Journal of Cell Biology*, 141(4), pp. 905-915.

Orlichenko, L., Huang, B., Krueger, E., & McNiven, M. A., 2006. Epithelial growth factor-induced phosphorylation of caveolin 1 at tyrosine 14 stimulates caveolae formation in epithelial cells. *Journal of Biological Chemistry*, 281(8), pp. 4570-4579.

Osanai, M., Murata, M., Chiba, H., Kojima, T., & Sawada, N., 2007. Epigenetic silencing of claudin-6 promotes anchorage-independent growth of breast carcinoma cells. *Cancer Sci.*, 98(10), pp. 1557-1562.

Ozdamar, B., Bose, R., Barrios-Rodiles, M., Wang, H. R., Zhang, Y., & Wrana, J. L., 2005. Regulation of the polarity protein Par6 by TGFbeta receptors controls epithelial cell plasticity. *Science*, 307no. 5715, pp. 1603-1609.

Palecek, S. P., Schmidt, C. E., Lauffenburger, D. A., & Horwitz, A. F., 1996. Integrin dynamics on the tail region of migrating fibroblasts. *Journal of Cell Science*, 109(5), pp. 941-952.

Parat, M. O., Anand-Apte, B., & Fox, P. L., 2003. Differential caveolin-1 polarization in endothelial cells during migration in two and three dimensions. *Molecular Biology of the Cell*, 149(8), pp. 3156-3168.

Parsons, M., Messent, A. J., Humphries, J. D., Deakin, N. O., & Humphries, M. J. 2008. Quantification of integrin receptor agonism by fluorescence lifetime imaging", *Journal of Cell Science.* 121(3), pp. 265-271.

Parton, R. G., Simons, K., & Dotti, C. G., 1992. Axonal and dendritic endocytic pathways in cultured neurons. *The Journal of Cell Biology.* 119(1), pp. 123-137.

Pasapera, A. M., Schneider, I. C., Rericha, E., Schlaepfer, D. D., & Waterman, C. M., 2010. Myosin II activity regulates vinculin recruitment to focal adhesions through FAK-mediated paxillin phosphorylation. *The Journal of Cell Biology*, 188(6), pp. 877-890.

Payne, C. K., Jones, S. A., Chen, C., & Zhuang, X., 2007. Internalization and trafficking of cell surface proteoglycans and proteoglycan-binding ligands. *Traffic.*, 8(4), pp. 389-401.

Pearse, B. M., Smith, C. J., & Owen, D. J., 2000. Clathrin coat construction in endocytosis. *Current Opinion in Structural Biology*, 10(2), pp. 220-228.

Pellinen, T., Tuomi, S., Arjonen, A., Wolf, M., Edgren, H., Meyer, H., Grosse, R., Kitzing, T., Rantala, J. K., Kallioniemi, O., Fassler, R., Kallio, M., & Ivaska, J., 2008. Integrin trafficking regulated by Rab21 is necessary for cytokinesis, *Dev.Cell*, 15(3), pp. 371-385.

Perez-Moreno, M. & Fuchs, E., 2006. Catenins: keeping cells from getting their signals crossed. *Dev.Cell*, 11(5), pp. 601-612.

Petit, V., Thiery, J.P., 2000. Focal adhesions: structure and dynamics. Biology of the Cell, 92, pp. 477-494.

Pichot, C. S., Hartig, S. M., Xia, L., Arvanitis, C., Monisvais, D., Lee, F. Y., Frost, J. A., & Corey, S. J., 2009. Dasatinib synergizes with doxorubicin to block growth, migration, and invasion of breast cancer cells. *Br.J.Cancer*, 101(1), pp. 38-47.

Pierini, L. M., Lawson, M. A., Eddy, R. J., Hendey, B., & Maxfield, F. R., 2000. Oriented endocytic recycling of alpha5beta1 in motile neutrophils. *Blood*, vol. 95, no. 8, pp. 2471-2480.

Pigors, M., Kiritsi, D., Krumpelmann, S., Wagner, N., He, Y., Podda, M., Kohlhase, J., Hausser, I., Bruckner-Tuderman, L., & Has, C., 2011. Lack of plakoglobin leads to lethal congenital epidermolysis bullosa: a novel clinico-genetic entity. *Hum.Mol Genet.*, 20(9), pp. 1811-1819.

Podar, K., Shringarpure, R., Tai, Y. T., Simoncini, M., Sattler, M., Ishitsuka, K., Richardson, P. G., Hideshima, T., Chauhan, D., & Anderson, K. C., 2004. Caveolin-1 is required for vascular endothelial

growth factor-triggered multiple myeloma cell migration and is targeted by bortezomib. *Cancer Research*, 64(20), pp. 7500-7506.

Polo, S., Sigismund, S., Faretta, M., Guidi, M., Capua, M. R., Bossi, G., Chen, H., De Camilli, P., & Di Fiore, P. P., 2002. A single motif responsible for ubiquitin recognition and monoubiquitination in endocytic proteins. *Nature (London)*, 416(6879), pp. 451-455.

Powelka, A.M., Sun, J., Li, J., Gao, M., Shaw, L.M., Sonnenberg, A. & Hsu, V.W., 2004. Stimulation-dependent recycling of integrin beta1 regulated by ARF6 and Rab11. *Traffic,* 5, pp. 20–36.

Praefcke, G. J. & McMahon, H. T., 2004. The dynamin superfamily: universal membrane tubulation and fission molecules? *Nat.Rev.Mol.Cell Biol.*, 5(2), pp. 133-147.

Presley, J. F., Mayor, S., McGraw, T. E., Dunn, K. W., & Maxfield, F. R., 1997. Bafilomycin A1 treatment retards transferrin receptor recycling more than bulk membrane recycling. *Journal of Biological Chemistry*, 272, 21, pp. 13929-13936.

Prigozhina, N. L. & Waterman-Storer, C. M., 2004. Protein kinase D-mediated anterograde membrane trafficking is required for fibroblast motility. *Curr.Biol.*, 14(2), pp. 88-98.

Prigozhina, N. L. & Waterman-Storer, C. M., 2006. Decreased polarity and increased random motility in PtK1 epithelial cells correlate with inhibition of endosomal recycling. *Journal of Cell Science*, 119(17), pp. 3571-3582.

Raiborg, C. & Stenmark, H., 2002. Hrs and endocytic sorting of ubiquitinated membrane proteins. *Cell Struct.Funct.*, 27(6), pp. 403-408.

Ramsay, A. G., Keppler, M. D., Jazayeri, M., Thomas, G. J., Parsons, M., Violette, S., Weinreb, P., Hart, I. R., & Marshall, J. F., 2007. HS1-associated protein X-1 regulates carcinoma cell migration and invasion via clathrin-mediated endocytosis of integrin alphavbeta6. *Cancer Research*, 67(11), pp. 5275-5284.

Rapoport, I., Boll, W., Yu, A., Bocking, T., & Kirchhausen, T., 2008. A motif in the clathrin heavy chain required for the Hsc70/auxilin uncoating reaction. *Molecular Biology of the Cell*, 19(1), pp. 405-413.

Rappoport, J. Z., Heyman, K. P., Kemal, S., & Simon, S. M. 2008. Dynamics of dynamin during clathrin mediated endocytosis in PC12 cells. *PLoS.One.*, 3(6), pp. e2416.

Rappoport, J. Z. & Simon, S. M. 2003. Real-time analysis of clathrin-mediated endocytosis during cell migration. *Journal of Cell Science*, 116(6), p. 847-855.

Rappoport, J. Z. & Simon, S. M., 2009. Endocytic trafficking of activated EGFR is AP-2 dependent and occurs through preformed clathrin spots. *Journal of Cell Science*, 122(9), pp. 1301-1305.

Rappoport, J. Z., Taha, B. W., Lemeer, S., Benmerah, A., & Simon, S. M., 2003. The AP-2 complex is excluded from the dynamic population of plasma membrane-associated clathrin. *Journal of Biological Chemistry*, 278(48), pp. 47357-47360.

Rappoport, J. Z., Taha, B. W., & Simon, S. M., 2003. Movement of Plasma-Membrane-Associated Clathrin Spots Along the Microtubule Cytoskeleton. *Traffic.*, 4(7), pp. 460-467.

Reddy, K. B., Smith, D. M., & Plow, E. F., 2008. Analysis of Fyn function in hemostasis and alphaIIbbeta3-integrin signalling. *Journal of Cell Science.* 121(10), pp. 1641-1648.

Reiber, G. E., Vileikyte, L., Boyko, E. J., del, A. M., Smith, D. G., Lavery, L. A., & Boulton, A. J., 1999. Causal pathways for incident lower-extremity ulcers in patients with diabetes from two settings. *Diabetes Care*, 22(1), pp. 157-162.

Ren, M., Xu, G., Zeng, J., De Lemos-Chiarandini, C., Adesnik, M., & Sabatini, D. D., 1998. Hydrolysis of GTP on rab11 is required for the direct delivery of transferrin from the pericentriolar recycling compartment to the cell surface but not from sorting endosomes. *Proc.Natl.Acad.Sci.U.S.A*, 95(11), pp. 6187-6192.

Ridley, A. J., Paterson, H. F., Johnston, C. L., Diekmann, D., & Hall, A., 1992. The small GTP-binding protein rac regulates growth factor-induced membrane ruffling. *Cell*, 70(3), pp. 401-410.

Ridley, A. J., Schwartz, M. A., Burridge, K., Firtel, R. A., Ginsberg, M. H., Borisy, G., Parsons, J. T., & Horwitz, A. R. 2003. Cell migration: integrating signals from front to back. *Science*, 302(5651), pp. 1704-1709.

Roberts, M., Barry, S., Woods, A., Van Der, S. P., & Norman, J., 2001. PDGF-regulated rab4-dependent recycling of alphavbeta3 integrin from early endosomes is necessary for cell adhesion and spreading. *Curr.Biol.*, 11(18), pp. 1392-1402.

Roberts, M. S., Woods, A. J., Dale, T. C., Van Der, S. P., & Norman, J. C., 2004. Protein kinase B/Akt acts via glycogen synthase kinase 3 to regulate recycling of alpha v beta 3 and alpha 5 beta 1 integrins. *Mol.Cell Biol.*, 24(4), pp. 1505-1515.

Saffarian, S., Cocucci, E., & Kirchhausen, T., 2009. Distinct dynamics of endocytic clathrin-coated pits and coated plaques. *PLoS.Biol*, 7(9), pp. e1000191.

Sahai, E., 2005. Mechanisms of cancer cell invasion. *Curr.Opin.Genet.Dev.*, 15(1), pp. 87-96.

Saitou, M., Furuse, M., Sasaki, H., Schulzke, J. D., Fromm, M., Takano, H., Noda, T., & Tsukita, S., 2000. Complex phenotype of mice lacking occludin, a component of tight junction strands. *Molecular Biology of the Cell*, 11(12), pp. 4131-4142.

Salanueva, I. J., Cerezo, A., Guadamillas, M. C., & del Pozo, M. A., 2007. Integrin regulation of caveolin function. *J.Cell Mol.Med.*, 11(5), pp. 969-980.

Samaniego, R., Sanchez-Martin, L., Estecha, A., & Sanchez-Mateos, P., 2007. Rho/ROCK and myosin II control the polarized distribution of endocytic clathrin structures at the uropod of moving T lymphocytes. *Journal of Cell Science*, 120(20), pp. 3534-3543.

Sancey, L., Garanger, E., Foillard, S., Schoehn, G., Hurbin, A., biges-Rizo, C., Boturyn, D., Souchier, C., Grichine, A., Dumy, P., & Coll, J. L., 2009. Clustering and internalization of integrin alphavbeta3 with a tetrameric RGD-synthetic peptide. *Mol.Ther.*, 17(5), pp. 837-843.

Sander, E. E., van, D. S., ten Klooster, J. P., Reid, T., van der Kammen, R. A., Michiels, F., & Collard, J. G., 1998. Matrix-dependent Tiam1/Rac signaling in epithelial cells promotes either cell-cell adhesion or cell migration and is regulated by phosphatidylinositol 3-kinase. *The Journal of Cell Biology*, 143(5), pp. 1385-1398.

Scales, T. M. & Parsons, M., 2011. Spatial and temporal regulation of integrin signalling during cell migration. *Curr.Opin.Cell Biol*, 23(5), pp. 562-568.

Scheiffele, P., Verkade, P., Fra, A. M., Virta, H., Simons, K., & Ikonen, E., 1998. Caveolin-1 and -2 in the exocytic pathway of MDCK cells. *The Journal of Cell Biology*, 140(4), pp. 795-806.

Schlunck, G., Damke, H., Kiosses, W.B., Rusk, N., Symons, M.H., Waterman-Storer, C.M., Schmid, S.L., & Schwartz, M.A., 2004. Modulation of Rac Localization and Function by Dynamin. *Molecular Biology of the Cell*, 15, pp. 256-267.

Schmoranzer, J., Goulian, M., Axelrod, D., & Simon, S. M., 2000. Imaging constitutive exocytosis with total internal reflection fluorescence microscopy. *The Journal of Cell Biology*, 149(1), pp. 23-32.

Schmoranzer, J., Kreitzer, G., & Simon, S. M., 2003. Migrating fibroblasts perform polarized, microtubule-dependent exocytosis towards the leading edge. *Journal of Cell Science*, 116(22), pp. 4513-4519.

Schneider-Poetsch, T., Ju, J., Eyler, D. E., Dang, Y., Bhat, S., Merrick, W. C., Green, R., Shen, B., & Liu, J. O., 2010. Inhibition of eukaryotic translation elongation by cycloheximide and lactimidomycin. *Nat.Chem.Biol*, 6(3), pp. 209-217.

Schoenenberger, C. A., Zuk, A., Zinkl, G. M., Kendall, D., & Matlin, K. S., 1994. Integrin expression and localization in normal MDCK cells and transformed MDCK cells lacking apical polarity. *Journal of Cell Science*, 107(2), pp. 527-541.

Schwab, A., 2001. Ion channels and transporters on the move. *News Physiol Sci.*, 16, pp. 29-33.

Servant, G., Weiner, O. D., Neptune, E. R., Sedat, J. W., & Bourne, H. R., 1999. Dynamics of a chemoattractant receptor in living neutrophils during chemotaxis. *Molecular Biology of the Cell*, 10(4), pp. 1163-1178.

Severs, N. J., 1988. Caveolae: static inpocketings of the plasma membrane, dynamic vesicles or plain artifact? *Journal of Cell Science*, 90(3), pp. 341-348.

Sheetz, M. P., Felsenfeld, D., Galbraith, C. G., & Choquet, D., 1999. Cell migration as a five-step cycle. *Biochem.Soc.Symp.*, 65, pp. 233-243.

Sher, I., Zisman-Rozen, S., Eliahu, L., Whitelock, J. M., Maas-Szabowski, N., Yamada, Y., Breitkreutz, D., Fusenig, N. E., rikawa-Hirasawa, E., Iozzo, R. V., Bergman, R., & Ron, D., 2006. Targeting perlecan in human keratinocytes reveals novel roles for perlecan in epidermal formation. *J.Biol Chem.*, 281(8), pp. 5178-5187.

Shi, F. & Sottile, J., 2008. Caveolin-1-dependent beta1 integrin endocytosis is a critical regulator of fibronectin turnover. *Journal of Cell Science*, 121(14), pp. 2360-2371.

Shieh, J. C., Schaar, B. T., Srinivasan, K., Brodsky, F. M., & McConnell, S. K., 2011. Endocytosis regulates cell soma translocation and the distribution of adhesion proteins in migrating neurons. *PLoS.One.*, 6(3), p. e17802.

Shih, S. C., Katzmann, D. J., Schnell, J. D., Sutanto, M., Emr, S. D., & Hicke, L., 2002. Epsins and Vps27p/Hrs contain ubiquitin-binding domains that function in receptor endocytosis. *Nat.Cell Biol.*, 4(5), pp. 389-393.

Shin, K., Wang, Q., & Margolis, B., 2007. PATJ regulates directional migration of mammalian epithelial cells. *EMBO Rep.*, 8(2), pp. 158-164.

Singh, R. D., Puri, V., Valiyaveettil, J. T., Marks, D. L., Bittman, R., & Pagano, R. E., 2003. Selective caveolin-1-dependent endocytosis of glycosphingolipids. *Molecular Biology of the Cell*, 14(8), pp. 3254-3265.

Sinha, B., Koster, D., Ruez, R., Gonnord, P., Bastiani, M., Abankwa, D., Stan, R. V., Butler-Browne, G., Vedie, B., Johannes, L., Morone, N., Parton, R. G., Raposo, G., Sens, P., Lamaze, C., & Nassoy, P., 2011. Cells respond to mechanical stress by rapid disassembly of caveolae. *Cell*, 144(3), pp. 402-413.

Skalski, M. & Coppolino, M.G., 2005. SNARE-mediated trafficking of alpha (5) beta (1) integrin is required for spreading in CHO cells. *Biochem. Biophys. Res. Commun*., 335, pp. 1199–1210.

Sorkin, A., 2001. Internalization of the epidermal growth factor receptor: role in signalling. *Biochem.Soc.Trans.*, 29(4), pp. 480-484.

Staehelin, L. A., 1974. Structure and function of intercellular junctions. *Int.Rev.Cytol.*, 39, pp. 191-283.

Stamatovic, S. M., Keep, R. F., Wang, M. M., Jankovic, I., & Andjelkovic, A. V., 2009. Caveolae-mediated internalization of occludin and claudin-5 during CCL2-induced tight junction remodeling in brain endothelial cells. *Journal of Biological Chemistry*, 284(28), pp. 19053-19066.

Steed, E., Balda, M. S., & Matter, K., 2010. Dynamics and functions of tight junctions. *Trends Cell Biol*, 20(3), pp. 142-149.

Steffens, S., Schrader, A. J., Vetter, G., Eggers, H., Blasig, H., Becker, J., Kuczyk, M. A., & Serth, J., 2012. Fibronectin 1 protein expression in clear cell renal cell carcinoma. *Oncol.Lett.*, 3(4), pp. 787-790.

Stratton, I. M., Adler, A. I., Neil, H. A., Matthews, D. R., Manley, S. E., Cull, C. A., Hadden, D., Turner, R. C., & Holman, R. R., 2000. Association of glycaemia with macrovascular and microvascular complications of type 2 diabetes (UKPDS 35): prospective observational study. *BMJ*, 321(7258), pp. 405-412.

Sturge, J., Hamelin, J., & Jones, G. E., 2002. N-WASP activation by a beta1-integrin-dependent mechanism supports PI3K-independent chemotaxis stimulated by urokinase-type plasminogen activator. *Journal of Cell Science*, 115(4), pp. 699-711.

Su, L., Mruk, D. D., Lee, W. M., & Cheng, C. Y., 2010. Differential effects of testosterone and TGF-beta3 on endocytic vesicle-mediated protein trafficking events at the blood-testis barrier. *Exp.Cell Res.*, 316(17), pp. 2945-2960.

Subramani, D. & Alahari, S. K., 2010. Integrin-mediated function of Rab GTPases in cancer progression. *Mol.Cancer*, 9(312).

Sweitzer, S. M. & Hinshaw, J. E., 1998. Dynamin undergoes a GTP-dependent conformational change causing vesiculation. *Cell*, 93(6), pp. 1021-1029.

Tagawa, A., Mezzacasa, A., Hayer, A., Longatti, A., Pelkmans, L., & Helenius, A., 2005. Assembly and trafficking of caveolar domains in the cell: caveolae as stable, cargo-triggered, vesicular transporters. *The Journal of Cell Biology*, 170(5), pp. 769-779.

Tan, J. L., Tien, J., Pirone, D. M., Gray, D. S., Bhadriraju, K., & Chen, C. S., 2003. Cells lying on a bed of microneedles: an approach to isolate mechanical force. *Proc.Natl.Acad.Sci.U.S.A*, 100(4), pp. 1484-1489.

Tawk, M., Joulie, C., & Vriz, S., 2000. Zebrafish Hsp40 and Hsc70 genes are both induced during caudal fin regeneration. *Mech.Dev.*, 99(1-2), pp. 183-186.

Tayeb, M. A., Skalski, M., Cha, M. C., Kean, M. J., Scaife, M., & Coppolino, M. G., 2005. Inhibition of SNARE-mediated membrane traffic impairs cell migration. *Exp.Cell Res.*, 305(1), pp. 63-73.

Thiery, J. P., 2002. Epithelial-mesenchymal transitions in tumour progression. *Nat.Rev.Cancer*, 2(6), pp. 442-454.

Traynor, D. & Kay, R. R., 2007. Possible roles of the endocytic cycle in cell motility. *Journal of Cell Science*, 120(14), pp. 2318-2327.

Trinkle-Mulcahy, L., Andersen, J., Lam, Y. W., Moorhead, G., Mann, M., & Lamond, A. I., 2006. Repo-Man recruits PP1 gamma to chromatin and is essential for cell viability. *J.Cell Biol*, 172(5), pp. 679-692.

Tsuruta, D., Gonzales, M., Hopkinson, S. B., Otey, C., Khuon, S., Goldman, R. D., & Jones, J. C., 2002. Microfilament-dependent movement of the beta3 integrin subunit within focal contacts of endothelial cells. *FASEB J*, 16(8), pp. 866-868.

Tzaban, S., Massol, R. H., Yen, E., Hamman, W., Frank, S. R., Lapierre, L. A., Hansen, S. H., Goldenring, J. R., Blumberg, R. S., & Lencer, W. I., 2009. The recycling and transcytotic pathways for IgG transport by FcRn are distinct and display an inherent polarity. *The Journal of Cell Biology*, 185(4), pp. 673-684.

Ullrich, O., Reinsch, S., Urbe, S., Zerial, M., & Parton, R. G., 1996. Rab11 regulates recycling through the pericentriolar recycling endosome. *The Journal of Cell Biology*, 135(4), pp. 913-924.

Upla, P., Marjomaki, V., Kankaanpaa, P., Ivaska, J., Hyypia, T., Van der Goot, F. G., & Heino, J., 2004. Clustering induces a lateral redistribution of alpha 2 beta 1 integrin from membrane rafts to caveolae and

subsequent protein kinase C-dependent internalization. *Molecular Biology of the Cell*, 15(2), pp. 625-636.

Valdembri, D., Caswell, P. T., Anderson, K. I., Schwarz, J. P., Konig, I., Astanina, E., Caccavari, F., Norman, J. C., Humphries, M. J., Bussolino, F., & Serini, G., 2009. Neuropilin-1/GIPC1 signaling regulates alpha5beta1 integrin traffic and function in endothelial cells. *PLoS.Biol.*, 7(1), p. e25.

van der Sluijs, P., Hull, M., Huber, L. A., Male, P., Goud, B., & Mellman, I., 1992. Reversible phosphorylation--dephosphorylation determines the localization of rab4 during the cell cycle. *The EMBO Journal*, 11, pp. 4379-4389.

Van Meer, G. & Simons, K., 1986. The function of tight junctions in maintaining differences in lipid composition between the apical and the basolateral cell surface domains of MDCK cells. *EMBO J.*, 5(7), 1455-1464.

Vassilieva, E. V., Gerner-Smidt, K., Ivanov, A. I., & Nusrat, A., 2008. Lipid rafts mediate internalization of beta1-integrin in migrating intestinal epithelial cells. *Am.J.Physiol Gastrointest.Liver Physiol*, 295(5), p. G965-G976.

Virata, M. L. A., Wagner, R. M., Parry, D. A., & Green, K. J., 1992. Molecular structure of the human desmoplakin I and II amino terminus. *Proc Natl Acad Sci U S A*, 89, pp. 544-548.

Volchuk, A., Narine, S., Foster, L. J., Grabs, D., De, C. P., & Klip, A., 1998. Perturbation of dynamin II with an amphiphysin SH3 domain increases GLUT4 glucose transporters at the plasma membrane in 3T3-L1 adipocytes. Dynamin II participates in GLUT4 endocytosis. *Journal of Biological Chemistry*, 273(14), pp. 8169-8176.

Wang, X., Kumar, R., Navarre, J., Casanova, J. E., & Goldenring, J. R., 2000. Regulation of vesicle trafficking in madin-darby canine kidney cells by Rab11a and Rab25. *Journal of Biological Chemistry*, 275(37), pp. 29138-29146.

Ward, E. S., Martinez, C., Vaccaro, C., Zhou, J., Tang, Q., & Ober, R. J., 2005. From sorting endosomes to exocytosis: association of Rab4 and Rab11 GTPases with the Fc receptor, FcRn, during recycling. *Molecular Biology of the Cell*, 16(4), pp. 2028-2038.

Webb, D. J., Donais, K., Whitmore, L. A., Thomas, S. M., Turner, C. E., Parsons, J. T., & Horwitz, A. F., 2004. FAK-Src signalling through paxillin, ERK and MLCK regulates adhesion disassembly. *Nat.Cell Biol*, 6(2), pp. 154-161.

Webb, D. J., Parsons, J. T., & Horwitz, A. F., 2002. Adhesion assembly, disassembly and turnover in migrating cells -- over and over and over again. *Nat.Cell Biol.*, 4(4), pp. E97-100.

Weisz, O. A. & Rodriguez-Boulan, E., 2009. Apical trafficking in epithelial cells: signals, clusters and motors. *Journal of Cell Science*, 122(23), pp. 4253-4266.

White, D. P., Caswell, P. T., & Norman, J. C., 2007. alpha v beta3 and alpha5beta1 integrin recycling pathways dictate downstream Rho kinase signaling to regulate persistent cell migration. *The Journal of Cell Biology*, 177(3), pp. 515-525.

Wilcox, E. R., Burton, Q. L., Naz, S., Riazuddin, S., Smith, T. N., Ploplis, B., Belyantseva, I., Ben-Yosef, T., Liburd, N. A., Morell, R. J., Kachar, B., Wu, D. K., Griffith, A. J., Riazuddin, S., & Friedman, T. B., 2001. Mutations in the gene encoding tight junction claudin-14 cause autosomal recessive deafness DFNB29. *Cell*, 104(1), pp. 165-172.

Wilson, P. D., 1997. Epithelial cell polarity and disease. *Am.J.Physiol*, 272(4;2), p. F434-F442.

Woodcock, S.A., Jones, R.C., Edmondson, R.D., and Malliri. A., 2009. A modified tandem affinity purification technique identifies that 14-3-3 proteins interact with Tiam1, an interaction which controls Tiam1 stability. *J Proteome Res.,* 8, pp. 5629-5641.

Woods, A. J., White, D. P., Caswell, P. T., & Norman, J. C., 2004. PKD1/PKCmu promotes alphavbeta3 integrin recycling and delivery to nascent focal adhesions. *Embo J*, 23(13), pp. 2531-2543.

Xia, W., Wong, E. W., Mruk, D. D., & Cheng, C. Y., 2009. TGF-beta3 and TNFalpha perturb blood-testis barrier (BTB) dynamics by accelerating the clathrin-mediated endocytosis of integral membrane proteins: a new concept of BTB regulation during spermatogenesis. *Developmental Biology*, 327(1), pp. 48-61.

Yadav, S., Puri, S., & Linstedt, A. D., 2009. A primary role for Golgi positioning in directed secretion, cell polarity, and wound healing. *Molecular Biology of the Cell*, 20(6), pp. 1728-1736.

Yonemura, S., Itoh, M., Nagafuchi, A., Tsukita, S.. 1995. Cell-to-cell adherens junction formation and actin filament organization: similarities and differences between non-polarized fibroblasts and polarized epithelial cells. *J. Cell Sci.,* 108*, pp.* 127-142*.*

Yoon, S. O., Shin, S., & Mercurio, A. M., 2005. Hypoxia stimulates carcinoma invasion by stabilizing microtubules and promoting the Rab11

trafficking of the alpha6beta4 integrin. *Cancer Research*, 65(7), pp. 2761-2769.

Yoshimori, T., Yamamoto, A., Moriyama, Y., Futai, M., & Tashiro, Y., 1991. Bafilomycin A1, a specific inhibitor of vacuolar-type H(+)- ATPase, inhibits acidification and protein degradation in lysosomes of cultured cells. *Journal of Biological Chemistry*, 266, pp. 17707-17712.

Yu, D. & Turner, J. R., 2008. Stimulus-induced reorganization of tight junction structure: the role of membrane traffic. *Biochimica et Biophysica Acta*, 1778(3), pp. 709-716.

Zamir, E. & Geiger, B., 2001. Molecular complexity and dynamics of cell-matrix adhesions. *Journal of Cell Science*, 114(20), pp. 3583-3590.

Zavadil, J. & Bottinger, E. P., 2005. TGF-beta and epithelial-to-mesenchymal transitions. *Oncogene*, 24(37), pp. 5764-5774.

Zeissig, S., Burgel, N., Gunzel, D., Richter, J., Mankertz, J., Wahnschaffe, U., Kroesen, A. J., Zeitz, M., Fromm, M., & Schulzke, J. D., 2007. Changes in expression and distribution of claudin 2, 5 and 8 lead to discontinuous tight junctions and barrier dysfunction in active Crohn's disease. *Gut*, 56(1), pp. 61-72.

Zeng, J., Ren, M., Gravotta, D., De Lemos-Chiarandini, C., Lui, M., Erdjument-Bromage, H., Tempst, P., Xu, G., Shen, T. H., Morimoto, T., Adesnik, M., & Sabatini, D. D., 1999. Identification of a putative effector protein for rab11 that participates in transferrin recycling. *Proc.Natl.Acad.Sci.U.S.A*, 96(6), pp. 2840-2845.

Zhang, W., Razani, B., Altschuler, Y., Bouzahzah, B., Mostov, K. E., Pestell, R. G., & Lisanti, M. P., 2000. Caveolin-1 inhibits epidermal growth factor-stimulated lamellipod extension and cell migration in metastatic mammary adenocarcinoma cells (MTLn3). Transformation suppressor effects of adenovirus-mediated gene delivery of caveolin-1. *Journal of Biological Chemistry*, 275(27), pp. 20717-20725.

Zhou, P., Porcionatto, M., Pilapil, M., Chen, Y., Choi, Y., Tolias, K. F., Bikoff, J. B., Hong, E. J., Greenberg, M. E., & Segal, R. A., 2007.Polarized signaling endosomes coordinate BDNF-induced chemotaxis of cerebellar precursors. *Neuron*, 55(1), pp. 53-68.

Zhou, X. Y., Murphy, F. R., Gehdu, N., Zhang, J. L., Iredale, J. P., & Benyon, R. C., 2004. Engagement of alpha(v)beta(3) integrin regulates proliferation and apoptosis of hepatic stellate cells. *Journal of Biological Chemistry*, 279(23), pp. 23996-24006.

Zhou, Z., Wang, J., Cao, R., Morita, H., Soininen, R., Chan, K. M., Liu, B., Cao, Y., & Tryggvason, K., 2004. Impaired angiogenesis, delayed

wound healing and retarded tumor growth in perlecan heparan sulfate-deficient mice. *Cancer Research*, 64(14), pp. 4699-4702.

Zhu, J. X., Goldoni, S., Bix, G., Owens, R. T., McQuillan, D. J., Reed, C. C., & Iozzo, R. V., 2005. Decorin evokes protracted internalization and degradation of the epidermal growth factor receptor via caveolar endocytosis. *Journal of Biological Chemistry*, 280(37), pp. 32468-32479.

Zieske, J. D., Hutcheon, A. E., Guo, X., Chung, E. H., & Joyce, N. C., 2001. TGF-beta receptor types I and II are differentially expressed during corneal epithelial wound repair. *Invest Ophthalmol.Vis.Sci.*, 42(7), pp. 1465-1471.

APPENDIX I

PUBLISHED PAPERS

Fletcher, S. J., Poulter, N. S., Haining, E. J., & Rappoport, J. Z., 2012. Clathrin-mediated endocytosis regulates occludin, and not focal adhesion, distribution during epithelial wound healing. *Biol.Cell*, 104(4), pp. 238-256.

Farquhar, M.J., Hu, K., Harris, H.J., Davis, C., Brimacombe, C.L., **Fletcher, S.J.,** Baumert, T.F., Rappoport, J.Z., Balfe, P. & McKeating, J.A., 2012. Hepatitis C virus induces CD81 and claudin-1 endocytosis. *J Virol.*, 86(8), pp,4305-4316.

Fletcher, S. J. & Rappoport, J. Z., 2010. Moving forward: polarised trafficking in cell migration. *Trends in Cell Biology*, 20(2), pp. 71-78.

Fletcher, S. J. & Rappoport, J. Z., 2009. The role of vesicle trafficking in epithelial cell motility. *Biochem.Soc.Trans.*, 37(5), pp. 1072-1076.

APPENDIX II

SUPPLEMENTARY METHODS

1 Cell culture medium

Dulbecco's Modified Eagle Medium (DMEM) Lonza supplemented with 10% FBS and 1% Pen/Strep (all Lonza) was sterile filtered through a 500ml Corning 0.1µM pore Vacuum Filter System (Corning) before use.

2 Trypsin

10X trypsin (Gibco) aliquoted, frozen then diluted to 1X trypsin in PBS.

3 LB Broth

20 g of LB Broth (Sigma) was dissolved in 1 L distilled H_20 and autoclaved at 121ºC for 20 minutes.

4 Pouring LB agar plates

35 g of LB Agar (Sigma) was dissolved in 1 L distilled H_20 and autoclaved at 121ºC for 20 minutes. As the agar was cooling but before setting, kanamycin or ampicillin was added to a final concentration of 50 µg/ml or 100 µg/ml respectively. In a laminar flow hood, 50ml of the LB agar antibiotic mix was

poured into 12cm plastic dishes. The dish lids were removed whilst the plates were setting. Plates were stored in sealed bag, upside down at 4ºC.

5 Cell Imaging Media (CIM)

1 pot of Hanks Balanced Salt (without phenol red and sodium bicarbonate) (Sigma) was added to 1L of distilled water. 2.38g HEPES (Fisher Scientific) was added to form a final concentration of 10mM. The solution was set to pH 7.4 with HCl (Fisher Scientific) was added until a pH of 7.4 was obtained using a Basic Denver Instrument pH meter (Denver Instrument). The media was then sterile filtered through a 500ml Corning 0.1µM pore Vacuum Filter System. 5% FBS was added prior to use (0.5ml FBS to 9.5ml filtered solution).

6 4% Paraformaldehyde

10ml of 16% Paraformaldehyde (Electron Microscopy Sciences) was diluted to a 4% Paraformaldehyde solution in 30ml of PBS.

7 Permeabilisation buffer

An initial 10% Triton-X100 (Sigma) solution was made, adding 1ml of Triton-X100 solution to 9ml of PBS and vortexed to mix thoroughly. A final 0.1% Triton-X100 solution was made by adding 1ml 10% Triton-X100 to 99ml of PBS.

8 GS-BSA Block buffer

A solution of 10% Normal goat serum (Gibco) and 5% BSA (Sigma) was made to a final volume of 20ml (18ml of PBS, 2ml Goat serum and 0.5g BSA).

9 Acrylamide gel solutions

Table S.M.1. Acrylamide gel solutions.

	4%	**10%**	**12.5%**	**15%**
Distilled H_2O	30ml	20ml	16.1ml	11.75ml
Tris-HCl*	12.5ml	12.5ml	12.5ml	12.5ml
Bis Acrylamide (Protogel)	6.7ml	16.5ml	20.8ml	25ml
10% SDS	0.5ml	0.5ml	0.5ml	0.5ml
APS	500µl	500µl	500µl	500µl
TEMED	75µl	75µl	75µl	75µl

Makes 50ml of gel solution (volumes scaled depending upon requirement).
* Tris for stacking gel 0.5M pH6.8.
Tris for resolving gel 1.5M pH8.8.

0.5M pH6.8 Tris-HCl: 60.57g Tris (Fisher Scientific) dissolved in 1L distilled H_2O.

1.5M pH8.8 Tris-HCl: 181.71g Tris (Fisher Scientific) dissolved in 1L distilled H_2O. (5M HCl used to obtain correct pH using a Basic Denver Instrument pH meter (Denver Instrument).

10% Ammonium Persulphate (APS): 1g APS dissolved in 10ml distilled H_2O frozen in 1ml aliquots.

10% Sodium Dodecyl Sulphate (SDS): 10g SDS dissolved in 100ml distilled H_2O.

10 Running buffer

1X running buffer was made by diluting 100ml of 10X Running buffer in 900ml distilled H_2O.

10X Running buffer: 144g Glycine (Fisher Scientific), 30g Tris, 4g SDS made up to 1L in distilled H_2O.

11 Transfer buffer

1X running buffer was made by diluting 100ml of 10X Transfer buffer in 700ml distilled H_2O and 200ml methanol.

10X Transfer buffer: 144g Glycine (Fisher Scientific), 30g Tris, made up to 1L in distilled H_2O.

12 TBST

1X TBST buffer was made by diluting 100ml of 10X TBS with 900ml distilled H_2O plus 1ml Tween20 (Sigma). To pipette Tween20 use a P1000 pipette tip with the tip end cut off, remove remnants of Tween20 from the tip by ejecting the tip into the solution after Tween20 addition and mix for 10 minutes (the tip was removed after mixing).

10X TBS: 200ml 1M Tris-HCl pH 7.5, 300ml 5M NaCl made up to 1L with 500ml distilled H_2O.

1M pH7.5 Tris-HCl: 121.14g Tris (Fisher Scientific) dissolved in 1L distilled H_2O, 5M HCl used to obtain correct pH.

5M NaCl: 292.2g NaCl (Fisher Scientific) dissolved in 1L distilled H_2O.

13 TBST-Marvil blocking buffer

A 5% skimmed milk solution (Marvil) was dissolved in TBST (S.M.14) - 10g Marvil skimmed milk powder was dissolved in 200ml TBST.

14 1% Triton-X100

1ml of 10% Triton-X100 (prepared as S8) in 9ml PBS. One Complete mini-cocktail protease inhibitor tablet (Roche) was added.

15 3X Sample buffer

18.8ml of 1M Tris pH 6.8 (Fisher Scientific) (as described in S.M.12), 6g Sodium dodecyl sulphate (SDS) (Sigma), 15ml Beta mercaptoethanol (Sigma) and 30ml Glycerol was made up to 100ml with distilled H_2O. A small spatula of bromophenol blue was added and sample buffer mixed thoroughly.

16 0.2M sodium borate pH 9.0

38.137g of Sodium teraborate decahydrate (Sigma) was dissolved in 500ml of distilled H_2O. 5M HCl was used to obtain pH 9.0 using a Basic Denver Instrument pH meter (Denver Instrument).

17 0.2M Ethanolamine pH 8.0

6.108g of Ethanolamine liquid (Sigma) was diluted in 500ml distilled H_2O. 5M HCl was used to obtain pH 8.0 measured with a Basic Denver Instrument pH meter (Denver Instrument).

18 0.1M Glycine pH 3.0

3.75g of Glycine (Fisher Scientific) was dissolved in 500ml distilled H_2O. 5M HCl was used to obtain pH 3.0 measured with a Basic Denver Instrument pH meter (Denver Instrument). 0.1M glycine pH3.0 was autoclaved at 123ºC for 20 minutes prior to use.

19 0.5% NP40 lysis buffer

A 10% NP40 (Sigma) solution was made adding 1ml NP40 to 9ml PBS. 0.5ml 10% NP40 solution was diluted to a 0.5% NP40 solution in 9.5ml PBS. 1x EDTA-free Protease Inhibitor Cocktail tablet and 1x PhosSTOP Phoshotase Inhibitor Cocktail tablet was added to 10ml of 0.5% NP40 lysis buffer and vortexed thoroughly.

20 1X NuPAGE Bis-Tris running buffer

1X NuPAGE Bis-Tris running buffer was prepared by dilution of 20ml of 20X NuPAGE Bis-Tris running buffer (Invitrogen), with 380ml of ultrapure H_2O.

21 100mM Ammonium bicarbonate solution

0.362g Ammonium Bicarbonate was added to 40ml MilliQ water and vortexed.

22 10mM DTT solution

0.00771g DTT was dissolved in 5ml of 100mM Ammonium Bicarbonate solution (S.M.21) and vortexed.

23 50mM 2-Iodoacetamide solution

0.0462g 2-Iodoacetamide was dissolved in 5ml of 100mM Ammonium Bicarbonate solution (S.M. 21), vortexed, wrapped in foil and kept in the dark until use.

24 Trypsin

To 46µl of trypsin (Progold), 360µl of Ammonium Bicarbonate solution (S.M. 21) and 400µl MillQ water were mixed.

25 Extraction Solution A

53µl Formic Acid (Fisher Scientific) was added to 100µl Acetonitrile and made up to 5ml with MilliQ water.

26 Extraction Solution B

53µl Formic Acid (Fisher Scientific) was added to 2ml Acetonitrile and made up to 5ml with MilliQ water.

27 Resuspension Solution

53µl Formic Acid (Fisher Scientific) was added to 250µl Acetonitrile and made up to 5ml with MilliQ water.

28 Biotinylation wash buffer

50ml of 1M Tris pH7.5 (made as described in S.M. 12), 32ml of 3.2M NaCl, made up to 1 L with distilled H_2O. Once the solution was cooled, it was set to pH to 8.6 using 10M NaOH using a Basic Denver Instrument pH meter (Denver Instrument).

3.2M NaOH: 187g NaCl (Fisher Scientific) dissolved in 1L distilled H_2O.

29 Biotinylation reducing buffer

40ml of pH 8.6 biotinylation wash buffer (S.M.28) was added to 60µM NaOH and 600mg MesNa (Sigma). The solution was made shortly before use.

30 Table of Antibodies

Table S.M.2. Primary Antibodies

Antibody	Dilution	Procedure	Company	Catalogue #
rabbit anti-occludin	1:250	IC	Invitrogen	71-1500
rabbit anti-ZO1	1:250	IC	Invitrogen	61-7300
rabbit anti-occludin	1:500	WB	Invitrogen	71-1500
mouse anti FAK (pY397)	1:100	IC	BD Transduction Labs	611807
mouse anti-occludin	1:500	IC	Invitrogen	33-1500
mouse anti-ZO1	1:500	WB	Invitrogen	33-9100

Table S.M.3. Secondary Antibodies

Antibody	Dilution	Procedure	Company	Catalogue #
donkey anti-rabbit-Alexa Fluor 568	1:200	IC	Invitrogen	A10042
goat anti-rabbit -Alexa Fluor 568	1:200	IC	Invitrogen	A11008
donkey anti-mouse – Alexa Fluor 568	1:200/ 1:100	IC	Invitrogen	A10037
goat anti-mouse – Alexa Fluor 488	1:200/ 1:100	IC	Invitrogen	A11001
goat anti-rabbit IgG horseradish peroxidase	1:10000	WB	Thermo Fisher Scientific	31460
sheep anti mouse IgG Horseradish peroxidase	1:5000	WB	GE Healthcare	RPN4201